ISSN 2313–5891 (Online)
ISSN 2304–974X (Print)

Ukrainian Food Journal

Volume 13, Issue 4
2024

Kyiv **Київ**

2024

Ukrainian Food Journal is an international scientific periodical journal that publishes articles by specialists in the field of food science, engineering and technology, chemistry, economics and management.

Ukrainian Food Journal – міжнародне наукове періодичне видання для публікації результатів досліджень фахівців у галузі харчової науки, техніки та технології, хімії, економіки і управління.

Ukrainian Food Journal is abstracted and indexed by scientometric databases:

Ukrainian Food Journal індексується наукометричними базами:

Index Copernicus (2012)
EBSCO (2013)
Google Scholar (2013)
UlrichsWeb (2013)
CABI full text (2014)
Online Library of University of Southern Denmark (2014)
Directory of Open Access scholarly Resources (ROAD) (2014)
European Reference Index for the Humanities and the Social Sciences (ERIH PLUS) (2014)
Directory of Open Access Journals (DOAJ) (2015)
InfoBase Index (2015)
Chemical Abstracts Service Source Index (CASSI) (2016)
FSTA (Food Science and Technology Abstracts) (2018)
Web of Science (Emerging Sourses Citaton Index) (2018)
Scopus (2022)

Ukrainian Food Journal включено у перелік наукових фахових видань України з технічних наук, категорія А (Наказ Міністерства освіти і науки України № 358 від 15.03.2019)

Editorial office address:

National University
of Food Technologies
68 Volodymyrska str.
Kyiv 01601, **Ukraine**

Адреса редакції:

Національний університет
харчових технологій
вул. Володимирська, 68
Київ 01601, **Україна**

e-mail: **ufj_nuft@meta.ua**

Ukrainian Food Journal is an open access journal published by the National University of Food Technologies, Kyiv, Ukraine. The Journal publishes original research articles, short communications, review papers, news, and literature reviews covering all areas of food science, technology, engineering, nutrition, food chemistry, economics, and management.

Studies must be new, have a clear link to food science, and be of general interest to the international scientific community.

Topics covered by the journal include:

- Food engineering
- Food chemistry
- Food microbiology
- Food quality and safety
- Food processes
- Automation of food processes
- Food packaging
- Economics
- Food nanotechnologies
- Economics and management

Please note that the Journal does not consider:

1. Articles with medical claims (this topic is not covered in the Journal); articles in which the subject of the study is humans and animals.
2. Articles that do not have scientific value (solutions of typical practical and engineering problems).

Periodicity of the Journal

4 issues per year (March, June, September, and December).

Reviewing a Manuscript for Publication

The editor-in-chief checks the content of a newly received article to ensure it complies with the journal's profile, approves the design, style, and illustrative material of the article, may make suggestions for their improvement and makes a decision on sending it for review.

Articles submitted for publication in the Ukrainian Food Journal undergo double-blind peer review by at least two scientists appointed by the editorial board: one member of the editorial board and one external to the editorial board and/or publisher.

The full guide for authors can be found on our website:

http://ufj.nuft.edu.ua

Contents

Food Technology…….. 657

Silvia Mironeasa, Mădălina Ungureanu-Iuga, Vasile-Florin Ursachi, Costel Mironeasa
Seedless grape pomace to increase fiber content in extruded corn snacks… 657

Yurii Bulii
Improvement of alcohol distillation plant operation…….. 675

Ilhama Kazimova, Elza Omarova, Ahad Nabiyev, Afet Gasimova
Comparative analysis of the composition of Bayan Shirey, Rkatsiteli and Cabernet Sauvignon grape varieties for production of brandy wine materials……..... 694

Irma Berulava, Maria Silagadze, Volodymyr Kovbasa, George Pkhakadze, Gulnara Khetsuriani, Marita Rukhadze
Fermented drink based on secondary raw milk materials…….. 708

Ana Batariuc, Mădălina Ungureanu-Iuga, Anca Becze, Lacrimioara Senila, Silvia Mironeasa
Impact of heat treatment of sorghum grains on flour properties…… 723

Mariia Blazhenko, Nataliia Falendysh, Vladyslav Shpak
Effect of hemp seed by-products on wheat dough fermentation……... 737

Vitalii Shutyuk, Olha Dushchak, Oleksandr Bessarab
Physico-chemical characteristics of dried green onion semi-finished products and their rehydration ability…… 753

Processes and Equipment..... 766

Oleksandr Gavva, Oleksandr Sokolskyi, Yuliia Herasymenko
Determination of opening force of hot-melt adhesive joints in flexible packaging…….. 766

Oleksandr Kozak, Volodymyr Telychkun
Mathematical model of vacuum cooling process for wheat bread……. 780

Economics and Management……. 794

Dávid Sütő, Péter Bajnai, Veronika Fenyves
Forecasting the financial performance of small and medium-sized enterprises: evidence from the Hungarian food retail sector……. 794

Viktoriia Khmurova, Olena Dragan, Iryna Fedulova, Maryna Dzhulai, Alina Berher
Evaluation of employer's brand of trade and food industry companies…… 809

Biotechnology, Microbiology……... 825

Tetiana Belemets, Viktoria Krasinko, Viktor Stabnikov
Characteristics and immunostimulating properties of chemical and microbial vaccine adjuvants……... 825

Instructions for authors……..... 862

Seedless grape pomace to increase fiber content in extruded corn snacks

Silvia Mironeasa[1], Mădălina Ungureanu-Iuga[1,2], Vasile-Florin Ursachi[1], Costel Mironeasa[1]

1 – "Ştefan cel Mare" University of Suceava, Romania;
2 – Mountain Economy Center (CE-MONT), Romanian Academy, Romania

Keywords:

Grape pomace
Corn
Snacks
Extrusion
Functional
Fiber

Article history:

Received 14.04.2024
Received in revised form 26.08.2024
Accepted 30.12.2024

Corresponding author:

Mădălina Ungureanu-Iuga
E-mail: madalina.iuga@usm.ro

DOI:
10.24263/2304-974X-2024-13-4-3

Abstract

Introduction. Extruded snack nutritional value can be enhanced by incorporating functional ingredients like seedless grape pomace – a winery's valuable by-product that is usually discarded.

Materials and methods. This work aimed to evaluate the impact of seedless grape pomace from two varieties (red and white) on extruded corn snack quality: expansion characteristics, starch digestibility, color, texture, and functional properties. The best formulation was evaluated by the nutritional profile, antioxidant activity, and polyphenol content.

Results and discussion. Grape variety affected the content of total starch, snacks porosity, starch digestion index, lightness, browning index, cutting, compression and puncture forces, chewiness, and functional properties of extruded snacks added with grape pomace. Increasing the amount of grape pomace in snacks resulted in a decrease in expansion index, water absorption and solubility indices, total starch content, lightness, friability, cutting, compression and piercing forces, and crispness, while chewiness, browning index, and starch digestibility index increased when as the addition level of the plant additive was higher. The recommended addition levels were 30% for white seedless grape pomace and 20% for the red one. The characterization of these two samples in comparison with the control demonstrated that if even the porosity, texture parameters, lightness, and functional properties were lower, the general quality of the final product was acceptable. The fortified samples had a higher content of protein, ash, lipids, and fiber, and they demonstrated significantly higher antioxidant activity compared to the control. The fiber content was more than 23 fold higher in the the white seedless pomace-containing sample and more than 37 fold in the red one compared to the control corn snack. Furthermore, some individual polyphenols like quercetin, luteolin, and myricetin were identified only in the fortified snacks, depending on grape variety. The FT-IR spectra registered higher absorbances for the fortified snacks than those of control.

Conclusion. The results confirmed the opportunity to valorize seedless grape pomace in the extrusion process to obtain functional snacks with potential health benefits.

Introduction

World grape production was estimated at 73.5 million tons in 2021 (Statista, 2023), and most of the grapes (around 75%) are used for winemaking (Stabnikova et al., 2023), which generates a large amount of by-products (seeds, skins, and stem residues) called grape pomace, most of which is not used and pose environmental problems (Andrade et al., 2019; Dwyer et al., 2014). Annual global production of grape pomace consists from 10.5 to 13.1 million tons (Gómez-Brandón et al., 2019; Oliveira et al., 2024). Meanwhile, grape pomace contains valuable compounds, and recently much research has been carried out on its use in the production of functional foods (Almanza-Oliveros et al., 2024; Baroi et al., 2022; Grevtseva et al., 2023; Stabnikova et al., 2021; Troilo et al., 2022).

Therefore, it is of crucial importance to reuse these by-products to enhance process economics and its sustainability. The strategy of recycling grape winemaking by-products involves reusing them as raw material for a subsequent process, such as extrusion, to produce higher value products. The incorporation of grape by-products in extruded snacks includes in addition to health benefits by creating value-added snacks with high nutritional profile, and, environmentally sustainable benefits.

Seedless grape pomace is well-known as good source of fibers (65–80%) (Llobera and Cañellas, 2008; Valiente et al., 1995), polysaccharides (Beres et al., 2017; Bordiga et al., 2019) containing also multiple types of polyphenols, such as anthocyanins, hydroxycinnamic acids, catechins, and flavonols (Kammerer et al., 2004). These polyphenols have been affirmed to have antioxidant properties (Deng et al., 2011; Ivanov et al., 2021) and inhibit low-density lipoprotein oxidation (Yıldırım et al., 2005). Additionally, dietary fiber is recognized as a beneficial component of a healthy diet, with benefits including lowering cholesterol and blood sugar levels, improving cardiovascular health, and preventing constipation and obesity (Deng et al., 2011; Sagar et al., 2018; Stabnikova and Paredes-Lopez, 2024). The phytochemicals content of seedless grape pomace is known to vary depending on the type of grape (red or white), grape cultivar, growth climates, and processing conditions. Deng et al. (2011) reported that total dietary fiber was the predominant composition in the red wine grape pomace but not in the white wine grape pomace in which soluble sugar was in the largest amount. The seedless grape pomace from the red variety are usually rich in anthocyanidins that are neglected in white varieties (Yu and Ahmedna, 2013).

Extrusion technology, one of process with high productivity and versatility, offers the possibility to incorporate different types of by-products in snacks to develop new products or to improve nutritionally the products that are carbohydrate-rich or glycemic-high (Paraman et al., 2015). Corn grits, the major ingredient used for the production of extruded snacks, contains a high amount of starch and less nutrients, and it's improvement with other raw materials has been approached in various studies. An increase of fiber level in extruded snacks would offer a nutritional benefit, and the seedless grape pomace shows the appropriate characteristics (Deng et al., 2011) since it contains a great quantity of hemicellulosic sugars (Bordiga et al., 2019). However, it is a food engineering challenge to design palatable extruded foods having high content of dietary fiber due to the low expansion capability of polymer matrices that contain large amounts of dietary fiber (Sozer and Poutanen, 2013). Expansion rates at high fiber content can be enhanced when there are present soluble non-digestible oligo- and polysaccharides. Grape skin cell walls are considered an important source of polysaccharides, with the content of soluble polysaccharides varying depending on the grape variety (Zhai et al., 2024). The oligosaccharides represent the natural by-products of the degradation of berry cell wall polysaccharides (Bordiga et al., 2019). These components will not only improve expansion rates but also provides additional functional

properties, acting as nutrients for the colonic microflora of humans (Bordiga et al., 2019; Sozer and Poutanen, 2013). The polysaccharide-lipid complexes formed during the extrusion process contribute to the insoluble fiber fraction, together with resistant starches formed under harsh extrusion conditions (Gualberto et al., 1997). Increasing the content of insoluble dietary fiber and reducing starch digestibility in nutritious snacks is desirable, but their acceptability by consumers from sensory and textural properties points of view must also be taken into account.

The possibility of using seedless grape pomace in high proportion in corn snack production with satisfactory physical, functional and textural properties, acceptable or desired for consumers has not investigated yet. The incorporation of by-products with a higher content of dietary fiber is known to cause lower expansion during extrusion, resulting products with unacceptable features (Stojceska et al., 2010). Until now, the investigations reported the valorization of grape by-products in extruded snacks at levels up to 20%. There is not known research about the application of seedless grape pomace above this limit in the production of expanded products based on corn flour so far.

The results of the present study could reveal the level of this ingredient, which can be added to corn flour to enhance the nutritional profile of snacks. The main aim of this research was to investigate the possibility of using seedless grape pomace from white and red grape varieties in considerable amounts in the production of corn snacks, and to estimate the best percentage that can be added in corn flour to obtain snacks with desired characteristics.

Materials and methods

Materials

The red and white grape pomaces were provided by the Iaşi Research and Development Center for Viticulture and Vinification, while the corn was purchased from a local Romanian producer. After drying the pomace in a convection oven (ZRD-A5055, Zhicheng Analysis Instrument, Shanghai, China) at 50°C until its moisture content became below 10%, the seeds were manually separated, and the remaining grape skins were ground using a laboratory mill (Perten 3100, Perten Instruments, Huddinge, Sweden). The ground grape skin was then sieved through a mesh smaller than 0.2 mm to obtain a uniform powder. Flour mixtures were created by blending corn flour with either white (SGPW) or red (SGPR) grape skin in varying proportions (10–40%), with the corn flour serving as the control.

Extrusion parameters

A laboratory single-screw extruder (Kompakt extruder KE 19/25, Brabender, Duisburg, Germany) was used. The extruder had a barrel diameter of 19 mm and a length-to-diameter ratio of 25:1, equipped with a 2 mm diameter nozzle. The feeding rate was maintained at 24 rpm, and the screw speed was set to 150 rpm. The temperature settings for the four processing stages were 50°C, 95°C, 175°C, and 180°C. After extrusion, the products were cooled to room temperature and left to equilibrate for 16 hours before storage.

Methods

Expansion characteristics

As extrusion leads to an expanded product, the expansion index (EI) was determined. EI was calculated by measuring 20 segments from each sample using a digital caliper. To

determine porosity, 15 product pieces were placed in a 250 mL cylinder filled with mustard seeds. The volume of mustard seeds without the snacks was also recorded, with the difference indicating the bulk volume. The same snacks were then ground into a fine powder, and the resulting volume was measured in the same cylinder, representing the apparent volume. The difference between the bulk and apparent volumes provided an estimate of the internal void volume, allowing the material's porosity to be assessed (Rathod and Annapure, 2017).

Digestibility of starch

Total starch content was measured using a Megazyme kit (K-DSTRS; Megazyme, Bray, Ireland) following the manufacturer's instructions (Batariuc et al., 2023). Total digestible starch was determined using a spectrophotometric method, and the starch digestion index (SDRI) was calculated as the ratio of rapidly digestible starch (after 20 min of digestion) to total starch.

Color

The ground snacks were placed in transparent petri dishes, and the surface was leveled. The color parameters—Lightness (L*), green to red hue (a*), and yellow to blue hue (b*) were measured using a CR-400 device (Konica Minolta, Tokyo, Japan). The browning index (BI) was then calculated based on methods described in the literature (Al-Hilphy et al., 2022).

Texture

The texture of the snacks was analyzed using a TVT 6700 texturometer (Perten Instruments, Hägersten, Sweden). A single-cycle compression test was conducted on 1 cm-long samples, applying a compression of 50% at a test speed of 1 mm/s with a 25 mm cylindrical probe. The cutting force was measured using a V-shaped cutting blade, perpendicular to 4 cm-long samples, also at a test speed of 1 mm/s. Crispness was assessed by analyzing the slope of the first peak during the test. Additionally, a puncture test was performed on 1 cm-long samples using a 3 mm diameter puncture probe, at the same speed of 1 mm/s.

Sensory analysis

The crunchiness and chewiness of the snacks were evaluated by 65 panelists from the Food Engineering Faculty at Stefan cel Mare University of Suceava. Each panelist was instructed to consume and swallow coded samples of the extruded snacks, rating the intensity of each attribute on a nine-point scale, following the guidelines of ISO 8589:2007. Mineral water was provided for mouth cleansing between tastings.

Functional properties

The water absorption index (WAI) was determined as outlined by Ratod and Annapure (Rathod and Annapure, 2017). A sample of 2.5 g of ground extrudates was suspended in 25 mL of water at room temperature for 30 min with intermittent stirring, followed by centrifugation at 3000 rpm for 15 min. After removing the supernatant, the hydrated residue was weighed. The supernatant was poured into a pre-weighed evaporating dish, and the water was evaporated to a constant weight to determine the dry solids. The water absorption index (WAI) was calculated as the weight of the hydrated residue per unit weight of the original dry solids. The water solubility index (WSI) was calculated as the weight of dry solids in the supernatant, expressed as a percentage of the original sample weight.

Polyphenols quantification

For the separation and quantification of individual phenolics, phenolic extracts were analyzed using a High-Performance Liquid Chromatography (HPLC) system (Shimadzu, Kyoto, Japan), which included a LC-20 AD liquid chromatograph, SIL-20A autosampler, CTO-20AC column oven, and SPD-M-20A diode array detector. Separation was performed on a Phenomenex Kinetex® 2.6 µm Biphenyl 100 Å HPLC column (150 × 4.6 mm) thermostated at 25°C. The injection volume was set at 10 µL, with solvents consisting of 0.1% acetic acid in water (solvent A) and acetonitrile (solvent B). The gradient started with 100% A, transitioning to 5% B at 6.66 min, 40% B at 66.6 min, and 80% B at 74 min. The solvent flow rate was maintained at 1 mL/min. Polyphenols were identified by comparing retention times with those of standard solutions, and quantification was based on absorbance in the chromatograms, measured relative to external standards at 320 nm for p-coumaric acid, rosmarinic acid, myricetin, luteolin, and quercetin. The standard calibration curves had regression coefficients of $R^2 > 0.99$.

FT-IR spectra acquisition

The molecular characteristics of the extruded products were analyzed using Fourier Transform Infrared (FTIR) spectroscopy with a Thermo Scientific Nicolet iS20 spectrophotometer (Waltham, MA, USA) equipped with an attenuated total reflection (ATR) accessory. Spectra were collected in the range of 650 to 4000 cm^{-1}, with a resolution of 4 cm^{-1} and 32 scans. The molecular features were identified based on established literature (Nogales-Bueno et al., 2017; Reinaldo et al., 2021) and analyzed using OMNIC software (version 9.9.549, Thermo Fisher Scientific, Waltham, MA, USA).

Nutritional profile

The nutrients composition (moisture, lipids, protein, and ash) of the snacks was determined by following the ICC standard instructions: moisture (101/1), fat (104/1), protein (105/2), and ash (105/1). The total dietary fiber was evaluated with a Megazyme kit (K-TDFR-200a 04/17) following the AACC 32-05.01 method.

For DPPH antiradical activity (AA DPPH), samples were extracted via ultrasonication by mixing 1 g of the sample with 10 mL of acetone: water acid solution (70:28:2) at 45°C for 1 h~~our~~. Cold water was added to the bath every 15 min to maintain the temperature. A 0.5 mL portion of the extract was mixed with 0.5 mL of 80% methanol and 5 mL of DPPH solution, then incubated for 30 min in the dark at room temperature. Absorbance was recorded at 517 nm using the same spectrophotometer.

Statistical analysis

The single and combined impact of grape pomace variety (red or white) and addition level (10, 20, 30, or 40%) on snacks quality in terms of porosity, expansion index, total starch, starch digestion index, L*, BI, cutting force, crispness, compression force, puncture force, crunchiness, chewiness, water absorption index, and the water solubility index were evaluated by using quadratic, cubic or 2FI models. Models fitting was checked by Analysis of Variance (ANOVA) at a significance level of $p < 0.05$ and by considering the F-value, p-value, R^2 and $Adj.\text{-}R^2$. The differences among samples were evaluated by using Tukey test ($p < 0.05$). The statistical modelation of data was performed by using XL STAT 2024 version and Stat Ease Design-Expert (trial version).

Results and discussion

The impact of seedless grape pomace variety and its addition level on corn snack quality was evaluated by applying different mathematical models (Table 1).

Porosity was affected significantly ($p < 0.05$) by grape variety, while the expansion index was influenced by the addition level and the interaction between grape variety and addition level. A slight increase of porosity with the addition level rise was observed (Figure 1).

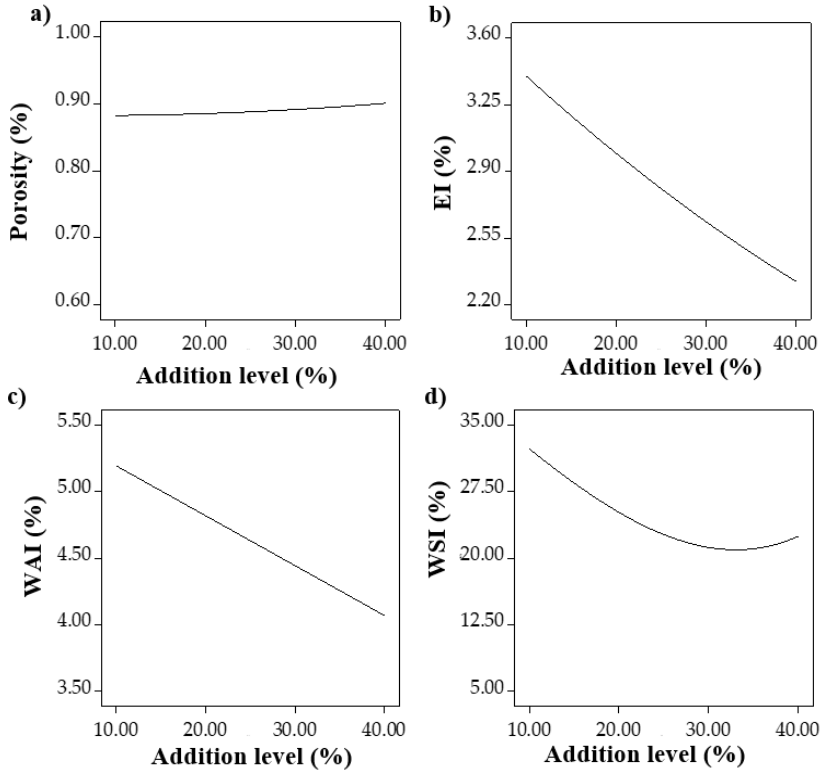

Figure 1. Dependence of porosity (a), expansion index (EI) (b), water absorption index (WAI) (c), and water solubility index (WSI) (d) on addition level of seedless grape pomace

On the other hand, higher amounts of seedless grape pomace caused the decrease of the expansion index. Similar, a reduction of the expansion index was reported by Soja et al. (2024) for snacks from potato starch and different plant pomaces due to the high amount of fiber present in the plant ingredient which led to lower expansion capacity. Another study reported that the incorporation of chokeberry and cherry pomaces in corn extruded snacks resulted in a lower expansion rate (Gumul et al., 2023). The results obtained in our study regarding the decrease of snacks porosity and expansion could be due to the simultaneous effect of fiber and polyphenols from seedless grape pomace which affected the final product texture (Soja et al., 2024). The expansion of snacks depends on the starch content of the flour because it presents viscoelastic characteristics. The bubbles generated during heating by the water evaporation enter into the swelling starch grains and determine their expansion (Karkle et al., 2012). Thus, replacing corn flour with seedless grape pomace rich in fiber generated a starch dilution effect and decreased the expansion.

Table 1

ANOVA results for mathematical models fitted for properties evaluated

Factor	Porosity (%)	EI (%)	Total starch (%)	SDRI	L*	BI	Cutting force (N)	Crispness (N/s)	Compression force (N)	Puncture force (N)	Crunchiness	Chewiness	WAI (%)	WSI (%)
Intercept	0.81	2.84	39.05	0.84	54.02	26.39	8.33	4.77	20.18	11.07	49.43	41.54	4.75	18.99
A-Variety	-0.08**	0.04	1.57**	-0.03**	-5.02**	-3.63**	1.89**	0.12	2.65**	2.60**	-0.73	-1.53**	0.11**	-3.66**
B-Level	0.03*	-0.40**	4.06**	0.02**	-4.17**	-0.72	-0.70*	0.08	-0.39	0.14	1.83	3.20*	-0.42**	-4.01
AB	0.02	0.14**	-1.87**	-0.01	-2.07**	-0.86*	1.10**	1.11**	6.63**	2.12**	2.96**	0.58	0.13**	2.04**
B^2	0.01	0.05	1.00	0.06**	-0.27		-1.01*		0.07	-0.26	2.15*	1.04		0.23
AB^2					1.32**						0.47	-0.17		-4.50**
B^3					-0.94						-0.91	-0.74		1.12
p-value	<0.01	<0.01	<0.01	<0.01	<0.01	<0.01	<0.01	<0.01	<0.01	<0.01	<0.01	<0.01	<0.01	<0.01
R^2	0.80	0.85	0.95	0.88	0.99	0.89	0.85	0.77	0.94	0.92	0.81	0.84	0.86	0.94
Adj.-R^2	0.76	0.81	0.93	0.85	0.99	0.87	0.82	0.73	0.93	0.90	0.75	0.89	0.84	0.91

* - significant at $p < 0.05$, ** - significant at $p < 0.01$

EI - expansion index; SDRI - starch digestion index; WAI - water absorption index; WSI - water solubility index

Snacks' functional properties were influenced by grape variety and its interaction with the addition level ($p < 0.05$), while the latest had a significant impact only on the water solubility index. Both the water absorption index and water solubility index showed a decreasing trend proportional with the addition level increase (Figure 1).

The water absorption index is a measure of the distribution of starch in excess water and is dependent on starch damage and the reduction in amylose and amylopectin mass during processing (Yağci and Göğüş, 2008). It depends on the number of hydrophilic groups and on the ability of starch to form a gel structure (Raleng et al., 2016). The great sugar content of grape pomace could have been reduced starch gelatinization due to the competition for water of these two types of molecules and/or could have been determined the formation of complexes between them (Lund, 1984). Similar results were reported by Raleng et al. (2016) for rice-pigeon pea snacks with pineapple pomace. The quantity of soluble polysaccharides released from starch during thermal processing through dextrinization can be estimated by the water solubility index (Ding et al., 2005). Poliszko et al. (2019) studied the impact of pumpkin flour on corn snacks properties and also reported a decrease of the water solubility index.

Total starch and starch digestion index (SDRI) were influenced by both grape variety and addition level ($p < 0.05$), but only total starch was affected by their interaction. Total starch content increased with the addition level increase, while the starch digestion index first decreased, then it raised at levels > 30% (Figure 2).

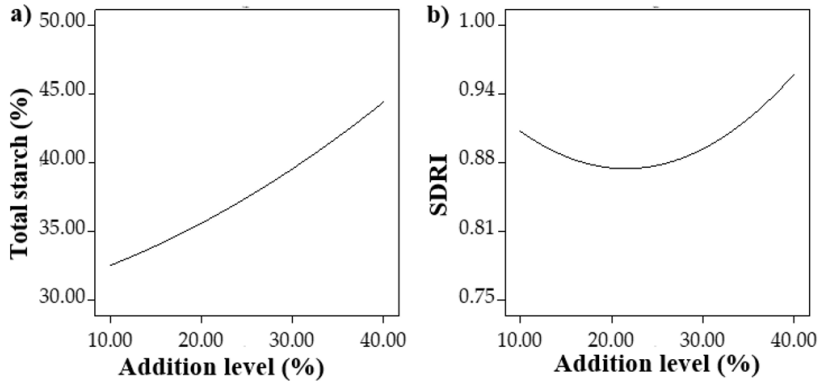

Figure 2. Dependence of total starch (a) and starch digestion index (SDRI) (b) on addition level of seedless grape pomace

The increase in starch digestibility could be due to a weaker snacks microstructure, and a greater contact surface determined by the presence of grape pomace (Raleng et al., 2022). Grape variety, the addition level, and their interaction had a significant effect ($p < 0.05$) on snacks lightness (L*). On the other hand, the browning index (BI) was influenced by grape variety and its interaction with the addition level. A reduction of L* values was observed as the addition level raised, while the browning index recorded slight changes (Figure 3).

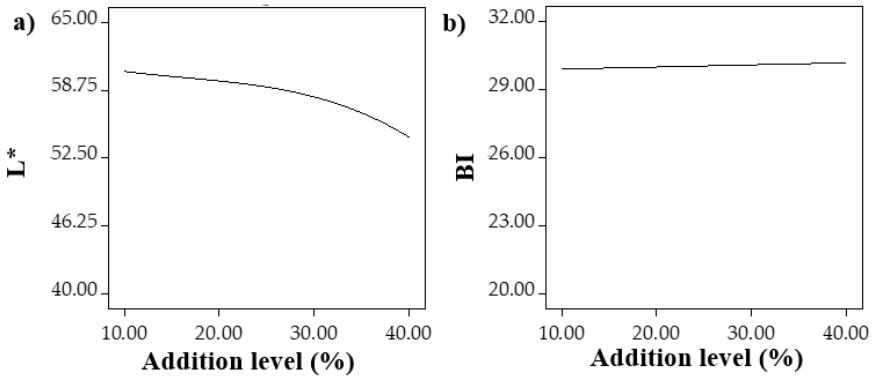

Figure 3. Dependence of L* (a) and browning index (BI) (b) color properties on addition level of seedless grape pomace

Altan et al. (2008) also reported a decrease of barley snacks L* values when tomato pomace was added. Non-enzymatic browning reactions and pigments degradation could be responsible for color changes during extrusion (Altan et al., 2008). The increase in pomace quantity led to the intensification of these modifications which may explain the reduction of L* and the increase of browning index.

All texture parameters (cutting force, crispness, compression force, and puncture force) were influenced by the interaction between grape variety and addition level, while the single effect of variety was significant ($p < 0.05$) only on cutting force, compression force, and puncture force. Only the cutting force was affected by the addition level ($p < 0.05$). All the texture properties (cutting force, crispness, compression force, and puncture force) decreased proportionally with the addition level increase (Figure 4). The decrease of these texture parameters could be possibly explained by the presence of pectin from grape peels, which may act as a lubricant and decrease snacks hardness (Singha et al., 2019). Similar trends for cutting force and hardness of corn snacks with dried fruits were reported by Różańska-Boczula et al. (2023). These results could be due also to the damage on the internal structure and the reduction of matrix cohesion because of high fiber and non-starch components content induced by grape pomace, which may lead to starch gelatinization disturbance.

Crunchiness was siginicanlty affected by the interaction of grape variety and addition level ($p < 0.05$). Chewiness was affected by both grape variety and addition level, with a greater impact of the grape type. The addition level increase caused a reduction of crunchiness and an increase of snacks chewiness (Figure 5). Różańska-Boczula et al. (2023) reported lower crispness as the amount of elderberry powder was higher in corn-based snacks. At low addition levels snacks structure encompasses bigger air bubbles that make them being more delicate. On the other hand, at higher grape pomace levels, the air pores are smaller and the structure is more rigid, leading to a less crunchy snack. The higher fiber content of grape pomace caused a denser structure, which resulted in higher chewiness, similar with the findings obtained by Dangal (2023).

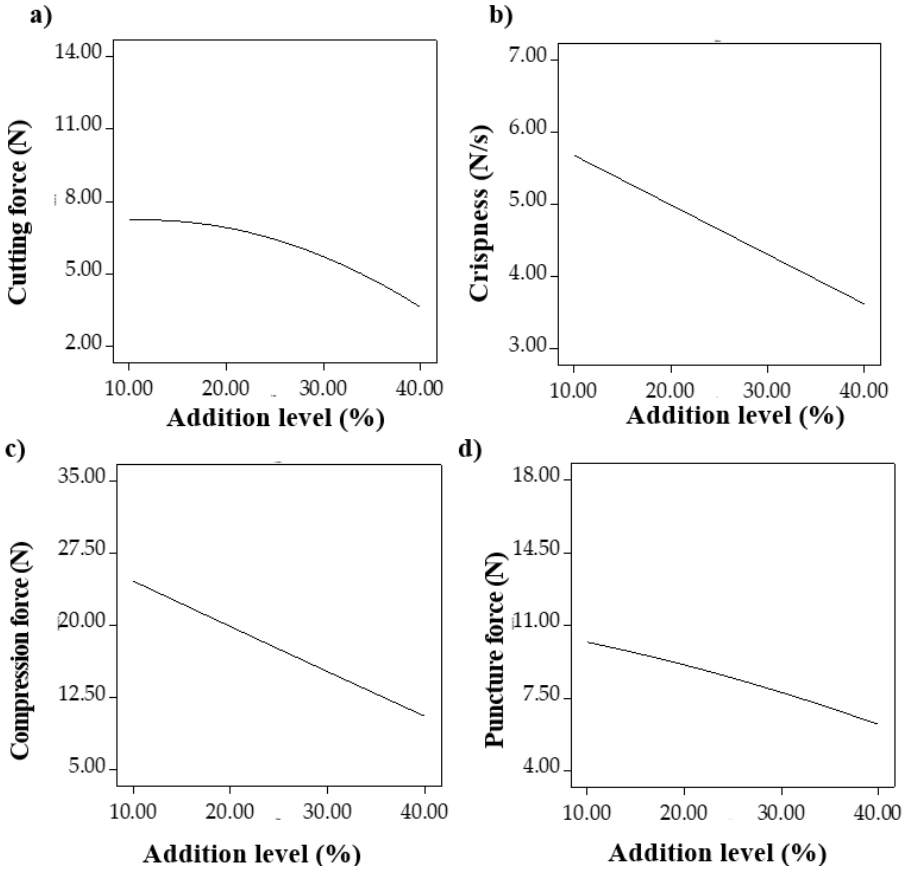

Figure 4. Dependence of cutting force (a), crispness (b), compression force (c), and puncture force (d) on addition level of seedless grape pomace

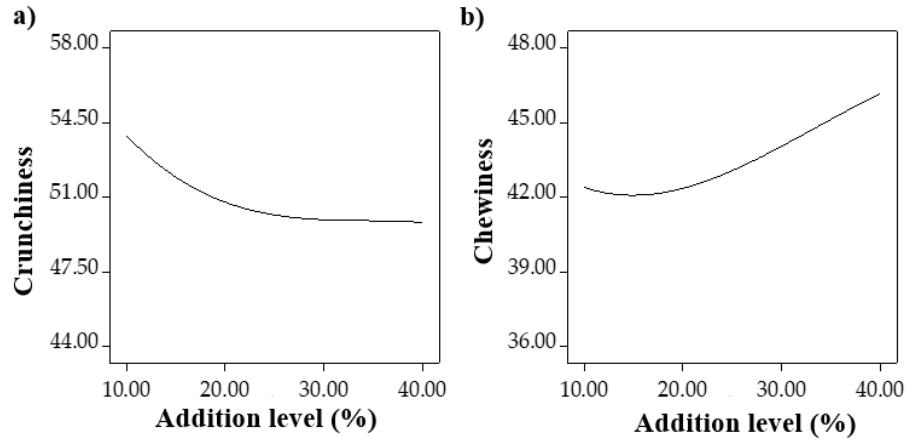

Figure 5. Dependence of crunchiness (a) and chewiness (b) texture properties on addition level of seedless grape pomace

To select the best formulations, the maximum porosity, EI, and chewiness, and the minimum cutting force, compression force, puncture force, and water absorption index were considered. Thus, an addition level of 30% for white seedless grape pomace (SGPWO) and 20% for the red seedless grape pomace (SGPRO) were recommended and further characterization of them was performed.

The highest porosity was observed for white seedless grape pomace, while the EI was better in the case of control sample (Table 2). This may be due to the high fiber content of the grape pomace incorporated. Both fortified samples exhibited higher total starch content compared to the control, while the greatest starch digestion index (SDRI) was found for white seedless grape pomace. These changes could be related to the structure density of the fortified snacks (Raleng et al., 2022). Both grape pomace types caused significant changes of L* and browning index by lowering the values obtained, which can be explained by the presence of pigments and/or the intensification of Maillard reactions due to the chemical composition of the ingredients added (Lohinova and Petrusha, 2023; Yu et al., 2018). Control sample exhibited greater cutting force, crispness and compression force compared to both fortified snacks. Red seedless grape pomace presented the highest puncture force. This may be explained by the more compact structure of the control and by the dilution effect of grape pomace fiber, which was different depending on the chemical composition of each grape variety (Różańska-Boczula et al., 2023). The white seedless grape pomace sample was more chewable compared to the red seedless grape pomace, while the crunchiness did not differ among them. The highest water absorption index was obtained for red seedless grape pomace, while the water solubility index of both fortified samples was lower compared to the control. A reduced water solubility index is desired from a nutritional perspective because it induces a lower digestion and intestinal absorption (Poliszko et al., 2019).

Table 2

Fortified samples properties compared with control sample

Indicators	SGPWO		SGPRO		C	
	Mean	SD	Mean	SD	Mean	SD
Level (%)	30	-	20	-	0	-
Porosity (%)	0.89^{a}	0.05	0.71^{b}	0.05	0.73^{b}	0.02
EI (%)	2.61^{c}	0.15	2.95^{b}	0.15	3.70^{a}	0.03
Total starch (%)	39.93^{a}	1.00	40.09^{a}	1.00	35.90^{b}	0.00
SDRI	0.89^{a}	0.02	0.81^{b}	0.02	0.84^{b}	0.00
L*	57.12^{b}	0.88	51.69^{c}	0.88	78.48^{a}	0.12
BI	30.08^{a}	1.46	23.20^{b}	1.46	31.98^{a}	0.40
Cutting force (N)	5.58^{c}	1.01	10.03^{b}	1.01	14.61^{a}	1.77
Crispness (N/s)	4.25^{b}	0.50	4.56^{b}	0.50	7.23^{a}	0.77
Compression force (N)	14.82^{b}	1.62	21.10^{a}	1.62	20.09^{a}	1.46
Puncture force (N)	7.56^{b}	1.01	12.90^{a}	1.01	10.10^{b}	1.13
Crunchiness	49.47^{a}	1.43	48.02^{a}	1.43	-	-
Chewiness	44.49^{a}	1.33	39.63^{b}	1.33	-	-
WAI (%)	4.41^{b}	0.16	4.94^{a}	0.16	4.52^{b}	0.19
WSI (%)	23.24^{b}	3.06	13.12^{c}	3.06	31.80^{a}	0.30

Mean values followed by different letters in the same row are significantly different ($p < 0.05$)

WAI - water absorption index; **WSI** - water solubility index; **SDRI** - starch digestion index; **BI** - browning index; **SGPWO** - white seedless grape pomace; **SGPRO** - red seedless grape pomace.

Characterization of the best samples

The appearance of the samples selected is shown in Figure 6.

C **SGPWO** **SGPRO**

Figure 6. Extruded corn snacks with white seedless grape pomace (SGPWO) and red seedless grape pomace (SGPRO) *vs.* control (C)

The content of polyphenols identified in the fortified and control snacks is presented in Figure 7. p-coumaric acid was present in all the analysed samples and showed very close values. Quercetin was found in both fortified snacks, with the red one (SGPRO) exhibiting the highest concentration. SGPWO contains rosmarinic acid, which was not found in the other sample. On the other hand, SGPRO contains significant amounts of luteolin and myricetin, which were not present in the other snacks. The results are in agreement with previous studies which reported higher content of myricetin and quercetin in red grapes compared to white varieties (Gomes et al., 2019), while rosmarinic acid is found in higher amounts in white grapes (Squillaci et al., 2021).

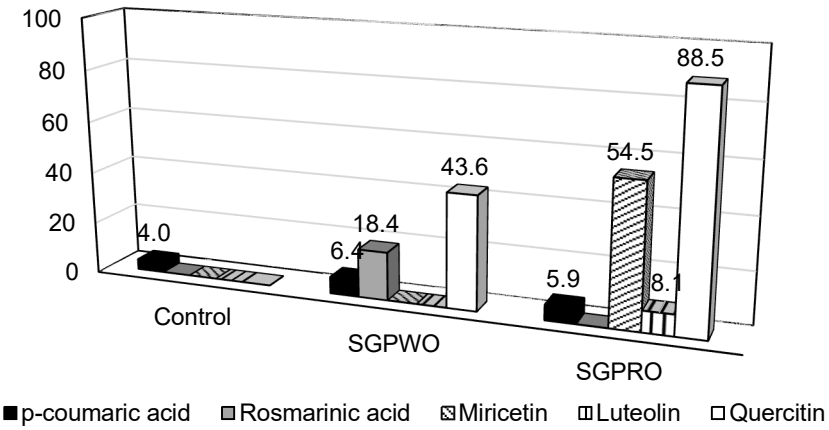

Figure 7. Polyphenols content of extruded corn snacks with white seedless grape pomace (SGPWO) and red seedless grape pomace (SGPRO) *vs.* control (C)

The addition of seedless grape pomace resulted in an increase of FT-IR peaks intensities compared to the control (Figure 8). More pronounced peaks at 2374 and 1745 cm^{-1} were observed for the fortified samples compared to the control.

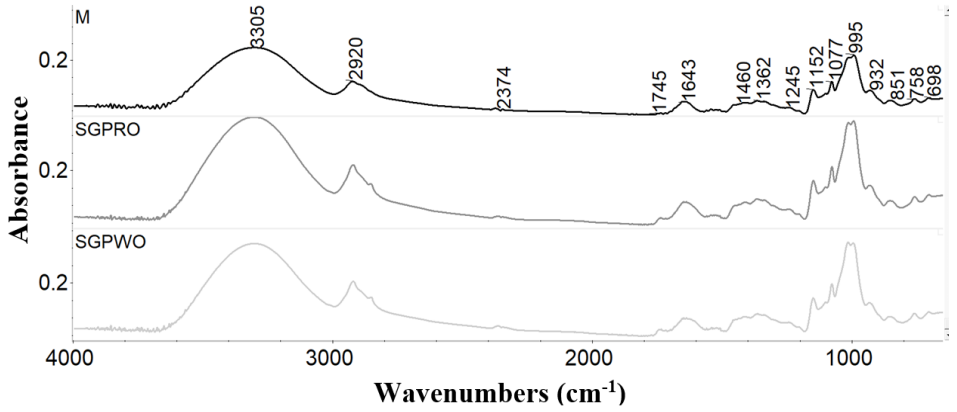

Figure 8. FT-IR spectra for extruded corn snacks with white seedless grape pomace (SGPWO) and red seedless grape pomace (SGPRO) *vs.* control (C)

The peak at 3305 cm^{-1} corresponds to the -OH stretching vibration, while the peaks at 2920 cm^{-1} correspond to the C-H stretching vibration (Zhao et al., 2015). The stretching vibration of C=O give the peak at 1745 cm^{-1}, while the peak at 1643 cm^{-1} was assigned to aromatic CH bonds (Zhao et al., 2015). The peak at 1077 could be related to the C-O stretching vibration of fibers (Singha et al., 2019). The protein band (1700–1600 and 1570–1534 cm^{-1}) was observed at 1745 cm^{-1}. The presence of a peak at 1745 cm^{-1} may be due to the pectin content in enriched samples, which were supplemented with seedless grape pomace (Amador-Rodríguez et al., 2019). C-O and C-C stretching of xyloglucan could give the peak at 1077 cm^{-1} (Amador-Rodríguez et al., 2019).

The nutritional profile of the fortified snacks compared to the control are showed in Table 3. It can be observed that the amount of nutrients (protein, ash, lipids, and fiber) increased significantly after grape pomace addition.

Table 3

Nutritional profile of extruded corn snacks with white seedless grape pomace (SGPWO) and red seedless grape pomace (SGPRO) *vs.* control (C)

Sample	SGPWO	SGPRO	C
Protein (% d.b.)	8.78 ± 0.03^{b}	9.58 ± 0.02^{a}	7.61 ± 0.02^{c}
Ash (% d.b.)	1.63 ± 0.01^{a}	1.34 ± 0.01^{b}	0.45 ± 0.01^{c}
Moisture (% d.b.)	6.57 ± 0.01^{c}	8.02 ± 0.02^{b}	8.33 ± 0.02^{a}
Lipids (% d.b.)	1.48 ± 0.05^{b}	1.70 ± 0.06^{a}	0.35 ± 0.07^{c}
Fiber (% d.b.)	17.08 ± 0.03^{a}	10.67 ± 0.14^{b}	0.46 ± 0.19^{c}
AA DPPH (%)	93.68 ± 0.10^{a}	91.73 ± 0.10^{b}	38.04 ± 0.10^{c}

Mean values followed by different letters in the same row are significantly different ($p < 0.05$)

The extruded corn snacks with red seedless grape pomace (SGPRO) presented higher protein and lipids content, while the extruded corn snacks with white seedless grape pomace (SGPWO) exhibited the greatest ash and fiber content. Significanlty higher ($p < 0.05$) antiradical activity was observed in the snacks with SGPWO presenting the greatest value. Drozdz et al. (2014) also reported higher antioxidant activity when corn snacks were enriched with apple and rosehip pomaces. Similar increase in protein, ash, fiber and protein content was reported for corn-based snacks with grape pomace (Yu et al., 2018) due to the intake of nutrients from the ingredients incorporated.

Conclusions

Seedless grape pomace can be incorporated in food formulations to increase the fiber and nutrients content. The suitability of this ingredient for the production of corn snacks at the recommended levels of 30% for the white variety and 20% for the red variety has been demonstrated without significant adverse effects on the quality and acceptability of the final product. The enriched snacks presented higher nutrients content, antioxidant activity and they were richer in some polyphenols like luteolin, quercetin, and myricetin compared to control, depending on the grape variety used. Even if the incorporation of seedless grape pomace determined the reduction of porosity, L*, texture parameters including crispness, and functional properties as the addition level increased, at the recommended doses the quality of the snacks is acceptable and the nutritional benefits are superior. In conclusion, seedless grape pomace is a promising ingredient for the development of new ready to eat healthy food like extruded snacks, with simultaneous benefits for environment protection.

Patent. The results were first used in a patent application entitled "Process for obtaining an extruded non-gluten product, direct-expanded and product so obtained", no. 24464010.8/ep24464010 from 14.11.2024 (“Procedeu de obţinere a unui produs aglutenic extrudat, direct-expandat şi produs astfel obţinut” no. a/00678 from 07.11.2024).

Acknowledgment. This work was supported by a grant of the Ministry of Research, Innovation and Digitization, CNCS - UEFISCDI, project number PN-III-P4-PCE-2021-0718, within PNCDI III.

References

Al-Hilphy A.R., Ali H.I., Al-IEssa S.A., Gavahian M., Mousavi-Khaneghah A. (2022), Assessing compositional and quality parameters of unconcentrated and refractive window concentrated milk based on color components, *Dairy*, 3(2), pp. 400–412, https://doi.org/10.3390/dairy3020030

Almanza-Oliveros A., Bautista-Hernández I., Castro-López C., Aguilar-Zárate P., Meza-Carranco Z., Rojas R., Michel M.R., Martínez-Ávila G.C.G. (2024), Grape pomace—Advances in its bioactivity, health benefits, and food applications, *Foods*, 13(4), 580, https://doi.org/10.3390/foods13040580

Altan A., McCarthy K. L., Maskan M. (2008), Evaluation of snack foods from barley-tomato pomace blends by extrusion processing, *Journal of Food Engineering*, 84(2), pp. 231–242, https://doi.org/10.1016/j.jfoodeng.2007.05.014

Amador-Rodríguez K.Y., Silos-Espino H., Valera-Montero L.L., Perales-Segovia C., Flores-Benítez S., Martínez-Bustos F. (2019), Physico-chemical, thermal, and rheological properties of nixtamalized creole corn flours produced by high-energy milling, *Food Chemistry*, 283, pp. 481–488, https://doi.org/10.1016/j.foodchem.2019.01.044

Andrade M.A., Lima V., Silva, A.S., Vilarinho F., Castilho M.C., Khwaldia K., Ramos F. (2019). Pomegranate and grape by-products and their active compounds: are they a valuable source for food applications? *Trends in Food Science & Technology*, 86, pp. 68-84, https://doi.org/10.1016/j.tifs.2019.02.010

Baroi A.M., Popitiu M., Fierascu I., Sărdărescu I.D., Fierascu R.C. (2022), Grapevine wastes: A rich source of antioxidants and other biologically active compounds, *Antioxidants*, 11(2), 393, https://doi.org/10.3390/antiox11020393

Batariuc A., Coțovanu I., Mironeasa S. (2023), Sorghum flour features related to dry heat treatment and milling, *Foods*, 12(11), 2248, https://doi.org/10.3390/foods12112248

Beres C., Costa G.N.S., Cabezudo I., da Silva-James N.K., Teles A.S.C., Cruz A.P.G., Mellinger-Silva C., Tonon R.V, Cabral L.M.C., Freitas S.P. (2017), Towards integral utilization of grape pomace from winemaking process: A review, *Waste Management*, 68, pp. 581–594, https://doi.org/10.1016/j.wasman.2017.07.017

Bordiga M., Travaglia F., Locatelli M. (2019), Valorisation of grape pomace: An approach that is increasingly reaching its maturity – a review, *International Journal of Food Science and Technology*, 54(4), pp. 933–942, https://doi.org/10.1111/ijfs.14118

Dangal R. (2023), Optimization of single screw extrusion processing variables of brewing spent grain, soy flour, rice flour and cranberry pomace blend extrudates on the physical and sensory properties of an extrudates, MS thesis, University of Wisconsin-Stout, USA, Available online: at 03 November, 2024: https://minds.wisconsin.edu/bitstream/handle/1793/84991/2023dangalr.pdf?sequence=1&isAllowed=y

Deng Q., Penner M.H., Zhao Y. (2011), Chemical composition of dietary fiber and polyphenols of five different varieties of wine grape pomace skins, *Food Research International*, 44(9), pp. 2712–2720, https://doi.org/10.1016/j.foodres.2011.05.026

Ding Q.B., Ainsworth P., Tucker G., Marson H. (2005), The effect of extrusion conditions on the physicochemical properties and sensory characteristics of rice-based expanded snacks, *Journal of Food Engineering*, 66(3), pp. 283–289, https://doi.org/10.1016/j.jfoodeng.2004.03.019

Drozdz W., Tomaszewska-Ciosk E., Zdybel E., Boruczkowska H., Boruczkowski T., Regiec P. (2014), Effect of apple and rosehip pomaces on colour, total phenolics and antioxidant activity of corn extruded snacks, *Polish Journal of Chemical Technology*, 16(3), pp. 7–11, https://doi.org/10.2478/pjct-2014-0042

Dwyer K., Hosseinian F., Rod M. (2014), The market potential of grape waste alternatives, *Journal of Food Research*, 3, 91, https://doi.org/10.5539/jfr.v3n2p91

Gomes T.M., Toaldo I.M., Haas I.C. da S., Burin V.M., Caliari V., Luna A. S., de Gois J.S., Bordignon-Luiz M.T. (2019), Differential contribution of grape peel, pulp, and seed to bioaccessibility of micronutrients and major polyphenolic compounds of red and white grapes through simulated human digestion, *Journal of Functional Foods*, 52, pp. 699–708, https://doi.org/10.1016/j.jff.2018.11.051

Gómez-Brandón M., Lores M., Insam H., Domínguez J. (2019), Strategies for recycling and valorization of grape marc, *Critical Reviews in Biotechnology*, 39(4), pp. 437–450, https://doi.org/10.1080/07388551.2018.1555514

Grevtseva N., Gorodyska O., Brykova T., Gubsky S. (2023), The use of wine waste as a source of biologically active substances in confectionery technologies. In: O. Stabnikova, O. Shevchenko, V. Stabnikov, O. Paredes-López (Eds.), *Bioconversion of Waste to Value-Added Products*, CRC Press, Boca Raton, London, pp. 69-111, https://doi.org/10.1201/9781003225287-3

Gualberto D.G., Bergman C.J., Kazemzadeh M., Weber C.W. (1997), Effect of extrusion processing on the soluble and insoluble fiber, and phytic acid contents of cereal brans, *Plant Foods for Human Nutrition*, 51, pp. 187–198, https://doi.org/10.1023/A:1007941032726

Gumul D., Berski W., Zięba T. (2023), The influence of fruit pomaces on nutritional, pro-health value and quality of extruded gluten-free snacks, *Applied Sciences (Switzerland)*, 13(8), 4818, https://doi.org/10.3390/app13084818

Ivanov V., Shevchenko O., Marynin A., Stabnikov V., Gubenia O., Stabnikova O., Shevchenko A., Gavva O., Saliuk A. (2021), Trends and expected benefits of the breaking edge food technologies in 2021–2030, *Ukrainian Food Journal*, 10(1), pp. 7–36, https://doi.org/10.24263/2304-974X-2021-10-1-3

Kammerer D., Claus A., Carle R., Schieber A. (2004), Polyphenol screening of pomace from red and white grape varieties (*Vitis vinifera* L.) by HPLC-DAD-MS/MS, *Journal of Agricultural and Food Chemistry*, 52(14), pp. 4360–4367, https://doi.org/10.1021/jf049613b

Karkle E.L., Alavi S., Dogan H. (2012), Cellular architecture and its relationship with mechanical properties in expanded extrudates containing apple pomace, *Food Research International*, 46(1), pp. 10–21, https://doi.org/10.1016/j.foodres.2011.11.003

Llobera A., Cañellas J. (2008), Antioxidant activity and dietary fibre of Prensal Blanc white grape (*Vitis vinifera*) by-products, *International Journal of Food Science and Technology*, 43(11), pp. 1953–1959, https://doi.org/10.1111/j.1365-2621.2008.01798.x

Lohinova A., Petrusha O. (2023), Maillard reaction in food technologies, *Ukrainian Journal of Food Science*, 11(2), pp. 81–109, https://doi.org/10.24263/2310-1008-2023-11-2-4

Lund D. (1984), Influence of time, temperature, moisture, ingredients, and processing conditions on starch gelatinization, *Critical Reviews in Food Science and Nutrition*, 20(4), pp. 249–273, https://doi.org/10.1080/10408398409527391

Nogales-Bueno J., Baca-Bocanegra B., Rooney A., Hernández-Hierro J.M., Byrne H.J., Heredia F.J. (2017), Study of phenolic extractability in grape seeds by means of ATR-FTIR and Raman spectroscopy, *Food Chemistry*, 232, pp. 602–609, https://doi.org/10.1016/j.foodchem.2017.04.049

Oliveira M., Teixeira B.M.M., Toste R., Borges A.D.S. (2024), Transforming wine by-products into energy: Evaluating grape pomace and distillation stillage for biomass pellet production, *Applied Sciences*, 14(16), 7313, https://doi.org/10.3390/app14167313

Paraman I., Sharif M.K., Supriyadi S., Rizvi S.S.H. (2015), Agro-food industry byproducts into value-added extruded foods, *Food and Bioproducts Processing*, 96, pp. 78–85, https://doi.org/10.1016/j.fbp.2015.07.003

Poliszko N., Kowalczewski P. Ł., Rybicka I., Kubiak P., Poliszko S. (2019), The effect of pumpkin flour on quality and acoustic properties of extruded corn snacks, *Journal Fur Verbraucherschutz Und Lebensmittelsicherheit*, 14(2), pp. 121–129, https://doi.org/10.1007/s00003-019-01216-6

Raleng A., Singh A., Singh B., Attkan A.K. (2016), Response surface methodology for development and characterization of extruded snack developed from food-by-products, *International Journal of Bio-Resource and Stress Management*, 7(6), pp. 1321–1329, https://doi.org/10.23910/IJBSM/2016.7.6.1691a

Raleng A., Singh N. G. J., Chavan P., Attkan A.K. (2022), Opportunities in valorisation of industrial food waste into extruded snack products - A review, *Indian Journal of*

Agricultural Sciences, 92(12), pp. 1167–1174, https://doi.org/10.56093/ijas.v92i10.113487

Rathod R.P., Annapure U.S. (2017), Antioxidant activity and polyphenolic compound stability of lentil-orange peel powder blend in an extrusion process, *Journal of Food Science and Technology*, 54(4), pp. 954–963, https://doi.org/ 10.1007/s13197-016-2383-9

Reinaldo J.S., Milfont C.H.R., Gomes F.P.C., Mattos A.L.A., Medeiros F.G.M., Lopes P.F.N., Filho M. de sá M.S., Matsui K.N., Ito E.N. (2021), Influence of grape and acerola residues on the antioxidant, physicochemical and mechanical properties of cassava starch biocomposites, *Polymer Testing*, 93, 107015, https://doi.org/10.1016/j.polymertesting.2020.107015

Różańska-Boczula M., Wójtowicz A., Piszcz M., Soja J., Lewko P., Ignaciuk S., Milanowski, M., Kupryaniuk, K., Kasprzak-Drozd, K. (2023), Corn-based gluten-free snacks supplemented with various dried fruits: characteristics of physical properties and effect of variables, *Applied Sciences (Switzerland)*, 13(19), 10678, https://doi.org/10.3390/app131910678

Sagar N.A., Pareek S., Sharma S., Yahia E.M., Lobo M.G. (2018), Fruit and vegetable waste: Bioactive compounds, their extraction, and possible utilization, *Comprehensive Reviews in Food Science and Food Safety*, 17(3), pp. 512–531, https://doi.org/10.1111/1541-4337.12330

Singha P., Singh S.K., Muthukumarappan K. (2019), Textural and structural characterization of extrudates from apple pomace, defatted soy flour and corn grits, *Journal of Food Process Engineering*, 42(4), e13046, https://doi.org/10.1111/jfpe.13046

Soja J., Combrzyński M., Oniszczuk T., Gancarz M., Oniszczuk A. (2024), Extrusion-cooking aspects and physical characteristics of snacks pellets with addition of selected plant pomace, *Applied Sciences*, 14(19), 8754, https://doi.org/10.3390/app14198754

Sozer N., Poutanen K. (2013), Fibre in extruded products, In: J.A. Delcour, K. Poutanen (Eds.), *Fibre-Rich and Wholegrain Foods*, Woodhead, pp. 256–272, https://doi.org/10.1533/9780857095787.3.256

Squillaci G., Zannella C., Carbone V., Minasi P., Folliero V., Stelitano D., La Cara F., Galdiero M., Franci G., and Morana A. (2021), Grape canes from typical cultivars of Campania (Southern Italy) as a source of high-value bioactive compounds: Phenolic profile, antioxidant and antimicrobial activities, *Molecules*, 26(9), 2746, https://doi.org/10.3390/molecules26092746

Stabnikova O., Marinin A., Stabnikov V. (2021), Main trends in application of novel natural additives for food production, *Ukrainian Food Journal*, 10(3), pp. 524–551, https://doi.org/10.24263/2304-974X-2021-10-3-8

Stabnikova O., Shevchenko A., Stabnikov V., Paredes-López O. (2023), Utilization of plant processing wastes for enrichment of bakery and confectionery products, *Ukrainian Food Journal*, 12(2), pp. 299-308, https://doi.org/10.24263/2304-974X-2023-12-2-11

Stabnikova O., Paredes-Lopez O. (2024), Plant materials for the production of functional foods for weight management and obesity prevention, *Current Nutrition & Food Science*, 20(4), pp. 401–422, https://doi.org/10.2174/1573401319666230705110854

Statista (2023), Global fruit production in 2021, by selected variety, Accessed on March 10, 2024,https://www.statista.com/statistics/264001/worldwide-production-of-fruit-byvariety

Stojceska V., Ainsworth P., Plunkett A., İbanoğlu Ş. (2010), The advantage of using extrusion processing for increasing dietary fibre level in gluten-free products, *Food Chemistry*, 121(1), pp. 156–164, https://doi.org/10.1016/j.foodchem.2009.12.024

Troilo M., Difonzo G., Paradiso V.M., Pasqualone A., Caponio F. (2022), Grape pomace as innovative flour for the formulation of functional muffins: How particle size affects the nutritional, textural and sensory properties, *Foods*, 11(12), 1799, https://doi.org/10.3390/foods11121799

Valiente C., Arrigoni E., Esteban R.M., Amado R. (1995), Grape pomace as a potential food fiber, *Journal of Food Science*, 60(4), pp. 818–820, https://doi.org/10.1111/j.1365-2621.1995.tb06237.x

Yağci S., Göğüş F. (2008), Response surface methodology for evaluation of physical and functional properties of extruded snack foods developed from food-by-products, *Journal of Food Engineering*, 86(1), pp. 122–132, https://doi.org/10.1016/j.jfoodeng.2007.09.018

Yıldırım H.K., Akçay Y.D., Güvenç U., Altındişli A., Sözmen E.Y. (2005), Antioxidant activities of organic grape, pomace, juice, must, wine and their correlation with phenolic content, *International Journal of Food Science and Technology*, 40(2), pp. 133–142, https://doi.org/10.1111/j.1365-2621.2004.00921.x

Yu J., Ahmedna M. (2013), Functional components of grape pomace: Their composition, biological properties and potential applications, *International Journal of Food Science and Technology*, 48(2), pp. 221–237, https://doi.org/10.1111/j.1365-2621.2012.03197.x

Yu J., Smith I.N., Chen G. (2018), Influence of grape pomace inclusion on physical and chemical properties of corn-based extrudates, *SDRP Journal of Food Science and Technology*, *3*(6), pp. 516–526, https://doi.org/10.25177/jfst.3.6.4

Zhai H., Ling M., Li S., Chen B., Zhao X., Tong W., Cheng C., Li J., Shi Y., Duan C. (2024), The characteristics of polysaccharide composition of red wines in China: Effects of grape varieties, origins and winemaking techniques, *Food Chemistry: X*, 22, 101283, https://doi.org/10.1016/j.fochx.2024.101283

Zhao X., Zhu H., Zhang G., Tang W. (2015), Effect of superfine grinding on the physicochemical properties and antioxidant activity of red grape pomace powders, *Powder Technology*, 286, pp. 838–844, https://doi.org/10.1016/j.powtec.2015.09.025

Cite:

UFJ Style

Mironeasa S., Ungureanu-Iuga M., Ursachi V.F., Mironeasa C. (2024), Seedless grape pomace to increase fiber content in extruded corn snacks, *Ukrainian Food Journal*, 13(4), pp. 657–674, https://doi.org/10.24263/2304-974X-2024-13-4-3

APA Style

Mironeasa, S., Ungureanu-Iuga, M., Ursachi, V.F., & Mironeasa, C. (2024). Seedless grape pomace to increase fiber content in extruded corn snacks. *Ukrainian Food Journal*, *13*(4), 657–674. https://doi.org/10.24263/2304-974X-2024-13-4-3

Improvement of alcohol distillation plant operation

Yurii Bulii

National University of Food Technologies, Kyiv, Ukraine

Keywords:

Alcohol
Distillation
Rectification
Impurities
Hydroselection

Article history:

Received 22.03.2024
Received in revised form 20.09.2024
Accepted 30.12.2024

Corresponding author:

Yurii Bulii
E-mail: yvbuliy@gmail.com

DOI:
10.24263/2304-974X-2024-13-4-4

Abstract

Introduction. The criteria for improving the operation of distillation plant include the degree of purification of rectified alcohol from impurities, the consumption of vapor, hot process water for hydroselection, and cooling water.

Materials and methods. The object of the study was the distillation plant equipped with columns of cyclic action. The concentration of volatile impurities was determined by the chromatographic method, degree of extraction and the multiplicity of concentration was determined by the calculation method, the flow rates of water, distillation residue and alcohol-containing vapor by using flow meters.

Results and discussion. Extending the residence time of the liquid on the plates of the impurity concentration column to 40 s ensures the complete removal of esters, methyl acetate and isopropyl alcohol, to increase the degree of extraction of higher alcohols of fusel oil and methanol by 38 %, to increase the multiplicity of concentration of the head impurities by 25 %, the upper intermediate and final impurities by 38 % and to reduce the consumption of heating vapor by 40 %. Reduction of the ethanol concentration in the epyurate to 25 % vol. allows fully removing esters, reducing the concentration of aldehydes and fusel oil in the epyurate by 43% and isopropyl alcohol by 62%. Through the recirculation of the distillation residues of the rectification column, impurity concentration column and the extractive rectification column, the specific consumption of water and the energy required for her heating are reduced by 80%. Feeding alcohol-containing fractions in the form of vapor to the impurity concentration column for 2% allows reducing water consumption for cooling by 2.1%, and heating vapor by 1.4%. With an increase in the amounts of non-condensable alcohol vapor from 2 to 5%, water consumption decreases by 5.1%, and heating steam by 1.9%.

Conclusion. The research results can be used to improve the operation of distillation plant by reducing the consumption of heating vapor, process water and water for cooling heat-exchange equipment.

Introduction

For the further development of the alcohol industry, the priority direction is the optimization of the operation of distillation plants (DP) by the development and implementation of resource- and energy-saving technologies (Shiyan et al., 2009). When using traditional methods of purification of alcohol from impurities in typical DP, some of them usually remain present in small quantities in commercial alcohol. For their more complete removal modern installations are retrofitted with an impurity concentration column, final purification, and extractive rectification columns, hydroselection of volatile impurities is carried out (Jacimovic et al., 2014; Tsygankov, 2010). The use of rational technological and design solutions allows to increase the degree of extraction and the multiplicity of concentration of the impurities, thereby improving the quality indicators of rectified alcohol, reducing the specific consumption of water and vapor, as well as increasing the yield of the finished product (Botshekan et al., 2022).

A relatively new and promising approach to solving the problem of optimizing the operation of the DP is the use of cyclic rectification technology (Andersen et al., 2018; Bedryk et al., 2023). Under the above conditions increase the driving force of the process of mass-exchange between liquid and vapor (Lita et al., 2014), increases the efficiency of plates operation and the specific consumption of heating vapor decreases (Chenyang et al., 2024; Kiss, 2014). Research in this direction began in the 60-70s of the twentieth century (Bastian et al., 2018; Nielsen et al., 2017), but due to the complexity of technical solutions installations did not find wide practical use (Rasmussen et al., 2020; Toftegard et al., 2016).

At the National University of Food Technologies (Ukraine), a design of column apparatuses has been developed, the operation of which allows increasing the contact time of steam and liquid until the phases reach a state close to equilibrium, and brings the efficiency of each physical plate closer to the efficiency of a theoretical plate (patent UA 141245. Method of liquid pouring through plates of a column mass-exchange apparatus; patent UA 139228. Column mass-exchange apparatus of cyclic action). On real plates such an equilibrium is rarely achieved. One of the good reasons for this is the short period of time that the contacting phases stay on the plate. To implement the method, the distillation column was equipped with plates with a variable free section, the movable segments of which were connected to mechatronic subsystems (Bulii et al., 2021). In the cyclic mode increases the driving force of the mass-exchange process and the efficiency of contact devices significantly (Flodman et al., 2012; Zhang et al., 2017).

One of the ways to optimize the work of the DP is carrying out of hydroselection of impurities. To increase the rectification coefficients of the head impurities of alcohol and the maximum removal of isopropanol hydroselection is carried out in the ether column (Linek et al., 2005). To do this the concentration of ethyl alcohol in the epyurate is reduced from 45–55 to 20–30 % vol. by supplying hot softened water or condensate of vapor to the upper plate of the column. Water consumption is 0.55-0.90 kg/kg of anhydrous alcohol (a.a.) introduced into the column. For extraction of head and upper intermediate impurities (fusel alcohol) in the impurity concentration column the concentration of distillation residue is maintained within 4–4.5 % vol., for the extraction of lower intermediate impurities (higher alcohols of fusel oil) in the extractive rectification column should not exceed 1.5–3.0 % vol. (Shiyan et al., 2009).

The disadvantages of the known methods are the increased consumption of process water and vapor for heating it (Nagy et al., 2015). To eliminate these shortcomings it is proposed an innovative technology (Bulii et al., 2021), the peculiarity of which is the recirculation of distillation residues of rectification column, impurity concentration column

and extractive rectification column for hydroselection of impurities (patent UA 116733. Method of obtaining rectified alcohol).

The operation of heat exchange equipment is an important component of the functioning of a distillation plant (Jacimovic et al., 2014; Pinto et al., 2011). From practical experience, it is known that the thermal load on the condensers of the ether and rectification columns, impurity concentration column and final purification column is insignificant: 0.5-2% of the vapor condenses in them (Tsygankov, 2010). Known methods provide for the supply of alcohol-containing intermediates and by-products in columns from condensers in the form condensate of vapor with a temperature of 25-30 °C (Matsuda et al., 2011; Mischenko et al., 2020). For the effective isolation and concentration of impurities of alcohol a prerequisite is additional heat costs for heating them to a temperature of 75-80 °C, as well as an increase in the consumption of heating vapor by 28.7 % (Shiyan et al., 2009).

To the optimize the operation of heat exchange equipment by reducing consumption vapor and water for cooling, a promising direction is the organization of supplying the columns with alcohol-containing vapor that has not condensed in dephlegmators (Sheikus, 2019; Simon et al., 2009). It has developed an innovative energy-saving technology, which provides for the supply of the impurity concentration column with alcohol-containing fractions in a vaporous state (patent UA 126533. Method for obtaining rectified alcohol). The technical solution allows for to reduction of the specific consumption of heating vapor, cooling water and the cost of installation due to the absence of condensers in the technological scheme.

The aim of research was to study the effectiveness of innovative ways to improve the operation of distillation plant: carrying out the processing of alcohol-containing fractions and epuration of beer distillate in cyclic mode, the recirculation of distillation residue of rectification and ether columns, impurity concentration column and extractive rectification column, as well as of the method which provides for the supply to the impurity concentration column of power in a vaporous state.

Research objectives were as follows:

1. To determine the degree of extraction, multiplicity of concentrating of volatile alcohol impurities and consumption of heating vapor in the impurity concentration column and ether column of cyclic action.
2. To determine the specific and total consumption of process water and energy costs for its heating for hydroselection in the ether column, impurity concentration and extractive rectification columns when the recirculation of their distillation residues.
3. To determine the water consumption for cooling of dephlegmators of distillation, ether, rectification and impurity concentration columns and vapor consumption for heating them in case of supplying the impurity concentration column with alcohol-containing vapors.

Materials and methods

Research objects

1. Experimental ether column (EC) and impurity concentration column (ICC) of cyclic action

To conduct research in the production conditions of the «Storonibabsky distillery» (Ukraine) an experimental EC with a diameter of 1200 mm and ICC with a diameter of 950

mm where installed of cyclic action (Figure 1). The EC contained 35 scaly plates, the distance between which was 300 mm. The ICC contained 30 scaly plates. In terms of design features the ICC did not differ from the EC.

The rotary segments of the plates were connected to standard double-acting pneumatic cylinders, the action of which took place in accordance with the controller's program. The movable segments opened and closed the overflow holes of the plates according to a given algorithm in such a way that the liquid synchronously overflowed through the formed overflow hole and all the holes of the plates (patent UA 124733. Column mass-exchange apparatus of cyclic action; patent UA 123918. Mass-exchange contact plate).

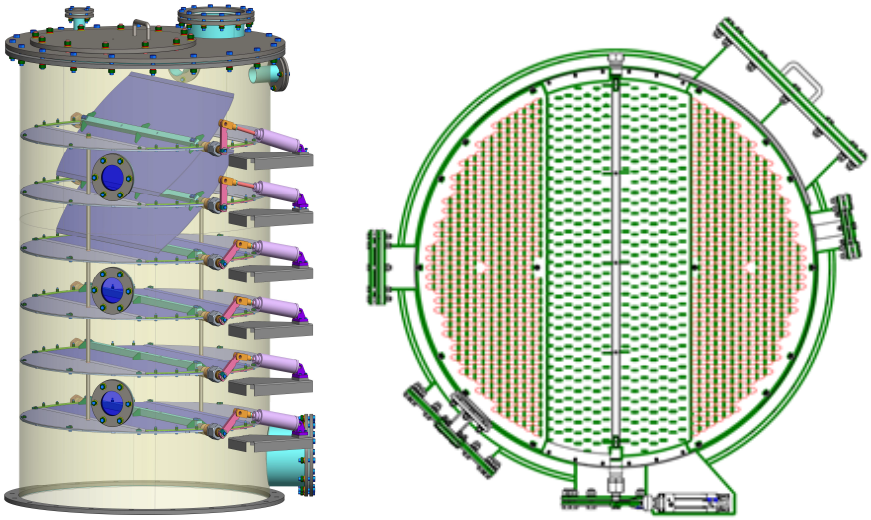

Figure 1. Fragment of an experimental column of cyclic action

3. Distillation plant (DP) with recirculation of distillation residues of rectification column, impurity concentration column (ICC) and extractive rectification column

Studies of the effectiveness of innovative technology with the recycling of distillation residue for hydroselection of alcohol impurities were carried out in the production conditions of the «Chudniv Distillery» (Ukraine). The technological scheme of resource- and energy-saving DP is presented in Figure 2.

The installation included distillation, ether and rectification column, an impurity concentration, extractive rectification, final purification columns and appropriate heat exchange equipment. To heat the columns heating vapor (HV) was supplied to their bottoms parts. Vapor condensate (C) was removed from the evaporators.

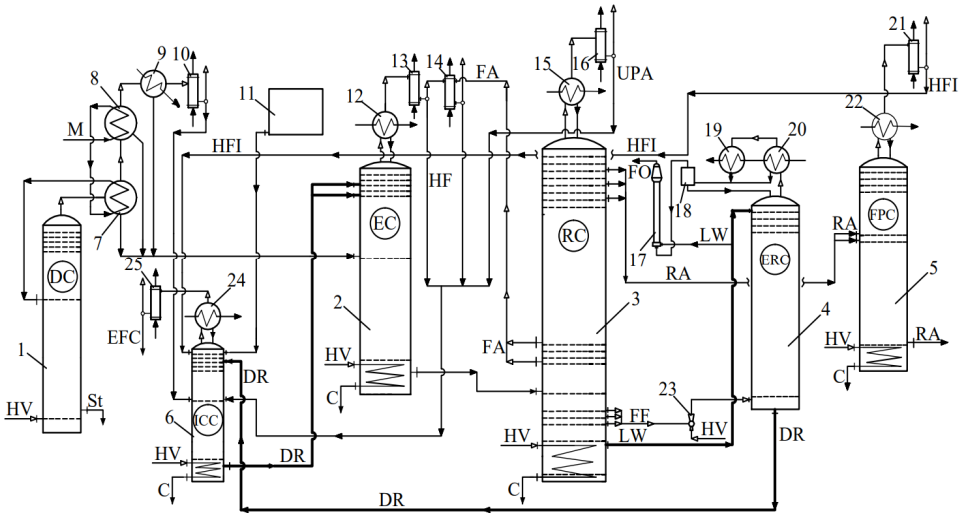

Figure 2. Resource- and energy-saving of distillation plant (DP) with distillation residues recirculation

1- distillation column (DC), 2 – ether column (EC), 3 – rectification column (RC), 4 – extractive rectification column (ERC), 5 – final purification column (FPC), 6 – impurity concentration column (ICC); 7, 8 – beer heaters; 9 – water section of the beer heater; 10, 13, 16, 19, 21, 25 – condensers; 12, 15, 20, 22, 24 – dephlegmators; 11 – pressure collector of hot softened water; 14 – fusel alcohol condenser; 17 – fusel oil extractor; 18 – decanter; 23 – vapor ejector.

Symbols: M – beer; St – stillage; HV – heating vapor; HF– head fraction of ethyl alcohol; LW – luther water; FO – fusel oil; FF – fusel fraction; RA – rectified alcohol; FA – fusel alcohol; EFC – ester-fusel concentrate; UPA – unpasteurized alcohol; C – condensate; HFI – head and final impurities; DR – distillation residue.

The beer (M) was sequentially fed through the second **8** and first **7** sections of the beer heater, in which it was heated with water-alcoholic vapor of the distillation column **1** to a temperature close to the boiling point and then directed to the upper plate of the distillation column, in which alcohol and related organic impurities were extracted. The beer distillate from the beer heaters **7** and **8** and the water section of the heater **9** was supplied to the feeding plate of the EC **2** and the vapor condensate from the condenser **10** to the feeding plate of the ICC **6**. From the bottom part of the column **1** stillage was removed. Concentration and extraction of the head and part of the intermediate impurities of alcohol were carried out in the EC **2**. For this purpose, distillation residue from the ICC **6** was supplied to the upper zone of its concentration part.

Concentrated impurities in the form of the head fraction of ethyl alcohol (HF) were taken from the condenser **13**. Fusel alcohol (FA) was taken from the vapor phase of 18-23rd plates of the rectification column **3** were fed into the interpipe space of the condenser **14** and after condensation of the vapor was removed from the unit together with the HF. The fusel fraction (FF) was taken from the vapor phase of the **5, 7, 9**, and **11**th plates of the rectification column **3**. In the upper pasteurization part of this column the concentration of the head impurities was carried out, which were not fully removed in EC **2.** These impurities in the form of unpasteurized alcohol (UPA) were discharged through condenser **16** together with HF from condenser **13**, fractions from condenser **10** and **14** to the feeding plate of the ICC **6.**

Rectified alcohol (RA) was taken from the liquid phase of the upper plates of column **3**, which then went to the feeding plate of the final purification column **5**. Its upper part was connected to the dephlegmator **22** and the condenser **21**. In column **5** alcohol was purified from the head and final impurities (HFI) were taken from condenser **21** and then directed to the upper plate of column **6**. Commercial rectified alcohol was taken from the bottom part of the column **5**. Vapors of the FF were mixed with heating vapor in ejector **23** and fed into the bottom part of the extractive rectification column **4**. Hot luther water (LW) from the bottom part of the rectification column **3** was supplied to its upper plate. In column **4** fusel oil (FO) alcohols were extracted and concentrated. The condensate of FO vapors from the dephlegmator **20** and condenser **19** was directed to the decanter **18**, in which the mixture was delaminated: the liquid from the bottom part of the decanter **18** was returned in the form of reflux to the upper plate of column **4** and the FO was sent to the extractor **17**. LW was supplied to the bottom part of the extractor to flush the oil. Concentrated of FO in the form of a marketable product was taken from the upper part of the extractor **17**.

Distillation residue (DR) of column **4** was supplied to 3-5th plate, counting from above, of the ICC **6** for hydroselection of intermediate impurities, including fusel oil components, and their concentration. In the process of separation of alcohol-containing fractions in column **6**, reflux was returned from the dephlegmator **24** to her upper plate, and ester-fusel concentrate (EFC) was taken from condenser **25**. To carry out hydroselection in the EC **2** in the upper zone of its concentration part the distillation residue purified from head and part of intermediate impurities from the ICC **6** was fed to the upper zone of its concentration part.

3. Distillation plant (DP) with feeding of impurity concentration column with alcohol-containing fractions in form of vapour

In the production conditions of the «Chudniv Distillery» the reconstruction of the existing indirect action DP equipped with the ICC was carried out. The technological scheme of the installation after its reconstruction is presented in Figure 3.

The operation of the unit was as follows. The matured alcohol beer (M) entered the beer heater **3**, in which it was heated with water-alcoholic vapor from distillation column (DC) **2** to a temperature of 70-85 °C, then into separator **1** to get rid of carbon dioxide and other non-condensed gases, after which it entered the DC **2** feeding plate. In separator **1** together with non-condensed gases a certain amount of alcohol was carried out. To extract it vapor from the upper part of the separator **1** was directed to the concentration part of the ICC **11** through a flow meter FIT4 and an analog damper VGA4. Heating vapor (HV) was continuously supplied to the bottom parts of DC **2**, EC **5**, rectification column (RC) **7** and ICC **11.** From the bottom part of the DC **2** stillage freed from alcohol and volatile impurities was removed. Water was supplied to the pipes of the dephlegmators **4, 6, 8, 9, 13**, condenser **17** and alcohol trap **18** for cooling.

Condensate of water-alcoholic vapor from the heater **3** and the water section of the dephlegmator **4** was supplied to the upper part of the EC **5**. Freed from the head (esters and aldehydes), parts of the upper intermediate (higher alcohols of fusel oil) and final (methyl alcohol) impurities of alcohol beer distillate — epyurate (E) was supplied as a power supply to the RC **7**. Low-boiling vapors of the head fraction (HF) uncondensed in the dephlegmator **6** were directed through the flow meter FIT3 and analog damper VGA3 to the concentration part of the ICC **11.** In the RC **7** ethyl alcohol was purified from intermediate and final impurities and its concentration. Rectified (pasteurized) alcohol (RA) was taken from the 5th, 7th and 10th plates, counting the RC **7** from above.

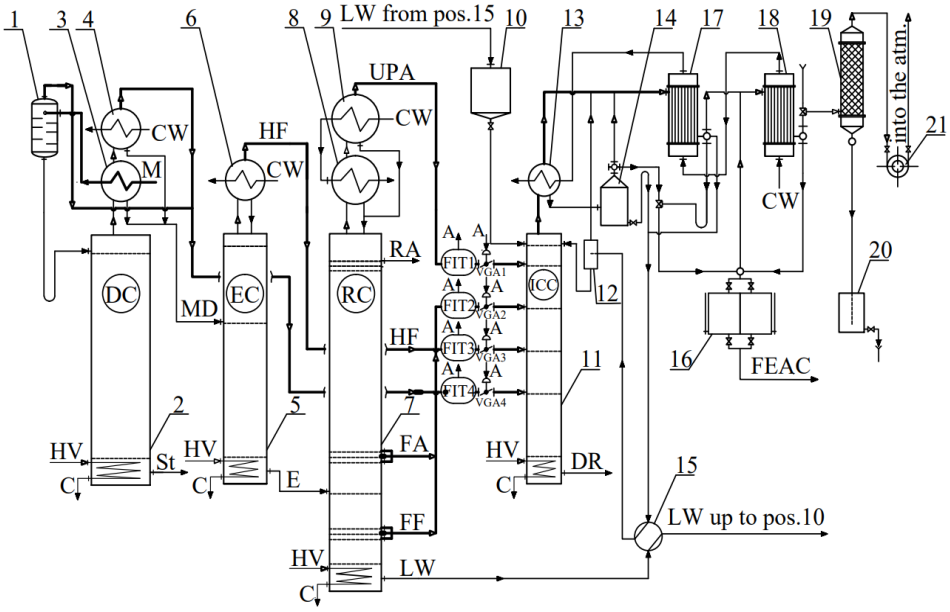

Figure 3. Resource- and energy-saving of distillation plant (DP) with feeding of the impurity concentration column alcohol-containing vapor

1 – carbon dioxide separator, 2 – distillation column (DC), 3 – beer heater, 4, 6, 8, 9, 13 – dephlegmators; 5 – ether column (EC); 7 – rectification column (RC); 10 – pressure collector of luther water, 11 – impurity concentration column (ICC), 12 – reflux separator, 14 – decanter; 15 – heat exchanger; 16 – collection of FEAC; 17 – upper stage condenser; 18 – alcohol trap; 19-barometric condenser; 20-barometric box; 21 – vacuum pump.

Symbols: M – beer; MD – beer distillate; St – stillage; CW – cooling water; E – epyurate; HF– head fraction of ethyl alcohol; HV – heating vapor; LW – luther water; FEAC – fusel-ester-aldehyde concentrate; FA – fusel alcohol; FF – fusel fraction; RA – rectified alcohol; DR – distillation residue; C – condensate; FIT – flow meter; VGA – analogue trap; A – analogue signal.

Intermediate impurities were removed from this column in the form of two products: fusel fraction (FF), which was taken from the vapor space of the 5, 7, 9 and 11th plates, counting from the bottom of the column, and fusel alcohol (FA), which was taken from the vapor space 17-20th and 25th plates, counting from the bottom. To extract ethyl alcohol FF and FA vapors were directed to the concentration part of the ICC **11** through the flow meter FIT2 and the analog damper VGA2. Low-boiling water-alcoholic vapors enriched with main and final impurities that did not condense in dephlegmators **8** and **9** through the flow meter FIT1 and analog damper VGA1 was directed to the upper zone of the concentration part of the ICC **11.**

All flow meters and dampers were installed on the corresponding vapor pipelines. The dampers were controlled by an analog signal (A), which came from the controller. For the supply of non-condensed vapor from the separator **1**, dephlegmators **4, 6, 9** and FF and FA pairs to the ICC **11,** the pressure difference at the points of their selection and introduction into the column was 4.9–9.8 kPa (patent UA 126533. Method of obtaining rectified alcohol).

To ensure this mode, the ICC **11** operated under vacuum, which was maintained by means of a vacuum pump **21** and a barometric condenser **19** connected to a barometric box **20**. To carry out hydroselection the upper plate of the column **11** from the pressure collector **10** continuously received LW with a temperature of 90–95 °C in the amount that provided the concentration of alcohol in the distillation residue within 4–8 % vol. In the ICC **11** alcohol-containing vapors of by-products and intermediate products of rectification were divided into two streams: the upper one, enriched with the head (esters, aldehydes) and intermediate (higher alcohols of FF and FA, including C_3, C_4, C_5), alcohol impurities, and the lower one — distillation residue. The vapor, coming out of the upper part of the column, was condensed in the dephlegmator **13** and its condensate flowed by gravity into the decanter **14**. In the decanter, the heterogeneous mixture was delaminated into fusel-ester-aldehyde concentrate (FEAC), which was taken from the upper part of the decanter, and the lower layer enriched with water, which was directed to the upper plate of the column **11** in the form of reflux for irrigation. The reflux was preheated with LW heat in heat exchanger **15** to a temperature of 90-95 °C, which corresponded to the temperature at the upper plate of column **11**, and passed through separator **12** to separate gases. FEAC was taken in the amounts of 0.4-0.5% to the amount of alcohol introduced into DC **2**, and the distillation residue, freed from the head, intermediate and part of the final impurities, was continuously removed from the lower part of the ICC **11** and then fed to the upper plate of DC **2.** The water pressure in the working collector was 245 kPa and provided water supply to the dephlegmators and its required speed in the pipes. For calculations, the water temperature at the inlet to the dephlegmators was 20 °C, at the outlet – 70 °C.

Research methods

To evaluate the results of the research, analytical, chemical, physico-chemical and calculation methods were used using devices and methods used in the production of rectified ethyl alcohol.

Liquid consumption. The flow rates of alcohol-containing fractions, water, distillation residue, rectified alcohol and concentrate of impurities were monitored using constant differential pressure flow meters RM (Polulyah et al., 2012). The principle of their operation is based on the perception of the dynamic pressure of the controlled medium, which depends on the flow, by a sensing element (float) placed in the flow. Because of the flow action, the sensing element moved along the height of the flow meter, and the amount of displacement served as a measure of flow. The readings were taken on the scale of a flow meter graduated by water in l/h.

Vapor cost. The flow rate of alcohol-containing steam was determined using TVA flow meters from Spirax Sarco. Their principle of operation is based on the measurement of mechanical stress, which causes an instantaneous flow rate in the measuring cone in one direction. This voltage is converted into mass-compensated flow rate and transmitted through 4-20 mA outputs with a single-loop power supply. The TVA flow meter design provides high ranges of parameter changes and high measurement accuracy (Dattarajan et al., 2019).

Concentration of ethyl alcohol in water-alcohol solutions. The concentration of ethyl alcohol in the liquid distillation residue of the aldehyde concentrate was determined by areometric method (Polygalina, 1999). The test solution was poured into a 250 ml glass cylinder, the temperature was measured with a thermometer with a division price of 0.1 °C, and then the ASP-1 alcoholmeter was immersed. The actual concentration of ethyl alcohol at a temperature of 20 °C was determined from the readings of the alcoholmeter and using special tables to make appropriate corrections for temperature.

Concentration of volatile alcohol impurities. Concentration of aldehydes was determined by reaction with fuchsin-sulfur reagent I; fusel oil – by the method based on the reaction of higher alcohols with salicylic aldehyde solution in the presence of sulfuric acid; free acids – by the amount of sodium hydroxide solution used for titration; complex esters – by titrometric method after their saponification with sodium hydroxide solution; volume fraction of methyl alcohol – by method based on the reaction of methanol oxidation with potassium permanganate and sulfuric acid to form formaldehyde, which forms a color with fuchsin-sulfur reagent II (Arslan, 2021).

The concentration of head volatile impurities (aldehydes, higher alcohols of fusel oil, acrolein, isopropyl alcohol) in alcohol-containing fractions, distillation residue of impurity concentration column, concentrate of impurities and rectified ethyl alcohol was determined on a gas chromatograph with an HP FFAP 50 m × 0.32 m column (Dewulf, 2002; Plutowska et al., 2008). The analysis of the experimental samples was carried out three times. The average values were chosen as determinative.

Grade of extraction and concentration ratio of volatile alcohol impurities

The degree of extraction *(α)* and multiplicity of concentration *(β)* of key organic impurities of alcohol were calculated by the formulas:

$$\alpha = \frac{X_f}{X_{cl}}, \quad \beta = \frac{X_{seac}}{X_f},$$

where X_f, X_{seac}, X_{cl} – accordingly, the concentration of volatile alcohol impurities on the feed plate, fusel and ester-aldehyde concentrate and distillation residue, mg/l in terms of a.a. (Linek, 2005; Shiyan et al., 2009).

Research stages

At the first stage, the efficiency of the technology of epyuration of the beer distillate and separation of alcohol-containing fractions in the specified hydrodynamic modes in the EC and the ICC of stationary and cyclic action was investigated. To improve the process a mathematical model, a control program and a human-machine interface (SCADA) were developed. Beer distillate was fed to the *EC* feeding plate. For maximum release of the epyurate from the head and upper intermediate impurities, their hydroselection was carried out by supplying the upper plate of the column of distillation residue from the bottom part of the ICC, freed from impurities, in the amount of 240 dal/h. Under such conditions the concentration of ethyl alcohol in the epyurate decreased to 25 % vol. In the process of its epyuration the head impurities of alcohol were extracted and concentrated, which were taken from the condenser in the form of the head fraction in the amount of 5% of the amount of rectified alcohol. The epyurate freed from these impurities was fed to the 16th plate of the rectification column. The pressure in the bottom part of the EC was maintained within 11.3–11.8 kPa; the temperature in the bottom part was 100.5–101 °C and above the upper plate 93.5–94 °C.

The feed plate of the experimental ICC was fed with the head fraction of ethyl alcohol from the EC condenser and alcohol-containing fractions from the condensers of the distillation column, the carbon dioxide separator, fusel alcohol, fusel rinse water and distillates from the alcohol traps. The total number of feed fractions was 688.3 l/h (250 l/h in terms of a.a.). For hydroselection of impurities, hot softened water in the amounts of 4050-

4500 l/h was continuously supplied to the upper plate, which provided a concentration of ethyl alcohol in a distillation residue of 3.8 % vol. The distillation residue from the ICC purified from impurities was supplied to the upper zone of the concentration part of the EC for hydroselection of the main and part of the intermediate impurities, including isopropyl alcohol. The liquid retention time on the column plates in cyclic mode was 40 s, the time of its overflow from plate to plate was 1.7 s. Aldehyde-methanol concentrate was taken from the ICC condenser in the amount of 7–9 l/h. From the upper zone of the decanter after separation of the water-alcoholic mixture, ester-fusel concentrate was taken in the amounts of 2–3 l/h. Both concentrates were mixed in a concentrate of impurities.

At the second stage, the efficiency of a typical DP indirect action with the recirculation of distillation residue was investigated. For hydroselection of impurities a distillation residue of the rectification column (luther water) was fed to the upper plate of the extractive rectification column; for 3–5th plate, counting from above, the ICC supplied the distillation residue of the extractive rectification column purified from the upper intermediate impurities and the distillation residue of the ICC freed from the head impurities and isopropanol was sent to the upper zone of the concentration part of the EC. The use of the luther water did not affect the quality of the RA, since the distillation residue of the extractive rectification column with a low content of ethyl alcohol (1.5–3.0 % vol.) freed from higher fusel oil alcohols was fed into the concentration zone of the ICC, in which intermediate impurities, including fusel oil components, were extracted and concentrated. In the process of research, the specific and total consumption of process water and energy consumption for its heating for hydroselection were determined.

At the **third stage** the efficiency of the operation of the DP in the mode of supplying the ICC with alcohol-containing fractions was investigated, which entered the feed plate in the form of vapor that did not condense in the dephlegmators of the main columns. According to the known method of rectification, 98% of the amount of vapor coming out of the upper part of each column was condensed in the dephlegmators of the main columns, of which vapor condensate in the amount of 2% was directed to the ICC feeding plate.

The effectiveness of the innovative technology was investigated in two ways. According to Method I, uncondensed in the carbon dioxide separator and dephlegmators of the main columns vapor was supplied to the ICC in the amount of 2%. According to Method II the water consumption for cooling the dephlegmators was reduced in such a way that 95% of the vapor from the amount of vapor coming out of each column condensed in the dephlegmators, and uncondensed vapor in the amount of 5% was supplied to the ICC feeding plate. In the course of the research, the quality indicators of rectified ethyl alcohol were monitored for compliance with the requirements of the standard.

Results and discussion

At the **first stage** the efficiency of the process of epyuration of the beer distillate in the EC of cyclic action was determined using hydroselection and without hydroselection and the process of extraction of ethyl alcohol from alcohol-containing fractions in the ICC of stationary and cyclic action (patent UA 136560. Method of mass-exchange between liquid and vapor in a column apparatus). Physicochemical parameters of beer distillate (BD), head fraction (HF), epyurate obtained without hydroselection (E1) and using hydroselection (E2) are given in Table 1.

Table 1

Composition of experimental samples of beer distillate (BD), head fraction (HF), and epyurate (E)

Impurities	Concentration of impurities, mg/l, in terms of a.a.			
	BD	**HF**	**E1**	**E2**
Ethanol, % vol.	50	92	40	25
Aldehydes	31.5	5252.0	4.5	1.8
methylacetate	traces	630.1	traces	traces
acetaldehyde	27.6	4621.9	2.7	1.8
Esters	83.1	14302.6	1.6	traces
ethylacetate	80.0	13905.6	traces	traces
isoamylacetate	3.1	325.2	1.6	traces
ethyl butyrate	traces	50.49	traces	traces
Methanol, %	0.044	2.4	0.027	0.010
Fusel oil	14116.7	4526.3	7786.3	4492.1
isopropanol	3.6	21.9	2.1	0.8
n-propanol	2565.8	558.2	1137.6	408.3
isobutanol	4014.2	3696.0	1627.1	566.5
n-butanol	39.4	8.2	38.8	38.4
isoamylol	7491.2	50.8	4966.9	3478.1
n-pentanol	4.5	191.1	13.8	traces

Table 1 demonstrates that in E2 epyurate the concentration of aldehydes decreased by 60%, acetaldehyde by 33.4%, methanol by 63%, fusel oil by 42.3%, and isopropyl alcohol by 62% compared to E1 epyurate. Furthermore, esters and n-pentanol were completely eliminated. This reduction in concentration of impurities can be attributed to the decrease of ethanol in the water-alcohol solutions to 30% vol. and below leading to rectification coefficients of the alcohol impurities become greater than one (Shiyan et al., 2009). At the same time, the intermediate and final impurities of alcohol take on the character of the head ones. The calculated values of the degree of extraction of key alcohol impurities (α) in the EC of cyclic action using hydroselection and without hydroselection are presented in the form of a diagram (Figure 4).

As can be seen from the diagram, in the hydroselection mode the degree of extraction of all impurities increased by 1.7–2.8 times. The head impurities of alcohol were best removed.

The results of chromatographic analysis of alcohol-containing fractions (F), which were supplied to the ICC, are given in Table 2.

They included HF, shoulder straps made from condensers of the distillation column (CDC) and carbon dioxide separator (CDSC), fusel alcohol (FA) and fusel rinse water (FRW). In the process of processing alcohol-containing fractions samples of distillation residue (DR), impurity concentrate (IC) and rectified ethyl alcohol (RA) were taken

The results of chromatographic analysis of experimental samples and the calculated values of the degree of extraction of volatile impurities of alcohol in the stationary (α1) and cyclic (α2) modes of operation of the ICC are given in Table 3.

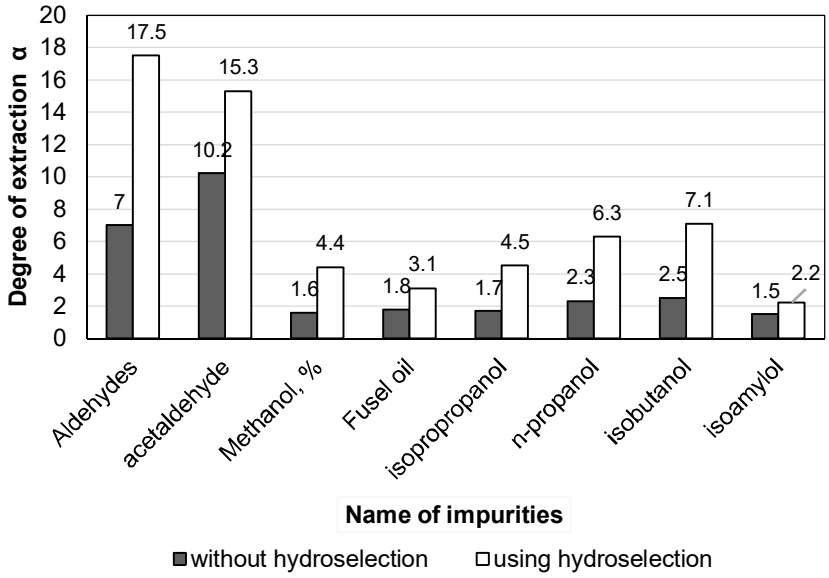

Figure. 4. Degree of extraction of volatile impurities of alcohol (α) in ether column (EC) of cyclic action with and without hydroselection

.

Table 2

Composition of alcohol-containing fractions

Impurities	Concentration of impurities, mg/l, in terms of a.a.					
	HF	CDC	CDSC	FA	FRW	F
Ethanol, % vol.	92.5	48.8	60	89	17.5	30.5
Aldehydes	1135.2	37.2	126.2	4.9	7.0	318.7
methylacetate	926.1	37.2	90.9	4.9	7.0	242.3
acetaldehyde	209.1	traces	35.3	traces	traces	76.4
Esters	2394.9	186.4	39.7	20.2	68.3	40.5
ethylacetate	2223.6	165.8	traces	2.1	traces	traces
isobutylacetate	23.0	13.0	7.9	10.1	traces	11.1
isoamylacetate	90.6	7.6	31.8	8.0	68.3	29.4
Methanol, %	0.49	0.025	0.1445	0.013	0.0032	0.18
Fusel oil	3113.1	18820	12583	48824	197726	105883
isopropanol	4.9	4.9	1.7	1.1	traces	1.2
n-propanol	1186.4	1403	699.6	14741	36681	20002
isobutanol	1640	606.1	4082	27557	36826	20297
n-butanol	2.7	6.4	16.5	35	705.2	362
isoamylol	279.1	1863.5	7783	6485.3	123514	65221

Table 3

Compositions of experimental samples and calculated values of degree of extraction (α) of alcohol impurities

Impurities	Concentration of impurities, mg/l, in terms of a.a.						Degree of extraction	
	DR1*	IC1*	DR2*	IC2*	RA1*	RA2*	α1	α2
Ethanol,% vol.	3.8	67	3.8	67	96.3	96.3	8.0	8.0
Aldehydes	3.7	1689.1	2.8	2302	0.20	0.18	85.4	113.8
Esters	0.5	334961	traces	446615	traces	traces	79.7	∞
Methanol, %	0.006	1.67	0.004	2.69	0.007	0.0003	28.5	45.0
Fusel oil	1163.5	434120	721.7	726463	1.2	0.88	91.0	146.7

* 1 – operation of the ICC in stationary mode

* 2 – operation of the ICC in cyclic mode

The analysis of the results showed that esters were fully removed in the cyclic mode and the degree of extraction of higher alcohols of fusel oil and methanol increased by 38 %. This is explained by the fact that when the time of stay of the liquid on the plates of the column was extended to 40 s the time of its contact with vapor increased and the efficiency of mass-exchange increased due to an increase in the gradient of concentrations of volatile components, and there was a more complete saturation of vapor with volatile components of the liquid, and liquids with heavy-volatile components of vapor. Because of optimizing the operation of the ICC, the quality of rectified alcohol improved (Kiss et al., 2014; Mischenko et al., 2020).

In the cyclic mode, the multiplicity of concentration (β) of the head impurities increased by 25%, the upper intermediate impurities – by 40% and the final ones – by 37% (Figure 5).

This can be explained by the fact that there was more of a complete vapor saturation with it volatile components of liquid on the plates of the column, the mixing of the liquid on adjacent plates, so that the grade of phase equilibrium achievement was increased (Chen et al., 2010). The prolonging in the residence time of the liquid on the plates longer than 40 s proved to be impractical due to an increase in the specific heating vapor consumption without a significant increase in the grade of impurity extraction. The determining impurity, by the content of which the degree of purification of rectified alcohol was assessed, was isopropyl alcohol. It is known that its concentration in the epyurate and the finished product should not exceed 1.5 mg/l (Pang et al., 2017).

It was found that the specific consumption of heating vapor in installations of cyclic action decreased by 40 % compared to installations operating in stationary mode: in the process of processing of alcohol-containing fractions from 25 to 15 kg/dal of a.a. introduced to the feed plate, and in the process of epuration of the beer distillate — from 15 to 8.2 kg/dal of a.a. This is explained by the fact that due to the increase in the contact time of vapor and liquid on the plates of columns of cyclic action the degree of phase equilibrium achievement increased. The consequence of this was a reduction in vapor consumption (Chenyang et al., 2024).

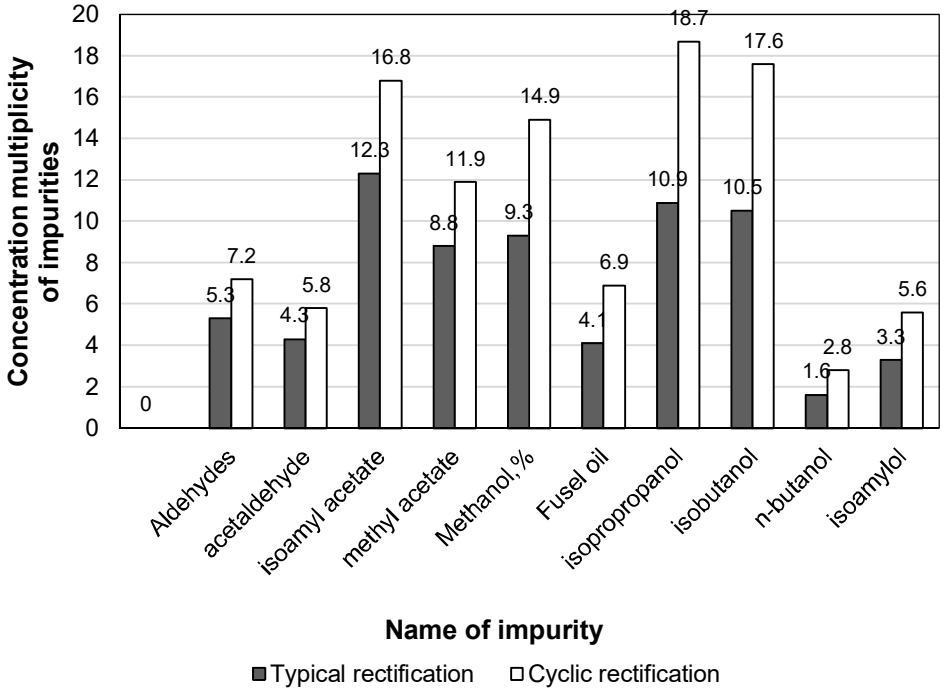

Figure 5. Multiplicity of concentration (β*)* of volatile alcohol impurities in impurity concentration column (ICC) under typical and cyclic rectification conditions

After the inclusion of the experimental ICC in the DP scheme the yield of rectified ethyl alcohol increased by 3.8 %, the total consumption of hot softened process water for hydroselection decreased by 80% and the quality indicators of rectified ethyl alcohol corresponded to the normative ones. The increase in the yield of alcohol was due to its extraction from the head fraction. Reduction of water consumption was due to the use of distillation residue of the ICC for hydroselection in the EC (Bulii et al., 2021).

At the second stage the effectiveness of innovative resource- and energy-saving technology, which provided for the recirculation of distillation residues of rectification column, the ICC and extractive rectification column was investigated. For hydroselection of impurities, distillation residue from the ICC was supplied to the EC, and distillation residue of the rectification column was supplied to the column of extractive rectification, so there was no consumption of hot process softened water in the EC and the column of extractive rectification. The specific consumption of process water and heating vapor for its heating (in terms of 1 kg of a.a. introduced into the column) is given in Tables 4 and 5.

Table 4

Specific and total process water consumption for hydroselection of volatile alcohol impurities

Method	Specific flow rates of process water, l/kg of a.a.			Total flow rates process water	
	ICC	EC	Column of extractive rectification	l/kg of a.a.	%
Typical	4.7	0.7	18.1	23.5	100
Innovative	4.7	—	—	4.7	20

Table 5

Specific and total energy consumption for heating process water for hydroselection of volatile impurities of alcohol

Method	Specific energy consumption for heating process water, kJ/kg of a.a.			Total energy consumption	
	ICC	EC	Column of extractive rectification	кJ/kg of a.a.	%
Typical	590.8	88.0	2275.2	2951.0	100
Innovative	590.8	—	—	590.8	20

According to Tables, it can be seen that the innovative method allows you to reduce the total consumption of process water and energy costs for its heating by 80%. This is explained by the fact that the supply of alcohol-containing fractions enriched with organic impurities from the EC condensers and rectification column to the ICC feeding plate, the distillation residue of the extractive rectification column above the feeding plate (3–5th plates, counting from above) and hot softened water for hydroselection of impurities to upper plate allows you to reduce the concentration of ethyl alcohol on the upper plates of the concentration part of the ICC and thereby reduce the consumption of process water in the ICC. The supply of distillation residue of the extractive rectification column to the ICC allows you to form a zone for effective concentration of intermediate impurities, including fusel oil components (Bausa et al., 2001).

At the third stage the effectiveness of the innovative technology was investigated, which provided for the supply of alcohol-containing fractions to the ICC feeding plate in the form of alcohol-containing vapor that did not condensed in the condenser of the carbon dioxide separator, dephlegmators of the distillation column, the EC (head fraction) and rectification column (unpasteurized alcohol), as well as fusel fraction vapors and fusel alcohol. Such a technical solution eliminated the need for additional consumption of heating vapor for preheating of these fractions to the boiling point for their evaporation in the ICC and made it possible to reduce the consumption of heating vapor and water for cooling the heat exchange equipment due to the absence of condensers in the technological scheme. The results of the research are given in Table 6.

The data presented in Table 6 indicates that using Method I resulted in a reduction of total water consumption for cooling by 0.013 m^3/dal of a.a. (2.1%).

Table 6

Water (W) and heating vapor (HV) consumption in distillation plant (DP) of indirect action equipped with the impurity concentration column (ICC)

Columns of distillation plant	W, m^3/dal of a.a.			HV, kg/dal of a.a.		
	known method	innovative		known method	innovative	
		method I	method II		method I	method II
Distillation	0.065	0.064	0.062	20	20	20
Ether	0.154	0.151	0.146	12	12	12
Rectification	0.282	0.276	0.268	22	22	22
ICC	0.128	0.125	0.121	10	9.1	8.8
DP	0.629	0.616	0.597	64	63.1	62.8

Additionally, the consumption of heating vapor in the ICC decreased by 0.9 kg/dal of a.a. (1.4%). With Method II, water consumption decreased by 0.032 m^3/dal of a.a. (5.1%), while heating vapor consumption dropped by 1.2 kg/dal of a.a. (1.9%). Importantly, the organoleptic and physicochemical parameters of the rectified ethyl alcohol remained within normative standards. Furthermore, when utilizing Method II the profit for a plant with a capacity of 3000 dal of alcohol per day increased by 33.3% compared to Method I. This is explained by the absence in the technological scheme of condensers and the reduced consumption of cooling water and steam to heat the alcohol fractions reaching the feed plate of the ICC.

Conclusions

1. Extension of the residence time of the liquid on the plates of the ICC up to 40 s in the selected hydrodynamic mode allows increasing the degree of extraction and the multiplicity of concentration of the head, intermediate and final impurities of alcohol by 25–40 %.
2. The consumption of heating vapor in the processes of epyuration of the beer distillate and processing of alcohol-containing fractions in cyclic mode is reducing by at least 40 %.
3. Recirculation of distillation residue of rectification column, ICC and extractive rectification column allows reducing the specific consumption of process water and vapor for its heating by 80% in the DP of indirect.
4. Feeding the ICC with alcohol-containing fractions in the form of vapor in the amount of 2% allows you to reduce the total water consumption for cooling by 0.013 m^3/dal of a.a. (2.1%) and consumption of heating vapor by 0.9 kg/dal of a.a. (1.4%).
5. In case of an increase in the amount of non-condensed vapor in the dephlegmators of the main columns from 2 to 5% and passing it to the ICC, the cooling water consumption is reduced by 0.032 m^3/dal of a.a. (5.1%), and of the heating vapor by 1.2 kg/dal of a.a. (1.9%).
6. The absence of condensers and alcohol traps of the main columns in the technological scheme allows you to reduce the metal intensity of the DP by 10%.

Considering the positive results obtained, it is advisable to continue research in this direction. Promising studies are those on the efficiency of the main columns in cyclic mode, as well as the operation of the ICC and other DP columns, if the volume of alcohol-containing vapors entering their feed trays increases to 10–25% or more.

References

Arslan M., Tahir H., Zareef M., Shi J., Allah A., Bilal M., Xiaowei H., Zhihua L., Xiaobo Z. (2021), Recent trends in quality control, discrimination and authentication of alcoholic beverages using nondestructive instrumental techniques, *Trends in Food Science & Technology,* 107, pp. 80–113, https://doi.org/10.1016/j.tifs.2020.11.021

Andersen B.B., Nielsen R.F., Udugama I.A., Papadakis E., Gernaey K.V., Huusom J.K., Mansouri S.S., Abildskov J. (2018), Integrated process design and control of cyclic distillation columns, *IFAC-Papers Online,* 51(18), pp. 542–547, https://doi.org/10.1016/j.ifacol.2018.09.368

Batista F.R.M., Follegatti-Romero L.A., Meirelles A.J.A. (2013), A new distillation plant for neutral alcohol production, *Separation and Purification Technology,* 118, pp. 784–793, https://doi.org/10.1016/j.seppur.2013.08.030

Bausa J., Tsatsaronis G. (2001), Reducing the energy demand of continuous distillation processes by optimal controlled forced periodic operation, *Computers & Chemical Engineering*, 25, pp. 359–370

Bedryk O., Shevchenko A., Mishchenko O.S., Maleta V.N., Kiss A.A. (2023), Industrial experience in using cyclic distillation columns for food grade alcohol purification, *Chemical Engineering Research and Design*, 192, pp. 102–109, https://doi.org/10.1016/j.cherd.2023.02.026

Botshekan M., Moheb A., Vatankhah F., Karimi K., Shafiei M. (2022), Energy saving alternatives for renewable ethanol production with the focus on separation/purification units: A techno-economic analysis, *Energy,* 239(PE), 122363, https://doi.org/10.1016/j.energy.2021.122363

Bulii Y., Kuts A., Yuryk I., Forsiuk A. (2021), Improving the efficiency of mass-exchange between liquid and steam in rectification columns of cyclic action, *Ukrainian Food Journal,* 10(2), pp. 346–360, https://doi.org/10.24263/2304974X-2021-10-2-11

Chen H., Huang K., Wang S. (2010), A novel simplified configuration for an ideal heat–integrated distillation column (ideal HIDiC), *Separation & Purification Technology,* 73, pp. 230–242, https://doi.org/10.1016/j.seppur.2010.04.006

Chenyang Y., Huaigong Z., Wangfeng C., Minqing Z., Yan W., Ying Z., Jianbing C. (2024), Research progress of cyclic distillation technology, *Chemical Industry and Engineering Progress*, 43, pp. 1109–1117, https://doi.org/10.16085/j.issn.1000-6613.2023-0469

Dattarajan S., Pali S., Fernandes N., Gadwal N., Hulwan D. (2019), Measurement of steam quality using a vortex flowmeter, *Flow Measurement and Instrumentation,* 65, pp. 227–232, https://doi.org/10.1016/j.flowmeasinst.2018.12.004

Dewulf J. (2002), Analysis of volatile organic compounds using gas chromatography, *Trac-nrends in Analitical Chemistry,* 21(9–10), pp. 637–646, http://hdl.handle.net/1854/LU-158121

Flodman H., Timm D. (2012), Batch distillation employing cyclic rectification and stripping operations. *ISA Transactions,* 51(3), pp. 454–460, https://doi.org/10.1016/j.isatra.2011.12.003

Jacimovic B.M., Srbislav B.G., Budimir N.J., Jarić M.S. (2014), Techno-economic optimization of plant for raw ethanol production based on experimental data, *International Journal of Heat and Mass Transfer,* 139, pp, 639–646, https://doi.org/10.1016/j.ijheatmasstransfer.2014.07.085

Kiss A.A. (2014), Distillation technology – still young and full of breakthrough opportunities, *Journal of Chemical Technology and Biotechnology,* 89, pp. 479–498, https://doi.org/10.1002/jctb.4262

Kiss A.A, Olujic Z. (2014), A review on process intensification in internally heat-integrated distillation columns, *Chemical Engineering and Processing,* 86, pp. 125–144, https://doi.org/10.16/j.cep.2014.10.017

Linek V., Moucha T., Prokopova E., Rejl J.F. (2005), Simultaneous determination of vapor and liquid-side volumetric mass transfer coefficients in a distillation column, *Chemical Engineering Research and Design,* 83, pp. 979–986, https://doi.org/10.1205/cherd.03311

Lita I., Bildea C., Kiss A. (2014), Catalytic cyclic distillation – A novel process intensification approach in reactive separations, *Chemical Engineering and Processing,* 81, pp. 1–12, https://doi.org/10.1016/j.cep.2014.04.006

Matsuda K., Kawazuishi K., Kansha Y. Fushimi C., Nagao M., Kunikiyo H., Masuda F., Tsutsumi A. (2011) Advanced energy saving in distillation process with self-heat recuperation technology, *Energy,* 36, pp. 4640–4645, https://doi.org/10.1016/j.energy.2011.03.042

Mischenko O.S., Kizyun G.O., Mozharovska A.A., Ollynik S.I. (2020), Energy-efficient technology of processing of ethyl alcohol head fraction with obtaining rectified ethyl alcohol, *Food Industry*, 28, pp. 115–122.

Nagy E., Mizsey P., Hancsok J., Boldyryev S., Varbanov P. (2015), Analysis of energy saving by combination of distillation and pervaporation for biofuel production, *Chemical Engineering and Processing: Process Intensification,* 98, pp. 86–94, https://doi.org/10.1016/j.cep.2015.10.010

Nielsen R., Huusom J., Abildskov J., Based D. (2017), Design of cyclic distillation, *Engineering Chemistry Research*, 56(38), pp. 10833–10844, https://doi.org/10.1021/acs.iecr.7b01116

Pang X., Li Z., Chen J., Gao L., Han B. (2017), A comprehensive review of spirit drink safety standards and regulations from an international perspective, *Journal of Food Protection,* 80(3), pp. 431–442, https://doi.org/10.4315/0362-028X.JFP-16-319

Pinto F.S., Zemp R., Jobson M., Smith R. (2011), Thermodynamic optimization of distillation columns. *Chemical Engineering Science,* 66(13), pp. 2920–2934, https://doi.org/10.1016/j.ces.2011.03.022

Plutowska B., Wardenski W. (2008), Application of gas hromatography-olfactometry (GC-O) in analysis and quality assessment of alcoholic beverages – a review, *Food Chemistry,* 107, pp. 449–463, https://doi.org/10.1016/j.foodchem.2007.08.058

Polulyah K., Topolov I. (2002), Determination of the optimum parameters of the autogenerator flowmeter, *Ukrainian Metrological Journal,* 4, pp. 48–50.

Rasmussen J.B., Mansouri S.S., Zhang X., Abildskov J., Huusom J.K. (2020), A mass and energy balance stage model for cyclic distillation, *AIChE Journal,* 66(8), e16259, https://doi.org/10.1002/aic.16259

Simon L.L., Kencse H., Hungerbuhler K. (2009), Optimal rectification column, reboiler vessel, connection pipe selection and optimal control of batch distillation con sidering hydraulic limitations, *Chemical Engineering and Processing*, 48, pp. 938–949, https://doi.org/10.1016/j.cep.2008.12.006

Sheikus A. (2019), Distillation process optimization using continuous mobile control actions by redistributing the feed flow, *Advanced Information Systems*, 3(3), pp. 30–36, https://doi.org/10.20998/2522-9052.2019.3.04

Shiyan P., Sosnytskyi V., Oliinichuk S. (2009), *Innovative technologies of the alcohol industry. Theory and practice,* Askania Publishing House, Kyiv.

Toftegard B., Clausen C.H., Jorgensen S.B., Abildskov J. (2016), New realization of periodic cycled separation, *Industrial & Engineering Chemistry Research,* 55(6), pp. 1720–1730, https://doi.org/10.1021/acs.iecr.5b03911

Tsygankov S. (2010), *Bioethanol,* LLC NPP Interservice, Kyiv.

Zhang M., Zhang B.Y., Zhao H.K., Zhao Y., Sun J., Ren Z.Q., Li Q.S. (2017), Hydrodynamics and mass transfer performance of flow-guided jet packing tray, *Chemical Engineering and Processing – Process Intensification*, 120, pp. 330–336, https://doi.org/10.1016/j.cep.2017.07.022

Cite:

UFJ Style

Bulii Yu. (2024), Improvement of alcohol distillation plant operation, *Ukrainian Food Journal*, 13(4), pp. 675–693, https://doi.org/10.24263/2304-974X-2024-13-4-4

APA Style

Bulii, Yu. (2024). Improvement of alcohol distillation plant operation. *Ukrainian Food Journal*, *13*(4), 675–693. https://doi.org/10.24263/2304-974X-2024-13-4-4

Comparative analysis of the composition of Bayan Shirey, Rkatsiteli and Cabernet Sauvignon grape varieties for production of brandy wine materials

Ilhama Kazimova[1], Elza Omarova[1], Ahad Nabiyev[2], Afet Gasimova[2]

1 – Azerbaijan State University of Economics, Republic of Azerbaijan
2 – Azerbaijan Technological University, Republic of Azerbaijan

Keywords:

Grapes
Bayan Shirey
Rkatsiteli
Cabernet Sauvignon
Wine
Brandy

Article history:

Received 17.03.2024
Received in revised form 6.07.2024
Accepted 30.12.2024

Corresponding author:

Ilhama Kazimova
E-mail:
Ilhama_Kazimova@unec.edu.az

DOI:
10.24263/2304-974X-2024-13-4-5

Abstract

Abstract. This study aimed to investigate the chemical compositions of different grape varieties used for production of brandy wine materials.

Materials and Methods. It were studied white technical grape varieties (Bayan Shirey and Rkatsiteli), widely distributed in the country's wineries, as well as Cabernet Sauvignon, a red technical grape variety recently introduced to the Ganja-Gazakh region of the Republic of Azerbaijan. Titratable acidity, contents of sugar, phenolic compounds, pectin substances, and vitamin C were determined using standard methods.

Results and Discussion. The yield of unclarified juice was 78.68% from the Bayan Shirey, 74.34% from Rkatsiteli, and 66.35% from Cabernet Sauvignon grape varieties. The low juice yield of Cabernet Sauvignon is due to its relatively dense skin, and higher number and mass of seeds in the berry. The Bayan Shirey variety has a high yield of unclarified juice, which makes it promising for the production of brandy wine material. The total sugar content in the ripe grape variety Bayan Shirey, grown in the Samukh and Goygol districts, was 18.7 and 17.8%; for Rkatsiteli this indicator was 21.6 and 19.3%, and for the Cabernet-Sauvignon variety, it was 22.1 and 19.4%, respectively. The active acidity of ripe grape varieties varied between 3.2 and 3.3. Active acidity changed between 3.8 and 4.1 in unripe and overripe grape varieties.

The content of phenolic compounds in ripe varieties of grapes was between 0.74 and 1.20 g/100 ml. Among studied variants, ripe grape varieties were the richest in phenolic compounds. Pectic substances in ripe varieties of grapes varied between 0.23 and 0.52 g/100 ml. Fully ripe grape varieties were richer in vitamin C than unripe and overripe varieties. The content of vitamin C in ripe varieties of grapes varied between 7.8 and 12.4 mg/l.

The research has revealed that the most suitable varieties for the production of brandy wine materials are Bayan Shirey and Rkatsiteli.

Conclusions. The results of the study showed that ripe grape varieties such as Bayan Shirey, Rkatsiteli, and Cabernet Sauvignon have the best chemical composition for the production of brandy wine materials, including high content of sugar, phenolic compounds, and vitamin C.

Introduction

The quality of the wine material used for brandy production depends on the chemical composition of the original grapes. In recent decades, there has been a growing interest in studying the chemical characteristics of grapes, since parameters such as acidity, amounts of sugar, phenolic compounds, anthocyanins, and pectic substances significantly affect the sensory properties of the final product. It is essential to understand how different grape varieties, including white and red technical ones, interact with the terroir and technological processes that allow achieving the desired balance of taste, aroma, and structure of the final liquor (Van Leeuwen et al., 2006).

In the wine industry, especially in the production of brandy wine material, the importance of choosing a grape variety with optimal chemical properties is increasing. However, in practice it is not always possible to determine exactly which grape varieties are most suitable for obtaining a quality product, especially given the different growing conditions and degree of ripeness of the fruit. In this regard, there is a need to conduct comparative studies of the chemical composition of different grape varieties and their impact on the quality of brandy wine material (Lončarić et al., 2022).

The study of the chemical characteristics of grapes is of key importance for the wine industry, especially in the context of the production of brandy wine materials. In recent decades, there has been an active interest in the chemical composition of various grape varieties, since it directly affects the sensory characteristics of the final product. Parameters such as acidity, levels of sugar, phenolic, and anthocyanins vary significantly depending on the variety, terroir, and growing conditions (Dimitrov et al., 2016; Louw and Lambrechts, 2012; Ranković et al., 2004).

To produce high-quality brandy, it is necessary first to prepare high-quality brandy wine material that meets modern requirements for sensory and chemical characteristics and provide a rich taste, aroma, and stability of the product. When producing brandy wine material, it is necessary to pay special attention to the grape varieties, their degree of maturity, richness in chemical components, and other factors (Dhiman et al., 2011).

Despite extensive research, many aspects of the chemical composition of grapes remain insufficiently studied. The aim of this study was to investigate the chemical characteristics of individual grape varieties used for the production of brandy wine materials to identify patterns that may be useful for optimizing the production process.

The goal of the study was to analyze the composition of the red grape variety Cabernet-Sauvignon and the white grape varieties Bayan Shirey and Rkatsiteli to determine their potential for the production of high-quality brandy wine materials.

Materials and methods

The objects of the research were white technical grape varieties Bayan Shirey and Rkatsiteli, as well as the red technical grape variety Cabernet-Sauvignon, grown in Ganja-Gazakh, Samukh, and Goygol districts of Azerbaijan.

Bayan Shirey. The homeland of this white technical variety is Azerbaijan, where it has been widely distributed thanks to adaptation to local conditions. The grape variety Bayan Shirey is more widespread in Uzbekistan, Turkmenistan, Kazakhstan, Tajikistan, Ukraine, Moldova, and other countries. It is successfully cultivated and used in winemaking. Its aroma is light and fruity, with a hint of citrus, the sugar level is 16-20%, and the acidity is 5.5–8 g/l. It belongs to varieties of the late ripening period.

Rkatsiteli. The homeland of this grape variety is Kakheti, Georgia. In Azerbaijan, most of Rkatsiteli grows in the Goygol and Samukh districts. Grape varieties grown in the foothills are more prone to sugar accumulation than those grown in flat areas are. Currently, in addition to table and brandy wine material, other varieties of fortified wines are also produced from the Rkatsiteli grape variety. This variety belongs to the mid-late ripening period. In a fully ripe Rkatsiteli variety, the sugar content reaches 18-24%, titratable acidity is 5.5–6.5 g/l. Rkatsiteli has good resistance to grape diseases.

Cabernet Sauvignon is a red technical grape variety that first appeared in the 17th century in Bordeaux, France. The Cabernet Sauvignon grape variety, bred in the late 19th – early 20th century, was planted in Azerbaijan in the collections of research institutions, and on the farms of Karabakh, Shirvan, and the Ganja-Gazakh regions. Currently, this variety is more common in the wineries of the Goygol and Samukh districts.

Research methods

Mechanical composition of grape varieties

When studying the mechanical composition of grape varieties, indicators such as the average cluster mass, the mass of the skin and the comb, the mass and number of berries, the mass of seeds and pulp were determined.

The percentage ratio of each component in relation to the total mass of the cluster was calculated using the formula

$$\% = \frac{component\ mass}{total\ \ mass\ of\ cluster} \times 100$$

Determination of sugar content

Grape samples were crushed and squeezed to determine the total sugar content. The resulting juice was filtered to remove pulp and sediment. Then, 1 ml of an invertase enzyme solution was added to 10 ml of the filtrate, which broke down sucrose into glucose and fructose. After 30 minutes at 37 °C, the glucose concentration was determined using glucose oxidase enzyme (Al-Mhanna et al., 2018).

Determination of titratable acidity

A titrimetric method was used to determine acidity. The content of titratable acids in grape juice was measured using a 0.1 N sodium hydroxide (NaOH) solution until a neutral reaction was achieved (pH 7.0) (Gąstoł, 2015). Titratable acidity was expressed as grams of tartaric acid per liter.

Determination of active acidity

Active acidity was measured using a pH meter.

Determination of vitamin C

The vitamin C content was determined by titration using 2,6-dichlorophenolindophenol. The grape was squeezed and filtered. A few drops of indicator were added to 10 ml of the

filtrate and then titrated with a 0.1% solution of 2,6-dichlorophenolindophenol until the color changed to pink. The concentration of vitamin C was calculated based on the expense of the titrant and expressed in milligrams per 100 ml of juice (Chang et al., 2016).

Determination of the content of pectic substances

The method for measurement of the content of pectic substances in grapes is based on the extraction and transfer of pectin to the dissolved state. Grapes are carefully squeezed to obtain juice. The resulting juice is filtered to remove pulp and sediment. For the extraction of pectic substances, a 0.1 N solution of hydrochloric acid is used. The samples are kept at a temperature of 80 °C for 30 minutes. Then, the extract is cooled and filtered. 1 ml of carbazole reagent (0.1% solution of carbazole in 95% ethanol) and 1 ml of concentrated sulfuric acid are added to 1 ml of the obtained extract. The resulting mixture is carefully mixed and kept in a water bath at a temperature of 60 °C for 10–15 minutes. Then the mixture is cooled at room temperature and the volume is brought up to 10 ml with distilled water. The optical density of the obtained solution is measured on a spectrophotometer at a wavelength of 520 nm. The concentration of pectic substances (including pectin and protopectin) is calculated according to a standard curve constructed based on a known concentration of a pectin standard (for example, apple pectin).

Determination of the content of phenolic compounds

The determination of the content of phenolic compounds was carried out using the Folin–Ciocalteu assay, which allows for the quantitative estimation of the content of phenols in wine samples (Kupina, 2019).

The method is based on oxidation-reduction reactions with the use of phosphorus-vanadate reagent (Folin–Ciocalteu reagent), which is reduced in the presence of phenols. This leads to a change in the color of the solution, and the intensity of the color can be used to judge the content of phenols. The wine is subjected to preliminary extraction in order to remove solid particles and other substances that may interfere with the reaction. In some cases, additional filtration is carried out. A solution of Folin–Ciocalteu reagent is added to the purified wine sample, which is a mixture of molybdate and vanadate. This reagent interacts with phenolic groups in wine. Then a solution of sodium carbonate (Na_2CO_3) was added to provide an alkaline medium necessary for the reaction. Phenols reduce molybdenum and vanadium, which causes a change in the color of the solution, usually to blue-green. The solution is incubated at room temperature or in a water bath for 30 minutes. After incubation, the optical density (or absorption) of the solution was measured at a wavelength of 760 nm, since the color change is proportional to the amounts of phenolic compounds.

For accurate estimation of the content of phenols, a calibration curve is constructed using a standard solution of phenolic compounds, for example, gallic acid. Based on this curve, the content of phenols in the sample is determined.

The content of phenols in wine was calculated using the established dependence between absorption and concentration of phenols in a standard solution.

Assessing the ripeness of grapes

The grapes were collected from different parts of the vineyard to ensure the representativeness of sampling. Only healthy berries were accepted, excluding damaged ones. The berries were divided into three categories: unripe, ripe, and overripe. Before

conducting chemical analyses, the berries were thoroughly washed and processed, after which they were crushed and juice was extracted.

Grape ripeness was determined by measuring sugar content and titratable acidity. Sugar content was measured using a refractometer, which provides a Brix reading, where 1°Brix is equivalent to 1 gram of sugar per 100 g of the solution (1°Brix = 1% sugar) (Jaywant et al., 2022; Reid, 2002). The ripeness of grapes was characterized by a soluble solid content of about 20°Brix and a titratable acidity value of 6–8 g/l (Lago et al., 2017). For the ripe Bayan Shirey and Rkatsiteli white varieties, sugar content varied between 17.8 and 21.6% and for the red Cabernet-Sauvignon variety – between 19.4 and 22.1%.

In white varieties of ripe grapes (Bayan Shirey and Rkatsiteli), the acidity varied between 6.7 and 7.8 g/l, for the red variety (Cabernet Sauvignon) – between 6.5 and 6.7 g/l. For a more accurate assessment of the stage of physiological maturity, the glucoacidometric method was used, which involves calculating the ratio of sugar content (in Brix) to titratable acidity. According to literary data, the optimal value of this ratio is considered to be between 2.5 and 3.5 (Lago et al., 2017). For Bayan Shirey and Rkatsiteli, it was 2.65–2.77 and for Cabernet Sauvignon it was 2.98–3.3.

Visual and organoleptic (taste) assessments were also carried out to assess the ripeness of the grapes. At this stage of the study, attention was paid to the condition of the berries (color, consistency, presence of aromas) and their taste qualities (sweetness, aroma, texture). All ripe berries were distinguished by a uniform color: Bayan Shirey had a golden-yellow color; Cabernet-Sauvignon had a dark red color, sweet taste, and a pronounced aroma, which also confirmed their ripeness.

Statistical analysis

The chemical parameters were determined in five replicates. The results are presented as mean ± standard deviation.

Results and discussion

Mechanical composition of grape varieties

The mechanical composition of white technical grape varieties Bayan Shirey and Rkatsiteli, and red technical grape variety Cabernet Sauvignon were studied. The mechanical composition of grapes includes grape skins and combs. A grape cluster consists of a comb, berries, skins, pulp, seeds, and juice (Reid, 2002). Depending on the degree of maturity of the grapes, growing conditions, environmental situation, and applied agrotechnical conditions, the components included in the mechanical composition changed differently in percentage terms.

The mechanical composition of the studied grape varieties is presented in Tables 1 and 2.

The mass of clusters and the number of berries were determined for three grape varieties grown under the conditions of the Goygol district: Bayan Shirey, Rkatsiteli, and Cabernet Sauvignon. The data presented in Table 1 show that the average mass of berries and the total number of berries in clusters vary significantly.

Table 1

Mechanical composition of technical grape varieties grown in Goygol district

Indicators	Grape varieties		
	Bayan Shirey	Rkatsiteli	Cabernet Sauvignon
Average mass of a grape cluster, g	194.98±0.02	152.50±0.01	132.70±0.01
Number of berries per cluster, g	94.00±0.04	87.00±0.03	65.00±0.01
Mass of grape comb per cluster, g	6.84±0.01	7.00±0.02	7.20±0.01
Mass of grapes per cluster, g	188.14±0.02	145.50±0.01	125.50±0.01
Mass of grape skin per cluster, g	6.08±0.01	7.40±0.00	7.40±0.01
Mass of grape seed per cluster, g	3.68±0.01	4.15±0.01	8.30±0.01
Mass of grape pulp per cluster, g	24.96±0.05	20.52±0.01	16.40±0.01
Percentage of the total mass of a grape cluster			
Comb	3.51±0.01	4.59±0.02	5.42±0.02
Skin	3.12±0.02	4.85±0.03	5.58±0.01
Seeds	1.89±0.03	2.72±0.01	6.25±0.01
Pulp	12.80±0.01	13.50±0.03	20.15±0.01
Juice with pulp	91.48±0.03	87.84±0.02	82.75±0.01
Unclarified juice without pulp	78.68±0.01	74.34±0.01	66.35±0.04

Table 2

Mechanical composition of technical grape varieties grown in Samukh district

Indicators	Grape varieties		
	Bayan Shirey	Rkatsiteli	Cabernet Sauvignon
Average mass of a grape cluster, g	201.50±0.04	156.40±0.01	128.60±0.01
Number of berries per cluster, g	98.00±0.01	91.00±0.01	63.00±0.01
Mass of grape comb per cluster, g	6.40±0.03	6.70±0.02	7.40±0.01
Mass of grapes per cluster, g	195.10±0.02	149.70±0.01	121.20±0.03
Mass of grape skin per cluster, g	6.48±0.01	7.80±0.02	7.60±0.01
Mass of grape seed per cluster, g	4.05±0.01	4.55±0.03	8.80±0.02
Mass of grape pulp per cluster, g	25.20±0.01	19.70±0.02	20.85±0.03
Percentage of the total mass of a grape cluster			
Comb	3.18±0.01	4.28±0.03	5.75±0.01
Skin	3.21±0.03	4.98±0.01	5.91±0.02
Seeds	2.01±0.01	2.91±0.02	6.84±0.01
Pulp	12.50±0.01	12.60±0.02	16.20±0.01
Juice with pulp	91.60±0.03	87.82±0.02	81.50±0.01
Unclarified juice without pulp	79.10±0.01	75.22±0.01	65.30±0.02

The Bayan Shirey variety had the highest average berry mass (188.14 g) and the highest number of berries in clusters (94.0). This may indicate a high yield potential for this variety, which is a positive aspect for winegrowers and winemakers. Larger and more numerous berries can result in a higher juice yield and, ultimately, better wine quality. The Rkatsiteli

variety, with a smaller average berry mass (145.5 g) and berry quantity (87.0), is inferior to Bayan Shirey in these indicators but remains competitive. Cabernet Sauvignon showed the lowest values: 125.5 g on average and only 65.0 berries per cluster. This can be considered a disadvantage in terms of yield. However, Cabernet Sauvignon is known for its high-quality characteristics and potential for creating complex wines.

A comparative analysis of grape varieties established the yield of unclarified juice. The Bayan Shirey grape variety had a yield of unclarified juice of 78.68%, Rkatsiteli – 74.34%, and Cabernet Sauvignon – 66.35%. The low juice yield of Cabernet Sauvignon is attributed to its relatively dense skin and higher number and mass of seeds in the berry.

Table 2 shows significant changes in the mechanical composition of grape varieties grown in the Samukh district. Depending on the variety, the mass of the grape cluster, the number and mass of berries, the yield of the comb and pulp differ. In the Samukh district, the mass of the cluster of the Bayan Shirey grape variety averaged 201.5 g, for the Rkatsiteli grape variety, this value was 156.4 g; while for the Cabernet Sauvignon variety, it was 128.6 g. The research revealed that the number of berries in different grape varieties also varied. Bayan Shirey significantly exceeded Rkatsiteli and Cabernet Sauvignon in cluster mass and number of berries. This could be seen as a positive result, as larger clusters could indicate higher yields (Reid, 2002).

Higher yields may contribute to the economic viability of wineries. Differences in stem mass may indicate different growth and development patterns of varieties (Reid, 2002). The higher stem mass of Cabernet Sauvignon may indicate a more robust structure, but this may also increase the amount of waste during processing. The lower skin mass of Bayan Shirey may be beneficial for wine production, as it may indicate less astringency and a sweeter taste.

According to Fataliyev (2012), varieties such as Chardonnay and Merlot also show similar patterns in mechanical composition. For example, Chardonnay has a large cluster mass and high yield, which makes it one of the most popular varieties in the world. Merlot, like Cabernet Sauvignon, has a high content of phenolic compounds, which affects its aroma and taste.

The results of the study show that the Bayan Shirey variety has advantages in terms of yield and cluster mass, which makes it more attractive for wineries. The Bayan Shirey grape variety had a seed mass of 4.05 g and a pulp mass of 25.2 g; the Rkatsiteli variety had a seed mass of 4.55 g and a pulp mass of 19.70 g; and the Cabernet Sauvignon variety had a seed mass of 8.8 g and a pulp mass of 20.85 g. The ratio of the yield of combs, skins, seeds, and pulp to the total mass of the grape cluster was also determined. Depending on the variety of grape, the comb makes up 2.5–6%, the skin 7–8%, the seeds 3–4% and the pulp with juice 80–92% (Salimov, 2022). The same grape variety grows in different districts, though their mechanical composition differs from each other.

The yield of unclarified juice varied depending on the districts and the variety. The Bayan Shirey grape variety grown in the Goygol district had a yield of unclarified juice of 78.68%, while in the Samukh district, the yield of unclarified juice obtained from the same variety was 79.1%.

Temperature, humidity, and rainfall can significantly affect the sugar and acid content of grapes, which in turn changes juice yield (Gąstoł, 2015). Different soil types can contain different levels of nutrients stipulating the growth and development of grapevines. The methods of harvesting, processing, and squeezing grapes can vary between districts and significantly affect the amount of juice obtained. Growing conditions and vineyard health (e.g. the presence of diseases or pests) can also influence juice yield. Thus, the yield of unclarified juice depends on many factors, and differences between grapes grown in different districts can be attributed to a combination of them (Gąstoł, 2015).

The yield of unclarified juice of different grape varieties grown in the Goygol and Samukh districts is shown in Figure 1. As seen in the figure, in the Samukh district, the yield of unclarified juice of the Bayan Shirey and Rkatsiteli varieties was higher than that of the same varieties grown in the Goygol district.

The largest amount of unclarified juice was obtained from the Bayan Shirey and Rkatsiteli varieties. The smallest yield of unclarified juice was obtained from the Cabernet Sauvignon variety, grown in both districts.

The average cluster mass of grape varieties grown in the Goygol and Samukh districts is shown in Figure 2.

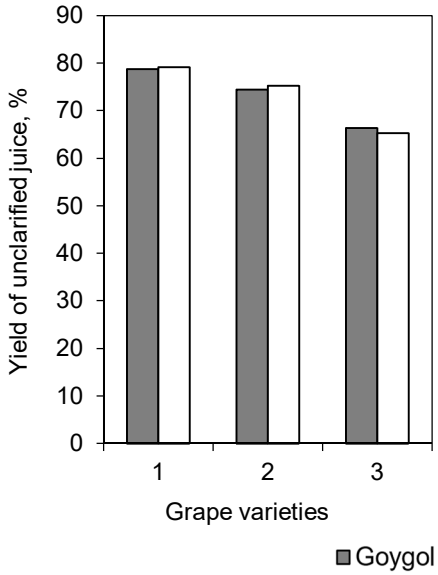

Figure 1. Yield of unclarified juice from grape varieties grown in Goygol and Samukh districts:
1 – Bayan Shirey, 2 – Rkatsiteli, 3 – Cabernet Sauvignon.

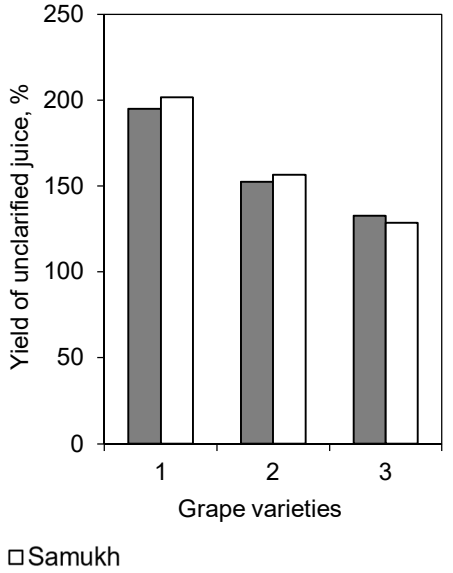

Figure 2. Average cluster mass of grape varieties grown in Goygol and Samukh districts, in grams:
1 – Bayan Shirey, 2 – Rkatsiteli, 3 – Cabernet Sauvignon.

The Bayan Shirey and Rkatsiteli grape varieties are more suitable for the production of brandy wine material than the Cabernet Sauvignon variety. Cabernet Sauvignon has a thicker skin and less water content in the berries and less juice is released when squeezing compared to Bayan Shirey and Rkatsiteli. A high juice yield is important for the production of brandy wine material, as this contributes to a greater amount of raw materials for fermentation and subsequent alcohol production. Bayan Shirey and Rkatsiteli have a higher sugar content and balanced acidity, which is important for further fermentation and distillation.

Since Cabernet Sauvignon is a red technical grape variety, it is recommended to use it for the production of other types of wine, mainly red table wines. From the above, it is clear that the quality of the produced brandy wine material largely depends on the mechanical composition of the grapes.

Chemical composition of grape varieties

Tables 3 and 4 present data on the quantitative change in some chemical indicators of grape varieties depending on the degree of ripeness.

Table 3

Changes in chemical composition of grape varieties grown in Samukh district depending on the degree of ripeness

Chemical indicators	Grape varieties								
	Bayan Shirey			Rkatsiteli			Cabernet Sauvignon		
	I	II	III	I	II	III	I	II	III
Total sugar, g/100 ml	18.70 ±0.02	16.50 ±0.04	17.80 ±0.01	21.60 ±0.03	18.20 ±0.05	19.40 ±0.02	22.10 ±0.04	18.60 ±0.01	19.40 ±0.03
Titratable acidity, g/100 ml	7.00 ±0.03	7.90 ±0.02	5.70 ±0.04	6.80 ±0.01	7.60 ±0.03	5.20 ±0.05	6.50 ±0.02	7.60 ±0.04	5.20 ±0.01
Active acidity, pH	3.20 ±0.04	3.80 ±0.01	3.90 ±0.02	3.30 ±0.04	3.90 ±0.01	4.00 ±0.03	3.30 ±0.05	4.00 ±0.02	4.10 ±0.03
Phenolic compounds, g/100 ml	0.78 ±0.02	0.70 ±0.03	0.54 ±0.04	0.74 ±0.02	0.65 ±0.04	0.50 ±0.01	1.05 ±0.03	0.95 ±0.05	0.68 ±0.03
Pectic ubstances, g/100 ml	0.25 ±0.05	0.31 ±0.03	0.18 ±0.04	0.23 ±0.01	0.28 ±0.02	0.20 ±0.04	0.50 ±0.01	0.62 ±0.03	0.36 ±0.05
Protopectin, g/100 ml	0.12 ±0.01	0.20 ±0.04	0.08 ±0.02	0.11 ±0.05	0.18 ±0.03	0.08 ±0.02	0.18 ±0.04	0.40 ±0.01	0.16 ±0.04
Pectin, g/100 ml	0.13 ±0.03	0.11 ±0.01	0.10 ±0.02	0.12 ±0.03	0.10 ±0.01	0.12 ±0.03	0.32 ±0.02	0.22 ±0.04	0.20 ±0.01
Vitamin C, mg/l	8.20 ±0.01	5.60 ±0.03	3.40 ±0.05	7.80 ±0.01	5.40 ±0.01	3.10 ±0.03	10.20 ±0.01	7.60 ±0.02	4.80 ±0.02

Note: I – Ripe grapes, II – Unripe grapes, III – Overripe grapes

Total sugar, which is the main indicator of grape quality, was the lowest in unripe grape varieties. The total sugar content in the unripe Bayan Shirey grape variety grown in the Samukh district was 16.5%, while in Rkatsiteli, this value was 18.2%, and in Cabernet Sauvignon, it was 18.6%. Depending on the degree of ripeness of grape varieties, the highest sugar content was observed in fully ripe varieties. Total or titratable acidity is important in the winemaking process. Organic acids of grapes are formed mainly because of the exchange of carbohydrates, amino acids, proteins, and other organic substances during photosynthesis.

The quality of grapes and wine largely depends on titratable acidity. Tartaric acid is the main titratable acidity of grapes (Baiano et al., 2012). Besides, grapes contain malic, succinic, citric, and other non-volatile acids (Nabiev and Moslemzade, 2008). The lowest titratable acidity was recorded in overripe grape varieties (Table 1). The acidity of the overripe Bayan Shirey grape variety was 5.7 g/l, while for the Rkatsiteli and Cabernet Sauvignon varieties, this value was 5.2 g/l. The low titratable acidity of overripe grape varieties compared to other variants is explained by the fact that, like other nutrients, it is spent on the respiratory process (Baiano et al., 2012).

Exceeding the titratable acidity of grapes is inappropriate. Mostly unripe grape varieties have high titratable acidity (Baiano et al., 2012). It is also known that unripe grapes contain

large amounts of malic acid. Brandy and table wines made from unripe grapes have an unpleasant, harsh taste due to the high level of malic acid (more than 2 g/l), called green acidity (Nabiev, 2010). Increased green acidity in wine creates conditions for the formation of various defects, including mousy taste, during the storage period of wine (Baiano et al., 2012). Therefore, to produce high-quality wines, including brandy, it is necessary to regulate the amount of titratable acidity of grapes.

Active acidity affects the quality of wine (Vicente et al., 2022). It directly affects the balance of taste, aroma, and stability of wine. While high acidity helps to preserve freshness and balance, high acidity can give the wine harshness and unpleasant sensations.

When making brandy wine material, it is important that the acidity maintain the taste without excessive harshness, ensuring the purity and complexity of the aroma. The correct level of acidity also contributes to better preservation of wine and prevents the development of unwanted defects during storage. High active acidity in grape juice and wine is undesirable because it can impart a harsh and unpleasant taste, interfering with the harmony of the overall profile of the drink. It can also hinder the balanced development of aroma and taste, making the wine less enjoyable to drink. In addition, excessive acidity can negatively affect the fermentation process and storage, increasing the risk of developing defects and reducing the stability of the wine (Fataliyev, 2012).

The change in pH depends on the grape variety, soil and climate conditions and other factors. When the pH is between 3.0 and 3.3, the active acidity of the environment or wine slows down oxidation and reduction processes. Therefore, the stability, transparency, color preservation, and other factors of wine largely depend on active acidity. As seen in Table 3, fully ripe grape varieties have normalized active acidity for wine production. Active acidity in fully ripe grape varieties changed between 3.2 and 3.3. In unripe and overripe grape varieties, active acidity varied within the range of pH values of 3.8-4.1. Fully ripe grape varieties are considered more optimal for wine production.

Phenolic compounds are widely distributed in plants, including grapes, and have important technological properties (Cosme et al., 2018). The quality of grapes and wine largely depends on phenolic compounds. The content of phenolic compounds in grape skins is higher than in juice and pulp (Bendaali et al., 2022). Some of the important biological and technological properties of phenolic substances are their antioxidant and antimicrobial propertiesGrape and wine varieties rich in phenolic substances are not only more resistant to diseases, but also rich in extractive substances (Nabiev and Moslemzade, 2008). As seen in Table 1, fully ripened grape varieties are richer in phenolic compounds compared to other varieties. The presence of phenolic compounds in grapes and wine stipulates their enrichment with aromatic substances.

The quality of the prepared brandy wine material also largely depends on pectic substances. The pectic substances are mainly represented by pectic acid, pectin, and protopectin. In addition, grapes, especially wine, contain pectin salts. These salts are mainly contained in grapes grown on soils rich in calcium and magnesium ions (Velioglu et al., 1998). According to their biological and technological properties, pectic substances are colloidal particles. The presence of pectic substances affects the yield of grape juice, and the transparency of juice and wine (Nabiev and Moslemzade, 2008). Therefore, the production of high-quality brandy wine materials largely depends on the content of pectic substances.

Table 4

Changes in chemical composition of grape varieties grown in Goygol district depending on the degree of ripeness

Chemical indicators	Grape varieties								
	Bayan Shirey			Rkatsiteli			Cabernet Sauvignon		
	I	II	I	I	I	III	I	II	I
Total sugar, g/100ml	17.80 ±0.01	16.10 ±0.03	17.20 ±0.05	19.30 ±0.02	17.40 ±0.03	18.20 ±0.01	19.40 ±0.03	17.60 ±0.04	18.50 ±0.02
Titratable acidity, g/100 ml	7.80 ±0.01	8.30 ±0.01	6.70 ±0.03	7.20 ±0.05	8.10 ±0.02	5.60 ±0.03	6.70 ±0.04	8.70 ±0.02	5.40 ±0.04
Active acidity, pH	3.30 ±0.01	4.0 ±0.04	4.20 ±0.01	3.20 ±0.03	3.90 ±0.05	4.10 ±0.03	3.20 ±0.02	3.60 ±0.04	3.90 ±0.02
Phenolic compounds, g/100 ml	0.82 ±0.03	0.74 ±0.02	0.58 ±0.05	0.80 ±0.01	0.74 ±0.03	0.55 ±0.02	1.20 ±0.04	1.02 ±0.01	0.70 ±0.04
Pectic substances, g/100 ml	0.28 ±0.01	0.34 ±0.04	0.23 ±0.03	0.25 ±0.02	0.32 ±0.01	0.21 ±0.03	0.52 ±0.04	0.64 ±0.05	0.40 ±0.02
Protopectin, g/100 ml	0.13 ±0.03	0.23 ±0.01	0.10 ±0.02	0.12 ±0.05	0.22 ±0.04	0.09 ±0.01	0.20 ±0.03	0.42 ±0.02	0.16 ±0.04
Pectin, g/100 ml	0.15 ±0.04	0.11 ±0.02	0.13 ±0.03	0.13 ±0.04	0.10 ±0.02	0.12 ±0.01	0.32 ±0.01	0.22 ±0.03	0.24 ±0.05
Vitamin C, mg/l	8.50 ±0.02	8.40 ±0.05	3.80 ±0.04	8.20 ±0.03	6.10 ±0.01	3.70 ±0.04	12.40 ±0.03	8.20 ±0.01	5.10 ±0.02

Note: I – Ripe grapes, II – Unripe grapes, III – Overripe grapes

Pectic substances, including protopectin, are mainly found in unripe grapes (Tables 2 and 3). For example, the content of pectic substances in unripe Rkatsiteli grapes grown in the Samukh district was 0.28 g/100 ml, while in ripe grapes, this parameter was 0.23 g/100 ml, and in overripe grapes, it was 0.20 g/100 ml.

The research revealed that the red grape variety is richer in pectic substances than the white grape variety. The total amount of pectic substances in the fully ripened Bayan Shirey grape variety grown under the conditions of the Goygol district was 0.28 g / 100 ml, while for the Rkatsiteli variety, this parameter was 0.25 g/100 ml, and for the Cabernet Sauvignon variety, it was 0.52 g/100 ml (Table 4).

The studies revealed that the unripe Rkatsiteli grape variety had a protopectin content of 0.18 g/100 ml, while the ripe variety had a protopectin content of 0.11 g/100 ml, and the overripe variety had a protopectin content of 0.08 g/100 ml (Table 3). As the grapes ripen, the amount of protopectin decreases and turns into pectin. The conversion of protopectin into pectin occurs under the action of the protopectinase enzyme. During this period, the grapes become relatively soft and are enriched with aromatic and other nutrients through the process of photosynthesis (Velioglu et al., 1998).

In wine materials, the content of protopectin above the norm is inappropriate, since protopectin is practically insoluble in water (Velioglu et al., 1998). This prevents the clarification and stability of the wine material. Therefore, when producing brandy, grape varieties should be selected so that the content of pectic substances, mainly protopectin, is lower. The amount of pectic substances in grapes depends to some extent on the specific characteristics of the variety, the degree of maturity, soil and climatic conditions, and other

factors (Rouxinol et al., 2023). The amount of pectin varies among grape varieties. For example, varieties with high acidity levels often contain more pectin, which can affect the fermentation and clarification process. At the stage of full ripening, pectin levels usually decrease. Unripe berries contain more pectin, which can lead to problems with clarification (Velioglu et al., 1998).

The quantitative content of vitamin C was also determined depending on the degree of ripeness of the grape varieties. The red grape variety Cabernet Sauvignon is richer in vitamin C than white grape varieties. In fully ripened Cabernet Sauvignon grapes, the content of vitamin C varied between 10.2 and 12.4 mg/l. In the Rkatsiteli variety, this indicator varied between 7.8 and 8.2 mg/l, and in the Bayan Shirey variety, between 8.2 and 8.5 mg/l (Tables 3 and 4).

It is known that fully ripened grape varieties are richer in vitamin C than unripe and overripe grape varieties. As seen in Table 3, vitamin C in the fully ripened Bayan Shirey grape variety was 8.2 mg/l, in unripe grapes this parameter was 5.6 mg/l, and in overripe grapes – 3.4 mg/l. Therefore, when producing brandy wine material, it is recommended to use fully ripened grapes.

Conclusions

1. To produce high-quality brandy wine material, the mechanical composition of grape varieties used as raw materials, as well as the juice yield, was determined. The yield of unclarified juice with and without pulp obtained from technical grape varieties, Bayan Shirey, Rkatsiteli, and Cabernet Sauvignon, grown in the Goygol and Samukh districts varied depending on the variety and region.
2. A comparative analysis of grape varieties established the yield of unclarified juice. The Bayan Shirey grape variety had a 78.68% yield of unclarified juice, Rkatsiteli – 74.34%, and Cabernet Sauvignon – 66.35%. The low juice yield of Cabernet Sauvignon is due to its relatively dense skin, and higher number and mass of seeds in the berry. The Bayan Shirey variety has a high yield of unclarified juice, which makes it promising for the production of brandy wine material.
3. Depending on the degree of ripeness of grape varieties, the highest sugar content was found in fully ripe varieties. The active acidity of fully ripe grape varieties changed between 3.2 and 3.3. In unripe and overripe grape varieties, the active acidity varied between 3.8 and 4.1. It was found that fully ripe grape varieties compared to other varieties are richer in phenolic substances.
4. In unripe grape varieties, Bayan Shirey, Rkatsiteli, and Cabernet Sauvignon, grown under the conditions of the Samukh district, the content of pectic substances was 0.20, 0.18, and 0.40 g/100 ml. In ripened grapes, this indicator was 0.12, 0.11, and 0.18 g/100 ml, and in overripe grapes – 0.08, 0.08, and 0.16 g/100 ml, respectively. As the grapes ripened, the amount of protopectin decreased. In wine materials, the content of protopectin above the norm is inappropriate, since protopectin is practically insoluble in water and this prevents the clarification and stability of the wine material.
5. The research has revealed that the most suitable varieties for the production of brandy wine materials are Bayan Shirey and Rkatsiteli.

References

Al-Mhanna N.M., Huebner H., Buchholz R. (2018), Analysis of the sugar content in food products by using gas chromatography mass spectrometry and enzymatic methods, *Foods*, 7(11), 185, https://doi.org/10.3390/foods7110185

Baiano A., Terracone C., Peri G., Romaniello R. (2012), Application of hyperspectral imaging for prediction of physico-chemical and sensory characteristics of table grapes, *Computers and Electronics in Agriculture*, 87, pp. 142–151, https://doi.org/10.1016/j.compag.2012.06.002

Bendaali Y., Vaquero C., González C., Morata A. (2022), Elaboration of an organic beverage based on grape juice with positive nutritional properties, *Food Science and Nutrition*, 10(6), pp. 1768–1779, https://doi.org/10.1002/fsn3.2795

Chang S.K., Ismail A., Daud Z.A.M. (2016), Ascorbic acid: Properties, determination and uses, *Encyclopedia of Food and Health*, pp. 275–284. https://doi.org/10.1016/b978-0-12-384947-2.00044-1

Cosme F., Pinto T., Vilela A. (2018), Phenolic compounds and antioxidant activity in grape juices: A chemical and sensory view, *Beverages*, 4(1), 22, https//doi.org/10.3390/beverages4010022

Dhiman A.K., Attri S., Ramachandran P. (2011), Technology of brandy production, In: V.K. Joshi (Ed.), *Handbook of Enology: Principles, Practices and Recent Innovations*, *Volume 1, Introduction to Vine and Wine*, pp. 531–552.

Dimitrov D., Yoncheva T., Haygarov V. (2016), Evaluation the risk of toxic compounds formation in grape and fruit brandies, *Journal of Microbiology, Biotechnology and Food Sciences*, 6(1), pp. 681–684, https://doi.org/10.15414/jmbfs.2016.6.1.681-684

Fataliyev H.K. (2012), Practical course in winemaking, Baku.

Gąstoł M. (2015), Vineyard performance and fruit quality of some interspecific grapevine cultivars in cool climate conditions, *Folia Horticulturae*, 27, pp. 21–31, https://doi.org/10.1515/fhort-2015-0011

Jaywant S.A., Singh H., Arif K.M. (2022), Sensors and instruments for Brix measurement: A review, *Sensors (Basel)*, 22(6), 2290, https://doi.org/10.3390/s22062290

Kupina S., Fields C., Roman M.C., Brunelle Sh.L (2019), Determination of total phenolic content using the Folin-C assay, *Journal of AOAC International*, 102(1), pp. 320–321, https://doi.org/10.1093/jaoac/102.1.320

Lago L.O., Nicolli K.P., Marques A.B., Zini C.A., Welke J.E. (2017), Influence of ripeness and maceration of the grapes on levels of furan and carbonyl compounds in wine – Simultaneous quantitative determination and assessment of the exposure risk to these compounds, *Food Chemistry*, 230, pp. 594–603, https://doi.org/10.1016/j.foodchem.2017.03.090

Lončarić A., Patljak M., Blažević A., Jozinović A., Babić J., Šubarić D., Pichler A., Flanjak I., Kujundžić T., Miličević B. (2022), Changes in volatile compounds during grape brandy production from 'Cabernet Sauvignon' and 'Syrah' grape varieties, *Processes*, 10(5), 988, https://doi.org/10.3390/pr10050988

Louw L., Lambrechts M.G. (2012), Grape-based brandies: production, sensory properties and sensory evaluation, *Alcoholic Beverages*, pp. 281–298, https://doi.org/10.1533/9780857095176.3.281

Nabiev A.A. (2010), *Chemistry of Wine*, Elm, Baku.

Nabiev A.A., Moslemzade E.A. (2008). *Biochemistry of food products*, Elm, Baku.

Ranković V., Palić R.M., Živković J., Mošić I., Stanković S., Stojanović, G.S. (2004), Investigation of the impact of grape cultivars on the grape brandies quality, *Facta*

Universitatis – Series: Physics, Chemistry and Technology, 3, pp. 61–66, https://doi.org/10.2298/fupct0401061r

Reid M.S. (2002), Maturation and maturity indices, In: A.A. Kader (Ed.), *Postharvest Technology of Horticultural Crops*, University of California, San Diego, pp. 55–62.

Rouxinol M.I., Martins M.R., Barroso J.M., Rato A.E. (2023), Wine grapes ripening: A review on climate effect and analytical approach to increase wine quality, *Applied Biosciences*, 2(3), pp. 347-372, https://doi.org/10.3390/applbiosci2030023

Salimov V. (2022), Examination of variability in morphological and biological characteristics of some grape varieties of Azerbaijan, *Viticulture Studies*, 2(2), pp. 81–93, https://doi.org/10.52001/vis.2022.13.81.93

Van Leeuwen C., Seguin G. (2006), The concept of terroir in viticulture, *Journal of Wine Research*, 17(1), pp. 1–10, https://doi.org/10.1080/09571260600633135

Velioglu Y.S., Mazza G., Gao L., Qomah B.D. (1998), Antioxidant activity and total phenolics in selected fruits, vegetables and grain prod, *Journal of Agricultural and Food Chemistry*, 46(10), pp. 4113–4117, https://doi.org/10.1021/jf9801973

Vicente J., Baran Y., Navascués E., Santos A., Calderón F., Marquina D., Rauhut D., Benito S. (2022), Biological management of acidity in wine industry: A review, *International Journal of Food Microbiology*, 375, 109726, https://doi.org/10.1016/j.ijfoodmicro.2022.109726

Cite:

UFJ Style

Kazimova I., Omarova E., Nabiyev A., Gasimova A. (2024), Comparative analysis of the composition of Bayan Shirey, Rkatsiteli and Cabernet Sauvignon grape varieties for production of brandy wine materials, *Ukrainian Food Journal*, 13(4), pp. 694–707, https://doi.org/10.24263/2304-974X-2024-13-4-5

APA Style

Kazimova, I., Omarova, E., Nabiyev, A., & Gasimova A. (2024), Comparative analysis of the composition of Bayan Shirey, Rkatsiteli and Cabernet Sauvignon grape varieties for production of brandy wine materials. *Ukrainian Food Journal*, *13*(4), 694–707. https://doi.org/10.24263/2304-974X-2024-13-4-5

Fermented drink based on secondary raw milk materials

Irma Berulava[1], Maria Silagadze[1], Volodymyr Kovbasa[2], George Pkhakadze[3], Gulnara Khetsuriani[3], Marita Rukhadze[3]

1 – Akaki Tsereteli State University, Kutaisi, Georgia
2 – National University of Food Technologies, Kyiv, Ukraine
3 – Agricultural University of Georgia, Tbilisi, Georgia

Keywords:

Milk
Fermentation
Milk whey
Laurel cherry
Biological value

Article history:

Received 01.03.2024
Received in revised form 16.09.2024
Accepted 30.12.2024

Corresponding author:

Maria Silagadze
E-mail: mariasilagadze@yahoo.com

DOI:
10.24263/2304-974X-2024-13-4-6

Abstract

Introduction. The aim of the research was production of fermented milk drink with increased biological value for preventive nutrition based on secondary milk processing raw materials.

Materials and methods. Skim milk, demineralized milk whey, retentate, the bacterial starter cultures, laurel cherry fruits, fermented acid drink were used in the research. Titrated acidity, the content of proteins, fat, ash, and pectins were determined by ISO standards, the content of sugars was estimated by Bertrand's method, the content of total phenols by Folin Chocalteau method, and the number of viable bacterial cells by plate counting method.

Results and discussion. The fermentation process of demineralized whey, skim milk or retentate under the influence of direct addition of matsoni, kefir, yogurt or propionic bacterial starters was investigated. The best results were observed with the use of matsoni starter. After a 12-hour fermentation of demineralized milk whey, the number of viable cells of matsoni bacterial starter was $118\pm38x10^6$ colony formed units (CFU)/mL, in skim milk it was $135\pm62x10^6$ CFU/mL, and in retentate it was 127±52 CFU/mL. After the bacterial starter culture of matsoni, the best results were shown by the bacterial starter cultures of kefir, yogurt and finally propionic. In the fermentation process, the desired result of titrated and active acidities (800T, pH 3.62) was achieved by using the bacterial starter culture of matsoni.

To achieve the final optimal acidity of a prophylactic fermented milk drink (80–1000T, pH 4.2–4.5), out of different compositions made by using bacterial starter cultures of matsoni, kefir, yogurt, and propionic, two compositions were considered the best, in which the ratio of matsoni, yogurt, and propionic was 1.0:0.5:1.0 and 1.0:0.5:0.5, respectively. During this time, the optimal duration of the fermentation process was 5-6.5 hours. In the composition of the fermented milk drink, laurel cherry fruits were used as fillers. Based on the study of their chemical composition, it was determined that laurel cherry fruits are characterized by a high content of main components – sugars (16.20±0.42%), nitrogenous substances (1.92±0.09%), vitamin C (16.10±0.22%), pectin substances (0.78±0.21%), and total phenolic compounds (420±0.35 mg/100 g). Based on the sensory evaluation, the optimal amount of laurel cherry puree (3–5%) was determined for the fermented milk product. Prophylactic fermented milk drink technology was proposed.

Conclusions. Fermented milk drink was proposed based on secondary raw materials of milk and vegetable raw materials (laurel cherry fruits).

Introduction

Due to the shortage of food resources in the world, the maximum utilization of valuable secondary products of processing raw materials is of particular importance (Ivanov et al., 2021; Jolanta et al., 2016; Stabnikova et al., 2021, 2024a). Secondary raw materials for milk processing deserve special attention, especially milk whey, whose utilization factor is currently unacceptably low. Only 35–40% of milk whey is recycled, and it is mostly poured into the sewer system, causing environmental pollution. Especially serious problems are caused by curd whey due to its high acidity (70–75 °T). The full utilization of milk whey and other secondary milk raw materials for use in the production of high biological value, low-calorie, and low-glycemic functional fermented milk drink is still a worldwide problem (Ayed et al., 2023; Kochubei-Lytvynenko et al., 2022).

The dairy industry in Georgia loses thousands of tons of that valuable raw material every year, of which milk whey deserves special attention (Rukhadze et al., 2021). It is a low-calorie product (18-20 kcal/100 g) and has a low glycemic index (24), which is why it is considered a universal bio-eco-friendly raw material of natural origin for the production of dietary and functional food products (Ahmed et al., 2023; Jolanta et al., 2016).

The production of liquid fermented beverages, which does not require large expenditures, can be considered as one of the areas of cost-effective use of whey (Jeličić et al., 2008). The development of food products based on the beneficial substances of milk passed into the milk whey, especially functional fermented milk drinks, remains very relevant today (Reis et al., 2021).

The main methods of increasing the biological value of fermented milk drinks and ensuring their pre- and probiotic properties are the use of highly effective multi-component bacterial starters (Amiranashvili et al., 2015; Pereira et all., 2015; Pescuma et al. 2010) with the addition of fruit juices (Chatterjee, 2015; Idan, 2021; Thakkar et al., 2018), fruit's pulp (Elkot et al., 2023a), extracts of phyto-raw materials (M'hir et al., 2023; Seyhan et al., 2016), germinated grains of various cereals and legumes (Criste et al., 2023; Emkani et al., 2022), soybean oil as a source of polyunsaturated fatty acids (Vlaseva et al., 2012), and algae (Elkot et al., 2023b).

The popularity of using plant extracts in fermented milk products is due to the presence of a wide range of biologically active substances such as vitamins, flavonoids, antioxidants, tannins, macro- and microelements. The combination of lactic acid microflora and biologically active substances of fruits and berries allows to significantly expanding the range of functional products (Farmani et al., 2024; Szafrańska et al., 2024).

Based on the above, it can be concluded that increasing the dietary and health properties of fermented milk products by enriching them with probiotic bacteria and prebiotics are a relevant area in the creation of functional food products.

The research aims to develop a high biological value fermented milk drink based on the secondary raw materials of milk processing to be used for preventive nutrition.

Materials and methods

Chemicals

All reagents used were of USP purity or higher. All solvents, including water, were used with an LC/MS label.

Materials

Secondary raw materials from milk processing, namely, skim milk, demineralized milk whey, and milk retentate; the bacterial starters, in particular, matsoni, kefir, yogurt, and propionic starters; a plant-based supplement (laurel cherry fruits); structure stabilizer (puree of fruits) were used as materials in the research. Skim milk, demineralized milk whey, and milk retentate were obtained from the milk processing enterprise LLC "Atinati".

Skim milk is a by-product in the production of cream, sour cream, and butter. The most valuable components in it are protein and carbohydrates. Skim milk contains high biological value protein (up to 4%), water- and fat-soluble vitamins.

Demineralized milk whey was obtained from LLC Atinati with a level of demineralization of 85–90% and a level of acidity neutralization of pH 6.0–6.5 (Rukhadze et al., 2021). Demineralized milk whey is a source of important food nutrients (Kochubei-Lytvynenko et al., 2023). It contains more than two hundred biologically active substances, almost all water-soluble and finely dispersed components of milk.

Milk retentate, or a milk ultraconcentrate, is a concentrated milk protein, which is obtained because of ultrafiltration of milk, semi-skim, or skim milk.

Matsoni, kefir, yogurt, and propionic starter cultures were purchased from LLC "SAMAIA".

Matsoni starter culture contains *Lactobacillus delbrueckii* subsp. *bulgaricus*, *Streptococcus salivarius* subsp. *thermophilus*, and *Lactobacillus delbrueckii* subsp. *lactis* (Amiranashvili et al., 2014; 2015).

Kefir starter culture contains *Lactococcus lactis* subsp. *lactis, L. lactis* subsp. *cremoris, Leuconostoc mesenteroides* subsp. *cremoris, L. lactis* subsp. *lactis biovar diacetylactis, Lactobacillus delbrueckii* subsp. *bulgaricus,* and *Saccharomyces cerevisiae*.

Yogurt starter culture consists of *Lactobacillus acidophilus*, *Lactobacillus casei*, *Streptococcus lactis*, *Lactobacillus plantarum*, *Streptococcus thermophilus*, and *Lactobacillus bulgaricus*.

Propionic starter culture was a propionic acid bacteria *Propionibacterium shermanii* – KM 186 strain.

A plant-based supplement laurel cherry fruits, grown in the Adjara region taken from the harvest of 2023 at perfect ripeness. Samples were stored in refrigerated chambers prior to analysis (Figure 1).

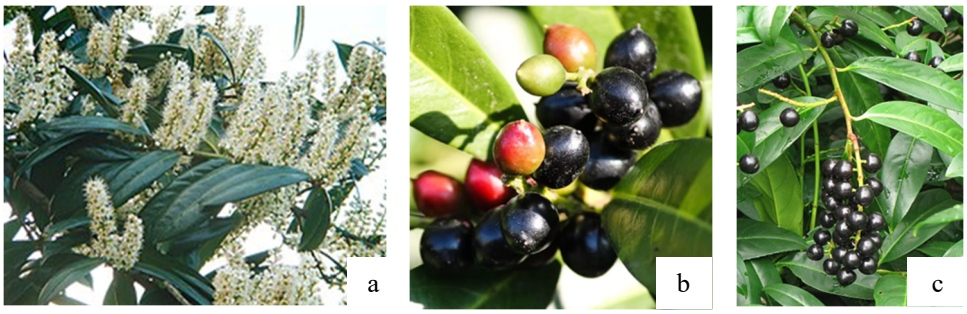

Figure 1. Laurel cherry during flowering (a); ripening fruits (b); ripe fruits of the wild-growing laurel cherry (c)

The laurel cherry is widespread in the subtropical zone of Georgia, especially in Adjara. The fruits of the plant have an individual, distinctive, unforgettable, velvety taste and aroma. The laurel cherry fruits contain polyphenols, among which anthocyanins are predominant, glycosides, tannins, and possess high antioxidant activity and can be used for the production of functional food (Minadze, 2006; Minadze et al., 2006; Stabnikova et al., 2024b).

The laurel cherry fruit puree was cooked in the following order: selected and washed fruits were peeled and blended. The obtained mass was rubbed through a sieve with a hole diameter of 0.5 mm, and then the mass prepared in this way was used in the preparation of a fermented milk drink.

Fermented milk drink was prepared from skim milk with a dry matter content of up to 9.5%, acidity of up to 20 °T; demineralized milk whey with a dry matter content of up to 7%, and milk retentate taken in a ratio of 1.0:2.0 :0.2 (Patent GEO No. 7334). All components were mixed, pasteurized at 72–75 °C, cooled to a temperature of 32–38 °C, and bacterial starter culture was introduced into it. Then, a sweetener and filler were added (laurel cherry fruit puree), which simultaneously played the role of a structure stabilizer and a flavor additive. Coagulation was carried out for 5.0–6.5 hours, at a temperature of 35–37 °C, until an acidity of 80–100 °T was reached. After that, it was pasteurized, homogenized, cooled, and bottled. The main components were used in the following ratio, wt. %: milky composition, 85–87; bacterial starter culture, 3–5; sweetener (palatinose), 1–3; laurel cherry fruit puree, 3-5.

Methods

Determination of dry matter content. The amount of dry matter in secondary milk raw materials and plant-based supplements was determined using a RADWAG MA 50r moisture meter (Finland), where drying was carried out under the influence of infrared rays. 5-10 g of samples were placed on the cup of this device, and drying was carried out at 105 ^{0}C. The screen recorded the moisture content in the analysis samples in %. The amount of dry matter was calculated as the difference: 100 minus the amount of moisture content.

Determination of acidity. Titrated acidity was determined by the titration method: for a plant-based supplement – according to ISO-750-1998 standard, for secondary milk raw materials – according to ISO/TS 22113:2012 standard, and active acidity was determined using PH-meter Metlter Toledo (USA).

Determination of total sugars. Total sugars were determined by the Bertrand's method (Surmanidze, 2023).

Determination of total phenolic content. Folin-Chokalteu method was used to determine the amount of phenolic substances in fruits (Bond et al., 2003; Tkesheliadze et al., 2022).

Determination of the total amount of proteins. The total amount of proteins was determined by the Kjeldahl method according to ISO 8968-1:2014.

Determination of the total amount of fats. The total amount of fats was determined by the Soxhlet method. Hydrolysis of the sample was carried out on the device HydrolEx H-506, and extraction was carried out on the extractor FatExtractor E-500. The resulting fat was dried to a constant weight and then weighed, and the fat content of the sample was calculated following ISO 14156:2001/IDF 172:2001.

Determination of total ash content. Total ash content was determined following ISO/CD 9877 IDF 258.

Determination of the amount of pectin substances. The amount of pectin substances was determined according to ISO 5773:2023(E).

Determination of vitamin C content. The quantitative determination of vitamin C in plant materials was carried out using a method based on reducing properties: a blue solution of 2,6-dichlorophenolindophenol is reduced to a colorless compound by plant extracts containing ascorbic acid (Surmanidze, 2023).

Determination of the number of microorganisms. The number of microorganisms was determined by counting colonies. 10 g of product were taken and mixed with 90 ml of buffered peptone water or a 0.85%-solution of table salt. 10 test tubes were placed on the test bench, each of which contained 9 mL of buffered peptone water. After the initial dilution, 1 mL of the test product was added to the first test tube with a sterile pipette. Using a sterile pipette, 1 mL was transferred from the first test tube to the next test tube, and so on. As a result, dilutions of 1:10, 1:100, and 1:1000 were obtained. The time from dilution preparation to inoculation exceeded 45 min. Before sowing, the cup was assigned a number. From each dilution, 1-1 mL of the analyte compound was taken and applied to two Petri dishes (for parallel determination). Then thawed and cooled to 45 °C food agar was added in the amount of 12-15 mL. With a circular movement of the hand, the cup was moved on the horizontal surface of the table, so that the contents were distributed in the form of equal layers over the entire area of the bottom. The process continued until the agar solidified. The cup with the seed was placed in a thermostat upside down for incubation at 30 °C for 72±3 hours. After this time, the colonies grown both on the surface and in the depth of the agar were examined. Colonies were counted using a colony counter. The arithmetic mean was calculated for each dilution separately.

Sensory evaluation. The sensory evaluation of the fermented milk drink was carried out on a 10-point scale according to the following indicators: homogeneous, slightly viscous, with liquid whey, characteristic color of the product, pure lactic acid taste, moderately sweet, and moderate taste of filler. In advance, the characteristics of each score were introduced. The best indicator was valued at 10 points, and the unsatisfactory one at 1 point. Five tasters participated in the sensory evaluation. They were selected from the staff and students of the Department of Food Technology of Akaki Tsereteli State University. The final scores were calculated by the arithmetic mean of the points assessed by each taster (Karchava et al., 2022).

Calculation of caloric content. To determine the caloric content of the research samples, the amount of proteins, fats, and carbohydrates contained in them were taken into account, multiplied by their conversion coefficient (4, 9, and 4 respectively), and the results were summed up.

Statistical analysis

Mathematical processing of the experimental data was performed according to the results of 3-5 times repetitions of the tests with the methods of statistics and regression analysis using Windows IBM SPSS Statistics software program (version 20.0, IBM, Armonk, New York, USA).

These studies were conducted at the Department of Food Technologies of Akaki Tsereteli State University (Georgia, Kutaisi) and the Western Georgian Regional Center of Chromatography Chromatographic Center of Shota Rustaveli State University in Batumi.

Results and discussion

Characteristics of secondary raw milk materials used for fermented milk drink

Skim milk, demineralized milk whey, and milk retentate were chosen as base for fermented milk drink creation. Their proximate composition was studied and caloric content was calculated (Table 1).

Table 1

Proximate composition of secondary raw materials

Compounds	Milk whey	Skim milk	Retentate
Moisture, %	93.28±1.31	90.30±1.08	80.4±1.32
Protein, %	0.87±0.11	3.60±0.08	10.7±0.15
Fat,%	0.11±0.05	0.08±0.02	0.72±0.02
Carbohydrate, %	5.75±0.06	6.02±0.05	8.90±0.09
Ash, %	0.63±0.04	0.72±0.05	0.20±0.01
Calorie content, kcal/100 ml	24.9	36.32	77.60

The content of dry matter in the secondary raw milk materials was as follows: in demineralized milk whey: 6.72±0.11%, in skim milk 9.7±0.08%, and in retentate 19.6%±0.13. The highest contents of proteins and carbohydrates were observed in the retentate and they were 10.7±0.15% and 8.7±0.11%, respectively. Fat and ash contents were recorded in insignificant amounts and did not exceed 0.11±0.05% and 0.72±0.02%, respectively. As for caloric content, it was 24.91 kcal/100 ml for demineralized milk whey, 36.32 kcal/100 ml for skim milk, and 77.6 kcal/100 ml for retentate. All secondary raw materials of milk are low-calorie (Ahmed et al., 2023) and acceptable for the preparation of prophylactic fermented milk drinks (Reis et al., 2021).

Development of starter cultures in secondary raw milk materials

To produce a fermented milk product, cheese whey, skim milk, and retentate were proposed, so it was necessary to study the development of starter cultures in this environment. Considering the data of several studies that noted that during the production and storage of milk and fermented milk drinks based on whey, especially when using various supplements, liquid stratification (separation of whey) occurs (Chavan et al., 2018; Paula et al., 2021), therefore demineralized whey was used – purified from suspended protein fragments and mineral salts. The activity of the development of starter microflora within 12 hours during the fermentation process was estimated by titrated active acidity and the number of viable cells of starter microorganisms (Table 2). The experiments were conducted at a 5%-dosage of starter cultures.

Table 2

Comparative characteristics of starter cultures in skim milk, whey, and retentate

Indicators	Starter culture			
	Propionic	Matsoni	Kefir	Yogurt
Demineralized cheese whey				
The number of vital cells, CFU/mL	90±51	118±38	110±42	102±62
Titrated acidity, °T	47±2	80±1	72±2	68±3
Active acidity, pH	4.75±0.01	3.62±0,02	4.02±0,01	4.35±0,01
Skim milk				
The number of vital cells, CFU/mL	125±68	135±62	127±52	119±82
Titrated acidity, °T	71±2	87±2	82±2	69±2
Active acidity, pH	4.06±0.01	3.92±0.01	4.21±0.02	4.42±0.01
Retentate				
The number of vital cells, CFU/mL	118±68	127±52	123±65	116±58
Titrated acidity, °T	68±2	79±2	71±1	62±3
Active acidity, pH	4.3±0.01	4.13±0.01	4.26±0.02	4.37±0.01

Based on the comparative analysis of the data presented in Table 1, it was revealed that the activity of bacterial starter cultures in demineralized milk whey, skim milk, and retentate did not differ significantly. Considering all indicators, the best results were achieved using the bacterial starter culture of matsoni. After a 12-hour fermentation of demineralized milk whey, the number of viable cells of matsoni bacterial starter was 118±38x10^6 CFU/mL, in skim milk 135±62x10^6 CFU/mL, and in retentate 127±52 x10^6 CFU/mL. After the bacterial starter culture of matsoni, the best results were shown by the bacterial starter cultures of kefir, yogurt, and finally propionic (Gungor et al., 2024). As for the titrated and active acidities (80 °T, pH 3.62), the bacterial starter culture of matsoni was considered dominant in this case as well.

Changes in titrated and active acidities during process of fermentation (coagulation) of secondary milk raw materials using different bacterial starter cultures.

The fermentation process in secondary raw milk lasted for 12 hours. Determination of titrated and active acidities was done every 3 hours (Figures 2 and 3).

As shown in Figures 3 and 4, the best results were achieved by using the matsoni starter culture in different secondary milk raw materials for 12 hours (80 °T, pH – 3.62). The lowest activity was observed with propionic. Considering that the properties of starter cultures of matsoni and kefir, as well as their fermentation activities are close to each other, the bacterial starter culture of kefir was excluded from the composition of bacterial starter cultures for further experiments.

Determining the ratio of bacterial starter cultures for a milky composition

Further, with different ratios of the starters used in the bacterial composition, the time required for curd formation and the final acidity of the fermented milk base were established. The following ratios of starter microflora were compiled:

1. M :Y : P= 1.0 : 1.0 : 1.0 ; 2. M : Y : P = 1.0 : 0.5 : 1.0 ;
3. M : Y: P = 1.0 : 0.5 : 0.5 ; 4. M : Y: P = 2.0 : 1.0 : 1.0 ;
5. M :Y: P = 1.0 : 0.5 : 1.0 .

(M – marsoni starter: K – kefir starter: Y – yogurt starter: P – propionic starter)

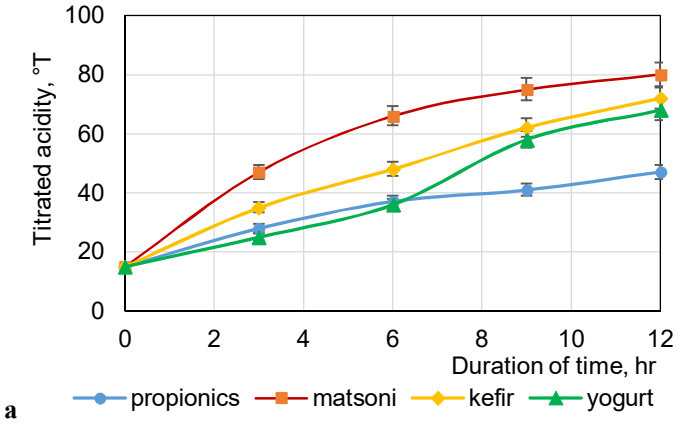

a

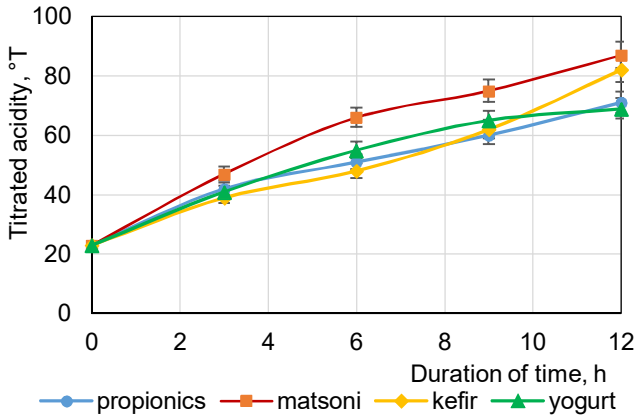

b

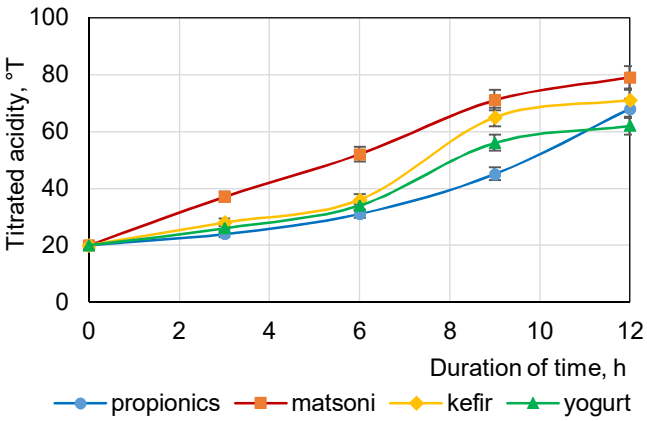

c

Figure 2. Change in titrated acidity during fermentation process using different bacterial starter cultures in: milk whey (a); skim milk (b); in retentate (c)

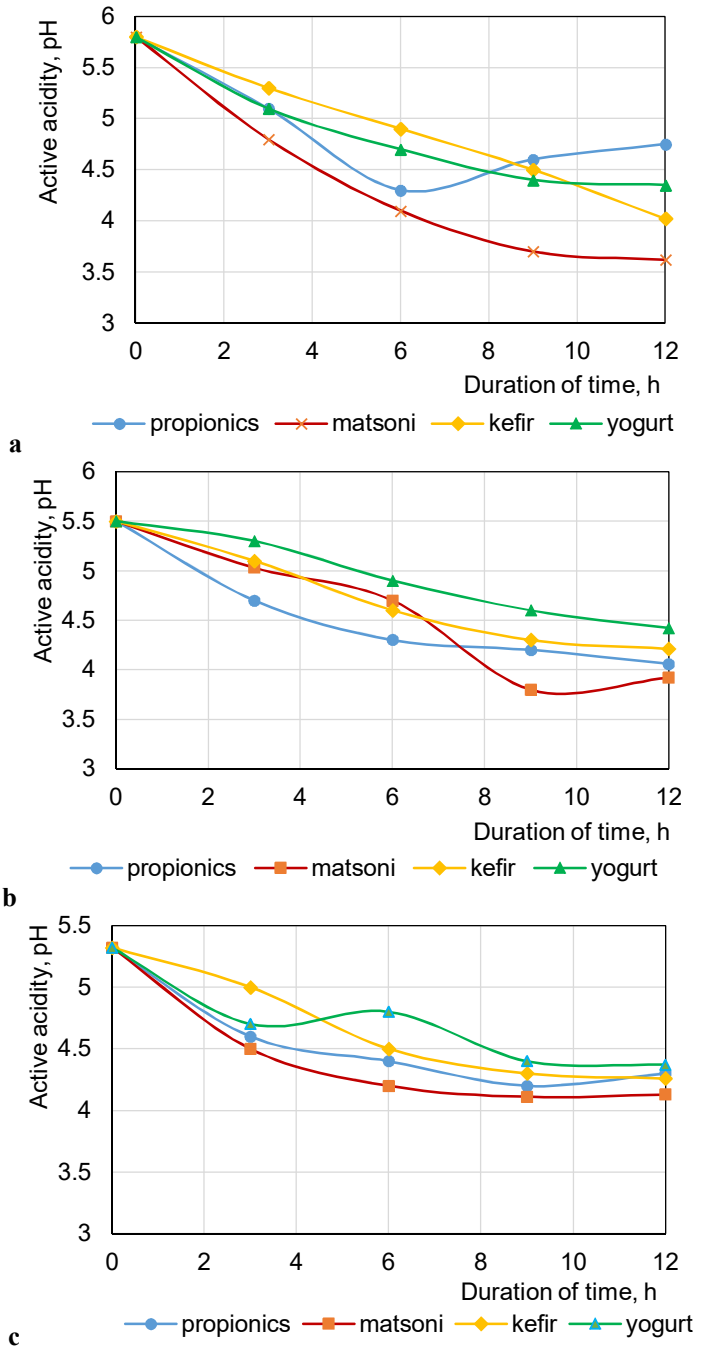

Figure 3. Change in active acidity during fermentation process using different bacterial starter cultures in: milk whey (a); in skim milk (b); in retentate (c)

Table 3 presents the activity of development of probiotic microorganisms in milk-whey medium with different initial ratios of starter microflora.

Table 3

Curd formation and changes in acidity during fermentation of milk-whey fermented drinks

Proportion of starters in the bacterial composition (dosage – 5%)	Time required for curd formation, h	Acidity	
		°T	pH
M : Y : P = 1.0 : 1.0 : 1.0	8.5	74±2	4.76±0.01
M : Y : P = 1.0 : 0.5 : 1.0	6.5	88±1	4.58±0.02
M : Y : P = 1.0 : 0.5 : 0.5	5.0	92±1	4.51±0.01
M : Y : P = 2.0 : 1.0 : 1.0	10.5	75±3	4.76±0.01
M : Y : P = 2.0 : 0.5 : 1.0	14.0	79±2	4.72±0.02

To achieve the predetermined final optimal acidity of a prophylactic fermented milk drink (80-100 ^{0}T, pH 4.2-4.5), the best result was shown by the composition of bacterial starter cultures in the following ratios: M : Y : P = 1.0 : 0.5 : 1.0; M : Y: P = 1.0 : 0.5 : 0.5.

Plant-based supplement for a fermented milk drink

The fruits of laurel cherry were used in the form of a plant-based supplement, as a structure stabilizer in the process of fermentation and delaying the milky composition.

Chemical composition of the laurel cherry fruits

The overall chemical composition of these fruits and the fractional composition of their pectin substances were determined (Table 4, Figure 4).

Table 4

Chemical composition of laurel cherry fruits

Characteristics	Samples of laurel cherry	
	Black-fruited, large	Wild-growing
Mass fraction of dry matter, %	21.80±0.21	17.10±0.32
Total sugars, %	16.20±0.42	11.71±0.35
Acidity, % (in terms of malic acid)	0.26±0.11	0.24±0.12
Pectin substances, % (in terms of the raw mass)	0.78±0.21	0.48±0.33
Total phenols, mg/100 g	420±0.35	480±0.15
Nitrogenous substances, %	1.92±0.09	1.87±0.10
Vitamin C, mg%	16.10±0.22	13.7±0.16

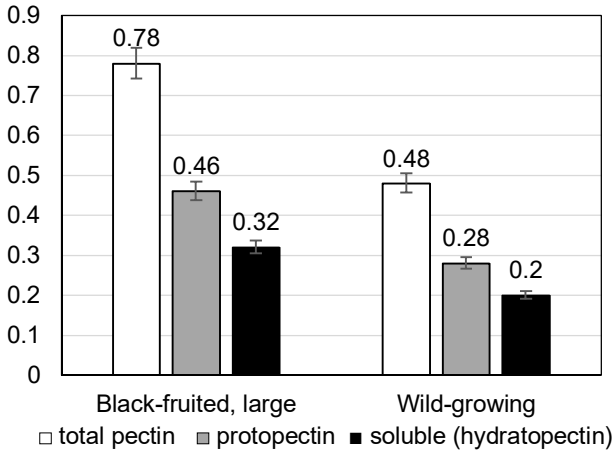

Figure 4. Fractional composition of pectin substances of the laurel cherry fruit

It was determined that the studied raw materials are valuable not only for their taste properties, but also due to their composition, high content of pectin substances, and phenolic compounds. These results are close to the results of research conducted by different researchers at different times. In particular, the chemical composition of the fruits of laurel cherry common in the subtropical zone of western Georgia and Adjara has been determined for use in the technology of food coloring (Surmanidze, 2023), confectionery (Minadze, 2006) and alcoholic beverages (Japaridze et al., 2005). Based on the analysis of the chemical composition of the fruits of laurel cherry (black-fruited large and wild growing), the black-fruited large fruits were used for further research.

Optimal amount of plant-based supplement for fermented milk drink

At the next stage of the research, the fermented milk product was mixed with the puree of the laurel cherry fruits in different percentages: 1, 3, 5 and 7%. To determine the optimal amount, an organoleptic evaluation was carried out. A fermented milk product with the addition of 3-5% of laurel cherry puree was considered the best. The results are illustrated in Figure 5.

Based on repeated experiments, the amount of filler and the technological parameters of the drink preparation were specified, which was reflected in the developed and proposed technology to produce a fermented milk drink, which is described in the section: “Materials and methods”.

The resulting fermented milk drink has a uniform, gentle consistency, natural color, and original aroma of the vegetable component – laurel cherry fruits. The ratio of secondary products of milk processing, bacterial starter culture, and fillers was selected not only based on their biological compatibility, but also based on the taste properties, to achieve a uniform organoleptic original range, which will additionally have a preventive effect on the human body.

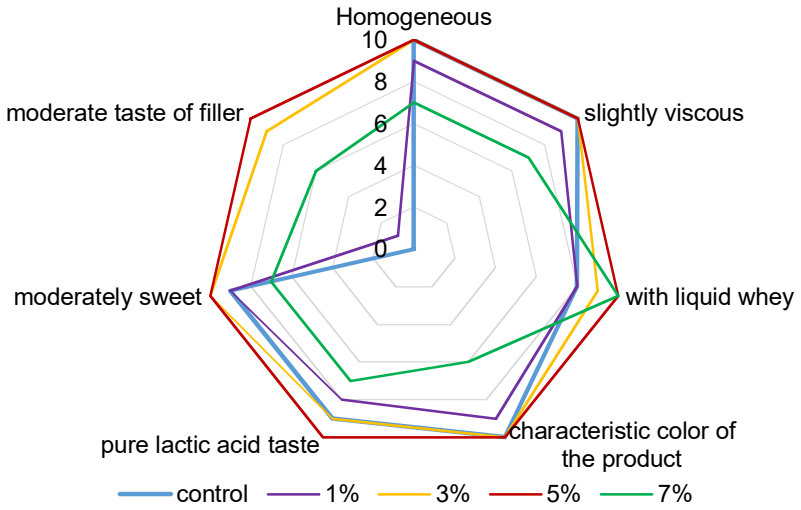

Figure 5. Influence of doses of laurel cherry puree on sensory parameters of fermented milk product

Conclusions

1. In the fermentation process of demineralized milk whey, skim milk, and retentate, with the action of direct application of the bacterial starter cultures – matsoni, kefir, yogurt, and propionic, the best results were observed with the use of matsoni bacterial starter culture. After a 12-hour fermentation of demineralized milk whey, the number of viable cells of matsoni bacterial starter was 118±38x10^6 CFU/mL, in skim milk 135±62x10^6 CFU/mL, and in retentate 127±52x10^6 CFU/mL. After the bacterial starter culture of matsoni, the best results were shown by the bacterial starter cultures of kefir, yogurt and finally propionic.
2. In the fermentation process, the desired result of titrated and active acidities (800T, pH 3.62) was achieved by using the bacterial starter culture of matsoni. The lowest activity was observed with propionic.
3. Various compositions of bacterial starter cultures were prepared. To achieve the final optimal acidity of a fermented milk drink (80–100 °T, pH 4.2–4.5), the composition of bacterial starter cultures was considered the best in the following ratios: M : Y : P = 1.0 :0.5 :1.0; M : Y: P = 1.0 : 0.5 : 0.5. At this time, the optimal duration of the fermentation process was 5-6.5 hours.
4. There was determined the feasibility of using a plant-based supplement (laurel cherry fruits) as a filler in a fermented milk drink due to its taste properties, chemical composition, sugars (16.20±0.42%), nitrogenous substances (1.92±0.09%), vitamin C (16.10±0.22%), considering the high content of pectin substances (0.78±0.21%) and total phenolic compounds (420±0.35 mg/100 g).
5. Based on the sensory evaluation, the optimal amount of laurel cherry puree for a fermented milk drink was determined as 3–5%.

Acknowledgements. This work was supported by Shota Rustaveli National Science Foundation of Georgia (SRNSFG) (FR-23-3721 Development of innovative technology for production of whey-based functional lactic acid drink).

References

Ahmed T., Sabuz A.A., Mohaldar A., Fardows H.M.S., Inbaraj B.S., Sharma M., Rana M.R., Sridhar K. (2023), Development of novel whey-mango based mixed beverage: Effect of storage on physicochemical, microbiological, and sensory analysis, *Foods,* 12(2), 237, https://doi.org/10.3390/foods12020237

Amiranashvili L., Gagelidze N., Varsimashvili Kh., Tolordava L., Tinikashvili L., Kirtadze E., Sadunashvili T., Kvesityadze G., Torok T., Mills D., Bokulich (2014), Antimicrobial activity of lactic acid bacteria isolated from traditional fermented milk products in Georgia, *The International Scientific Conference on Probiotics and Prebiotics,* Budapest, Hungary, 21st – 23rd June 2016, pp. 63-64.

Amiranashvili L., Gagelidze N., Varsimashvili K., Tolordava L., Tinikashvili L., Sadunashvili T. (2015), Prospects for usage of lactic acid bacteria isolated from different regions of Georgia as Matsoni starters, *International scientific-practical conference: Innovative technologies for production of functional foods,* Kutaisi, Georgia, pp. 194-198.

Ayed L., M'hir S., Asses N. (2023), Sustainable whey processing techniques: Innovations in derivative and beverage production, *Food Bioscience*, 53, 102642, https://doi.org/10.1016/j.fbio.2023.102642

Bond T.J., Lewis J.R., Davis A., Davis A.P. (2003), Methods of polyphenols analysis, In: Santos-Bulga C., Williamson G. (Eds.), *Analysis and Purification of Catechins and their Transformation Products*, The Royal Society of Chemistry.

Chatterjee G., De Neve J., Dutta A., Das S. (2015), Formulation and statistical evaluation of a ready-to-to-drink whey based orange beverage and its storage stability, *Revista Mexicana de Ingeniería Química*, 14(2), pp. 253-264, https://www.researchgate.net/publication/283099865

Chavan M., Gat Y., Harmalkar M., Waghmare R. (2018), Development of non-dairy fermented probiotic drink based on germinated and ungerminated cereals and legume, *LWT,* 91, pp. 339-344, https://doi.org/10.1016/j.lwt.2018.01.070

Criste A.D., Urcan A.C., Coroian C.O., Copolovici L., Copolovici D.M., Burtescu R.F., Oláh, N.K. (2023), Plant-based beverages from germinated and ungerminated seeds, as a source of probiotics, and bioactive compounds with health benefits—Part 1: Legumes*, Agriculture,* 13(6), 1185, https://doi.org/10.3390/agriculture13061185

Elkot W.F., El-Sawah T.H., Abdeldaiem M.A., Alnuzaili E.S., Eljeam A.R.A.H., Al-Farga A., Elmahdy A. (2023a), Effect of using dried white sapote fruit (*Casimiroa edulis*) on the quality characteristics of bio-low-fat goat milk yoghurt drink, *Saudi Journal of Biological Sciences,* 30(2), 103844, https://doi.org/10.1016/j.sjbs.2023.103844

Elkot W.F., Elmahdy A., El-Sawah T.H., Alghamdia O.A., Alhag S.K., Al-Shahari E.A., Al-Farga A., Ismail H.A. (2023b), Development and characterization of a novel flavored functional fermented whey-based sports beverage fortified with *Spirulina platensis*, *International Journal of Biological Macromolecules*, 258(Pt 2), 128999, https://doi.org/10.1016/j.ijbiomac.2023.128999

Emkani M., Oliete B., Saure R. (2022), Effect of lactic acid fermentation on legume protein, *Fermentation*, 8(6), 244, https://doi.org/10.3390/fermentation8060244

Farmani B., Bodbodak S., Yerlikaya O. (2024), Development of a novel milk-based product fortified with carrot juice, *Food Bioscience,* 58, 103792, https://doi.org/10.1016/j.fbio.2024.103792

Paula N.R.F., Araújo É.O., Martins C.R., Martins V.R. (2021), Processing of fermented milk drink with different whey concentrations and addition of fruit pulps, *Australian Journal of Crop Science,* 15(7), pp. 1013-1019, https://doi.org/10.21475/ajcs.21.15.07.p3022

Gungor G., Akpinar A., Yerlikay O. (2024), Production of plant-based fermented beverages using probiotic starter cultures and *Propionibacterium* spp., *Food Bioscience*, 59, 103840, https://doi.org/10.1016/j.fbio.2024.103840

Idan M.A., Al-Shawi S.G., Khudhair N.A., (2021), Developing of grape-flavored whey probiotic beverage, *Annals of the Romanian Society for Cell Biology,* 25(1), pp. 4732-4741, https://www.researchgate.net/publication/349869476

ISO 14156:2001 | IDF 172:2001. Milk and milk products — Extraction methods for lipids and liposoluble compounds.

ISO 5773:2023(E). Textiles — Determination of components in flax fibres. Paragraph 7.4.
ISO 750:1998. Fruit and vegetable products — Determination of titratable acidity.
ISO 8968-1:2014. Milk and milk products – Determination of nitrogen content. Part 1: Kjeldahl principle and crude protein calculation.
ISO/CD 9877 | IDF 258. Milk and milk products — Determination of ash.
Ivanov V., Shevchenko O., Marynin A., Stabnikov V., Gubenia O., Stabnikova O., Shevchenko A., Gavva O., Saliuk A. (2021), Trends and expected benefits of the breaking edge food technologies in 2021–2030, *Ukrainian Food Journal,* 10(1), pp. 7-36, https://doi.org/10.24263/2304-974X-2021-10-1-3
Kochubei-Lytvynenko O., Bilyk O., Bondarenko Y., Stabnikov V. (2022), Whey proteins in bakery products, In: O. Paredes-López, O. Shevchenko, V. Stabnikov, V. Ivanov, (Eds.), *Bioenhancement and Fortification of Foods for a Healthy Diet*, CRC Press, Boca Raton, London, pp. 67-88, https://doi.org/.1201/9781003225287-5
Kochubei-Lytvynenko O., Bilyk O., Stabnikov V., Dubivko A. (2023), Milk whey enriched with magnesium and manganese for food production, In: O. Stabnikova, O. Shevchenko, V. Stabnikov, O. Paredes-López (Eds.), *Bioconversion of Waste to Value-Added Products*, pp. 113-128, CRC Press, Boca Raton, London, https://doi.org/10.1201/9781003329671-4
Japaridze I.V., Papunidze G.R., Vanidze M.R., Kalandia A.G. (2005), Bioflavonoids of cherry laurel fruits, *Beer and Beverages*, 3.
Jeličić I., Božanić R., Tratnik L., (2008), Whey-based beverages – a new generation of dairy products, *Mljekarstvo,* 58(3), pp. 257-274, https://www.researchgate.net/publication/228631581
Jolanta B.K., Tomasz D., Emilia J.T., Bartosz S. (2016), Use of whey and whey preparations in the food industry – a review, *Polish Journal of Food and Nutrition Sciences,* 66(3), pp. 157–165, https://doi.org/10.1515/pjfns-2015-0052
Karchava M., Berulava I., Khetsuriani G. (2022), *Food Chemistry*, Akaki Tsereteli State University Publishing House, Kutaisi.
M'hir S., Ziadi M., Mejri A., Ayed L. (2023), Mixture of whey-milk and palm sap for novel kefir beverage using simplex-centroid mixture design, *Kuwait Journal of Science,* 50(6), pp. 690-696, https://doi.org/10.1016/j.kjs.2023.04.008
Minadze N. (2006), Chemical-technological investigation of laurel cherry common in western Georgia with aim of producing food products, PhD thesis.
Minadze N., Khetsuriani G., Silagadze M. (2006), Cherry laurel fruit phenolic compounds, *Problems of Agricultural Sciences*, pp. 82-85.
Pereira C., Henriques M., Gomes D., Gomez-Zavaglia A., De Antoni G. (2015), Novel functional whey-based drinks with great potential in the dairy industry, *Food Technology and Biotechnology,* 53(3), pp. 307–314, https://doi.org/10.17113/ftb.53.03.15.4043
Pescuma M., Hébert E.M., Mozzi F., de Valdez G.F. (2010), Functional fermented whey-based beverage using lactic acid bacteria, *International Journal of Food Microbiology*, 141(1–2), pp. 73-81, https://doi.org/10.1016/j.ijfoodmicro.2010.04.011
Reis de M.S., Mendes G.D.R.L., Mesquita B.M.A.C., Lima W.J.N., Pinheiro C.A.F.D., Ruas F.A.O., Santos G.L.M., Brandi I.V. (2021), Development of milk drink with whey fermented and acceptability by children and adolescents, *Journal of Food Science and Technology*, 58(7), pp. 2847–2852, https://doi.org/10.1007/s13197-021-05003-w
Rukhadze S., Pkhakadze G., Silagadze M., Khetsuriani G., (2021), The technological process improvement for lactose production from milk whey using the method of bipolar electrodialysis, *Austrian Journal of Technological and Natural Sciences* 3(4), pp. 37-41, https://doi.org/10.29013/ajt-21-3.4-37-42
Seyhan E., Yaman H., Özer B. (2016), Production of a whey-based functional beverage supplemented with soy isoflavones and phytosterols, *The International Journal of Dairy Technology*, 69(1), pp. 114-121, https://doi.org/10.1111/1471-0307.12229
Stabnikova O., Marinin A., Stabnikov V. (2021), Main trends in application of novel natural additives for food production, *Ukrainian Food Journal*, 10(3), pp. 524–551, https://doi.org/10.24263/2304-974X-2021-10-3-8
Stabnikova O., Shevchenko A., Stabnikov V., Paredes-López O. (2024a), Utilization of plant processing wastes for enrichment of bakery and confectionery products, *Ukrainian Food Journal*, 12(2), pp. 299-308, https://doi.org/10.24263/2304-974X-2023-12-2-11

Stabnikova O., Stabnikov V., Paredes-López O. (2024b), Fruits of wild-grown shrubs for health nutrition, *Plant Foods for Human Nutrition*, 79(1), pp. 20-37, https://doi.org/10.1007/s11130-024-01144-3

Surmanidze D. (2023), Laurel cherry bioresources in Adjara, biovalue and promising processing technologies, PhD thesis.

Szafrańska J.O., Waraczewski R., Bartoń M., Wesołowska-Trojanowska M., Maziejuk W., Nowak P., Sołowiej B.G. (2024), The effect of organic fruit juices on physicochemical, microbiological and antioxidative aspects of organic goat's and cow's fermented whey beverages produced on laboratory and industrial scale, *Journal of Dairy Science*, 107(12), pp. 10481-10496, https://doi.org/10.3168/jds.2024-25350

Thakkar P., Vaghela, B., Patel A., Modi H.A. Prajapati J.B. (2018), Formulation and shelf life study of a whey-based functional beverage containing orange juice and probiotic organisms, *International Food Research Journal,* 25(4), pp. 1675-1681, https://www.researchgate.net/publication/327415913

Tkesheliadze E., Gagelidze N., Sadunishvil T., Herzig C. (2022), Fermentation of apple juice using selected autochthonous lactic acid bacteria, *Ukrainian Food Journal,* 11(1), pp. 52-63, https://doi.org/10.24263/2304-974X-2022-11-1-7

Vlaseva R., Perifanova-Nemska M., Denev P., Ivanova M. (2012), Development of technology for lactic acid beverage enriched with omega-3 and omega-6 fatty acids and dietary fiber, *International Conference for Renewable Resources and Plant Biotechnology 18th conference, NAROSSA® in Magdeburg,* Germany, June 4–5, 2012.

Cite:

UFJ Style

Berulava I., Silagadze M., Kovbasa V., Pkhakadze G., Khetsuriani G., Rukhadze M. (2024), Fermented drink based on secondary raw milk materials, *Ukrainian Food Journal*, 13(4), pp. 708–722, https://doi.org/10.24263/2304-974X-2024-13-4-6

APA Style

Berulava, I., Silagadze, M., Kovbasa, V., Pkhakadze, G., Khetsuriani, G., & Rukhadze M. (2024). Fermented drink based on secondary raw milk materials. *Ukrainian Food Journal*, *13*(4), 708–722. https://doi.org/10.24263/2304-974X-2024-13-4-6

Impact of heat treatment of sorghum grains on flour properties

Ana Batariuc[1], Mădălina Ungureanu-Iuga[1,2], Anca Becze[3], Lacrimioara Senila[3], Silvia Mironeasa[1]

1 – "Ştefan cel Mare" University of Suceava, Romania
2 – Mountain Economy Center (CE-MONT), Romanian Academy, Romania
3 – National Institute for Research and Development of Optoelectronics Bucharest INOE 2000, Romania

Keywords:

Red sorghum
Particle size
Nutritional profile

Article history:

Received 29.04.2024
Received in revised form 18.06.2024
Accepted 30.12.2024

Corresponding author:

Mădălina Ungureanu-Iuga
E-mail: madalina.iuga @usm.ro

DOI:
10.24263/2304-974X-2024-13-4-7

Abstract

Introduction. This paper aimed to evaluate the nutritional and rheological properties of heat-treated and untreated sorghum flour with medium size fraction (M) and integral.

Materials and methods. Amino acids were determined by high-performance liquid chromatography, fatty acids and volatiles by gas chromatography, minerals by atomic absorption spectrophotometry, and rheology by dynamic testing methods.

Results and discussion. The application of dry heat treatment on sorghum flour led to a reduction in the content of essential amino acids. However, a higher lysine content was observed in the treated M fraction compared to the control fraction. The content of non-essential amino acids significantly decreased after the application of heat treatment and grinding. The dry heat treatment temperature of 133 °C applied to the red sorghum grains, along with fractionation, resulted in an increase in the content of mono- and polyunsaturated fatty acids and a decrease in the saturated fatty acid content in the treated M fraction compared to the control fraction. There were considerable differences between samples regarding sodium, iron, zinc, and copper content. Heat treatment led to a decrease in the percentage of 2,4-pentadienenitrile volatile compound and the identification of 2,4-hexadienenitrile in the treated M fraction compared to the control fraction.

The obtained elastic modulus values showed that the dough prepared from the treated fraction M red sorghum flour possessed slightly higher elastic energy compared to the sample prepared from whole red sorghum flour treated at 133 °C. The maximum gelatinization temperature for the sample with the treated M fraction of red sorghum flour was lower than that of the control sample. The dough from treated M fraction of red sorghum flour showed higher compliance for both creep and recovery compared to that made from the control fraction.

Conclusion. Sorghum dry heat treatment and fractionation led to significant differences in nutritional and rheological profile.

Introduction

Sorghum (*Sorghum bicolor* L. Moench) originates from East Africa (Sudan and Ethiopia) and has come to be cultivated worldwide, being the fifth most cultivated cereal after corn, wheat, rice, and barley (Ratnavathi et al., 2016), due to its agronomic advantages, as it is resistant to drought, pests, and diseases (Pérez et al., 2010). The cultivation of sorghum is significant for semi-arid regions of the world, especially in Africa and Asia, due to its agronomic benefits in harsh environments, drought resistance, high productivity, and low production costs (Adebowale et al., 2020). Since the year 2000, the area allocated to this crop has come to represent approximately 3% of the total area occupied by cereal crops. Global production reached around 59 million tons in 2018 (Cabrera-Ramírez et al., 2020; Pezzali et al., 2020). The world's top five sorghum producers are the United States (25%), India (21.5%), Mexico (almost 11%), China (9%), and Nigeria (almost 7%). Together, these five countries account for 73% of total global production. Based on the region of cultivation and/or use by different populations, sorghum has various names. In Africa, it is known as large millet, milo, durra, and orshallu, while in China it is called gaoliang, and Indians call it jowar, cholam, or jonna (Djameh et al., 2015; Rashwan, 2017). Globally, the largest consumer of sorghum is China, and within the European Union, it is Spain. In the European Union, the most significant sorghum-cultivating countries are France and Italy.

In Romania, the surface used for sorghum cultivation in 2020 was 8.4 million hectares, with a production of 26.6 thousand tons (National Institute of Statistics: Bucharest, Romania, 2022), followed by Spain, Hungary, and Bulgaria. In Romania, both red and white sorghum hybrids are cultivated. Sorghum is an excellent source of starch and protein, containing phenolic compounds, such as flavonoids (Shahidi and Naczk, 1995), phenolic acids, and tannins. Starch and sugar are released more slowly from sorghum than from other cereals (Klopfenstein and Hoseney, 1995), which is beneficial for people with diabetes. As a potential source of resistant starch and β-glucans (Niba and Hoffman, 2003), sorghum can be used as a prebiotic food ingredient in value-added food products. Processed sorghum is consumed worldwide in various forms: bread, biscuits, cakes, couscous, tortillas, porridge, alcoholic and non-alcoholic beverages, extruded products, and pasta.

It has been asserted that sorghum has low protein quality due to the structural properties of kafirin, the predominant protein, a deficiency of amino acids such as threonine, tryptophan, and lysine, and interactions with phenolic molecules, such as condensed tannins, which form complexes with proteins and reduce their digestibility (Martinez et al., 2020). However, the gluten-free bakery industry is challenging, and currently, many researchers are focusing on composite flour formulations. Current research on heat-treated sorghum flour is limited, and a gap in food product development using this flour has been identified.

Understanding how certain physical treatments applied to sorghum grains affect the physicochemical composition of whole meal flour and different-sized sorghum flour particles, as well as their functionality, is important for managing the quality of finished products. The heat generated during the dry heat treatment process, as well as the frictional heat and mechanical energy required for grinding, can affect the structural and molecular properties of starch as well as other properties of sorghum grains. There is limited information on the characteristics of different-sized sorghum flour particles when sorghum grains are subjected to physical treatments. Additionally, knowledge of the nutritional and rheological properties of sorghum flour plays an essential role in explaining the complex interactions between components, along with the nature of the environment in which they are associated and investigated. Thus, this paper aimed to explore the characteristics of integral and fractionated red sorghum flour with or without heat treatment applied to the sorghum grains. For this purpose, the fatty acids, amino acids, volatile compounds, minerals content, and rheological behavior were determined.

Materials and methods

Materials

For the experimental research, red sorghum grains from a hybrid sorghum variety cultivated in Romania, specifically in the northern region of Moldova, were used. The red sorghum grains (ES Alize) were sourced from a retail vendor in Fălticeni (Suceava, Romania).

The sorghum grains were processed using two methods: first, a dry heat treatment was applied, and then they were milled. The optimal conditions were established before and they are presented in our previous paper (Batariuc et al., 2023). The dry heat treatment was applied to the sorghum grains spread in a uniform 10 mm layer on a tray, and placed in a convection oven (Binder ED53 L, Tuttlingen, Germany) for 15 minutes at 133°C. For milling the sorghum grains, a KitchenAid grain mill (model 1065 KGM, Whirlpool Corporation, Benton Harbor, MI, USA) was used. The whole sorghum flour was then separated using a vibrating sieve system (Retsch AS, Haan, Germany) to obtain the M particle size (200 μm < M < 250 μm). Samples codifications were the following: I_TOM – integral treated sample, OM – treated sample with M particle size, CM – control untreated sample with M particle size.

Amino acids profile

The amino acids were determined using a Vanquish UHPLC high-performance liquid chromatograph with a fluorescence detector, Thermo Fisher, equipped with a chromatographic column (Hypersil Gold 150 x 4.65 μm, with a flow rate of 0.80 mL/min). A sample of 5 g was hydrolyzed with 20 mL of 4 M hydrochloric acid at a temperature of 95°C for 24 hours. After filtering through filter paper, the obtained extract was neutralized with 15 mL of 10% potassium hydroxide solution. The samples were then re-filtered through 0.45 μm pore size filters and injected into the equipment. Derivatization was performed on a pre-column with ortho-phthalaldehyde (OPA) at a 1:2 ratio, using the automatic sample injection program, with an injection volume of 1 μL.

Fatty acids profile

The fatty acid analysis was performed using a gas chromatograph CG-FID (Agilent Technologies, 6890N GC, Wilmington, DE, USA) equipped with a DB-WAX capillary column with a polyethylene glycol stationary phase (30 m × 0.25 mm × 0.25 μm) and a flame ionization detector (FID). Approximately 30 ± 0.1 mg of flour sample was dissolved in 2 mL of iso-octane. The mixture was subjected to transesterification with 200 μL of methanolic potassium hydroxide solution (2 mol/L) under vigorous stirring. The resulting organic phase was mixed with sodium hydrogen sulfate. After collecting the supernatant, 1 μL of the sample was directly injected into the gas chromatograph (GC). The gases used for FID analysis were hydrogen at 40 mL/min, air at 450 mL/min, and helium at 30 mL/min. The injection volume was 1 μL in a 1:20 split mode. The temperature program was as follows: the initial oven temperature was set to 60°C, held for 1 min, increased from 60 to 200°C at a rate of 10°C/min, held for 2 min, then from 200 to 220°C at a rate of 5°C/min, and held for 20 min. The injector and detector temperatures were set at 250°C. Fatty acid identification in the samples was completed by comparing their retention times with those of a standard mixture (Senila et al., 2020).

The desirable fatty acid content (DFA) was determined as the sum of MUFA, PUFA, and stearic acid (Medeiros et al., 2014). The thrombogenic index was calculated as the sum of C14:0, C16:0 and C18:0 divided by (0.5 x MUFA + 0.5 x n6 + 3 x n3 + n3/n6) (Renna et al., 2012).

Minerals content

The determination of mineral content was carried out using a Shimadzu AA7000 atomic absorption spectrophotometer, ASC-7000 (air-acetylene), equipped with an ASC-6100 autosampler. The mineral content profile was determined for Ca, Na, Fe, Cu, and Zn, elements predominant in sorghum flour. The samples were prepared according to the method described in the technical manual of the Shimadzu AA7000, ASC-7000 spectrophotometer. Five grams of sample were placed in a crucible and calcined at 550°C for 12 hours. If calcination was incomplete, 1 mL of 65% nitric acid was added to the crucible, and after the evaporation of nitric acid, the process was repeated until the ash turned white. After cooling, 1 mL of 65% nitric acid was added to the crucible, and the contents were transferred to a 50 mL volumetric flask and brought to the mark with deionized water (Avramia and Amariei, 2021). The concentrations of macro- and microelements were expressed in mg/kg of analyzed sorghum flour.

Volatile compounds

The determination of volatile organic compounds (VOCs) was performed using a gas chromatograph coupled with a mass spectrometer (GC-MS). A sample amount of 3 g was transferred into a 20 mL headspace vial, and 3 g of sodium chloride was added to enhance VOCs in the headspace and inhibit any enzymatic reactions. The headspace vials were sealed with crimp-top caps with TFE-silicone headspace septa. Identification criteria for compounds required a mass spectrum match score of ≥ 80%. Results were expressed as the percentage of relative peak area (% RPA) for each peak in each sample, calculated by dividing the peak area by the total area of all identified peaks in each chromatogram. The total ion chromatogram (TIC) of each sample was used to integrate peak areas. All measurements were performed in triplicate, and data are presented as mean ± standard deviation.

The GC oven temperature was set at 35 °C (held for 1 min), increased to 100 °C (held for 1 min) at a rate of 5 °C/min, then to 250 °C (held for 3 min) at a rate of 7 °C/min, and finally increased to 250 °C (held for 1 min) at a rate of 10 °C/min. The transfer line temperature was set at 280 °C, and the ion source temperature was set at 250 °C. The mass spectrometer was operated in electron ionization (EI) mode at 70 eV, following the method reported by Dippong et al. (2023).

Rheological properties

The rheological properties of the sorghum flour dough were determined using dynamic testing methods, including oscillatory testing and creep-recovery testing. A preliminary test was also conducted to identify the boundaries of the linear viscoelastic region of the samples, with a constant oscillatory frequency of 1 Hz and increasing the stress from 0 to 100 Pa. Dynamic rheological measurements were performed with a Thermo-HAAKE MARS 40 dynamic rheometer (Karlsruhe, Germany) with parallel plates, equipped with a Peltier heating system that maintained a constant sample temperature of 21 °C during testing.

Dough samples, prepared from 50 g of sorghum flour and 50 mL of water, were rested for 5 minutes before testing to reach equilibrium. During testing, the gap between the plates was set to 2 mm, and any excess dough was removed. To prevent moisture loss from the sample during testing, a layer of petroleum jelly was applied around the sample edges. Data processing was carried out using the RheoWin Data Manager software, version 4.85 (Thermo Scientific).

Frequency sweep test. The determination of the variation in elastic (G') and viscous (G") modulus with frequency was carried out by applying a constant stress of 10 Pa, positioned within the linear viscoelastic region, over a frequency range from 0.01 to 20 Hz.

Temperature sweep test. By applying the oscillatory test at a constant frequency of 1 Hz, where the dough was heated at a rate of 4 ± 0.1 °C/min from 20 to 100 °C, values for the elasticity and viscosity moduli were determined.

Creep and recovery. The low-stress oscillatory test was complemented by a creep and recovery test. This involved the sudden application of a 50 Pa stress (within the linear viscoelastic range) for 60 seconds, followed by a 180-second recovery period after the stress was removed, allowing the dough to relax (Iuga et al., 2020).

Statistics

The data were reported at least in triplicate. XL STAT 2023 version was used for means comparisons by ANOVA with the Tukey test ($p \leq 0.05$).

Results and discussion

Nutritional composition

The amino acid profile in integral red sorghum flour heat treated (I_TOM), the heat-treated sample with fraction M (OM), and the untreated control fraction M (CM) is displayed in Figure 1.

Among the essential amino acids, leucine exhibited the highest levels across all samples analyzed. Heat treatment of red sorghum grains led to a decrease in leucine content, though the fraction OM still showed higher leucine levels than the integral sorghum flour heat-treated (I_TOM). Additionally, the heat treatment reduced the levels of proline, isoleucine, and histidine. Conversely, the heat-treated fraction OM showed a higher lysine content than the control fraction CM. Similarly, Paucar-Menacho et al. (2018) reported reductions in amino acid content ranging from 17-31% in quinoa grains after puffing, attributing these losses to chemical changes in protein fractions induced by heat treatment, such as glycation, glycoxidation, and oxidation. Moreover, Maillard reactions promoted by heat treatment involve the initial condensation between the carbonyl group of a reducing sugar and amino groups in proteins (Arena et al., 2017; Lohinova and Petrusha, 2023).

Other heat-induced protein changes may include oxidative deamination of N-terminal amino acids, β-elimination of cysteine, and formation of cross-linked lysinoalanine and histidinoalanine derivatives (Arena et al., 2017).

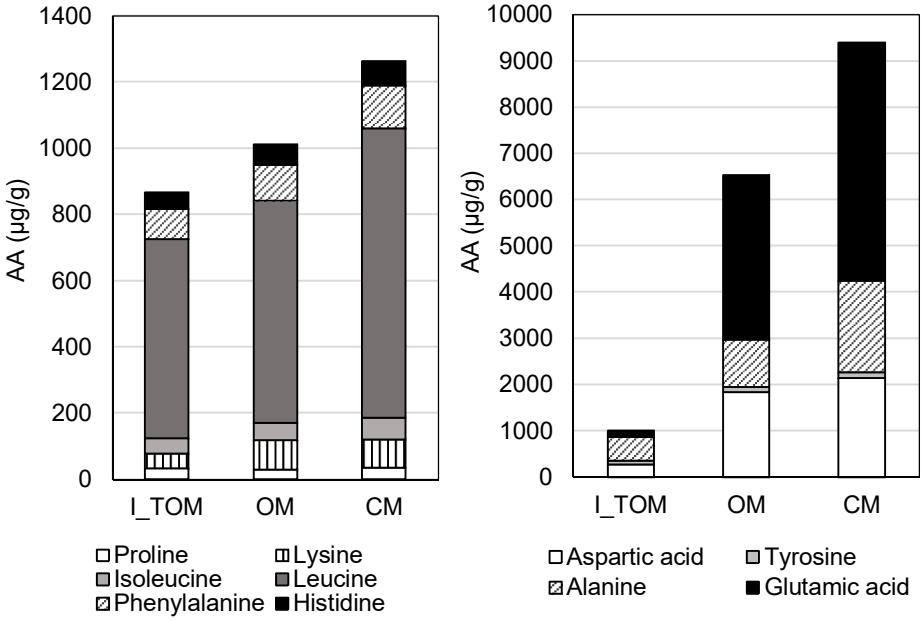

Figure 1. Amino acids (AA) content of sorghum flours

The control fraction of red sorghum (CM) showed a high content of glutamic acid, alanine, and aspartic acid, which diminished after the dry heat treatment (Figure 1). For the treated sample with M fraction (OM), higher levels of non-essential amino acids were observed compared to the values obtained for the integral red sorghum flour heat-treated (I_TOM). It is hypothesized that during heat treatment, condensed tannins bind with proteins to form insoluble complexes (Mohapatra, 2019).

The total saturated fatty acids (SFA), monounsaturated fatty acids (MUFA), and polyunsaturated fatty acids (PUFA) content in red sorghum grains heat-treated shows significant variations depending on the sample type ($p < 0.05$) (Figure 2).

The application of dry heat treatment led to a decrease in SFA content and an increase in MUFA and PUFA levels in the heat-treated OM sample compared to the untreated sample (CM). In contrast, for integral red sorghum flour heat-treated (I_TOM), there was a decrease in MUFA and PUFA content, while SFA levels increased. Torbica et al. (2021) also reported a decrease in SFA and the rise of PUFA after heat treatment of sorghum. After dry heat treatment, an increase in n-6 PUFA content was observed, with the highest value recorded for the heat-treated red sorghum flour with M fraction (OM). Integral red sorghum flour heat-treated (I_TOM) showed a significantly lower value compared to OM. Paucar-Menacho et al. (2018) similarly reported a higher omega-6 fatty acid content in quinoa grains after puffing. The omega-3 polyunsaturated fatty acid content displayed significant differences depending on the type of red sorghum flour sample. The highest value was found in the heat-treated M fraction (OM), followed by the untreated sample (CM), and finally, integral red sorghum flour heat-treated (Figure 2). Meanwhile, increasing the intake of omega-3 fatty acids in the diet is essential for human health and well-being (Stabnikova and Paredes-Lopez, 2024). The treatment of red sorghum grains also led to an increase in the MUFA/PUFA ratio in the heat-treated M fraction (OM) compared to the control sample (CM). Integral red sorghum flour heat-treated displayed a lower MUFA/PUFA ratio than OM.

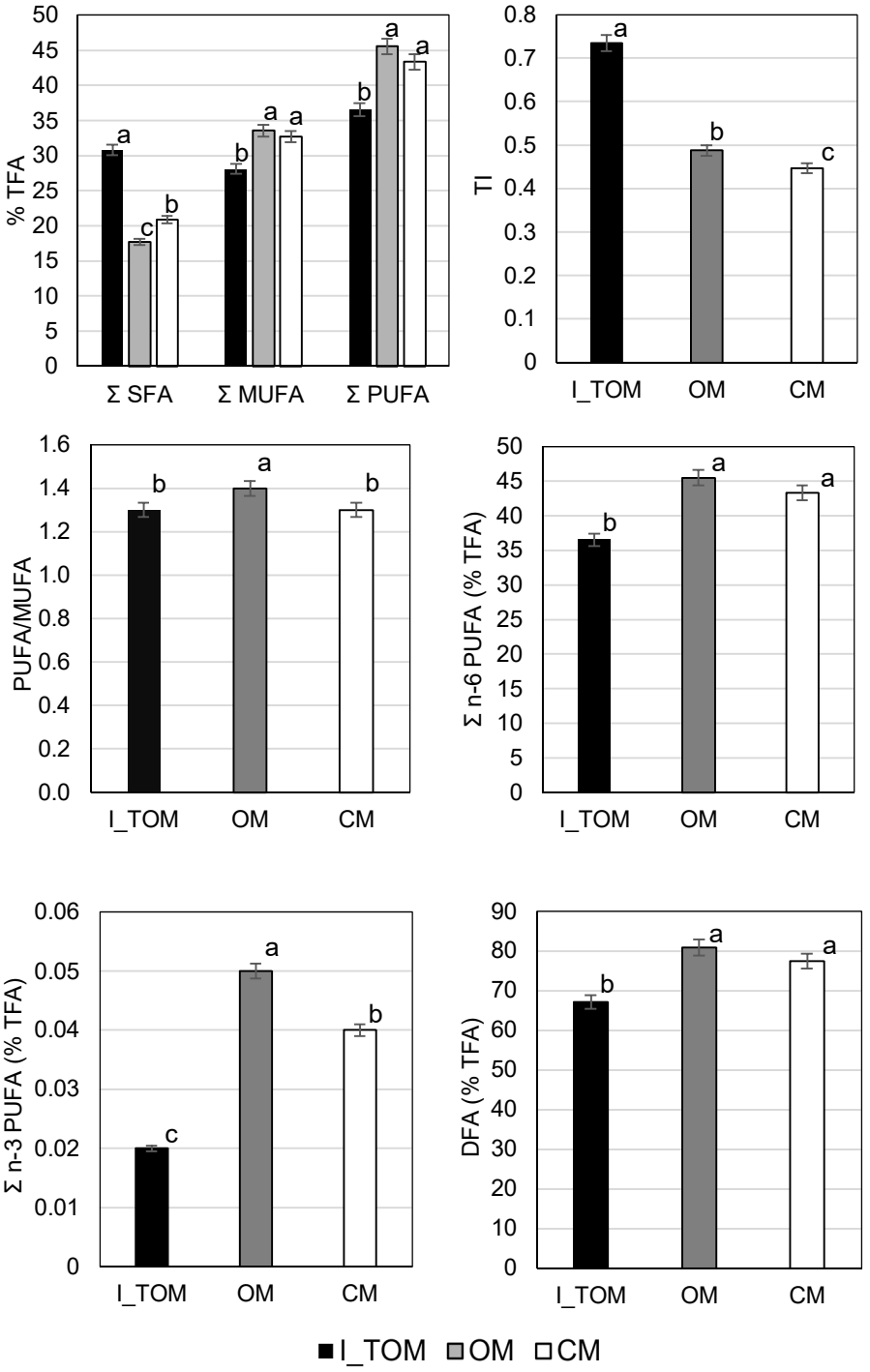

Figure 2. Fatty acids content and thrombogenic index of sorghum flours: Means with different superscripts are significantly different at $p \leq 0.05$

Torbica et al. (2021) reported that hydrothermal treatment reduced the lipid content of barley, rye, triticale, oat, sorghum, and millet flours and modified the profile of fatty acids in flours as a result of complex formation between amylose and protein. Furthermore, the ratio of ω-6 to ω-3 fatty acids raised after heat treatment of barley, rye, triticale, oat, and sorghum (Torbica et al. 2021).

Dry heat treatment and fractionation of red sorghum grains did not lead to significant changes in desirable fatty acids (DFA) content. However, integral red sorghum flour heat-treated (I_TOM) exhibited a significantly lower ($p < 0.05$) DFA value compared to OM (Figure 2). The thrombogenic index (TI) showed significant differences ($p < 0.05$) across the analyzed samples. The heat-treated red sorghum flour, M fraction, (OM) exhibited higher TI values compared to the control fraction (CM). Heat treatment led to an increase in TI in red sorghum flour, but fractionation reduced the thrombogenic index. No data on thrombogenic index variation in sorghum flour were found in the consulted literature. Capouchová et al. (2021) reported that oat samples TI ranged from 0.41 to 0.49, depending on the cultivar.

The mineral composition of the analyzed samples includes calcium and sodium as macroelements, and iron, zinc, and copper as microelements (Table 1).

Table 1

Mineral composition of sorghum flours

Sample	Content (mg/kg)				
	Calcium	Sodium	Iron	Zinc	Copper
I_TOM	18.41±0.46^{a}	61.82±1.55^{b}	56.49±1.41^{b}	20.36±0.51^{b}	2.62±0.07^{c}
OM	16.99±0.42^{b}	63.01±1.58^{a}	64.18±1.60^{a}	22.56±0.56^{a}	4.79±0.12^{a}
CM	16.22±0.41^{b}	59.71±1.49^{c}	38.87±0.97^{c}	18.47±0.46^{c}	3.33±0.08^{b}

Means within the same row with different superscripts are significantly different at $p \leq 0.05$.

No significant differences were identified between the heat-treated sample (OM) and the control sample (CM) of red sorghum flour in terms of calcium content. A higher calcium content was observed in integral red sorghum flour heat-treated (I_TOM) compared to the calcium content in the OM sample. Significant differences ($p < 0.05$) were observed between OM and CM regarding sodium, iron, zinc, and copper content. The molar ratio between phytate and minerals is crucial for determining the potential bioavailability of minerals, with a lower molar ratio indicating greater bioavailability, and vice versa (Wu et al., 2018). Mohapatra et al. (2020) also reported an increase in Na and Ca content after sorghum grains cooking. The reduction of moisture content during dry heat treatment and milling could explain the increase in the mineral content of sorghum flour. This observation was made also by Keya and Sherman (1997) for sorghum grains treated with intense infrared radiation.

The volatile compounds identified in the analyzed red sorghum flours include 2.4-pentadienenitrile, 2.4-hexadienenitrile, and 1,4-pentadiene (Figure 3). In integral red sorghum flour heat-treated, a high percentage of 1,4-pentadiene was identified. In the heat-treated M fraction (OM), 2,4-pentadienenitrile and 2,4-hexadienenitrile were determined. The thermal treatment led to a decrease in the percentage of 2,4-pentadienenitrile and the identification of 2,4-hexadienenitrile in the OM, compared to the control fraction. The reduction of 2,4-pentadienenitrile in the OM fraction was considerable when compared to the percentage identified in the control (CM) and in whole red sorghum flour heat-treated (I_TOM). 1,4-pentadiene aroma compound comes from the ethenolysis of linoleic acid ester present in plants Marvey (2008). It was identified also in other plant sources (Yan et al., 2022).

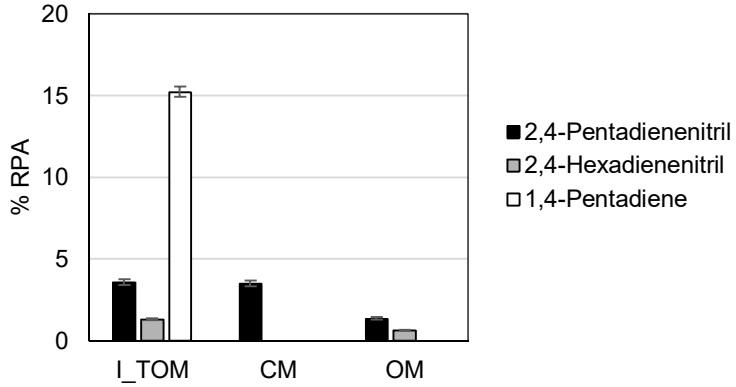

Figure 3. Volatile profile of sorghum flours

Rheological properties

The values obtained for the elastic modulus (G′), which represents the energy stored during deformation, showed that the dough from the heat-treated M fraction (OM) of red sorghum flour exhibited slightly higher elastic energy compared to the dough made from integral red sorghum flour heat-treated (I_TOM) (Figure 4).

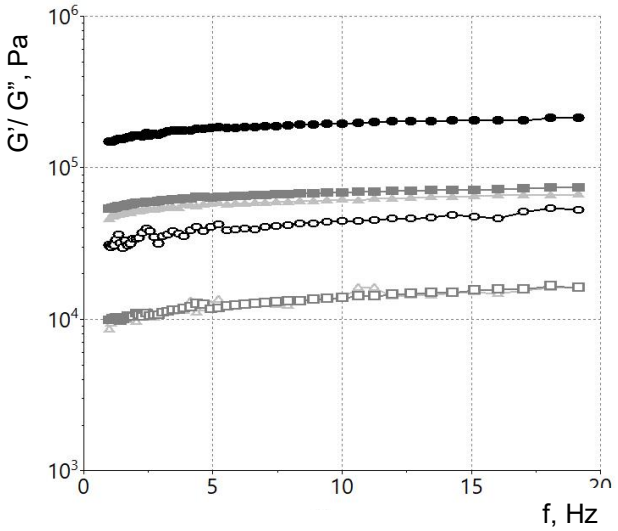

Figure 4. Variations of elastic modulus G′ (filled symbol) and viscous modulus G″ (empty symbol) with frequency for I_TOM (-▲-), OM (-■-) and CM (-●-) samples

The viscous modulus (G″) followed a similar trend in the heat-treated M fraction (OM) sample, with the energy lost during deformation being close in value to that of the treated

integral red sorghum flour sample. The highest values for both G′ and G″ were observed in the control fraction (CM) dough. These findings indicate that for all samples, G′ values were much higher than G″, suggesting a more elastic than viscous behavior. This behavior is likely due to intermolecular associations among the various components in both treated and untreated red sorghum flour. Similar results were reported by Huang et al. (2022), who found higher G′ values than G″ when examining the effects of thermal treatments and γ-irradiation on millet flour rheology. Measuring the elasticity modulus (G′) and viscosity modulus (G″) provides insight into the rigidity and extensibility of the dough: a high G′ and lower G″ value suggests a rigid dough, while a lower G′ indicates a softer, more extensible dough (Weipert, 1990). Huang et al. (2022) reported higher G′ for sorghum flour after dehulling.

The dough made from the heat-treated M fraction (OM) of red sorghum flour exhibited a behavior similar to that of the dough prepared from integral red sorghum flour heat-treated. The elastic modulus (G′) and viscous modulus (G″) values were higher than those observed in the control fraction (CM) dough (Figure 5).

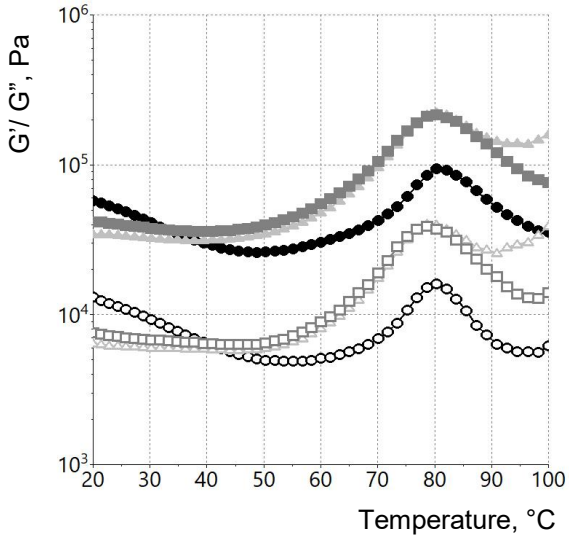

Figure 5. Variations of elastic modulus G′ (filled symbol) and viscous modulus G″ (empty symbol) with temperature for I_TOM (-▲-), OM (-■-) and CM (-●-) samples

The peak gelatinization temperature for the heat-treated M fraction (OM) sample was 78.59 °C, which was lower than that of the control fraction (CM) sample, which has a gelatinization temperature of 80.33 °C. However, there was no significant difference between the OM and the I_TOM sorghum flour sample in terms of peak gelatinization temperature. This suggests that while the heat-treated M fraction shows slight variations in gelatinization properties, it remains largely comparable to the treated integral flour, likely due to similar structural and compositional characteristics achieved through thermal treatment. During heat treatment, the amylose fraction is prone to interact more freely with the amylopectin fractions found in the branched crystalline areas which led to the decrease of mobility of the amylopectin chains and thus generate higher gelatinization temperature (Sun et al., 2014).

Creep and recovery curves of sorghum dough are presented in Figure 6.

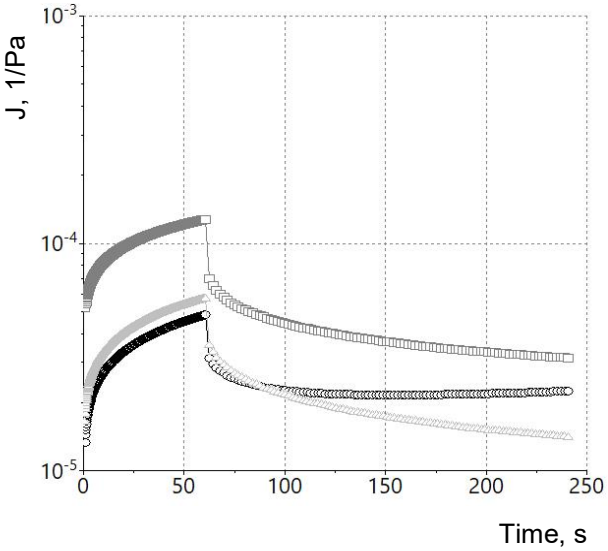

Figure 6. Creep and recovery curves for I_TOM (-■-), OM (-▲-) and CM (-●-) samples

The integral heat-treated sample (I_TOM) of red sorghum flour stood out for its higher maximum compliance in both the creep and recovery phases compared to the control fraction (CM). This suggests that the I_TOM dough has an enhanced ability to deform under stress and recover once the stress is removed, indicating a more elastic and resilient structure compared to the control sample.

The heat-treated M faction (OM) presented higher compliance in the creep phase and lower in the recovery phase compared to the control (CM), indicating a less resilient structure. Creep and recovery behavior is predominantly governed by reorientation of the linkages in the viscoelastic dough (Ahmed, 2014).

Conclusions

Dry heat treatment and fractionation led to significant changes of sorghum flour nutritional properties. Furthermore, the rheological behavior depends on the particle size and treatment applied to sorghum grains. The results obtained showed changes in amino acid profile and an enhancement of n-3, n-6 PUFA and minerals content after application of heat treatment and fractionation. Dough behavior during processing exhibited differences between integral and treated and untreated samples, with the control exhibiting the lowest creep compliances and gelatinization temperatures. These results are helpful for further development of gluten-free backed goods based on sorghum flour.

Acknowledgment
This work was supported by Romania National Council for Higher Education Funding, CNFIS, project number CNFIS-FDI-2024-F-0155.

References

Adebowale O.J., Taylor J.R.N., de Kock H.L. (2020), Stabilization of wholegrain sorghum flour and consequent potential improvement of food product sensory quality by microwave treatment of the kernels, *LWT-Food Science and Technology*, 132, 109827, https://doi.org/10.1016/j.lwt.2020.109827

Ahmed J. (2014), Effect of particle size and temperature on rheology and creep behavior of barley β-d-glucan concentrate dough, *Carbohydrate Polymers*, 111, pp. 89–100, https://doi.org/10.1016/j.carbpol.2014.03.098

Arena S., Renzone G., D'Ambrosio C., Salzano A. M., Scaloni A. (2017), Dairy products and the Maillard reaction: A promising future for extensive food characterization by integrated proteomics studies, *Food Chemistry*, 219, pp. 477–489, https://doi.org/10.1016/j.foodchem.2016.09.165

Avramia I., Amariei S. (2021), Purification of spent brewer's yeast for obtaining beta glucans: a factor in the valorization of by-products and waste reduction, *International Multidisciplinary Scientific GeoConference: SGEM*, 21(4.1), pp. 155–163, 21st International Multidisciplinary Scientific GeoConference SGEM 2021, 16 - 22 August, 2021, Albena, Bulgaria.

Batariuc A., Coțovanu I., Mironeasa S. (2023), Sorghum flour features related to dry heat treatment and milling, *Foods*, 12(11), 2248, https://doi.org/10.3390/foods12112248

Cabrera-Ramírez A. H., Luzardo-Ocampo I., Ramírez-Jiménez A. K., Morales-Sánchez E., Campos-Vega R., Gaytán-Martínez M. (2020), Effect of the nixtamalization process on the protein bioaccessibility of white and red sorghum flours during in vitro gastrointestinal digestion, *Food Research International*, 134, pp. 1–13, https://doi.org/10.1016/j.foodres.2020.109234

Capouchová I., Kouřimská L., Pazderů K., Škvorová P., Božik M., Konvalina P., Dvořák P., Dvořáček V. (2021), Fatty acid profile of new oat cultivars grown via organic and conventional farming, *Journal of Cereal Science*, 98, 103180, https://doi.org/10.1016/j.jcs.2021.103180

Dippong T., Senila L., Muresan L. E. (2023), Preparation and characterization of the composition of volatile compounds, fatty acids and thermal behavior of paprika, *Foods*, 12(10), 2041, https://doi.org/10.3390/foods12102041

Djameh C., Saalia F. K., Sinayobye E., Budu A., Essilfie G., Mensah-Brown H., Sefa-Dedeh S. (2015), Optimization of the sorghum malting process for pito production in Ghana: Sorghum malting process for pito production, *Journal of the Institute of Brewing*, 121(1), pp. 106–112, https://doi.org/10.1002/jib.191

Huang H.H., Dikkala P.K., Sridhar K., Yang H.T., Lee J.T., Tsai F.J. (2022), Effect of heat treatment and γ-irradiation on pasting, rheological, and fungal load of whole and dehulled millets, *Food Science and Technology International*, 28(3), pp. 273–282, https://doi.org/10.1177/10820132211017683

Iuga M., Boestean O., Ghendov-Mosanu A., Mironeasa S. (2020), Impact of dairy ingredients on wheat flour dough rheology and bread properties, *Foods*, 9(6), 828, https://doi.org/10.3390/foods9060828

Keya E. L., Sherman U. (1997), Effects of a brief, intense infrared radiation treatment on the nutritional quality of maize, rice, sorghum, and beans, *Food and Nutrition Bulletin*, 18(4), pp. 1–6. https://doi.org/10.1177/1564826597018004

Klopfenstein C.F., Hoseney R.C. (1995), Nutritional properties of sorghum and the millets, In: D.S.A.V. Dendy (Ed.), *Sorghumand millet: Chemistry and technology,* American Association of Cereal Chemists, pp. 125–168.

Lohinova A., Petrusha O. (2023), Maillard reaction in food technologies, *Ukrainian Journal of Food Science*, 11(2), pp. 81–109, https://doi.org/10.24263/2310-1008-2023-11-2-4

Marvey B.B. (2008), Sunflower-based feedstocks in nonfood applications: Perspectives from olefin metathesis, *International Journal of Molecular Sciences*, 9(8), pp. 1393–1406, https://doi.org/10.3390/ijms9081393

Medeiros E., Queiroga R., Oliveira M., Medeiros A., Sabedot M., Bomfim M., Madruga M. (2014), Fatty acid profile of cheese from dairy goats fed a diet enriched with castor, sesame and faveleira vegetable oils, *Molecules*, 19(1), pp. 992–1003, https://doi.org/10.3390/molecules19010992

Martinez O.D.M., Toledo R.C.L., Queiroz V.A.V., Pirozi M.R., Martino H.S.D., de Barros, F.A.R. (2020), Mixed sorghum and quinoa flour improves protein quality and increases antioxidant capacity *in vivo*, *LWT-Food Science and Technology*, 129, 109597, https://doi.org/10.1016/j.lwt.2020.109597

Mohapatra D., Patel A.S., Kar A., Deshpande S.S., Tripathi M.K. (2019), Effect of different processing conditions on proximate composition, anti-oxidants, anti-nutrients and amino acid profile of grain sorghum, *Food Chemistry*, 271, pp. 129–135, https://doi.org/10.1016/j.foodchem.2018.07.196

Mohapatra D., Patel A. S., Kar A., Deshpande S. S., Tripathi M. K. (2021), Effect of different processing conditions on essential minerals and heavy metal composition of sorghum grain. *Journal of Food Processing and Preservation*, 45(1), e14909, https://doi.org/10.1111/jfpp.14909

National Institute of Statistics (2022), *Romanian Statistical Yearbook*, Bucharest.

Niba L.L., Hoffman J. (2003), Resistant starch and β-glucan levels in grain sorghum (*Sorghum bicolor* M.) are influenced by soaking and autoclaving, *Food Chemistry*, 81(1), pp. 113–118, https://doi.org/10.1016/S0308-8146(02)00386-2

Paucar-Menacho L. M., Martínez-Villaluenga C., Duenas M., Frias J., Penas E. (2018), Response surface optimisation of germination conditions to improve the accumulation of bioactive compounds and the antioxidant activity in quinoa, *International Journal of Food Science & Technology*, 53(2), pp. 516–524, https://doi.org/10.1111/ijfs.13623

Pérez A., Saucedo O., Iglesias J., Wencomo H. B., Reyes F., Oquendo G., Milián I. (2010), Caracterización y potencialidades del grano de sorgo (*Sorghum bicolor* L. Moench), *Pastos y Forrajes*, 33(1), pp. 1–17.

Pezzali J. G., Suprabha-Raj A., Siliveru K., Aldrich C. G. (2020), Characterization of white and red sorghum flour and their potential use for production of extrudate crisps, *PLOS ONE*, 15(6), e0234940, https://doi.org/10.1371/journal.pone.0234940

Rashwan A.K. (2017), *Biochemical and technological studies on some sorghum varieties grown in Upper Egypt (electronic master thesis)*, Sohag University Egypt.

Ratnavathi C.V., Patil J.V., Chavan U.D. (2016), *Sorghum biochemistry: An industrial perspective*, Elsevier/Academic Press.

Renna M., Lussiana C., Cornale P., Fortina R., Mimosi A. (2012), Changes in goat milk fatty acids during abrupt transition from indoor to pasture diet, *Small Ruminant Research*, 108(1–3), pp. 12–21, https://doi.org/10.1016/j.smallrumres.2012.06.007

Senila L., Neag E., Cadar O., Kovacs M.H., Becze A., Senila M. (2020), Chemical, nutritional and antioxidant characteristics of different food seeds, *Applied Sciences*, 10(5), 1589, https://doi.org/10.3390/app10051589

Shahidi F., Naczk M. (1995), *Food Phenolics: Sources, Chemistry, Effects and Applications*, Technomic Publishing Co., Lancaster.

Stabnikova O., Paredes-Lopez O. (2024), Plant materials for the production of functional foods for weight management and obesity prevention, *Current Nutrition & Food Science*, 20(4), pp. 401–422, https://doi.org/10.2174/1573401319666230705110854

Sun Q., Han Z., Wang L., Xiong L. (2014), Physicochemical differences between sorghum starch and sorghum flour modified by heat-moisture treatment, *Food Chemistry*, 145, pp. 756–764. https://doi.org/10.1016/j.foodchem.2013.08.129

Torbica A., Belović M., Popović L., Čakarević J. (2021), Heat and hydrothermal treatments of non-wheat flours, *Food Chemistry*, 334, 127523, https://doi.org/10.1016/j.foodchem.2020.127523

Weipert D. (1990), The benefits of basic rheometry in studying dough rheology, *Cereal Chemistry*, 67(4), pp. 311–317.

Wu G., Ashton J., Simic A., Fang Z., Johnson S. K. (2018), Mineral availability is modified by tannin and phytate content in sorghum flaked breakfast cereals, *Food Research International*, 103, pp. 509–514, https://doi.org/10.1016/j.foodres.2017.09.050

Yan T., Lin J., Zhu J., Ye N., Huang J., Wang P., Jin S., Zheng D., Yang J. (2022), Aroma analysis of Fuyun 6 and Jinguanyin black tea in the Fu'an area based on E-nose and GC–MS, *European Food Research and Technology*, 248(4), pp. 947–961, https://doi.org/10.1007/s00217-021-03930-8

Cite:

UFJ Style

Batariuc A., Ungureanu-Iuga M., Becze A., Senila L., Mironeasa S. (2024), Impact of heat treatment of sorghum grains on flour properties, *Ukrainian Food Journal*, 13(4), pp. 723–736, https://doi.org/10.24263/2304-974X-2024-13-4-7

APA Style

Batariuc, A., Ungureanu-Iuga, M., Becze, A., Senila, L., & Mironeasa, S. (2024). Impact of heat treatment of sorghum grains on flour properties. *Ukrainian Food Journal*, *13*(4), 723–736. https://doi.org/10.24263/2304-974X-2024-13-4-7

Effect of hemp seed by-products on wheat dough fermentation

Mariia Blazhenko, Nataliia Falendysh, Vladyslav Shpak

National University of Food Technologies, Kyiv, Ukraine

Keywords:

Hemp
Protein
Kernels
Wheat dough
Amino acids
Fermentation

Article history:

Received 22.05.2024
Received in revised form 18.09.2024
Accepted 30.12.2024

Corresponding author:

Mariia Blazhenko
E-mail: blagmary@ukr.net

DOI:
10.24263/2304-974X-2024-13-4-8

Abstract

Introduction. The aim of the research was to determine the chemical composition of hemp seed by-products, namely hemp seed flour, hemp seed protein, and hemp seed kernels and the effect of their addition on the fermentation activity of yeast in wheat dough.

Materials and methods. Hemp seed flour, hemp seed kernels, and hemp seed protein were obtained from the non-narcotic variety of hemp "Liryna" (Ukraine). Starch content was determined by the Evers polarimetric method, fractional composition of proteins by electrophoresis, amino acid composition by the method of ion exchange chromatography.

Results and discussion. The by-products of hemp processing, namely hemp seed protein, hemp seed flour, hemp seed kernels, contained protein 4.8, 3.4, and 2.5 times higher, and fat 10.4, 8.8, and 30 times higher than first-grade wheat flour. While, the content of carbohydrates in hemp by-products was lower than in wheat flour. The percentage content of starch, mono- and disaccharides, and dietary fiber in hemp seed processing products was as follows: 24.5, 23.2, and 52.3% in hemp seeds protein; 18.0, 20.3, and 61.7% in hemp seed flour; 23.5, 19.8, and 56.7% in hemp seed kernels, respectively. The content of the globular protein fraction was predominant in hemp seed processing products from 49.6% to 61.7%, while in first grade wheat flour their content was only 10.7%. The content of the albumin fraction in hemp seed processing products varied from 28.1% to 32.1% compared to 7.2% in first grade wheat flour. It was determined that the content of essential amino acids in hemp by-products was higher than in first grade wheat flour. The amount of released carbon dioxide decreased from 10 to 70 ml with the addition of hemp seed by-products: 10% hemp seed flour instead of wheat flour, 15% hemp seed protein instead of wheat flour and the combined application of 15% hemp seed protein to replace wheat flour and 7% of hemp seed kernels to the mass of flour, however, the fermentation process intensified. The first peak of gas formation was observed simultaneously in all samples after 60 min of fermentation. The second peak of gas formation in the dough with the replacement of part of the wheat flour with hemp seed-processing products was after 120 min of fermentation, which was 30 min earlier than in the control sample. At the same time, the largest amount of carbon dioxide released in the dough with the replacement of 10% of wheat flour with hemp seed flour.

Conclusions. Hemp by-products had a relatively higher content of proteins, fats, micro- and macro-elements, a balanced composition of carbohydrates, amino- and fatty acids. Different from wheat flour chemical composition affected the course of the dough fermentation process and caused changes in the carbohydrate-amylase complex of the dough.

Introduction

Enrichment of bread and bakery products with non-traditional plant raw materials is a new direction in the manufacturing of functional foods (Ivanov et al., 2021; Stabnikova et al., 2021; Shevchenko, 2022; Shevchenko et al., 2023). To increase the nutritional and biological value of bread and intensify the technological process of its production, hemp seed by-products could be used (Hayit and Gül, 2020). Hemp seeds contain 20–25% easily digestible proteins with a high content of essential amino acids, up to 34% of dietary fiber, as well as a large amount of macro- and microelements (Farinon et al., 2020). In addition to high nutritional value, hemp seeds were also characterized by the presence of various biologically active substances, including phenolic compounds, as well as bioactive peptides with antioxidant, anti-inflammatory, neuroprotective, and antihypertensive properties (Farinon et al., 2020).

The possibility of using hemp seeds in the production of bread was demonstrated (Rusu et al., 2021). It was found that the content of proteins and essential amino acids, lipids and unsaturated fatty acids, fiber and minerals increased in bread when adding 5% hemp flour, which did not significantly affect the rheological properties of bread.

Incorporation of 5 – 40% (w/w) hemp seed flour in wheat flour increased the total phenolic content in the bread, thus significantly increasing its antioxidant activity (Capcanari et al., 2023). It was found that the protein content in the bread increased from 11.11% (control sample) to 18.18% (for a sample with 40% of hemp seed flour). However, the addition of hemp seed flour led to a decrease in the porosity of the bread, an increase in the hardness, and a decrease in the elasticity of the dough.

Replacement of 5 to 20% wheat flour with hemp flour in the production of cookies led to an increase in the content of ash, protein, fat, total phenolic content and antioxidant activity of the final product (Ertas and Aslan, 2020). The highest content of ash, 2.11%, was found in cookies prepared with 20% of roasted hemp flour (in control it was just 1.33%), and the highest content of protein, 11.81%, was detected in cookies with 20% of raw hemp flour (in control it was 8.55%). The antioxidant activity of cookies with 20% of roasted hemp flour was 40.88% and cookies made with 20% of raw hemp flour had an antioxidant activity 38.21%. At the same time, cookies with raw hemp flour up to 20% and roasted hemp flour up to 15 % demonstrated good overall acceptability.

Addition of 10% hemp flour or 5% hemp protein decreased elasticity of bread crumbs Addition of hemp by-products increased the dough yield, which was 165.38% for dough with 10% of hemp flour and 163.91% for dough with 5% of hemp protein (Mullerova et al., 2016). Sensory analysis of gluten-free bread with the addition of 5% hemp flour did not show significant difference from the control bread and it was acceptable to consumers (Hayward and McSweeney, 2020).

Thus, application of hemp seed by-products in manufacturing of bread needs to be deepened and detailed. The aim of the present study was to determine the effect of hemp seed by-products, namely hemp seed flour, hemp seed protein, and hemp seed kernels on the fermentation activity of yeast in wheat flour dough.

Materials and methods

Materials

Hemp seed flour, hemp seed protein and hemp seed kernels were used for research (Desnaland LLC, Ukraine).

Hemp seed flour was obtained from the seeds after oil extraction by cold pressing, without the use of heat or chemicals. Hemp seed protein was obtained from hemp seeds that

had been cold-pressed and oil extracted, and further sifted. Ready-to-eat hemp seeds were shelled steamed kernels (Irakli et al., 2019).

The dough was prepared from first grade wheat flour, pressed baker's yeast – 2% to the mass of flour, table salt – 1.5% to the mass of flour, white sugar – 3 – 5% to the mass of flour, sunflower oil – 2% to the mass of flour, barley-malt extract – 10% to the mass of flour. 10% hemp seed flour was added to replace equal amount of wheat flour, 15% hemp seed protein to replace equal amount of wheat flour, and composition of 15% hemp seed protein to replace equal amount of wheat flour containing 7% of hemp seed kernels to the mass of flour. The control was dough without hemp by-products. Therefore, the aim of the research was to determine the effect of hemp seed byproducts, namely hemp seed flour, hemp seed protein and hemp seed kernels on the fermentation activity of yeast in wheat flour dough.

Methods

Determination of protein content

Determination of the protein content in first grade wheat flour, hemp seed flour, hemp seed protein, and hemp seed kernels was carried out by the biuret method.

1.5 g of the product was weighed with an accuracy of 0.0001 g and placed in a dry conical flask with a capacity of 250 – 300 ml with a stopper. A portion of the product was completely moistened with 2 ml of carbon tetrachloride to remove fat. Then 100 ml of the biuret reagent was added, the flask was closed with a cork and shaken with a non-mechanical shaker for 60 min. After that, obtained extract was centrifuged for 10 min at 4500 rpm. The transparent centrifuge was placed in the cuvette of the photoelectrocolorimeter with a solution layer thickness of 5 mm. The optical density of the hood was measured at a wavelength of 550 nm. Based on the obtained value of the optical density of the protein extract, the protein content was determined using a calibration graph for the biuret method. The result was expressed as a percentage of the dry matter of the product (López-Bascón and de Castro, 2020).

Determination of fat content

Determination of the fat content in first grade wheat flour, hemp seed flour, hemp seed protein, and hemp seed kernels was carried out by the method of multiple extraction of fat from the appropriate weight of the product.

From the sample of the above-mentioned raw materials, two measurements were separated, each with a mass of (10±0.1) g. One was transferred to a filtering separatory funnel, (25±0.5) ml of diethyl ether was added, closed with a ground stopper and extraction was carried out by intensive shaking for 1 min. The obtained fat extract was sucked by a water-jet pump into a receiver attached to the filtering funnel, into which 2 – 3 ml of diethyl ether was poured before the extraction to prevent possible losses of the concentrated part of the first extract. The extract from the receiver was filtered through a pleated paper filter into a pre-dried and weighed flask. Similarly, the extraction was repeated in the same flask. Ether was driven off the flask using a Soxhlet apparatus. Then the flask with fat was placed in a drying cabinet and dried for 2 hours at a temperature of (105 ± 5) ºC, cooled in a desiccator and weighed with an error of ± 0.0002 g (López-Bascón and de Castro, 2020).

Determination of the starch content

The determination was made by the Evers method (Koshova et al., 2020). 5±0.01 g of the product was put into a volumetric flask, where 25 ml of 0.31 mol/l HCl solution was added. An additional 25 ml of HCl was put to rinse the residue into the flask. The flask was shaken, water was brought up to the neck and after 15 minutes 25–30 ml of distilled water was poured. For the precipitation of proteins and clarification, 5 ml of ammonium molybdate solution or 5 ml of phosphorous-tungstic acid solution or 2 ml of Carrez reagent I and II was added to the flask. After 5 minutes, the solution was filtered. On the saccharimeter, the angle of rotation of the plane of polarization was measured, the length of the polarizing tube was 200 mm. In parallel, a control experiment was conducted, which differred in that the flask must be kept in a boiling water bath for 15 minutes.

The starch content was calculated according to the formula (1):

$$C = \frac{\left(a_g - a_k\right) \cdot F \cdot 100}{100 - W}, \quad (1)$$

where a_g is the value of the angle of rotation of the plane of polarization by optically active substances in the main experiment, degree of saccharimeter;

a_k is the value of the angle of rotation of the plane of polarization by water-soluble optically active substances in the control experiment;

F is Evers coefficient, $1000/\left[a\right]_D^{20}$

W is the moisture content in the product, %.

Determination of mono- and disaccharides content

The determination was made by the Schorl method (Pokrzywnicka and Koncki, 2017). 30 ml of extract or hydrolyzate was put to a 250 ml conical flask, 10 ml of Feling I and Feling II reagents was added with a pipette, boiled for 2 minutes and cooled. To determine the amount of unreacted copper, 10 ml of a 30% potassium iodide solution and 10 ml of 25% sulfuric acid were added. The released iodine was immediately titrated with a 0.1 mol/l solution of sodium thiosulfate to a light yellow color, 2 ml of a 1% solution of soluble starch was added as an indicator, and the titration continued until the blue color disappeared.

In parallel, a control experiment was conducted in which everything was done similarly, replacing the sugar solution with the appropriate amount of distilled water.

Sugar content x, % to dry matter, in the product was calculated according to the formula (2):

$$x = \frac{\left(V_k - V_p\right) \cdot K \cdot 100 \cdot 100}{H\left(100 - W\right)}, \quad (2)$$

where V_k is the amount of 0.1 mol/l sodium thiosulfate solution used for titration in the control experiment, ml;

V_p is the amount of 0.1 mol/l sodium thiosulfate solution used for titration in the working solution, ml;

K is conversion factor for the type of sugar;

H is the amount of the product corresponding to the volume of extract or hydrolyzate taken for reaction with Fehling reagents, mg;

W is the moisture content in the product, %.

Determination of dietary fiber content

A general study was conducted to determine the total content of dietary fiber in products by the enzymatic-gravimetric method. Dietary fiber was calculated as the residual weight minus the weight of protein and ash (Shevchenko and Litvynchuk, 2022).

Determination of ash content

Ash content in wheat flour, hemp seed flour, hemp seed protein, and hemp seed kernels was determined by burning the sample with the subsequent determination of the unburned residue. Ashing was carried out using a nitric acid accelerator (Sahayam et al., 2009). The sample was weighed: for flours and protein – 1.5–2.0 g, for hemp seed kernels – 1.0–1.5 g into two crucibles pre-heated to a constant mass and cooled in a desiccator.

Weighed crucibles with a measuring scale were placed near the door of a muffle furnace heated to a temperature of 400–500 °C, the measuring scale was charred, preventing ignition of dry distillation products. After the separation of dry distillation products stopped, the crucibles were placed in a muffle furnace and the door was closed. The contents of the crucibles were ashed until they turned into a loose mass of gray color, cooled in air to room temperature, 2–3 drops of nitric acid were added and placed near the door of the muffle furnace, and the acid was carefully evaporated to dryness without allowing boiling. Then the crucibles were placed inside the muffle furnace, heated to a temperature of 600 – 900 °C, and ashed for 20–30 minutes. When there were no dark spots at the bottom of the crucible, ashing was considered complete. After the crucible was cooled to room temperature in a desiccator and weighed.

The ash content of product X, % to dry matter, was calculated according to the formula (3):

$$X = \frac{m_3 \cdot 100 \cdot 100}{m_н \cdot (100 - W)}, \quad (3)$$

where m_3 – mass of ash, g, $m_н$ – mass of the product, g, W – mass fraction of moisture in the product, %.

Determination of the moisture content

5±0.001 g of the product was put to the dried bags, placed in an open oven at a temperature of 100–105 °C for 4 hours. Further, they were cooled in a desiccator, weighed and again placed for drying, the end of drying was considered when the difference between the weight was no more than 0.004 g or the weight of the sample began to increase.

The moisture content (W) was calculated according to the formula (4):

$$W = \frac{m_1 - m_2}{m} \cdot 100, \quad (4)$$

where m is mass of the product, g;

m_1 is mass of the product with the bushing before drying, g;

m_2 is mass of the product бюксою the bushing after drying, g (Pasichnyi et al., 2023).

Determination of fractional composition of proteins

Fractional protein composition of raw materials was carried out by electrophoresis.

Electrophoresis was performed at a current of 40 mA and a voltage of 100–150 V based on two gel plates with 12 samples each. The speed of movement of proteins in the gel was controlled by bromophenol blue (0.1 mol/l). The protein separation time was 12 hours.

Determination of amino acid composition

The content of amino acids was determined using the method of ion exchange chromatography. The quantity of amino acids was determined by hydrolysis of proteins using automatic amino acid analyzer T–339 with polystyrene sulfonate ions. Amino acids were detected at a wavelength of 560 nm by rectification with a ninhydrin solution on a Unicam SP 800 photometer (Litvynchuk et al., 2022).

Determination of fatty acid composition

Fatty acid content was determined by gas-liquid chromatography (Chowdhury, 2007). The gas-liquid chromatograph was equipped with a flame ionization detector and a stainless steel column. The column was heated at 180 ºC for about 2 hours to achieve thermal stability before use. The operating mode was programmed in the oven at a temperature of 150 °C (holding time 5 min), the rate of increase from 80 ºC/min to 190 °C (holding time 0 min), from 20 °C/min to 200 °C (holding time 10 min), injection temperature 250 0 C and 312 Studies on the Fatty Acid 42(3) 2007 detector temperature 250 ºC. Nitrogen was used as a carrier gas with a flow rate of 20 ml/min.

Determination of micro- and macroelements content

The content of micro- and macroelements was determined using atomic absorption spectrometry and optical emission spectrometry with inductively coupled plasma (Başgel and Erdemoğlu, 2006; Malik et al., 2008).

The method of atomic absorption spectrophotometry was based on the phenomenon of absorption of resonant radiation with the corresponding wavelength by free atoms of the element, which were determined to be formed as a result of spraying the analyzed solution in the flame of a combustible mixture: air-acetylene, air-propane-butane.

Determination of gas-forming capacity of the dough

The kneaded dough was divided in such a way that each piece of dough contained 25 g of flour. Each piece was placed in a vessel for fermentation and kneaded with a rolling pin. The vessel was placed in the water thermostat of the AG–1 device, closed with a rubber stopper with a tube. The cylinder was filled with oil; the access of carbon dioxide to the tube was opened. Results were foxed every 30 minutes during 5 hours. The average arithmetic value of two parallel determinations was multiplied by 4 to remove from 25 g of flour to 100 g.

Results and discussions

Chemical composition of hemp seed by-products

Food products, including bakery products, are the main source of energy and nutrients for the human body (Drobot and Shevchenko, 2017).

Hemp by-products were not sufficiently studied in terms of their chemical composition and technological properties. It was appropriate to determine the general chemical composition of hemp seed by-products: hemp seed flour (Figure 1a), hemp seed protein (Figure 1b), and hemp seed kernels (Figure 1c) in comparison with first grade wheat flour (Table 1).

Figure 1. Hemp seed by-products:
hemp seed flour (a), hemp seed protein (b), hemp seed kernels (c)

The protein content in hemp seeds was 4.8 times higher, in hemp seed flour 3.4 times higher, in hemp seed kernels 2.5 times higher than in first-grade wheat flour. The total fat content of hemp seed by-products was also higher than that of first grade wheat flour. Hemp seed protein, hemp seed flour, and hemp seed kernels contained 10.4, 8.8, 30 times more fat, respectively, than wheat flour.

It was found that the content of carbohydrates in hemp by-products was lower than in first grade wheat flour. However, the content of total carbohydrates in wheat flour was largely provided by starch (92% of the total amount of carbohydrates), while in hemp by-products the content of total carbohydrates had more balanced composition among starch, mono- and disaccharides and dietary fibers: in hemp seed protein – 24.5, 23.2, and 52.3%, in hemp seed flour – 18.0, 20.3, and 61.7%, in hemp seed kernels – 23.5, 19.8, and 56.7%, respectively.

Table 1

Chemical compositions of first grade wheat flour and hemp seed by-products

Components	Content, %			
	First grade wheat flour	Hemp seed protein	Hemp seed flour	Hemp seed kernels
Protein,	11.6±0.23	55.4±0.26	38.1±0.42	29.3±0.24
Fat	1.4±0.45	14.5±0.13	12.3±0.23	42.1±0.26
Carbohydrates				
Starch	68.0±0.31	4.0±0.20	6.0±0.52	4.4±0.16
Mono- and disaccharides	1.8±0.12	3.8±0.33	6.8±0.11	3.7±0.14
Fiber	3.5±0.43	8.5±0.32	20.7±0.24	10.6±0.17
Ash	0.75±0.11	4.8±0.22	4.9±0.15	4.2±0.19
Moisture	13.0±0.28	9.0±0.30	11.2±0.18	5.7±0.26

Results are presented as mean ± standard deviation of three replicates.

In the study of Capcanari et al. (2023), the protein, fat and dietary fiber contents in hemp seed flour were 31.6, 8.2%, and 23%, which are consistent with the values obtained in the present study.

Fractional compositions of proteins of first grade wheat flour and hemp seed by-products are shown in Table 2.

Table 2

Fractional compositions of proteins of first grade wheat flour and hemp seed by-products

Products	Content, %				
	albumins	globulins	prolamins	glutelins	non-protein nitrogen
First-grade wheat flour	7.2±0.52	10.7±0.65	23.5±0.35	58.6±0.58	5.4±0.32
Hemp seed flour	32.1±0.94	58.4±0.96	6.6±0.26	2.9±0.21	9.7±0.41
Hemp seed protein	30.2±0.87	61.7±0.98	5.5±0.24	2.6±0.19	12.8±0.49
Hemp seed kernels	28.1±0.73	49.6±0.84	20.9±0.45	1.4±0.15	11.9±0.47

Results are presented as mean ± standard deviation of three replicates

Fraction of glutelins dominated in first grade wheat flour where it consisted 58.6%, while content of glutelins in the proteins of hemp seed by-products was very low (Table 2). This is consistent with the results reported in (Apetroaei et al., 2024).

The globular protein fraction was predominant in hemp seed processing products, and its content varied from 49.6% to 61.7%, while in first grade wheat flour their content was only 10.7%. The content of the albumin fraction in hemp seed processing products varied from 28.1% to 32.1% compared to 7.2% in first grade wheat flour.This confirmed that hemp by-products will not contribute to the formation of the gluten framework, as they do not contain gluten proteins (Marinopoulou et al., 2024).

It was shown that the amino acid composition of seed proteins differs depending on the varieties of hemp (Russo et al., 2015). The amino acid compositions of first grade wheat flour and hemp seed by-products used in the present study are shown in Table 3.

The content of essential amino acids in hemp by-products was higher than in first grade wheat flour. In particular, the content of leucine was 2.4, 2.3, and 1.1 times, content of lysine 5.8, 5.2, and 3.2 times, content of methionine 3.6, 3.3, and 1.6 times, threonine 3.4, 3.3, and 1.8 times, phenylalanine 2.7, 2.5, and 1.3 times higher in hemp seed protein, hemp seed flour, and hemp seed kernels compared to their contents in first grade wheat flour, respectively. This indicated the feasibility of increasing the biological value of bread when such raw materials are added to the recipe.

The chemical composition of first grade wheat flour and hemp by-products differed significantly in terms of total fat content. The research results showed (Table 4) a diverse fatty acid composition; however, it was necessary to distinguish the content and ratio of ω – 3 and ω – 6 fatty acids. They prevent the development of atherosclerosis, coronary heart disease, stroke, myocardial infarction, have antioxidant properties, According to World Health Organization recommendations, the ideal ratio of ω–6/ω–3 fatty acids in food products is considered to be 4:1 (Simopoulos, 2002; Stabnikova and Paredes-Lopez, 2024; WHO, 2003).

Analysis of the fatty acid composition showed that the ratio of ω–6/ω–3 fatty acids was the closest to the ideal: for hemp seed kernels it was 3.91, while for hemp seed flour it was 3.5:1, and for hemp seed protein it was 3.4:1 (Table 4).

Table 3

Amino acid compositions of first grade wheat flour and hemp seed by-products

Amino acids	Content, mg/100 g of protein			
	First grade wheat flour	Hemp seed protein	Hemp seed flour	Hemp seed kernels
Alanine	330±15	1556±31	1462±30	735±27
Arginine	400±20	3589±52	3411±45	1647±32
Aspartic acid	340±16	2263±62	2224±26	1359±62
Valin	470±22	885±31	910±56	445±28
Histidine	200±12	870±32	806±47	41±3
Glycine	350±15	1272±47	1319±66	740±56
Glutamic acid	3080±57	4445±88	4625±91	2870±87
Isoleucine	430±22	782±24	813±38	374±23
Leucine	806±35	1951±42	1877±63	913±62
Lysine	250±17	1458±39	1300±52	788±48
Methionine	190±12	686±25	630±24	302±22
Proline	970±64	1358±38	1305±40	673±32
Serin	500±32	1597±37	1514±48	824±35
Tyrosine	250±25	1078±36	955±36	469±28
Threonine	311±33	1056±34	1029±37	555±56
Phenylalanine	500±45	1350±35	1271±42	653±65
Cysteine	200±19	594±24	545±22	197±20

Results are presented as mean ± standard deviation of three replicates.

Table 4

Fatty acid compositions of hemp by-products

Fatty acids	Content, % to the total mass		
	Hemp seed flour	Hemp seed protein	Hemp seed kernels
Saturated fatty acid			
Myristic acid (C14:0)	0.32±0.06	0.35±0.01	0.20±0.01
Palmitic acid (C16:0)	6.44±0.12	8.01±0.16	7.22±0.42
Stearic acid (C18:0)	3.04±0.08	4.66±0.05	3.87±0.01
Arachinic acid (C20:0)	4.37±0.03	4.1±0.05	4.53±0.06
Geneicosanoic acid (C21:0)	1.13±0.08	1.09±0.06	1.11±0.07
Monounsaturated fatty acid			
Palmitoleic acid (C 16:1, ω-7)	0.13±0.01	0.14±0.01	0.11±0.01
Oleic acid (cis-18:1, ω -9)	12.87±0.13	12.59±0.012	12.68±0.08
Elaidic acid (9-trans-C18:1, ω-9)	0.1±0.01	0.64±0.01	0.11±0.01
Gondoic acid (C20:1, ω-9)	0.003±0.00012	0.41±0.02	0.33±0.07
Polyunsaturated fatty acids			
Linoleic acid (C18:2, ω-6)	54.55±0.20	51.44±0.2	54.97±0.2
γ-linolenic acid (C18:3, ω-6)	0.14±0.01	0.15±0.01	0.05±0.01
α-linolenic acid (C18:3, ω-3)	15.8±0.19	15.18±0.18	14.17±0.18
Arachidonic acid (C20:4, ω-6)	0.04±0.01	0.08±0.01	0.01±0.001
Ratio of ω-6 : ω3	3.5 : 1	3.4 : 1	3.9 : 1

Results are presented as mean ± standard deviation of three replicates.

Hemp by-products were less refined than first-grade wheat flour, in particular, hemp seed flour was whole-ground, so, it could be assumed that they contain high levels of macro- and microelements (Table 5).

By-products of hemp processing contain large amounts of magnesium, which is essential for the proper functioning of the body participating in the regulation of blood pressure, blood sugar levels and preventing the development of osteoporosis (Glasdam et al., 2016). Content of magnesium in hemp seed protein, hemp seed flour and hemp seed kernels was by 29.1, 26.8, and 22.1 times higher than in first grade wheat flour. Content of potassium, which reduces the risk of cardiovascular diseases, regulates heart rhythm, and maintains normal muscle tone (McLean and Wang, 2021) was by 9.5, 8.9, and 8.6 times higher in hemp seed protein, hemp seed flour and hemp seed kernels, than its content in wheat flour. The amount of calcium that regulates blood clotting, ensures the strength of bones and teeth, and is important for the functioning of human immune system (Beto, 2015) was by 12.8, 12.0, and 3.3 times higher in hemp seed protein, hemp seed flour and hemp seed kernels than its content in wheat flour. Content of zinc, which is essential for normal function of brain and immune system (Kiouri et al., 2023) was by 11.6, 10.5, and 9.9 times higher in hemp seed protein, hemp seed flour and hemp seed kernels than its content in wheat flour. Content of selenium, which play an important role in thyroid hormone metabolism, immune responses, and protection from oxidative damage (Stabnikova et al., 2022) was by 2.4, 3.6, and 8.2 times higher in hemp seed protein, hemp seed flour and hemp seed kernels than its content in wheat flour.

Table 5

Content of macro- and microelements in first grade wheat flour and hemp seed by-products

Macroelements	**First grade wheat flour**	**Hemp seed protein**	**Hemp seed flour**	**Hemp seed kernels**
	Content, mg/g			
Magnesium	0.22±0.01	6.40±0.08	5.9±0.05	4.86±0.05
Calcium	0.15±0.01	1.92±0.02	1.8±0.02	0.5±0.01
Phosphorus	1.08±0.03	11.17±0.02	9.2±0.08	8.2±0.09
Potassium	1.07±0.02	10.20±0.15	9.6±0.07	9.2±0.08
Microelements	**Content, µg/g**			
Manganese	57.0±0.08	129.0±0.26	152.9±0.27	68.2±0.16
Zinc	7.0±0.06	80.9±0.19	73.8±0.20	69.6±0.17
Iron	12.6±0.06	147.9±0.23	127.5±0.23	72.1±0.19
Cobalt	0.1±0.01	0.9±0.01	0.6±0.01	0.2±0.01
Copper	7.4±0.12	19.1±0.09	15.9±0.15	10.7±0.05
Selenium	0.34±0.01	0.83±0.01	1.22±0.02	2.77±0.02

Results are presented as mean ± standard deviation of three replicates.

Hemp seed flour used in the study of Capcanari et al. (2023) had similar content of minerals, mg/g: magnesium, 8.83; phosphorus, 18.51; potassium, 15.94; µg/g: zinc, 120; iron, 110, and copper, 20.

Effect of hemp seed by-products on wheat dough fermentation

The effect of hemp by-products on the carbohydrate-amylase complex of the dough was determined. The main process during the ripening of the dough is fermentation, during which carbon dioxide is released, which ensures the loosening of the dough.

It was found that the amount of released carbon dioxide in the samples with the replacement part of wheat flour with hemp by-products was lower compared to the control sample (Figure 2). In the dough with replacement of 10% of wheat flour with hemp seed flour 10 ml carbon dioxide released less compared to the control. When replacing 15% of wheat flour with hemp protein, 20 ml carbon dioxide released less and when replacing 15% of wheat flour with hemp seed protein and adding 7% of hemp seeds, 70 ml carbon dioxide released less.

The decrease in gas formation in dough with hemp seed by-products compared to the control is explained by the features of the protein composition of additives, namely the differences in the fractional composition of proteins compared to proteins of wheat flour (Table 2).

Glutelins and gliadins are the main types of wheat flour proteins responsible for the formation of the gluten framework of the dough (Urade et al., 2018). The protein composition of hemp seed by-products consists mostly of globular (albumin and globulin) proteins (Table 2), which have a compact spatial structure, greater strength, thereby not contributing to the stretchability of the dough and the creation of an elastic gluten frame compared to glutelins in the composition of wheat flour proteins (El- Sohaimy et al., 2022; Marinopoulou et al., 2024).

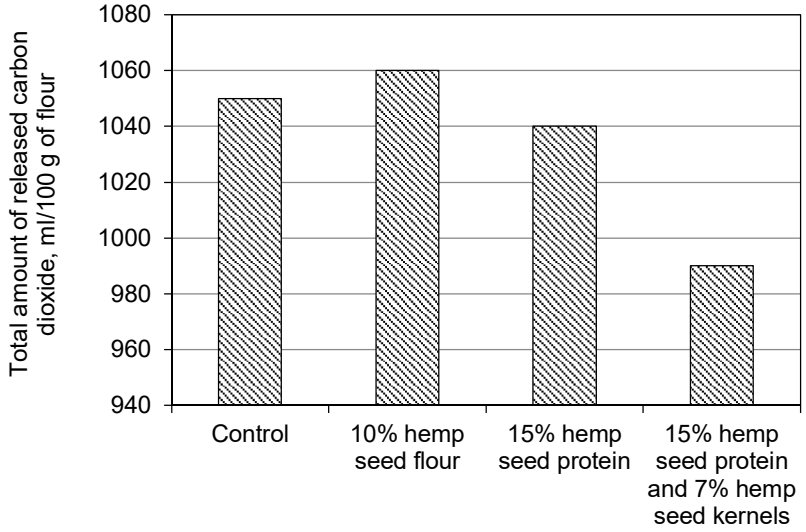

Figure 2. Influence of hemp by-products on amount of released carbon dioxide in the dough during fermentation

The dynamics of carbon dioxide release during 5 hours of fermentation is shown in Figure 3.

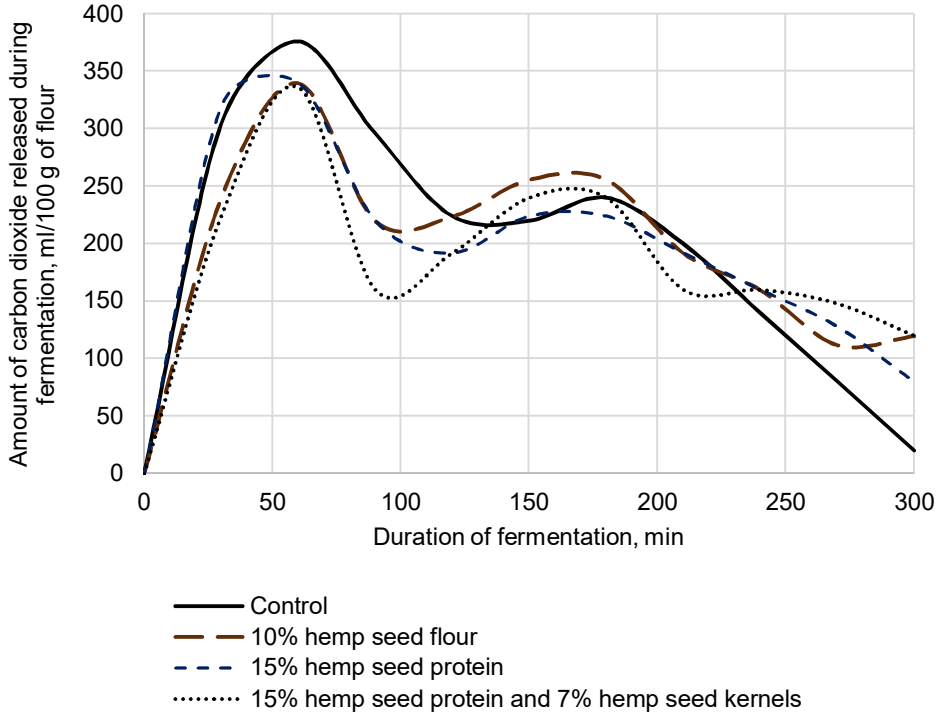

Figure 3. Influence of hemp by-products on dynamics of gas formation in dough during fermentation

It was found that the sugars of the control (dough without hemp by-products) were fermented most intensively (Figure 3). However, the first peak of gas formation was observed simultaneously in all samples after 60 min of fermentation. The second peak of gas formation, which indicates the beginning of maltose fermentation (Hackenberg et al., 2018), in the dough with the replacement of part of the wheat flour with hemp by-products began after 120 min of fermentation, which was 30 min earlier than in the control sample. At the same time, the highest amount of carbon dioxide was released in dough with the replacement of 10% of wheat flour with hemp by products.

The dynamics of gas formation in the dough with the replacement of 10% of wheat flour with organic hemp flour of the "Richoil" brand was studied (Tomashpolska et al., 2021). The first peak was observed after 150 min of fermentation, which was 90 min more compared to our results, which indicated a longer dough fermentation process. The addition of hemp seed flour to wheat bread recipe reduced gas formation. This is explained by the absence of gluten proteins and the increased fiber content in hemp flour (Istrate et al., 2021).

Replacing 30–50% of wheat flour with hemp seed flour in wheat bread recipes worsened the elasticity of the dough, reduced the gas formation (Mikulec et al., 2019), and, therefore, reduced the specific volume of bread. So, it was recommended to use no more than 30% hemp seed flour in wheat bread recipes. It was shown that the replacement of 10, 15 and 20% of wheat flour with hemp seed by-products led to a decrease in the amount of carbon dioxide formed during the fermentation of test samples of the dough for 180 minutes by 23-

30% compared to the control sample wheat dough without the addition of hemp seed by-products (Sokolova et al., 2020).

Based on the results of the research, it was found that hemp seed by-products have a rich chemical composition, a high content of protein and polyunsaturated fatty acids, they were balanced in terms of amino and fatty acid composition, and have an increased content of dietary fiber and micro- and macroelements compared to wheat flour. Therefore, hemp seed by-products can be considered promising raw materials for the use in bread production. However, the chemical composition different from wheat flour affected the course of the dough fermentation process and changes in the carbohydrate-amylase complex of the dough.

Conclusions

1. Determination of the chemical composition showed that the hemp by-products had 2.5–4.8 times more total protein and 8.8–30 times more fats, as well as a balanced composition of carbohydrates than first grade wheat flour.

2. As a result of determining the fractional composition of proteins, it was found that wheat flour of the first grade contained mostly the glutenin fraction, unlike hemp by-products, which were dominated by the albumin and globulin fractions. Hemp by-products had higher content of essential amino acids than in first grade wheat flour.

3. It was found that hemp by-products contained ω – 3 and ω – 6 fatty acids. In particular, in hemp seed kernels the ratio was 1:3.9, while in hemp seed flour – 1:3.5, in hemp hemp seed protein – 1:3.4.

4. The content of micro- and macroelements in hemp seed by-products was several times higher than in wheat flour of the first grade. Magnesium content was more than 20 times higher compared to wheat flour, potassium content – 8–9 times higher, zinc – 9–11 times higher, calcium content in hemp seed flour and hemp seed protein was 12 times higher compared to wheat flour, but hemp seed kernels - lower 3.3 times.

5. The amount of released carbon dioxide in the dough with the replacement of part of wheat flour with hemp by-products was lower compared to the control dough by 10–70 ml during 5 hours of dough fermentation.

6. The total amount of released carbon dioxide in dough with the addition of hemp by-products was less compared to the control sample, however, the second peak of gas formation, which indicates the fermentation of maltose, occured faster by 30 min, which indicates the intensification of the dough fermentation process. This result makes it possible to speed up the dough ripening process and accordingly reduce the time spent on the technological process of bread production with the appropriate recipe composition.

References

Apetroaei V.T., Pricop E.M., Istrati D.I., Vizireanu C. (2024), Hemp seeds (*Cannabis sativa* L.) as a valuable source of natural ingredients for functional foods – A review, *Molecules*, 29, 2097, https://doi.org/10.3390/molecules29092097

Başgel S., Erdemoğlu S.B. (2006), Determination of mineral and trace elements in some medicinal herbs and their infusions consumed in Turkey, *Science of the Total Environment,* 359(1–3), pp. 82–89, https://doi.org/10.1016/j.scitotenv.2005.04.016

Beto A.J. (2015), The role of calcium in human aging, *Clinical Nutrition Research,* 4(1), pp. 1–8, https://doi.org/10.7762/cnr.2015.4.1.1

Chowdhury K., Banu L.A., Khan S., Latif A. (2007), Studies on the fatty acid composition of edible oil, *Bangladesh Journal of Scientific and Industrial Research,* 42(3), pp. 311–316, https://doi.org/10.3329/bjsir.v42i3.669

Capcanari T., Covaliov E., Negoiţa C., Siminiuc R., Chirsanova A., Reşitca V., Ţurcanu D. (2023), Hemp seed cake flour as a source of proteins, minerals and polyphenols and its impact on the nutritional, sensorial and technological quality of bread, *Foods*, 12(23), 4327, https://doi.org/10.3390/foods12234327

Drobot V., Shevchenko A. (2017), Nutritional value and consumer properties of bakery products with fructose for diabetic nutrition, *Ukrainian Food Journal*, 6(3), pp. 480–493, https://doi.org/10.24263/2304-974X-2017-6-3-8

Ertas N., Aslan M. (2020), Antioxidant and physicochemical properties of cookies containing raw and roasted hemp flour, *Acta Scientiarum Polonorum: Technologia Alimentaria,* 19(2), pp. 177–184, https://doi.org/10.17306/J.AFS.2020.0795

El-Sohaimy S.A., Androsova N.V., Toshev A.D., El Enshasy H.A. (2022). Nutritional Quality, Chemical, and Functional Characteristics of Hemp (Cannabis sativa ssp. sativa) Protein Isolate., *Plants*, 11(21), 2825. https://doi.org/10.3390/plants11212825

Farinon B., Molinari R., Costantini L., Merendino N., (2020), The seed of industrial hemp (*Cannabis sativa* L.): Nutritional quality and potential functionality for human health and nutrition, *Nutrients*, 12(7), 1935, https://doi.org/10.3390/nu12071935

Glasdam S.M., Glasdam S., Peters G.H. (2016), The importance of magnesium in the human body: a systematic literature review, *Advances in Clinical Chemistry,* 73, pp. 169–193, https://doi.org/10.1016/bs.acc.2015.10.002

Hackenberg S., Leitner T., Jekle M., Becker T. (2018), Maltose formation in wheat dough depending on mechanical starch modification and dough hydration, *Carbohydrate Polymers*, 185, pp. 153–158, https://doi.org/10.1016/j.carbpol.2017.12.064

Hayıt F., Gül H. (2020), The importance of cannabis and its use in bakery products, *Electronic Letters on Science and Engineering*, 16(1), pp. 17–25.

Hayward L., McSweeney M., (2020), Acceptability of bread made with hemp (*Cannabis sativa* subsp. *sativa*) flour evaluated fresh and following a partial bake method, *Journal of Food Science*, 85(9), pp. 2915–2922, https://doi.org/10.1111/1750-3841.15372.

Irakli M., Tsaliki E., Kalivas A., Kleisiaris F., Sarrou E., Cook C.M., (2019), Effect of genotype and growing year on the nutritional, phytochemical, and antioxidant properties of industrial hemp (*Cannabis sativa* L.) seeds, *Antioxidants*, 8(10), 491, https://doi.org/10.3390/antiox8100491

Istrate A.M., Dabija A., Codina G.G., Rusu L. (2021), Influence of hemp flour on dough rheology and bread quality, *Scientific Study & Research*, 22 (4), pp. 521–531

Ivanov V., Shevchenko O., Marynin A., Stabnikov V., Gubenia O., Stabnikova O., Shevchenko A., Gavva O., Saliuk A. (2021), Trends and expected benefits of the breaking edge food technologies in 2021–2030, *Ukrainian Food Journal*, 10(1), pp. 7-36, https://doi.org/10.24263/2304-974X-2021-10-1-3

Kiouri D.P., Tsoupra E., Peana M., Perlepes S.P., Stefanidou M.E., Chasapis C.T. (2023), Multifunctional role of zinc in human health: An update, *EXCLI Journal*, 22, pp. 809–827, https://doi.org/10.17179/excli2023-6335

Koshova V., Mukoid R., Parkhomenko A. (2020), Influence of low-gluten grain crops on beer properties, *Ukrainian Food Journal*, 9(3), pp. 600–609, https://doi.org/10.24263/2304-974X-2020-9-3-9

López-Bascón M.A., de Castro M.L. (2020), Soxhlet extraction, In: F. Colin (Ed.), *Liquid-phase Extraction*, *Elsevier*, pp. 327–354, https://doi.org/10.1016/C2018-0-00618-0

Litvynchuk S., Galenko O., Cavicchi A., Ceccanti C., Mignani C., Guidi L., Shevchenko A. (2022), Conformational changes in the structure of dough and bread enriched with pumpkin seed flour, *Plants*, 11, 2762, https://doi.org/10.3390/plants11202762

Malik J., Szakova J., Drabek O., Balik J., Kokoska V. (2008), Determination of certain micro and macroelements in plant stimulants and their infusions, *Food Chemistry,* 111(2), pp. 520–525, https://doi.org/10.1016/j.foodchem.2008.04.009

Marinopoulou A., Sevastopoulou N., Farmouzi K., Konstantinidou E., Alexandri A., Papageorgiou M. (2024), Impact of hemp (*Cannabis sativa* L.) protein addition on the rheological properties of wheat flour dough and bread quality, *Applied Sciences*, 14, 11633. https://doi.org/10.3390/app142411633

McLean R.M., Wang N.X. (2021), Potassium, *Advances in Food and Nutrition Research,* 96, pp. 89–121, https://doi.org/10.1016/bs.afnr.2021.02.013

Mikulec A., Kowalski S., Sabat R., Skoczylas L., Tabaszewska M., Wywrocka-Gurgul A. (2019), Hemp flour as a valuable component for enriching physicochemical and antioxidant properties of wheat bread, *LWT - Food Science and Technology*, 102, pp. 164–172, https://doi.org/10.1016/j.lwt.2018.12.028

Mullerova M., Hryvna L., Dostalova Y., Kong J.L.H. , Ruban A., Machalkova L., Sottnikova V., Mrkvicova E., Vyhnanek T., Trojan V. (2016), Use of hemp raw materials in common bakery product recipes, *Students Conference on MendelNet*, 23, pp. 610–615, Available at https://mendelnet.cz/pdfs/mnt/2016/01/109.pdf

Pasichnyi V., Marynin A., Stabnikova, O., Shubina Y., Svyatnenko R. (2023), Functional and technological characteristics of semifinished products with shell of dough, *Ukrainian Journal of Food Science*, 11(2), pp. 65–80, https://doi.org/10.24263/2310-1008-2023-11-2-3

Pokrzywnicka M., Koncki R. (2017), Disaccharides determination: A review of analytical methods, *Critical Reviews in Analytical Chemistry*, 48(3), pp. 186–213, https://doi.org/10.1080/10408347.2017.1391683

Rusu I., Marc R., Mureşan C., Mureşan A., Mureşan V., Pop C., Chiş M., Man S., Filip M., Onica B., (2021), Hemp (*Cannabis sativa* L.) flour-based wheat bread as fortified bakery product, *Plants,* 10, 1558, https://doi.org/10.3390/plants10081558

Russo R., Reggiani R. (2015), Evaluation of protein concentration, amino acid profile and antinutritional compounds in hempseed meal from dioecious and monoecious varieties, *American Journal of Plant Sciences*, 6, pp. 14–22, https://doi.org/10.4236/ajps.2015.61003

Sahayam A.C., Venkateswarlu G., Chaurasia S.C. (2009), Nano platinum-catalyzed dry ashing of flour samples for the determination of trace metals by inductively coupled plasma optical emission spectrometry, *Atomic Spectroscopy*, 30(4), pp. 139–142.

Shevchenko A. (2022), Artichoke powder and buckwheat bran in diabetic bakery products, In: O. Paredes-López, O. Shevchenko, V. Stabnikov, V. Ivanov (Eds.), *Bioenhancement and Fortification of Foods for a Healthy Diet* (pp. 115-134), CRC Press, Boca Raton, London, https://doi.org/10.1201/9781003225287-8

Shevchenko A., Litvynchuk S. (2022), Influence of rice flour on conformational changes in the dough during production of wheat bread, *Ukrainian Journal of Food Science*, 10(1), pp. 5–15, https://doi.org/10.24263/2310-1008-2022-10-1-3

Shevchenko A., Fursik O., Drobot V., Shevchenko O. (2023), The use of wastes from the flour mills and vegetable processing for the enrichment of food products, In: O. Stabnikova, O. Shevchenko, V. Stabnikov, O. Paredes-López (Eds.), *Bioconversion of Waste to Value-added Products* (pp. 1–35), CRC Press, Boca Raton, London, https://doi.org/10.1201/9781003329671-1

Simopoulos A.P. (2002), The importance of the ratio of omega-6/omega-3 essential fatty acids, *Biomedicine & Pharmacotherapy,* 56(8), pp. 365–379, https://doi.org/10.1016/s0753-3322(02)00253-6

Sokolova N., Iorgacheva K. (2020), The potential of flour from solvent-extraction hemp oilcake as an ingredient of low-moisture bakery products, *Food Science and Technology*, 14, pp. 44–53, https://doi.org/10.15673/fst.v14i3.1789

Stabnikova O., Marinin A., Stabnikov V. (2021), Main trends in application of novel natural additives for food production, *Ukrainian Food Journal*, 10(3), pp. 524–551, https://doi.org/10.24263/2304-974X-2021-10-3-8

Stabnikova O., Stabnikov V., Antoniuk M., Arsenieva L., Ivanov V. (2022), Bakery products enriched with organoselenium compounds, In: O. Paredes-Lopez, V. Stabnikov, O. Shevchenko, V. Ivanov (Eds.), *Bioenhancement and Fortification of Foods for a Healthy Diet* (pp. 89–111), CRC Press, Boca Raton, London, https://doi.org/10.1201/9781003225287

Stabnikova O., Paredes-Lopez O. (2024), Plant materials for the production of functional foods for weight management and obesity prevention, *Current Nutrition & Food Science*, 20(4), pp. 401–422, https://doi.org/10.2174/1573401319666230705110854

Tomashpolska E., Shymanska A., Socolova N. (2021), New opportunities for the use of hemp products in breadmaking, *Procedicing of the International Competition of Student Scientific Works,* pp. 27–36.

Urade R., Sato N., Sugiyama M. (2018), Gliadins from wheat grain: an overview, from primary structure to nanostructures of aggregates, *Biophysical Reviews*, 10(2), pp. 435–443, https://doi.org/10.1007/s12551-017-0367-2

WHO (2003), World Health Organization, Diet, nutrition and the prevention of chronic diseases, Available from: http://apps.who.int/iris/bitstream/handle/10665/42665/WHO_TRS_916.pdf;jsessionid=9B8899CB77BAAEC360BEA529147672A4?sequence=1

Cite:

UFJ Style

Blazhenko M., Falendysh N., Shpak V. (2024), Effect of hemp seed by-products on wheat dough fermentation, *Ukrainian Food Journal*, 13(4), pp. 737–752, https://doi.org/10.24263/2304-974X-2024-13-4-8

APA Style

Blazhenko, M., Falendysh, N., & Shpak, V. (2024). Effect of hemp seed by-products on wheat dough fermentation. *Ukrainian Food Journal*, *13*(4), 737–752. https://doi.org/10.24263/2304-974X-2024-13-4-8

Physico-chemical characteristics of dried green onion semi-finished products and their rehydration ability

Vitalii Shutyuk, Olha Dushchak, Oleksandr Bessarab

National University of Food Technologies, Kyiv, Ukraine

Keywords:

Green onion
Drying
Hydration
Color

Article history:

Received 22.04.2024
Received in revised form 15.09.2024
Accepted 30.12.2024

Corresponding author:

Vitalii Shutyuk
E-mail: schutyuk@i.ua

DOI:
10.24263/2304-974X-2024-13-4-9

Abstract

Introduction. Studies of the drying process of green onions were conducted to determine the physico-chemical characteristics of dried semi-finished products and their ability to rehydrate.

Materials and methods. Green onions were dried at three different drying agent temperatures of 50, 60 and 70 °C. The speed of the airflow through the layer of raw materials was 1.3 m/s. For combined drying, a laboratory setup consisting of a DHG-9000 A drying chamber and an LG MF 6543 AF household microwave oven was used. Color parameters were determined by processing photos in the Adobe Photoshop graphic editor taken with a CANON EOS 80D camera using the HunterLab scale.

Results and discussion. During convective dehydration of green onions at drying agent temperatures of 50 and 60 °C, a constant speed section is observed, namely for 50 °C from 150 to 240 min of drying, and for 60 °C from 90 to 150 min of drying. For an air temperature of 70 °C, the section is almost absent.

The use of a two-stage method of drying green onions is more efficient in terms of energy and dehydration time. This technology involves two stages: the first convective method lasting 60 min at a drying agent temperature of 60 °C and the second one being microwave drying.

When restoring dried green onions, the rehydration rate increases with increasing water temperature from 0.026 min^{-1} at a water temperature of 50 °C to – 0.028 min^{-1} at a temperature of 70 °C. The equilibrium moisture content also increases from 5.65 to 6.15 kg of moisture per kg of dry product, respectively.

The drying temperature affected the parameters L, a, b on the HunterLab scale. Thus, the value of parameter "a" for fresh onions is 34, and for onions dried at a drying agent temperature of 50 °C is –10, for 70 °C it makes –12. The total color difference ΔE is about 33, which indicates a significant influence of drying duration on the color change of green onions.

Conclusions. The obtained results of the study of the physico-chemical characteristics of dried green onions in various ways will allow the production of higher-quality semi-finished products and competitive food products based on them.

Introduction

The global Spices and Seasonings market size was estimated at USD 20.19 billion in 2024 and is expected to grow at a CAGR (compound annual growth rate) of 4.89% from 2025 to 2032 (Spices and Seasonings Market, 2024). The use of spices and seasonings has been around throughout human history, and these natural plant products are included as ingredients in the formulation of various foods and drinks to give them specific taste and aroma (Kochubei-Lytvynenko et al., 2022; Lamkey, 2022; Stabnikova et al., 2021).

Green onion (also known as Welsh onion: *Allium fistulosum* L. belonging to the onion family *Alliaceae*) is originated from Central Asia, and are cultivated and traded around the world now as vegetable being fresh, or as spice being dried and grounded. *Allium* is a large genus of monocotyledonous flowering plants and its representatives including *Allium fistulosum* are widely used as ornamental flowers to decorate garden landscapes. It is a stable ingredient in different culinary dishes and at the same time is well known as a traditional medicinal plant because of its antioxidant, anti-inflammatory, and antimicrobial properties (Kim et al., 2023). Green onions used in folk medicine to treat colds, headaches, wounds, eyesight problems, reduce blood pressure, cholesterol level, fat accumulation and the risk of ischemic heart disease (Singh and Ramakrishna, 2017). Recent research showed in a randomized, double-blind, placebo-controlled trial on humans that Welsh onion green leaves extract may support and enhance immune function in healthy adults and help prevent infectious diseases such as colds and flu (Hirayama et al., 2019).

Allium fistulosum leaves contain, mg/100 g FW: dry matter, 10.6 – 10.8, total sugars, 3.9 – 4.0 (Čepulienė et al., 2024), soluble proteins, 730 (Štajner et al., 2006), and fat, 200 (Kim et al., 2023). Green onion leaves contain also vitamins of group B, μg/100 g FW: thiamine (B1), 0.05; riboflavin (B2), 0.09; niacin (B3), 0.40; and folic acid (B 9), 16 (Singh and Ramakrishna, 2017). Content of minerals consist, mg/100 g FW: calcium, 18; magnesium, 23; phosphorus, 49; iron, 1.2, and zinc, 0.52 (Singh and Ramakrishna, 2017).

Allium fistulosum leaves is a good source of β-carotene, and its content in leaves was 4.63 mg/100 g of fresh weight (FW) (Umehara et al., 2006). The main carotenoid determined in the onion leaves was lutein, followed with β-carotene, neoxanthin, violaxanthin, and antheraxanthin, with total content of carotenoids 5.47 mg/100 g FW (Kopsell et al., 2010). However, much higher carotenoid content, 287 mg/100 g FW was reported in (Štajner et al., 2006). Content of vitamin C in green onions consisted 16.1 mg/100 g FW (Štajner et al., 2006).

Green onion leaves are rich in polyphenolic compounds, containing, μg/100 g FW: p-coumaric acid,11.05; ferulic acid, 499.01; isoquercitrin, 29.14; quercitrin, 73.22; quercetol, 101.97; kaempferol, 153.94 (Vlase et al., 2013), and especial high content of flavonoids, 4.66 g/100 g FW (Štajner et al., 2006). Due to high content of these bioactive compounds, *Allium fistulosum* leaves exhibit significant antioxidant activity (Chang et al., 2013).

Green onion possess antibacterial properties, and it was shown inhibition effect of water, ethanolic, and petroleum ether extracts from leaves of *Allium fistulosum* on the growth of opportunistic pathogens, mainly bacteria *Staphylococcus aureus*, *Pseudomonas aeruginosa*, and *Escherichia coli* (Kumbhkar et al., 2023).

Green onions are a low-calorie product containing around 32 kcal/100 g FW (Kim et al., 2023). Being rich in biological active compounds and low in fat and calorie, green onions are fully satisfy requirements of diet for weight management and obesity prevention (Stabnikova and Paredes-Lopez, 2024; Sung et al., 2018).

Therefore, the physical and chemical characteristics of fresh green onions have been well studied. However, when harvested, spice plants may lose quality during drying, which

is fundamental process to keep the product good quality. The changes occurring in the green part during the drying process to obtain semi-finished products have not been sufficiently investigated, and there is not enough data on the ability of dried semi-finished products to rehydrate.

Drying is one of the most commonly used methods for preserving the material with high initial moisture contents helping to maintain minerals, inhibit microbial activity, as well as reduce transportation costs, handling, and storage. It removes much of the water from the plant soon after physiological maturity aiming to reach the moisture content ideal for long-term storage. Post-harvest conservation by drying relies on the fact that microorganisms, enzymes, and the metabolic mechanism require a certain amount of water to perform their activities. Reducing the water available in the plant will consequently reduce water activity, the rate of chemical reactions, the enzymatic degradation, and the microorganism growth (Hansen et al., 1993). However, due to undesirable changes in the quality of products dried with the pre-treatments and drying conditions, this process needs further studies (Maskan, 2000).

Thus, the aim of the present study was to investigate the drying process of green onions and their ability to rehydrate to determine the modes that allow producing higher quality semi-finished products.

Materials and methods

Materials

Green onions of the Parade variety was used in the research. When selecting raw materials for analysis, the following indicators were taken into account: the presence of a green stem of the uniform color, a light and pleasant taste with notes of onion and aroma, and the absence of defects.

Methods

Determination of physical-chemical characteristics of green onion

Green onion leaves (only green part) were washed and cut into pieces about 1 cm long. To determine the composition of the raw material generally accepted standard methods were used. Content of vitamin C was determined according to (Mohammed et al., 2014)

Kinetics of drying

To study the kinetics of dehydration, a layer of raw material with a height of about 3 cm of material was used. Green onions were dried at three different temperatures of the drying agent 50, 60 and 70 °C (taking into account the limitation of the browning temperature). The speed of the air flow through the layer of raw material was 1.3 m/s. All experimental results were obtained during drying by weighing the samples every 15 minutes until a constant weight was reached. Next, the mass fraction of moisture in the dried samples was determined. The mass fraction of moisture at different drying times was determined from the mass of the sample and its final moisture content. The obtained samples were analyzed using the dimensionless coefficient of moisture content (W, kg of moisture/kg of material).

Rehydration rate

The rehydration rate analysis was performed with samples dried at 50, 60 and 70 °C. In all cases, the mass fraction of moisture in the sample was less than 10.4%. The samples were weighed, placed in a special paper bag, weighed again, and then immersed in heated water. At a certain time, they were removed from the water and weighed. The rehydration rate was calculated using equation (1) (Krokida et al., 1997). The weight of the moistened bag was determined earlier.

$$d(W)/d\tau = -k(W - W^{eq}), \quad (1)$$

where W is the moisture content in the material during rehydration, kg/kg; τ is the rehydration time, min.; k is the rehydration rate, min^{-1}; W^{eq} is the equilibrium moisture content in the material, kg/kg.

Color

Color parameters were determined by processing photos in Adobe Photoshop taken with a CANON EOS 80D-camera на штативі QZSD (Beike) Q160H. The color parameters on the HunterLab scale were L (light or black-white axis), a (green-red axis) and b (blue-yellow axis). For each sample of green onion (fresh or dried at 50, 60 or 70 °C) five repetitions were made, the photos were previously blurred in a graphics editor. Another generalizing color parameter was the total color difference (ΔE):

$$\Delta E = \sqrt{(L - L_0)^2 + (a - a_0)^2 + (b - b_0)^2} \quad (2)$$

Statistics

All experiments were carried out at least in triplicate, and mean ± standard deviation are shown.

Results and discussion

Proximate composition of green onion

Proximate composition of green onion and the content of vitamin C is shown in Table 1.

Table 1

Proximate composition of green onion

Plant object	Moisture content, %	Total sugars, %	Proteins, %	Fats, %	Fiber, %	Vitamin C, mg/100 g
Green onion	93±0.5	3.2±0.4	1.1±0.4	0.1±0.02	1.5±0.2	15.4±1.0

The most important component determine the yield and quality of dried products are the content of dry matter, sugars, and main biochemical components (Martinazzo et al., 2016). It was found that the average content of moisture varied between 91 and 92%. It is worth noting that the content of sugars is one of the most important characteristics that determine the possibility of drying a particular type of raw material (Luciano et al., 2007). Content of total sugars in green onion was 3.2±0.4% FW. It was shown that the predominant sugars in green onions are monosaccharides, namely glucose and fructose (Kim et al., 2023), but they also consist of maltose, rhamnose, galactose, arabinose, mannose, and xylose in low amounts (Singh and Ramakrishna, 2017). The total carbohydrate content of the studied sample was 4.9%, with fiber accounting 53% of the total amount of carbohydrates. Low contents of protein, 1.2%, and fat, 0.8%, were determined in fresh green onion with the moisture content 93%. The content of vitamin C in the green onion was 15.4%. Green onion with established chemical composition were used as origin material for further studies.

Kinetics of drying

The process of heat treatment of raw materials was considered complete when the control value of moisture content W_c = 0.104 kg/kg (10.4%) was reached. Studies of the process of drying green onions under constant conditions at different temperatures showed that increasing the temperature of the drying agent significantly reduces the drying time (Kumar et al., 2021; Yevchuk et al., 2023). Thus, at a hot air speed of 1.3 m/s, the duration of drying raw materials is more than 300 min at a temperature of 50 °C and less than 150 min at 70 °C (Figure 2).

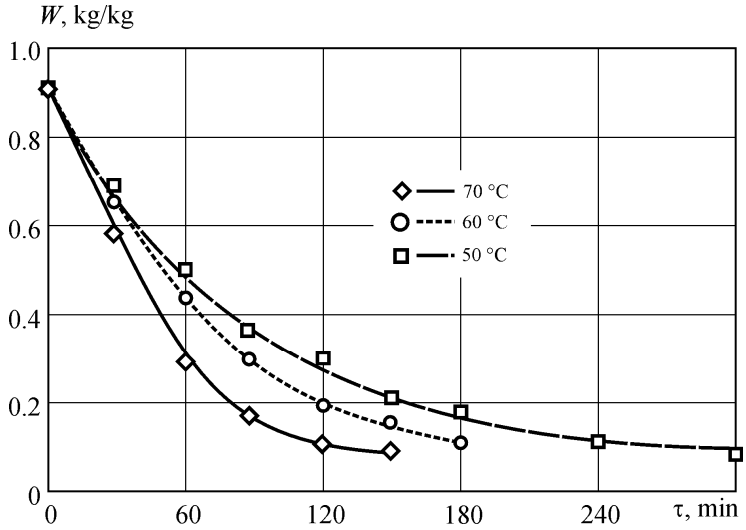

Figure 2. Change in content of moisture in green onions during drying at different temperatures and drying agent speed of 1.3 m/s

The maximum rate of change in the mass fraction of moisture significantly depends on the temperature of the drying agent (Fig. 3). Thus, an increase in the hot air temperature from 50 to 70 °C for 30 minutes of dehydration led to an increase in the maximum rate of change

in moisture content in green peas from 0.0083 kg/(kg·min) to 0.0115 kg/(kg·min) (Kumar et al., 2021). In the curves of the dehydration rate of green onions for drying agent temperatures of 50 and 60 °C, a constant speed section is observed, namely for 50 °C from 150 to 240 min of drying (0.001 kg/(kg min)), and for 60 °C from 90 to 150 min of drying (0.004 kg/(kg min)). For an air temperature of 70 °C, the section, in our opinion, is not significant and in Fig. 2 is absent, which is confirmed by its decrease for temperatures of 50 and 70 °C from 90 to 60 min.

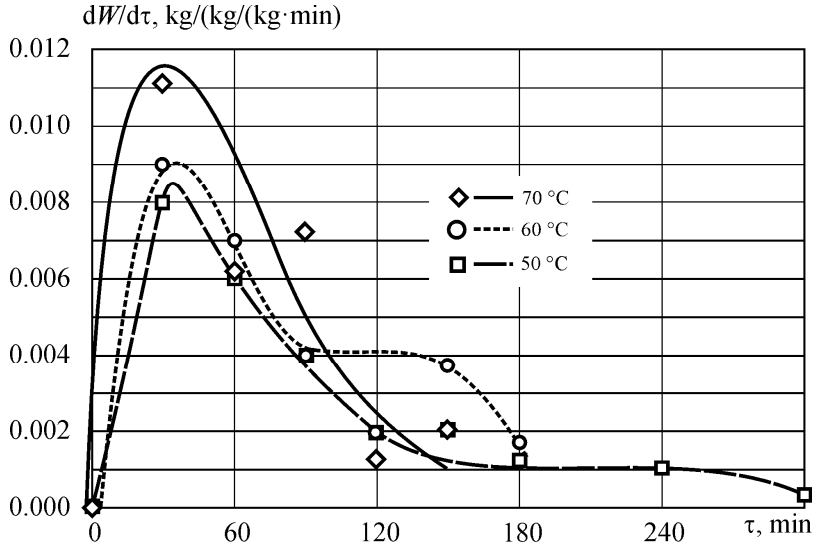

Figure 3. Change in rate of dehydration of green onions during drying at different temperatures of drying agent and speed of 1.3 m/s

The experiments conducted to determine the kinetics of green onion drying confirmed the feasibility of combining microwave and convective methods (Fig. 3). They indicate that the duration of drying by microwave is significantly shorter compared to the traditional convective method. Thus, for green onions, the difference in the duration of drying by these methods is about 130 minutes.

Using only microwave drying for green onions significantly reduces the duration of the process, but the quality of the product received deteriorates due to partial carbonization of the tissues. In this case, one of the main reasons affecting the quality of dried products is the need to change the power of the microwave emitter, due to the periodicity of the installation, and microwave emitters have discrete positional power control, which cannot sufficiently provide the necessary change in the drying mode.

Given the significant energy costs of microwave drying, the authors conducted additional studies that involved drying in two stages: the first is a convective method lasting 60 min (to a moisture mass fraction of 0.41 kg/kg); the second is microwave drying. The two-stage drying method proved to be effective and significantly reduced the dehydration time, these results correlate with the results of combined dehydration of banana, carrot and grape (Dehnad et al., 2012). In addition, it was achieved to obtain dry green onions with a lower moisture content compared to the convective method.

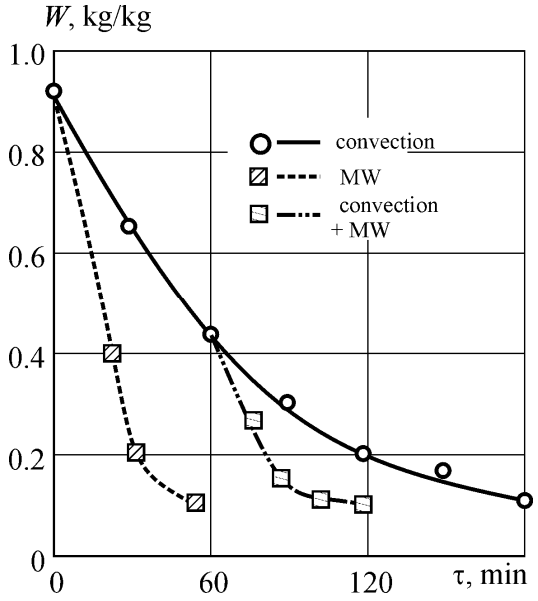

Figure 3. Change in moisture content of green onions during drying process by microwave and convective methods in different combinations

Rehydration rate

The kinetics of rehydration of dry green onions was studied at water temperatures of 50, 60 and 70 °C. The results of measuring the mass fraction of moisture in the material show that the rehydration rate and equilibrium humidity are higher for higher water temperatures (Fig. 4). Thus, for a temperature of 50 °C, the equilibrium humidity is 5.5 kg/kg, and at 70 °C it is 6.0 kg/kg. Moreover, the data indicate that the equilibrium moisture content during hydration is reached after 120 s, and almost three quarters of the equilibrium state of the product is reached by 30 s of the rehydration process.

The kinetics of rehydration of dried green onions depending on the water temperature (see Fig. 4) can be described with sufficient accuracy in the form of logarithmic dependences given in Table 2; while the rehydration rate determined by equation (1) increases from 0.026 min^{-1} at a water temperature of 50 °C to – 0.028 min^{-1} at a temperature of 70 °C. Also, with increasing hydration temperature, the value of the equilibrium moisture content W^{eq} increases from 5.65 to 6.15 kg/kg, respectively (Fig. 5). The obtained data and dependences correspond in nature to the results of studies (Shutiuk et al., 2014) on the rehydration of potatoes, mushrooms, pumpkins, apples and carrots.

Color

During the drying of green onions, significant color changes occurred. The drying temperature affected the parameters L, a, b. The parameters L and “a” of the dried samples differed significantly from the fresh material (Fig. 6).

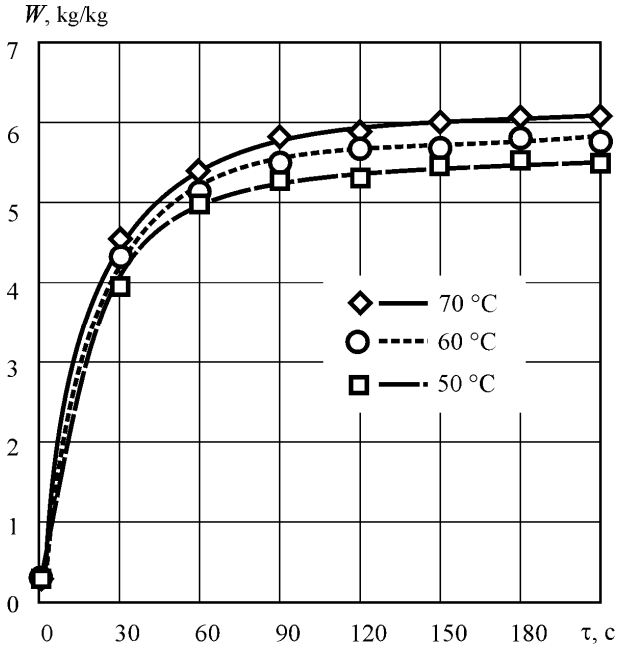

Figure 4. Change in moisture content of dried green onions depending on temperature of water during hydration

Table 2

Correlation of mass fraction change of green onions during rehydration

Water temperature (t, °C)	**Regression equation** *(W = f(τ))*	**R²**
50	$W = 1.0325\ln(\tau) + 0.3643$	0.9856
60	$W = 1.0915\ln(\tau) + 0.3798$	0.9844
70	$W = 1.1412\ln(\tau) + 0.3939$	0.9840

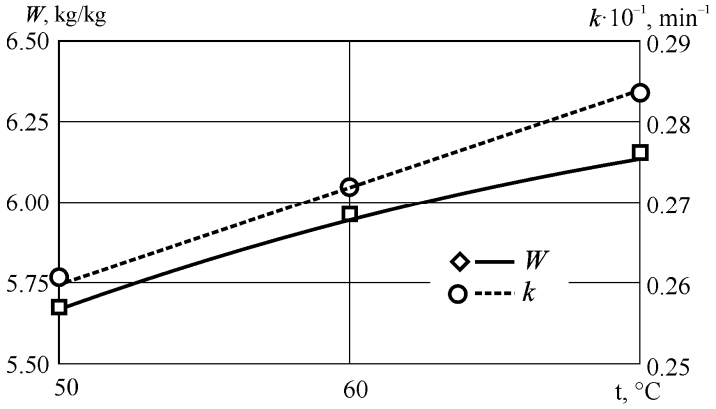

Figure 5. Effect of hydration temperature on rehydration coefficient (*k*) and equilibrium moisture content (W^{eq})

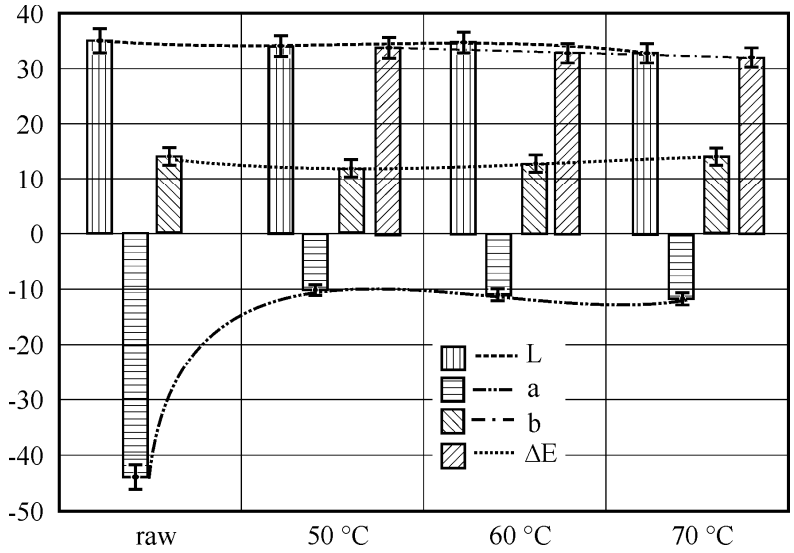

Figure 6. Changes in color parameters of raw green onions and those dried at different drying temperatures in the Lab color system

The parameters L are higher in the dried product (lighter), and the parameters a have significantly smaller negative values, which indicates a decrease in the intensity of the green color. Thus, the value of the parameter "a" for fresh onions is 34, and for those dried at a drying agent temperature of 50 °C it is 10, for 60 °C it makes 11 and for 70 °C it is 12 (respectively). The total color difference ΔE is about 33, which indicates a significant influence of the drying duration on the color change of green onions. The greatest color changes during drying occur at a drying agent temperature of 70 °C (Fig. 7).

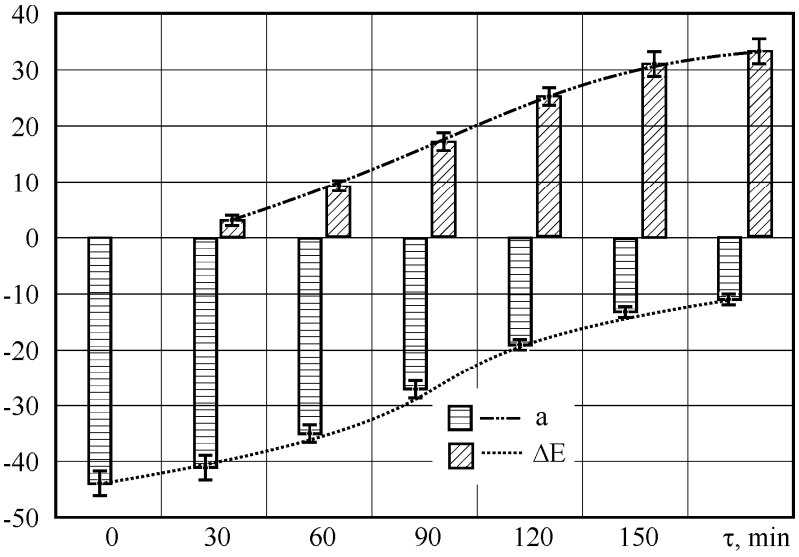

Figure 7. Changes in color parameters a and ΔE in the Lab color system of green onions drying at a drying agent temperature of 70 °C

Similar results with color changes were obtained in study (Demirhan and Özbek, 2014) during drying of basil in various ways. When using the microwave drying method, a sharp change in the values of a from –44 to –7 and, accordingly, the total color difference ΔE to 37 is observed (Fig. 6), which is explained, according to the Lab system, by the degradation of the green pigment of chlorophyll and its transition to yellow.

The use of the combined drying method at the stage of the beginning of the decreasing rate of dehydration (see Fig. 3) significantly reduces the duration of the process, but has less effect on the loss of green pigment compared to microwave drying. Thus, the value of the parameter a for the microwave drying method is –7, for the convective method it is –11, and for the combined method –9 (Fig. 8) significantly reduces the duration of the process, but has less effect on the loss of green. Accordingly, the use of the combined drying method allows not only to reduce the dehydration time compared to the convective method, but also to lose less green pigment compared to the microwave method.

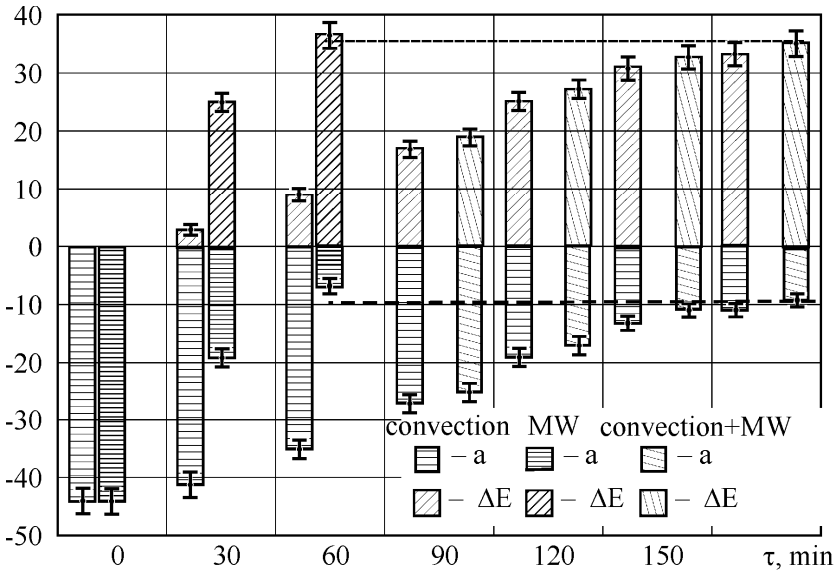

Figure 8. Changes in color parameter a and the total color difference ΔE of raw green onions during drying in different ways

Conclusions

1. The results of the research show that the dehydration rate of green onions for drying agent temperatures of 50 and 60 °C shows a constant speed section, namely for 50 °C from 150 to 240 min of drying (0.001 kg/(kg min)), and for 60 °C from 90 to 150 min of drying (0.004 kg/(kg min)); and for an air temperature of 70 °C, the section is almost absent.
2. The two-stage method of drying green onions is more effective and significantly shorter in terms of dehydration time. It involves two stages: the first convective method lasting

60 min (to a mass fraction of moisture of 0.41 kg/kg) at a drying agent temperature of 60 °C and the second one being microwave drying.

3. The rehydration rate increases with increasing water temperature from 0.026 min^{-1} at a water temperature of 50 °C to – 0.028 min^{-1} at a temperature of 70 °C. The value of the equilibrium moisture content W^{eq} also increases from 5.65 to 6.15 kg/kg, respectively.
4. The drying temperature affected the parameters L, a, b on the HunterLab scale. Thus, the value of parameter a for fresh onions is 34, and for onions dried at a drying agent temperature of 50 °C is –10, for 60 °C it is –11 and for 70 °C it makes –12 (respectively). The total color difference ΔE is about 33, which indicates a significant influence of drying duration on the color change of green onions.

References

Čepulienė V., Juškevičienė D., Viškelis J., Karklelienė R. (2024), Productivity and quality parameters of *Allium fistulosum* L., *Acta Agriculturae Scandinavica*, *Section B — Soil & Plant Science*, 74(1), https://doi.org/10.1080/09064710.2024.2392506.

Chang T., Chang H., Chang S., Lin S., Chang Y., Jang H. (2013), A comparative study on the total antioxidant and antimicrobial potentials of ethanolic extracts from various organ tissues of *Allium* spp., *Food and Nutrition Sciences*, 4, pp. 182–190, https://doi.org/10.4236/fns.2013.48A022.

Dehnad D., Jafari S.M., Ganje M., Ghambari V. (2012), Simultaneous heat and mass transfer during microwave drying of foods, *The First Middle East Drying Conference*, Shahid Chamran University of Ahvaz, Iran.

Demirhan E., Özbek B. (2009), Color change kinetics of microwave-dried basil, *Drying Technology*, 27(1), pp.156–166, https://doi.org/10.1080/07373930802566101.

FAO. (2024), Food and Agricultural Organization, Area and production data, www.fao.org. Access date 01 Dec 2024.

Hansen R., Keener H., Elsohly H. (1993), Thin layer drying of cultivated taxus clippings, *Transactions of the ASAE*, 36, pp. 1387–1391, https://doi.org/10.13031/2013.28475.

Hirayama Y., Takanari J., Goto K., Ueda H., Tanaka A., Nishihira J. (2019), Effect of Welsh onion (*Allium fistulosum* L.) green leaf extract on immune response in healthy subjects: A randomized, double-blind, placebo-controlled study, *Functional Foods in Health and Disease*, 9, pp. 123–133, https://doi.org/10.31989/ffhd.v9i2.569.

Kim S.H., Yoon J.B., Han J., Seo Y.A., Kang B.H., Lee J., Ochar K. (2023) Green onion (*Allium fistulosum*): An aromatic vegetable crop esteemed for food, nutritional and therapeutic significance, *Foods*, 12(24), 4503, https://doi.org/10.3390/foods12244503.

Kochubei-Lytvynenko O., Kuzmyk U., Yushchenko N. (2022), Spices for dairy products, In: O. Paredes-López, O. Shevchenko, V. Stabnikov, V. Ivanov, (Eds.), *Bioenhancement and Fortification of Foods for a Healthy Diet*, CRC Press, Boca Raton, London, pp. 157-178, https://doi.org/ 10.1201/9781003225287-11.

Kopsell D., Sams C., Deyton D., Abney K., Kopsell D., Robertson L. (2010), Characterization of nutritionally important carotenoids in bunching onion, *HortScience*, 45(3), pp. 463–465, https://doi.org/10.21273/hortsci.45.3.463.

Krokida M., Maroulis Z. (1997), Effect of drying method on shrinkage and porosity, *Drying Technology*, 10, pp. 1145–1155, http://dx.doi.org/10.1080/07373939708917369.

Kumar R., Malik M., Sharma A. (2021), Drying kinetics and effects of different drying methods and nutritional quality of raw and differently blanched green peas, *Journal*

of Current Research in Food Science, 2(2) pp. 44–56, https://doi.org/10.22271/foodsci.2021.v2.i2a.44.

Kumbhkar L., Choudhary R., Nayak B., Tiwari R. (2023), Antimicrobial potential of *Ipomoea aquatica*, *Allium fistulosum* and *Cucurbita moschata* against *Staphylococcus aureus*, *Pseudomonas aeruginosa* and *Escherichia coli*, Scope, 13(4), pp. 687-691.

Lamkey J.W. (2022), Spices, seasonings and flavors - achieving the desired result, *Meat and Muscle Biology*, 5(3), 13016, https://doi.org/10.22175/mmb.13016.

Luciano C., Guiné R., Barroca M. (2007), Onion drying: Kinetic study and chemical characterization, *Scientific Repository of the Polytechnic Institute of Viseu*, pp. 633-636.

Maskan M. (2000), Microwave/air and microwave finish drying of banana, *Journal of Food Engineering*, 44, pp. 71-78, https://doi.org/10.1016/S0260-8774(99)00167-3.

Martinazzo A., Corrêa Filho L., Teodoro C., Berbert P. (2016), Drying kinetics and microbiological quality of green onions, *Revista Ceres*, 63(6), pp. 769–774, https://doi.org/10.1590/0034-737x201663060004.

Mohammed Q., Hamad M., Mohammed E. (2009), Spectrophotometric determination of total vitamin C in some fruits and vegetables at Koya Area-Kurdistan Region/Iraq, *Journal of Kirkuk University–Scientific Studies*, 4(2), pp. 46–54. https://doi.org/10.13140/RG.2.1.2126.7603.

Singh B.K., Ramakrishna Y. (2017), Welsh onion (*Allium fistulosum* L.): A promising spicing-culinary herb of Mizoram, *Indian Journal of Hill Farming*, 30(2), 201–208.

Shutyuk V., Bessarab O., Samiylenko S., Tsyomka Yu., Omelchenko A. (2014), Research of rehydration kinetics of dried vegetable feedstock, *Ukrainian Food Journal*, 3(5), pp. 121–128.

Spices and Seasonings Market. (2024), Spices and Seasonings market size, share & industry analysis, by type (pepper, chili, ginger, cinnamon, cumin, turmeric, nutmeg and mace, cardamom, cloves, and others), by application (meat and poultry, bakery and confectionery, frozen food, snacks & convenience food, and others), and regional forecast, 2024-2032, Source: https://www.fortunebusinessinsights.com/industry-reports/spices-and-seasonings-market-101694, Available 13.01.2025

Stabnikova O., Marinin A., Stabnikov V. (2021), Main trends in application of novel natural additives for food production, *Ukrainian Food Journal*, 10(3), pp. 524–551, https://doi.org/10.24263/2304-974X-2021-10-3-8.

Stabnikova O., Paredes-Lopez O. (2024), Plant materials for the production of functional foods for weight management and obesity prevention, *Current Nutrition & Food Science*, 20(4), pp. 401–422, https://doi.org/10.2174/1573401319666230705110854.

Štajner D., Milić N., Čanadanović-Brunet J., Kapor A., Štajner M., Popović B. (2006), Exploring *Allium* species as a source of potential medicinal agents, *Phytotherapy Research*, 20(7), pp. 581–584, https://doi.org/10.1002/ptr.1917.

Sung Y., Kim D., Kim S., Kim H. (2018), Aqueous and ethanolic extracts of welsh onion, *Allium fistulosum*, attenuate high-fat diet-induced obesity, *BMC Complementary and Alternative Medicine*, 18, 105, https://doi.org/10.1186/s12906-018-2152-6.

Umehara M., Sueyoshi T., Shimomure K., Iwai M., Shigyo, M., Hirashima K., Nakahara T. (2006), Interspecific hybrids between *Allium fistulosum* and *Allium schoenoprasum* reveal carotene-rich phenotype, *Euphytica*, 148, pp. 295–301, https://doi.org/10.1007/s10681-005-9029-8.

Vlase L., Parvu M., Parvu E., Toiu A. (2013), Phytochemical analysis of *Allium fistulosum* L. and *A. ursinum* L., *Digest Journal of Nanomaterials and Biostructures*, 8(1), pp. 457–467, https://www.chalcogen.ro/457_Parvu.pdf.

Yevchuk Y., Ivanov D., Shutyuk V. (2023), Research of convective drying regimes of viburnum fruits, *Trends in LEAN Food Production and Packaging, Proceedings of the 12th International Specialized Scientific and Practical Conference*, September 20, Kyiv, pp. 96-98, https://conference.nuft.edu.ua/leanfoodpack/Books/Abstracts/A_2023.pdf.

Cite:

UFJ Style

Shutyuk V., Dushchak O., Bessarab O. (2024), Physico-chemical characteristics of dried green onion semi-finished products and their rehydration ability, *Ukrainian Food Journal*, 13(4), pp. 753–765, https://doi.org/10.24263/2304-974X-2024-13-4-9

APA Style

Shutyuk, V., Dushchak, O., & Bessarab, O. (2024), Physico-chemical characteristics of dried green onion semi-finished products and their rehydration ability. *Ukrainian Food Journal*, *13*(4), 753–765. https://doi.org/10.24263/2304-974X-2024-13-4-9

Determination of opening force of hot-melt adhesive joints in flexible packaging

Oleksandr Gavva[1], Oleksandr Sokolskyi[2], Yuliia Herasymenko[2]

1 – National University of Food Technologies, Kyiv, Ukraine;
2 – National Technical University of Ukraine «Igor Sikorsky Kyiv Polytechnic Institute», Kyiv, Ukraine

Keywords:

Adhesive
Flexible
Packaging
Strength

Article history:

Received
21.05.2024
Received in
revised form
29.06.2024
Accepted
30.12.2024

Corresponding author:

Oleksandr Gavva
E-mail:
gavvaoleksandr@
gmail.com

DOI:
10.24263/2304-974X-2024-13-4-10

Abstract

Introduction. Numerical modeling of the strength of hot-melt adhesive joints in flexible packaging materials allows for predicting the peel force values to achieve consumer-friendly packaging joint strength.

Materials and methods. For experimental tensile strength testing, three types of packaging materials were used: offset paper, cardboard, and polyethylene, which were subsequently bonded with a hot-melt adhesive. The hot-melt adhesive is based on EVA (ethylene-vinyl acetate). Numerical modeling was conducted to analyze the failure of the hot-melt adhesive joint, aiming to predict the initiation and propagation of failure under static loads.

Results and discussion. A mathematical model is proposed that allows experimentally determined resistance values to be used to calculate the maximum failure force. A numerical determination of the contact zone strength was performed, which enables the calculation of the failure force. The dependencies of the force at the edges of samples made from the three packaging materials on displacement for both experimental values and those obtained from numerical modeling were found. It was shown that plasticity zones arise on the interface surface when maximum stress is reached, leading to unloading in the local zone of the sample material. As the joint continues to fail, the breaking forces gradually decrease. The dependencies of forces at the edges of samples made from paper, cardboard, and polyethylene on the displacement of the sample edges during stretching were obtained. The appearance of the experimental curves of the dependence of the applied forces on the displacement corresponds to the model of nonlinear elastic-plastic failure of the adhesive zone. It was found that under the considered bonding conditions, the total peel force for paper materials is 0.1 N/mm, for cardboard materials – 0.22 N/mm, and for polyethylene materials – 0.75 N/mm. The highest force value among the bonded samples was observed for polyethylene. This can be explained by the fact that, during bonding with hot-melt adhesive, some films undergo welding rather than just bonding.

Conclusions. The considered model and methodology of numerical modeling of the strength of hot-melt adhesive joints provide the ability to predict the necessary and sufficient values of their strength.

Introduction

The technology of joining with hot-melt adhesive material is widely used in the chemical, food, and textile industries for forming joints in cardboard, paper, polymer, and combined packaging (Brockmann et al., 2008). This type of joint is used for joining and sealing various flexible and semi-rigid packages, such as those for flour, building bulk materials, confectionery products, and applying labels. Examples of the use of hot-melt adhesive joining are shown in Figure 1.

Figure 1. Examples of hot-melt adhesive use
a – manual application;
b – semi-automatic application;
c – automated equipment for application;
d – product packaged with hot-melt adhesive joints

Hot-melt adhesive joining has advantages compared to conventional glue. Traditional adhesive joints require a significant amount of time to achieve the planned strength, create solvent vapors in the workspace, and pose a risk of interaction with the packaged product. These disadvantages are absent when using hot-melt adhesive joining.

The use of hot-melt adhesive speeds up the process of labeling packaging, which directly affects productivity and production volumes. Additionally, hot-melt adhesive ensures effective and reliable label fixation, as it is resistant to external factors (moisture, heat, and cooling). In this case, the label will remain neat, and presentable, and not slip off during transportation.

Therefore, the task is to ensure the strength and reliability of the hot-melt adhesive bond to meet consumer demands during its use. Understanding the behavior of hot-melt adhesive joints during failure will allow the creation of high-quality joints in packaging elements.

The reliability of adhesive joints depends not only on the damage mechanisms but also on their ability to resist separation (Banea et al., 2015; Bennati et al., 2009; Campilho et al., 2013).

For example, in the works (Banea et al., 2009; 2010), the J-integral method is used to assess the strength of adhesive joints, which allows for determining the fracture toughness the driving force of crack propagation. For calculating flexible joined elements, it is advisable to consider the critical rate of energy release during deformation, taking into account large displacements (Zhao et al., 2016).

Mathematical models based on the adhesion zone method are most commonly used for modeling fracture processes (Stigh et al., 2016). Tasks of this type are solved using linear and nonlinear fracture mechanics. In most such mathematical models, the ratio of tensile and fracture stresses at the interface boundary is such that, as the interfacial distance increases, the adhesive strength at the interface reaches a maximum (crack initiation), then decreases, and afterward the crack propagates, leading to complete separation. The adhesion zone model simulates the fracture process by extending the concept of continuum mechanics, including the fracture zone, and using strength and energy parameters to characterize the separation process (Budzik et al., 2021; Leffler et al., 2007).

The reviewed works well describe the energy-force parameters of the fracture of rigid plate joints with a large contact surface area. However, they do not allow for a correct study of the fracture of joints in flexible materials with a narrow contact area, as is the case with flexible packaging.

Traditional mathematical models of fracture in the adhesion zone (De Moura et al., 2017; Valoroso et al., 2010) require experimental determination of the crack opening length as a function of the displacement of the sample edges. In the case of studying the fracture of hot-melt adhesive joints in flexible packaging materials, such measurements are difficult due to the narrow width of the bond zone and large displacements of the edges.

This study aims to numerically model the strength of hot-melt adhesive joints in flexible packaging materials to predict the opening force. This will allow for achieving consumer-friendly packaging joint strength, while also preventing unintentional self-unsealing.

Materials and methods

Materials

For the experimental study of tensile strength, three types of packaging materials were used – offset paper, cardboard, and polyethylene, which were subsequently bonded with hot-melt adhesive.

The mechanical properties of the materials used in the study are as follows:

- paper samples: elastic modulus – 2000 MPa, Poisson's ratio – 0.276;
- cardboard samples: elastic modulus – 1500 MPa, Poisson's ratio – 0.16;
- polyethylene samples: elastic modulus – 150 MPa, Poisson's ratio – 0.44.

Hot-melt adhesive from EVA-based material: elastic modulus – 90 MPa, tensile strength – 8 MPa, Poisson's ratio – 0.3.

The experimental study of the destruction process of hot-melt adhesive joints of paper, cardboard, and polyethylene samples was conducted according to the methodology outlined (Sokolskyi et al., 2020).

Methodology of numerical modeling

For the analysis of the fracture of thermoplastic adhesive joints, numerical modeling was performed using the finite element method to predict the initiation and propagation of fracture under static loads. The modeling of the double cantilever beam specimen, based on the adhesion zone methodology and fracture mechanics theory, accounts for irreversible failure at the interface, which is an advantage for modeling adhesive joints.

Figure 2 shows the general view of the finite element model. The model of the specimen consists of two strips of packaging material connected by a layer of hot-melt adhesive (red line), subjected to the action of two transverse symmetric forces. On the other side, the beam is rigidly fixed.

Figure 2. Finite element model of specimen bonded with hot-melt adhesive

Fracture of the adhesive occurs in Mode I (opening mode). It involves tensile stresses that lead to the crack formation (normal opening occurs in the field of normal stresses, and the displacement of the crack faces is perpendicular to the plane of the crack).

A numerical model was developed to study the behavior of the hot-melt adhesive joint during delamination, and a numerical calculation of the displacements and stresses occurring in the adhesive joint under tensile loading was performed.

A series of numerical experiments on fracture were conducted until the reaction values at the ends of the specimen matched those obtained during the experiment. By numerically selecting the values of the critical fracture energy, the threshold of bond strength energy is determined, and then, using this value, the force at the edges of the specimen, at which failure occurs, is calculated.

Experimental setup and procedure for conducting research

Tensile testing of bonded packaging material samples with hot-melt adhesive was conducted on the experimental setup shown in Figure 3 (Herasimenko et al., 2020).

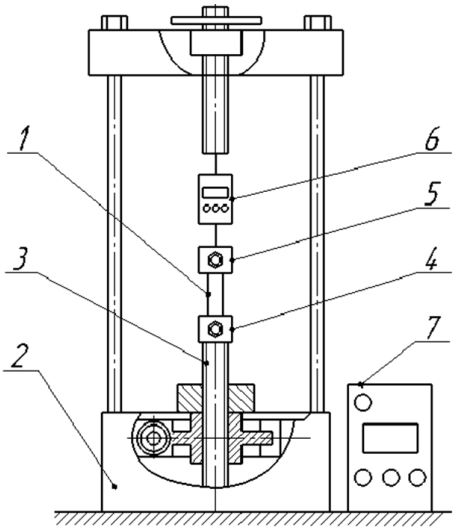

Figure 3. Experimental setup for tensile strength testing
1 – specimen; 2 – frame; 3 – tensile device; 4 – lower clamping jaws;
5 – upper clamping jaws; 6 – electronic dynamometer; 7 – control unit.

The experimental setup operates as follows. The test sample 1 is clamped between the lower 4 and upper 5 clamping jaws. A set tensile speed is established on the control unit 7. After activating the device, the lower jaw 4 moves downward at a constant speed and the electronic dynamometer 6 records the applied force. The displacement of the jaw is displayed on the indicator of the control unit 7.

The experiment was conducted as follows. First, the packaging material is bonded with hot-melt adhesive. The bonded strip of packaging material is then cut into individual samples. The test sample is clamped in the clamping jaws 4 and 5 of the setup (Fig. 3).

By stretching the sample at a set speed, we determine the force at the sample edges and plot its dependence on displacement.

Results and discussion

Mathematical model of the fracture process of the hot-melt adhesive joints

The geometry of the double cantilever beam is the most common test sample for analyzing the strength of adhesives and the delamination of composites. The double cantilever beam scheme is shown in Figure 4.

The specimen is rigidly fixed on one side, while symmetric forces are applied on the other side. The beam also has an initial crack, so the crack propagation continues in the opening mode.

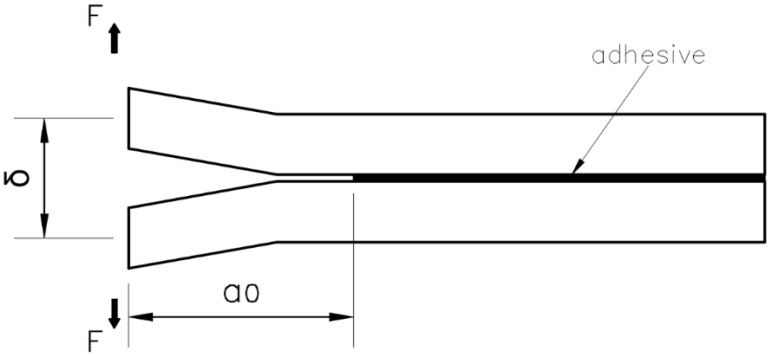

Figure 4. Scheme of the failure of the hot-melt adhesive bonded specimen

It is proposed to apply a mathematical model that allows the experimental determination of the fracture resistance of the joint to be used for calculating the maximum fracture force without measuring the crack length (Škec et al., 2018). It allows for avoiding the experimental determination of the crack opening length depending on the displacement of the sample edges for calculating the critical fracture energy. This model is proposed to be used for determining the opening force of the packaging, i.e., solving the inverse problem – numerical determination of the contact zone strength, from which the fracture force can be calculated.

For the mathematical description of the adhesive joint failure process, the adhesion zone model is used, in which the formation of failure is considered a gradual phenomenon, and the separation of surfaces occurs due to the deformation in the area of the failure initiation, which propagates along the adhesive layer.

To model the nonlinear elastic-plastic failure of a specimen with a central crack, we consider the crack propagation process based on the nonlinear adhesion zone model (Figure 5) (Škec et al., 2018).

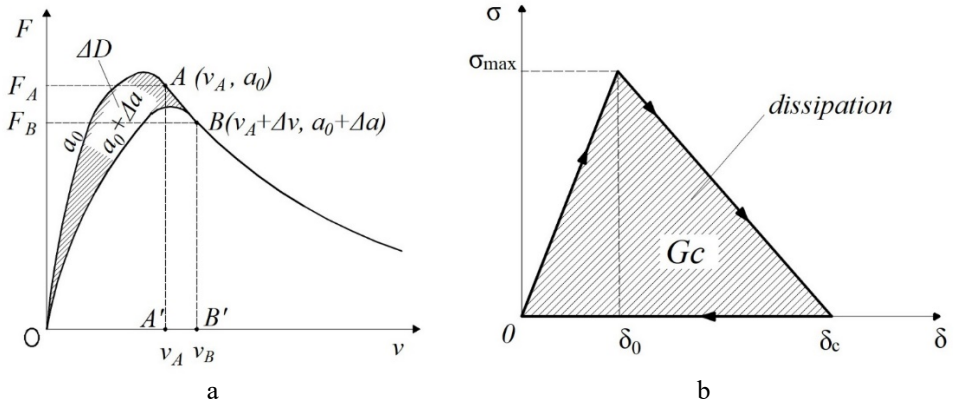

Figure 5. Behavior of the interface surface of the adhesion zone
a – dependence of the reaction force on the displacement;
b – equivalent adhesion zone law for the damaged point.

In these figures: F – reaction force at the edges, N; v – displacement vector, mm; a – crack opening length, mm; D – dissipation energy, J; σ – stress, Pa; G_c – critical energy release rate, J/m²; δ – relative displacement.

This model assumes that when the maximum stress $\sigma_{\max}$ is reached on the interface surface, plasticity zones form, leading to unloading in the local area of the specimen material.

The graphical representation of the power balance, shown in Figure 5a, illustrates the values of energy and its increment as the crack-opening zone propagates from the initial position a_0 to the new position $a_0 + \Delta a$. Point A corresponds to the displacement v_A and force F_A at which the crack-opening zone begins to propagate. At point A, the crack-opening zone extends by Δa, accompanied by an increase in displacement v_A from v_B and a decrease in force from F_A to F_B. The shaded area represents the increment in dissipation energy ΔD during the failure process.

Figure 5b illustrates that the propagation of the separation zone essentially involves the material failure at the tip of this zone, accompanied by energy dissipation when the deformation reaches the critical value $\delta = \delta_c$. While $\delta < \delta_c$, no energy is dissipated, and the stress increases linearly. When the separation zone propagates, the stress at its tip decreases from $\sigma_{\max}$ to zero, and the reaction force at the edges also decreases.

For this type of specimen deformation, the system's state is determined by the specified displacements and the crack length. In this case, the total potential energy can be expressed as a function of v and a.

In general form, the rate of change of the total potential energy $\dot{\Pi}$ is equal to the mechanical energy $\dot{W}$ transferred to the solid body, taking into account the dissipation energy $\dot{D}$:

$$\dot{\Pi} = \dot{W} - \dot{D},$$

where the dot denotes the derivative with respect to t; $\dot{W}$ is the mechanical energy, J; $\dot{D}$ is the dissipation energy, J.

From the perspective of thermodynamics, the equation takes the form of an inequality:

$$\dot{D} = \dot{W} - \dot{\Pi} = \left(F - \frac{\partial \Pi}{\partial v} \right) \dot{v} - \frac{\partial \Pi}{\partial a} \dot{a} \geq 0 \quad \text{for all } \dot{v} \text{ i } \dot{a}.$$

where F is the reaction force, N.

Moreover, $-\partial \Pi / \partial a$ is a thermodynamic variable. Since $-\partial \Pi / \partial a \leq 0$ and $\dot{a} \geq 0$ it is necessary for the dissipation energy $\dot{D}$ to be non-negative. In this case, the rate of energy G release:

$$G = -\frac{1}{b} \frac{\partial \Pi}{\partial a} \quad (\dot{a} > 0).$$

Within the framework of the Euler–Bernoulli hypothesis, the total potential energy is given by:

$$\Pi_v = \frac{3EIv^2}{4a_{eq}^3}$$

where E is the modulus of elasticity, Pa; $I = bh^3/12$ is the moment of inertia of the cross-sectional area of each of the connected parts of the double cantilever beam, mm^4; a_{eq} is the equivalent crack length, mm.

The equivalent length of the failure zone:

$$a_{eq} = \sqrt[3]{\frac{3\nu EI}{2F}}$$

The critical fracture energy:

$$G_C = \frac{F^2 a_{eq}^2}{bEI} \quad (1)$$

where b is the width of the specimen, mm.

The presented mathematical model allows for determining the critical fracture energy without considering the experimental value of the crack opening length as a function of the displacement of the sample edges.

The applied mathematical model allows using the experimental determination of the fracture resistance of the joint to calculate the maximum fracture force without measuring the crack length. Figure 6 shows the distribution of displacements and stresses in the testing model of the bonded paper specimen under tensile testing.

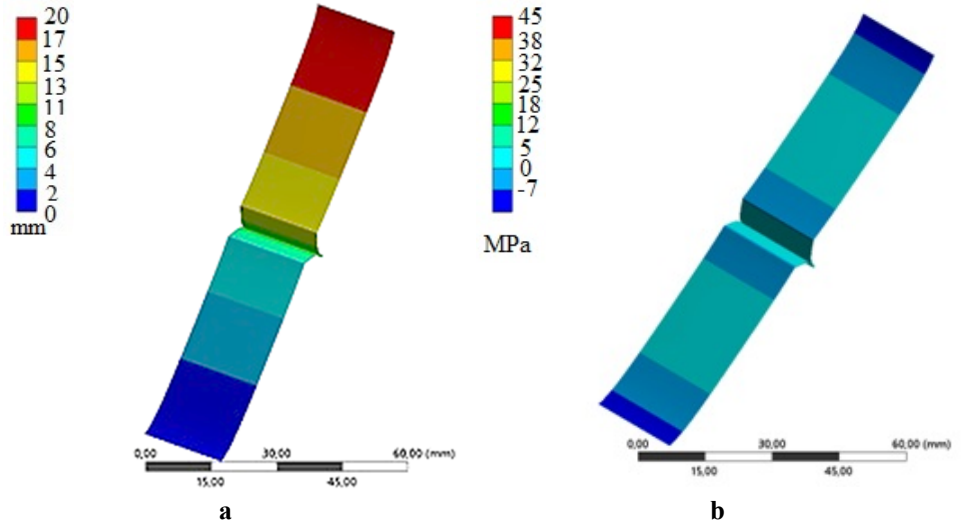

Figure 6. Model of tensile testing of the bonded paper sample: a – distribution of displacements; b – distribution of stresses

From Figure 6, it is evident that at a displacement of 10 mm, the stress values at the edges are 14.2 MPa.

Figure 7 shows the graphs of the dependence of the force at the sample edges on the displacement for experimental values and those obtained from numerical modeling.

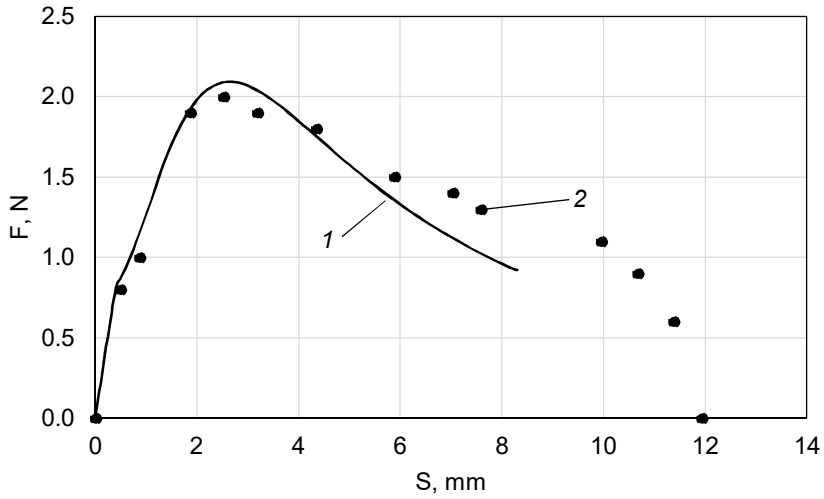

Figure 7. Dependencies of force at edges of paper sample on displacement 1 – modeling; 2 – experiment.

A comparison of the numerical calculations with the experimental values (Figure 7) shows almost complete agreement. The maximum force occurs at a displacement of 2-3 mm from the start of the crack opening, and then it gradually decreases. The total crack-opening force is 0.1 N/mm.

As the research results show (Millán et al., 2016; Xu et al., 2017), rigid material specimens, such as metal and composite plates, are typically studied. However, the shape of the 'force-displacement' curves qualitatively reproduces for the flexible packaging materials we investigated.

When the maximum stress is reached on the interface, plastic zones form, leading to unloading in the local area of the specimen material. As the joint continues to fracture, the tensile forces gradually decrease.

Figure 8 shows the distribution of displacements and stresses in the testing model of the bonded cardboard specimen under tensile testing.

From Figure 8, it can be seen that at a displacement of 10 mm, the stress at the edges is 10.08 MPa.

Figure 9 shows the graphs of the dependence of the force at the sample edges on the displacement for experimental values and those obtained from numerical modeling for cardboard samples.

The maximum force of 4.3 N occurs at a displacement of 5 – 6 mm from the start of the crack opening, and then it gradually decreases. The total crack-opening force is 0.22 N/mm. For the maximum force value, the discrepancy between the experimental data and numerical calculations is 7%, which is acceptable.

The fracture studies of hot-melt adhesive joints in cardboard materials are also described in (Hallbäck et al., 2014; Korin et al., 2007). The results obtained for slightly different cardboard materials and adhesives show qualitative agreement with the data obtained in this work.

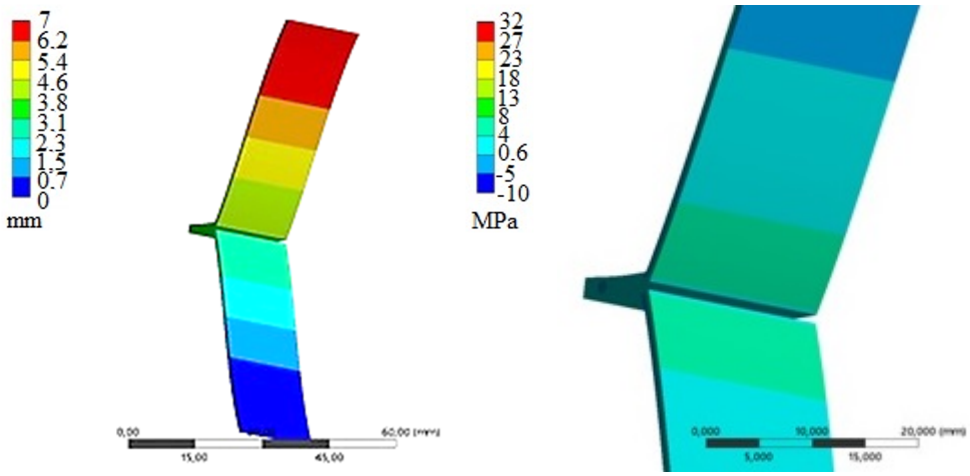

Figure 8. Model of tensile testing of the bonded cardboard sample
a – distribution of displacements; b – distribution of stresses.

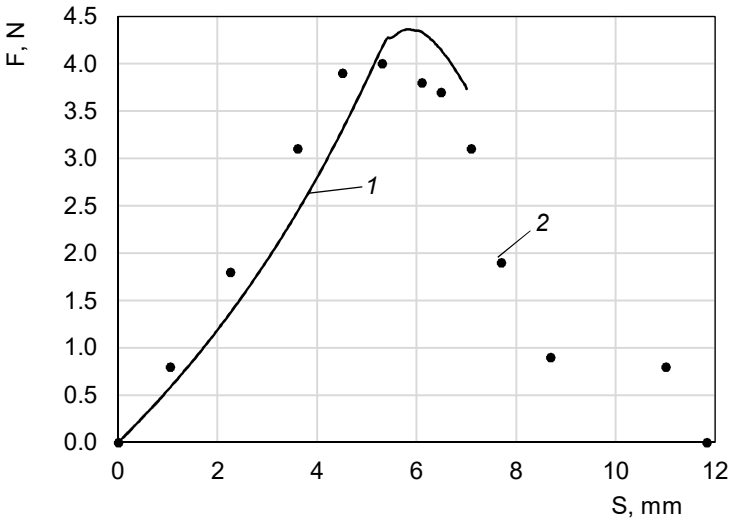

Figure 9. Dependencies of force at the edges of the cardboard sample on displacement
1 – modeling; 2 – experiment

Figure 10 shows the distribution of displacements and stresses in the model of tensile testing of the bonded polyethylene sample.

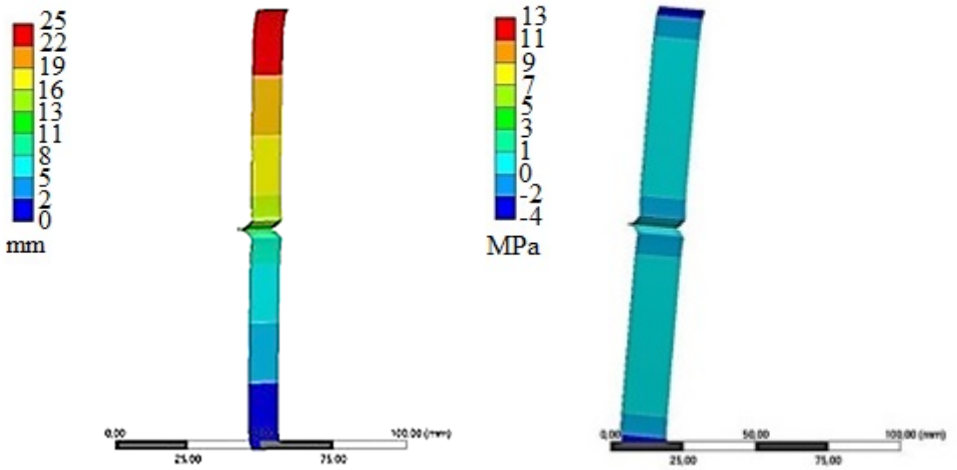

а б

Figure 10. Model of tensile testing of the bonded polyethylene sample:
a – distribution of displacements; b – distribution of stresses

From Figure 10, it can be seen that at a displacement of 10 mm, the stress value at the edges is 4.13 MPa.

Figure 11 shows the graphs of the dependence of the force at the sample edges on displacement for experimental values and those obtained from numerical calculations for polyethylene samples.

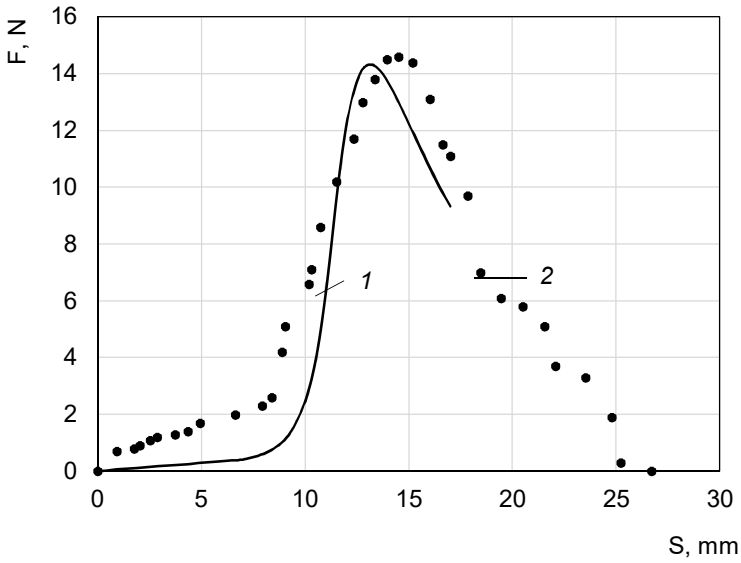

Figure 11 – Dependencies of force at the edges of the polyethylene sample on displacement:
1 – modeling; 2 – experiment.

The experimental curves in Figures 7, 9, and 11 qualitatively correspond to the curve shown in Figure 5a. That is, during stretching, the resistance force increases to a maximum, at which point the joint begins to fracture, and subsequently, with a further displacement of the edges, the fracture zone increases with a gradual decrease in forces until complete separation.

The maximum force of approximately 15 N occurs when the displacement is 12 – 13 mm from the beginning of the bond separation, and then it gradually decreases. The total opening force is 0.75 N/mm. For the maximum force value, the discrepancy between experimental data and numerical calculations is 2 %, which is within acceptable limits.

It has been established that the maximum force occurs at the beginning of the bond separation, and then it gradually decreases. As seen from the graphs, it requires twice as much force to break the hot-melt joint of the cardboard sample compared to the paper sample. The highest force value among the bonded samples is observed in polyethylene. This can be explained by the fact that during the bonding with hot-melt adhesive, some films undergo welding rather than gluing (a glue layer forms in the middle of the joint), meaning a chemical interaction of polymer macromolecules occurs, resulting in the disappearance of the interface between the bonded surfaces. An inseparable joint is formed, and further rupture occurs through the continuous material, as described in (Bennati et al., 2009; Waseem et al., 2014).

Numerical modeling of the strength of hot-melt adhesive joints allows for predicting the necessary and sufficient strength of adhesive joints for convenient disassembly by the consumer while ensuring the package's seal.

By numerically selecting the values of the critical fracture energy, it was possible to establish the strength limits of the bond energy, which illustrates good agreement between the theoretical and calculated graphs of the force-displacement dependence. From this value, the force at the edges of the sample at which it fractures can be calculated using the formula (1).

Conclusions

1. The considered model and method of numerical modeling of the strength of hot-melt adhesive joints allow for predicting the necessary and sufficient strength of the joints for convenient disassembly by the consumer, while also preventing self-unsealing.
2. The fracture of the hot-melt adhesive joint occurs after reaching its strength limit; the force value initially increases to the limit and then decreases until complete failure. Thus, it is possible to determine the maximum forces for opening packages made from different types of packaging materials, bonded under various conditions, for which the adhesive strength has been determined through modeling.
3. To assess the strength of the hot-melt adhesive joint, the dependencies of forces at the edges of paper, cardboard, and polyethylene samples on the displacement of the sample edges during stretching were obtained. It was established that, under the considered bonding conditions, the total opening force for paper materials is 0.1 N/mm, for cardboard – 0.22 N/mm, for polyethylene – 0.75 N/mm.

References

Banea M.D., da Silva L.F. (2009), Adhesively bonded joints in composite materials: an overview, *Proceedings of the Institution of Mechanical Engineers, Part L: Journal of Materials: Design and Applications*, pp. 1–18, https://doi.org/10.1243/14644207JMDA219.

Banea M.D., da Silva L.F., Campilho R.D.S.G. (2010), Temperature dependence of the fracture toughness of adhesively bonded joints, *Journal of Adhesion Science and Technology*, pp. 2011–2026, https://doi.org/10.1163/016942410X507713.

Bennati S., Colleluori M., Corigliano D., Valvo P. S. (2009), An enhanced beam-theory model of the asymmetric double cantilever beam (ADCB) test for composite laminates, *Composites Science and Technology*, pp. 1735–1745, https://doi.org/10.1016/j.compscitech.2009.01.019.

Banea M.D., da Silva L.F.M., Campilho R.D. (2015), The effect of adhesive thickness on the mechanical behavior of a structural polyurethane adhesive, *The Journal of Adhesion*, pp. 331–346, https://doi.org/10.1080/00218464.2014.903802.

Brockmann W., Geiß P.L., Klingen J., Schröder K.B. (2008), Adhesive bonding: materials, applications and technology, John Wiley & Sons.

Budzik M.K., Heide-Jorgensen S., Aghababaei R. (2021), Fracture mechanics analysis of delamination along width-varying interfaces, *Composites Part B: Engineering*, pp. 1–11, https://doi.org/10.1016/j.compositesb.2021.108793.

Campilho R.D.S.G., Moura D.C., Gonçalves D.J., Da Silva J.F.M.G., Banea M.D., da Silva L.F. (2013), Fracture toughness determination of adhesive and co-cured joints in natural fibre composites, *Composites Part B: Engineering*, pp. 120–126, https://doi.org/10.1016/j.compositesb.2013.01.025.

De Moura M.F.S.F., Moreira R.D.F. (2017), Fatigue analysis of composite bonded repairs, *Journal of Adhesion Science and Technology*, pp. 2164–2179, https://doi.org/10.1080/01694243.2017.1307497.

Hallbäck N., Korin C., Barbier C., Nygårds M. (2014), Finite element analysis of hot melt adhesive joints in carton board, *Packaging Technology and Science*, pp. 701-712, https://doi.org/10.1002/pts.2060.

Herasimenko Y.Y., Sokolskyi A.L. (2020), Investigation of the flexible packaging elements joining by hot melt adhesive, *Modern Engineering and Innovative Technologies*, pp. 5–8, https://doi.org/10.30890/2567-5273.2020-11-01-011.

Korin C., Lestelius M., Tryding J., Hallbäck N. (2007), Y-peel characterization of adhesively-bonded carton board: An objective method, *Journal of Adhesion Science and Technology*, pp. 197–210, https://doi.org/10.1163/156856107780437426.

Leffler K., Alfredsson K. S., Stigh U. (2007), Shear behaviour of adhesive layers, *International Journal of Solids and Structures*, pp. 530–545, https://doi.org/10.1016/j.ijsolstr.2006.04.036.

Millán J.S., Armendáriz I., García-Martínez J., González R. (2016). *Strategies for static failure analysis on aerospace structures.* In: A.S.H. Makhlouf and M. Aliofkhazraei (Eds.), *Handbook of Materials Failure Analysis with Case Studies from the Aerospace and Automotive Industries*, Butterworth-Heinemann, pp. 3–28.

Sokolskyi O., Herasimenko Yu. (2020), Simulation of the damage process of thermal glue bond, *KPI Science News* 4(131), pp. 93-98, https://doi.org/10.20535/kpisn.2020.4.227126

Stigh U., Biel A., Svensson D. (2016), Cohesive zone modelling and the fracture process of structural tape, *Procedia Structural Integrity*, pp. 235–244, https://doi.org/10.1016/j.prostr.2016.06.031.

Škec L., Alfano G., Jelenić G. (2018), On Gc, Jc and the characterisation of the mode-I fracture resistance in delamination or adhesive debonding, *International Journal of Solids and Structures*, 144–145, pp. 100–122, https://doi.org/10.1016/j.ijsolstr.2018.04.020.

Valoroso N., Fedele R. (2010), Characterization of a cohesive-zone model describing damage and de-cohesion at bonded interfaces, Sensitivity analysis and mode-I parameter identification, *International Journal of Solids and Structures*, pp. 1666–1677, https://doi.org/10.1016/j.ijsolstr.2010.03.001.

Waseem M.H.S., Kumar K. (2014), Finite element modeling for delamination analysis of double cantilever beam specimen, *SSRG International Journal of Mechanical Engineering*, pp. 1–11, https://doi.org/10.14445/23488360/IJME-V1I5P105.

Xu Y., Guo Y., Liang L., Liu Y., Wang X. (2017), A unified cohesive zone model for simulating adhesive failure of composite structures and its parameter identification, *Composite Structures*, pp. 555–565, https://doi.org/10.1016/j.compstruct.2017.09.012.

Zhao Y., Seah L.K., Chai G.B. (2016), Measurement of interlaminar fracture properties of composites using the J-integral method, *Journal of Reinforced Plastics and Composites*, pp. 1143–1154, https://doi.org/10.1177/0731684416642031

Cite:

UFJ Style

Gavva O., Sokolskyi O., Herasymenko Yu. (2024), Determination of opening force of hot-melt adhesive joints in flexible packaging, *Ukrainian Food Journal*, 13(4), pp. 766–779, https://doi.org/10.24263/2304-974X-2024-13-4-10

APA Style

Gavva, O., Sokolskyi, O., & Herasymenko, Yu. (2024). Determination of opening force of hot-melt adhesive joints in flexible packaging. *Ukrainian Food Journal*, *13*(4), 766–779. https://doi.org/10.24263/2304-974X-2024-13-4-10

Mathematical model of vacuum cooling process for wheat bread

Oleksandr Kozak, Volodymyr Telychkun

National University of Food Technologies, Kyiv, Ukraine

Keywords:

Wheat bread
Vacuum cooling
Modelling
Structural and mechanical properties

Article history:

Received 25.04.2024
Received in revised form 17.08.2024
Accepted 30.12.2024

Corresponding author:

Oleksandr Kozak
E-mail: oleksandrkozak2@gmail.com

DOI: 10.24263/2304-974X-2024-13-4-11

Abstract

Introduction. Vacuum cooling is an innovative method that reduces the cooling time of bakery products, improves their structural and mechanical properties, and extends their shelf life.

Materials and methods. A mathematical model of vacuum cooling of bread (loaf) from high-grade wheat flour with weight 0.5 kg was created. The results of experimental studies of the structural and mechanical properties of the crumb, gas permeability of the crust and crumb, and analysis of literature sources were used.

Results and discussion. The crust of the bread formed during the baking process is characterized by low gas permeability (D = 0.32 $m^3/m^2 \cdot s$), which significantly hinders the escape of water vapor from the inner layers of the product. Bread crumb has high gas permeability, which contributes to the even evaporation of moisture throughout the product. Its structural and mechanical properties vary with temperature: at high temperatures, the crumb is less durable (1500 Pa at 100 °C, 3600 Pa at 30 °C) and more vulnerable to mechanical stress, which necessitates a controlled pressure drop. In the process of vacuum cooling, phase transitions from liquid to vapor occur adiabatically, which ensures a rapid decrease in product temperature due to internal energy.

A mathematical model of the vacuum cooling process of wheat bread includes calculations of physical and mechanical processes: moisture evaporation, heat and mass transfer, the gas permeability of the crust and structural and mechanical properties of the bread crumb. This makes it possible to predict changes in product quality properties, including its temperature and moisture during cooling after baking.

At the optimal vacuum cooling parameters, the required bread temperature can be reached in just 68 seconds. This is much more efficient than traditional methods that take several hours.

Conclusion. A mathematical model of vacuum cooling of bread from high-grade wheat flour with weight 0.5 kg was created, which helps to optimize the cooling process and improve product quality.

Introduction

Bakery items cooling is an important final stage of the technological process that affects product quality. It is necessary to achieve structural and mechanical properties that allow cutting and packaging without the risk of product deformation, loss of structure or porosity, or condensation inside the package (Everington, 2003; Kozak et al., 2024; Stefanov et al., 2011). The duration of the traditional cooling method depends on the type, size of the product, and the ambient temperature: from 30 minutes for the buns to several hours for the loaves or rye breads (McDonald, 2001).

Traditional cooling methods are characterized by significant energy consumption and duration. In this context, the vacuum cooling process, which is based on adiabatic moisture evaporation, offers significant advantages. It ensures rapid cooling of the product by reducing the pressure in the chamber, which reduces the boiling point of the moisture (Primo-Martín et al., 2008; Zhu et al., 2018). However, excessive pressure reduction can cause undesirable defects, such as cracking of the crust or separation of the crust from the bottom crust (Kozak et al., 2024).

Vacuum cooling is widely used in the food industry to cool vegetables, herbs, and meat products (Ivanov et al., 2021; Peng et al., 2017; Zhang et al., 2014). Studies demonstrate the effectiveness of this method in reducing process time, minimizing energy consumption, and ensuring high product quality (Guo et al., 2018; Wang et al., 2020). However, when cooling bakery products, it is important to take into account the specifics of the product structure, in particular the gas permeability of the crust, and the structural and mechanical properties of the crumb (Kozak et al., 2023; 2024).

Despite significant progress in research, issues remain unresolved regarding the exact determination of the optimal vacuum cooling parameters for bakery products (Everington, 2003; Kinner et al., 2021). A mathematical model is needed that takes into account a complex of physical processes, including the gas permeability of the crust and the structural and mechanical properties of the crumb.

The aim of the study is to create a mathematical model of the process of vacuum cooling of bakery products, which will allow calculating the parameters of the mode taking into account the characteristics of the product.

Materials and methods

Materials

The study was conducted on a 0.5 kg loaf of wheat made from high-grade wheat flour. Important quality characteristics of the finished product of wheat flour products, namely the loaf, are: length – 300 mm, width (product diameter) – 150 mm, height – 80 mm.

Thermal and physical parameters for wheat bread varieties were as follows: humidity, 38–45%; thermal conductivity (λ), 0.2–0.3 W/m·K; heat capacity (c), 2.5–3.0 kJ/kg·K; density (ρ), 200–300 kg/m³; porosity of the crumb, 68 %.

Important quality indicators for wheat flour products are their sensory characteristics: appearance, cut, texture, color, smell, and taste of the finished product.

Requirements for the sensory characteristics of the product were as follows: appearance corresponds to the mold in which it was baked, without side spills. A mold in the form of a product or part of it cut into slices is allowed.

Surface (crust): light yellow to brown, without burning. Slight wrinkling is allowed for packaged products; for sliced products with traces of cuts.

Crumb condition: baked, elastic, not wet to the touch, no traces of unleavened bread.

Taste: typical for this type of product, without off-flavors.

Methods

To create a mathematical model for vacuum cooling of a 0.5 kg loaf from high-grade wheat flour, an integrated approach was used including a literature review and experimental studies. The research covers the parameters of vacuum cooling, as well as the structural and mechanical properties of the crumb and the gas permeability of the crust and crumb of the loaf. The results were the basis for building a mathematical model that takes into account key aspects of the process.

Results and discussion

Influence of product structural properties on vacuum cooling

During the study of the operating parameters of the vacuum cooling process of a loaf, it was found that the crust formed during baking has significant resistance (low gas permeability). This significantly hinders the escape of water vapor from the inner layers of the loaf to the environment of the vacuum chamber, which affects the cooling efficiency (Kozak et al., 2023). It has been found that the cooling intensity is determined by the gas permeability of the crust and the structural and mechanical properties of the crumb, which vary depending on the product temperature (Kozak et al., 2023).

To determine the operating parameters of the vacuum cooling process, studies were conducted that allowed us to establish the following indicators. The throughput of the loaf crust is D = 0.32 $m^3/m^2 \cdot s$, area of loaf crust, F = 0.091 m^2, and the volume of steam formed during vacuum cooling is equal to V = 0.444 m^3 (Kozak et al., 2023).

The study of the structural and mechanical properties of the loaf crumb showed a linear dependence of the tensile strength on temperature, as shown by equation (Kozak et al., 2024):

$$\sigma = -30 \cdot t + 4500; \quad (1)$$

where: σ is the tensile strength of the loaf crumb (Pa);

t is the temperature of the loaf crumb (˚C).

At a temperature of 100 °C, the tensile strength of the crumb is 1500 Pa, and at 30 °C it is 3600 Pa (Kozak et al., 2024).

Scheme of vacuum cooling of bread on the example of loaf

Based on the analysis of literature sources (Everington, 2003; Kinner et al., 2021) and the results of experimental studies of vacuum cooling of the loaf, as well as the determination of the structural and mechanical properties of the crumb and gas permeability of the loaf crust, a scheme for vacuum cooling of the loaf was created (Figure 1) (Kozak et al., 2023; 2024).

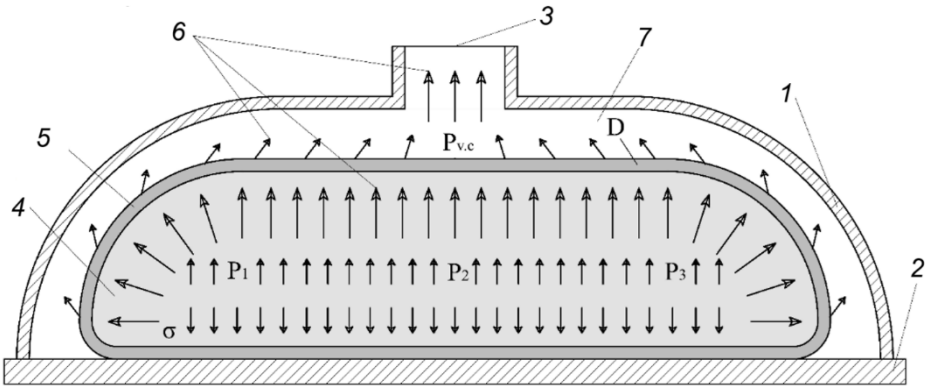

Figure 1. Scheme of vacuum cooling of loaf:
1 – vacuum chamber; 2 – vacuuming table; 3 – vacuum supply; 4 – loaf crumb; 5 – loaf crust; 6 – visualization of steam movement during the process; 7 – vacuum chamber environment.

Vacuum cooling of the loaf occurs as follows (Figure 1): a vacuum is created in the vacuum chamber Pv.c. (1) through the vacuum inlet (3). Because of the pressure decrease, adiabatic boiling of moisture begins in the entire volume of the loaf due to the fact that $P_1 = P_2 = P_3 = P_l$ (crumb 4). The main obstacle to the escape of steam (6) from the loaf is the crust (5) with gas permeability G. In order to avoid product destruction, the process should be carried out in such a way that the pressure gradient between the vacuum chamber environment (7) and the environment inside the loaf (crumb 4) does not exceed the tensile strength of the crumb $\Delta P < \sigma$.

Determination of operating parameters of vacuum cooling process of loaf

Based on the scheme for determining the operating parameters of the loaf vacuum cooling process (Figure 2), the following provisions were formulated:

Structural characteristics of the loaf:

A loaf after baking is considered as a capillary-porous body (Everington, 2003; McDonald, 2001).

The porosity of the loaf is 68%, which indicates a significant number of small pores in its structure (Kinner et al., 2021).

The crust of the loaf has low gas permeability, i.e., it does not allow moisture evaporating during the process to pass through (Kozak et al., 2023).

The crumb of the loaf is characterized by high gas permeability, which facilitates easy evaporation of moisture, allowing the cooling process to occur simultaneously throughout the entire volume (Kozak et al., 2023).

Structurally, the mechanical properties of the crumb vary linearly with temperature: the higher the temperature, the lower the tensile strength. This means that a loaf at high temperatures is softer and less resistant to mechanical stress (Kozak et al., 2024).

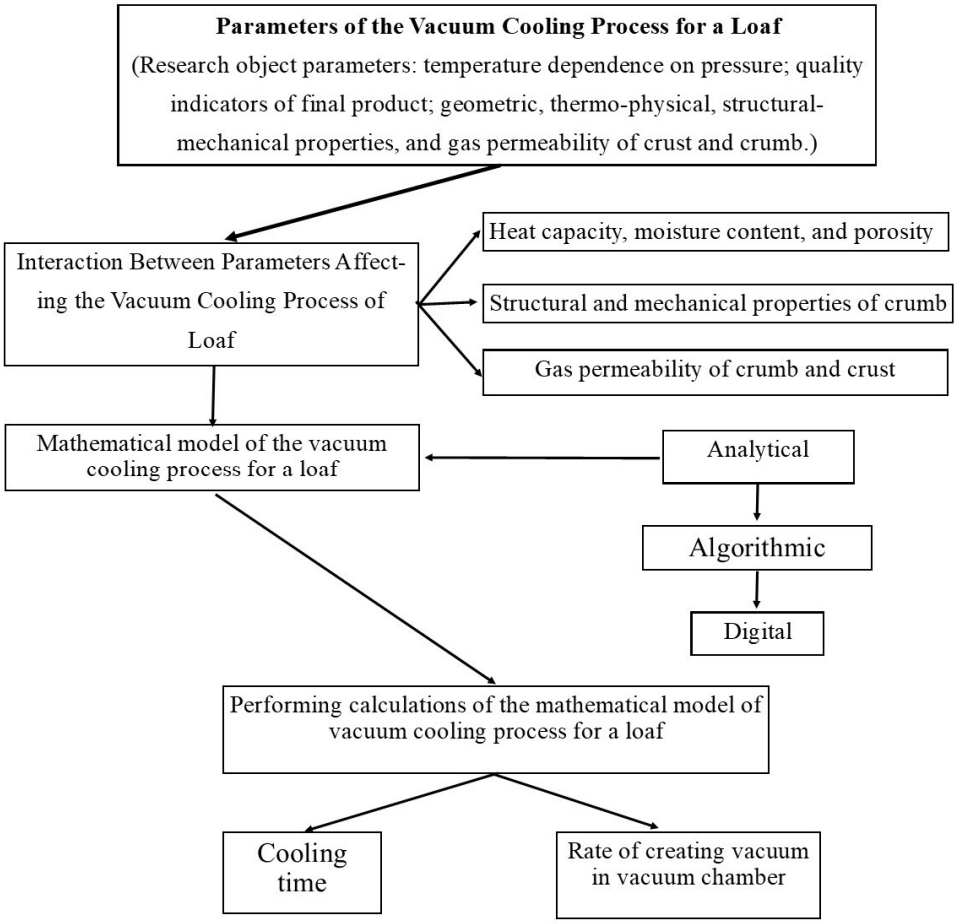

Figure 2. Scheme for determining operating parameters of loaf vacuum cooling process

Phase transitions:

The liquid-to-vapor phase transitions occur evenly throughout the loaf, which guarantees uniform moisture evaporation and ensures uniform cooling of the product (McDonald, 2001; Kozak et al., 2023).

Energy balance:

The phase transition occurs without additional heat input from the outside, due to a decrease in the internal energy of the product. This means that the loaf is cooled by its own energy, which is spent on moisture evaporation. As a result, the temperature of the product decreases, which ensures fast and efficient cooling (Ajani et al., 2022; Peng et al., 2017)

Thus, vacuum cooling of the loaf effectively reduces the temperature of the product by evaporating moisture, distributing it evenly throughout the volume, and reducing the internal energy of the product (Wang et al., 2020; Zhang et al., 2014).

Based on the above provisions, a mathematical model of the process of vacuum cooling of bakery products has been developed on the example of a loaf.

Analytical model of loaf vacuum cooling process

The analytical model, based on calculations of moisture evaporation, heat transfer, mass transfer, and mechanical strength of the bread crumb, allows you to assess the dynamics of changes in product quality, in particular during cooling after baking.

Structural and mechanical properties.

From the study of the structural and mechanical properties of the loaf crumb, we obtained a linear dependence of the tensile strength on temperature (Kozak et al., 2024):

$$\sigma = -30\,t + 4500; \tag{2}$$

where σ is a tensile strength of bread crumb (Pa);

t is a temperature (˚C).

Pressure drop between the media.

The Boyle-Mariotte gas law was used to calculate the pressure generated inside the loaf during the vacuum cooling process. This law states that for a constant amount of gas, its pressure and volume are inversely proportional to (Kozak et al., 2023):

$$P_1 \cdot V_1 = P_2 \cdot V_2 \tag{3}$$

where: P_1 is an initial pressure inside the loaf (Pa);

V_1 is an initial gas volume inside the loaf (m^3);

P_2 is a pressure inside the loaf during vacuum cooling (Pa);

V_2 is a gas volume inside the loaf during vacuum cooling (m^3);.

The gas flow through the crust of the loaf is described by the equation (Kozak et al., 2023):

$$J = \frac{P \cdot D}{L} \tag{4}$$

where J is gas flow through the loaf crust (m^3/s);

P is pressure difference between the internal and external environments (i.e. P= P1-P2),

D is gas permeability of the loaf crust ($m^3/(m^2 \cdot s)$),

L is thickness of the loaf crust (m).

Then the pressure P_2 inside the loaf:

From the permeability-concentration equation, we can express the pressure difference P (Kozak et al., 2023):

$$P = \frac{J \cdot L}{D} \tag{5}$$

Substituting this value of the pressure difference P into the Boyle-Mariotte law, we obtain (Kozak et al., 2023):

$$P_1 \cdot V_1 = (P_1 - P) \cdot V_2 \tag{6}$$

Where we get it:

$$P_1 \cdot V_1 = \left(P_1 - \frac{J \cdot L}{D} \right) \cdot V_2 \tag{7}$$

Given that the volume of gas inside the loaf does not change during vacuum cooling, we can assume that $V_1 \approx V_2$. In this case, the equation is simplified to (Kozak et al., 2023):

$$P_1 \approx P_2 + \frac{J \cdot L}{D} \tag{8}$$

Hence, we can derive the value of the pressure in the loaf P2 that occurs during vacuum cooling (Kozak et al., 2023):

$$P_2 = P_1 - \frac{J \cdot L}{D} \tag{9}$$

Evaporation of moisture.

In order for the moisture in the middle of the loaf to turn into steam, a certain amount of heat must be consumed, which is determined by the heat of phase transition. To estimate the amount of evaporated moisture W(τ) per unit mass of product, we use the equation (Everington, 2003; McDonald, 2001):

$$W(\tau) = \frac{q(\tau) \cdot g_p}{r} \tag{10}$$

where: τ – time, sec

q(τ) is amount of heat consumed for the phase transition of water to steam (J/kg);

r – heat of phase transition (J/kg);

g_p is weight of the product (kg).

The amount of heat used to cool the product (Everington, 2003; McDonald, 2001):

$$q(\tau) = (c_{d.m.} g_{d.m.} + c_m g_m)(t_l - t_{c.l.}) \tag{11}$$

where: $q(\tau)$ is the amount of heat consumed for cooling a unit mass of loaf (J/kg);;

$c_{d.m.}$ is a specific heat capacity of the loaf dry matter (J/(kg °C));

t_l is a temperature of the loaf after leaving the oven (°C);

$t_{c.l.}$ is an emperature of the cooled loaf (°C).

$g_{d.m.}$ is a dry matter content in the loaf determined by the formula (Everington, 2003; McDonald, 2001).

$$g_{d.m.} = \frac{100 - W_l}{100} \tag{12}$$

where W_l is a moisture content in the hot loaf.

Moisture content in the loaf (kg):

$$g_m = \frac{W_l}{100}. \tag{13}$$

Because 1 kg of steam at different pressures occupies a different volume, it is necessary to calculate the volume of steam generated as a result of cooling (Kozak et al., 2023):

$$V = V` \cdot W. \tag{14}$$

where: V`is a volume occupied by 1 kg of steam at the corresponding pressure (Figure 3).
W is a mass of moisture evaporated because of cooling.

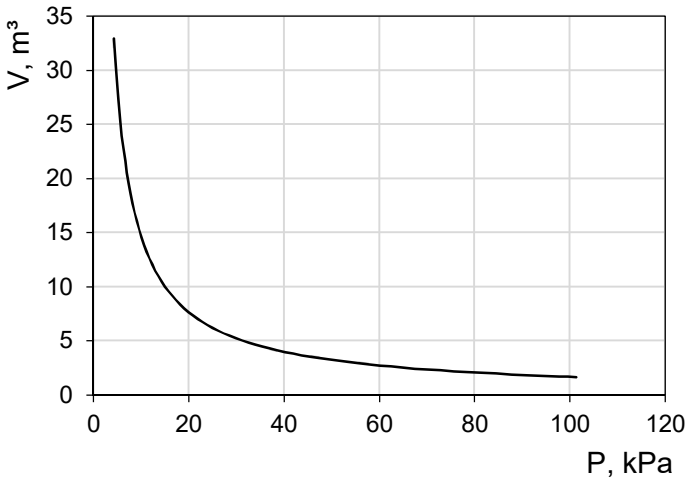

Figure 3. Dependence of steam volume on pressure

Mass transfer.

The amount of moisture that evaporates depends on the amount of heat removed from the bread to cool the product. The process of mass transfer due to moisture evaporation is described by the equation (Ajani et al., 2022):

$$\frac{dW(\tau)}{d\tau} = \frac{q_{v(\tau)}}{r}. \tag{14}$$

where W(τ) –is a change in moisture mass in the product.

Heat transfer.

The temperature depends on the amount of heat transferred, the heat capacity of the product, and its density (Gao et al., 2018; Guo et al., 2018):

$$\frac{dt(\tau)}{d\tau} = -\frac{q_v(\tau)}{c_p \cdot \rho}. \quad (15)$$

where:

q_v is an intensity of internal heat flow (W);

c_p is a specific heat capacity (J/kg·˚C);

ρ is a density of the product (kg/m^3).

There is no heat flux on the surface of the loaf, so there are no boundary conditions for heat flux:

$$q(0,\tau) = q(L,\tau) = 0. \quad (16)$$

Determine the pressure inside the vacuum chamber.

According to the temperature of product, the pressure is determined at which the moisture boils in the center of bread (Figure 4) (Everington, 2003; McDonald, 2001):

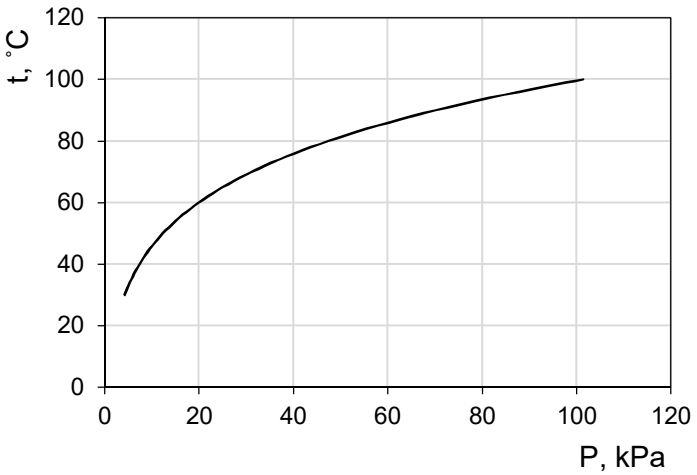

Figure. 4. Dependence of the boiling point of moisture on pressure

Boundary conditions.

For heat transfer:

$$t(0, \tau)=t(L, \tau)=t_f, \quad (17)$$

where T_f is a temperature of the medium.

For pressure:

$$P(0, \tau)=P(L, \tau)=P_k \quad (18)$$

For the strength of the crumb:

$$\sigma(\tau)\geq\Delta P(\tau) \quad (19)$$

Algorithmic model for calculating process of vacuum cooling of loaf

Initial data: Temperature after baking t_0; initial moisture content of the product W_0; initial pressure P_0.

Material properties: specific heat capacity c_p; density ρ; heat of phase transition r; gas permeability of the crust G; crust area F, tensile strength of the crumb.

Algorithm steps.

Initialization of parameters: temperature 100 °C, humidity 42%, pressure 101.325 kPa. We set the time step Δ τ (1 s) and the total simulation time τ_{fin}.

Strength calculation (Kozak et al., 2024):

$$\sigma = -30t + 4500; . \tag{20}$$

Determine the pressure drop between media (Kozak et al., 2023):

$$P_2 = P_1 - \frac{J \cdot L}{D}. \tag{21}$$

$$\Delta P = P_1 - P_2 . \tag{22}$$

Calculation of mass transfer.

Determine the weight and volume of evaporated moisture at each step (Ajani et al., 2022):

$$W\left(\tau + \Delta\tau\right) = W\left(\tau\right) - \frac{q_v \cdot \Delta\tau}{r}. \tag{23}$$

$$V = V` \cdot W \tag{24}$$

Calculation of heat transfer.

Calculate the temperature field of the product at the next time step (Gao et al., 2018; Guo et al., 2018):

$$t\left(\tau + \Delta\tau\right) = t\left(\tau\right) - \frac{q_v}{c_p \cdot \rho} \cdot \Delta\tau \tag{25}$$

$$q_v = \frac{r \cdot \Delta W}{\Delta\tau} \tag{26}$$

According to the temperature of the product, we determine the pressure at which the roll in the middle of the product will boil

Moving to the next time step.

- Increase the time τ by Δ τ.
- $\tau < \tau_{fin}$, return to step 2 to calculate the parameters at a new time step.

End of modelling.

- When the time reaches τ_{fin}, the model is complete.
- It is analysed the results: temperature field, moisture evaporation dynamics, product strength, and other parameters.

Results of calculations

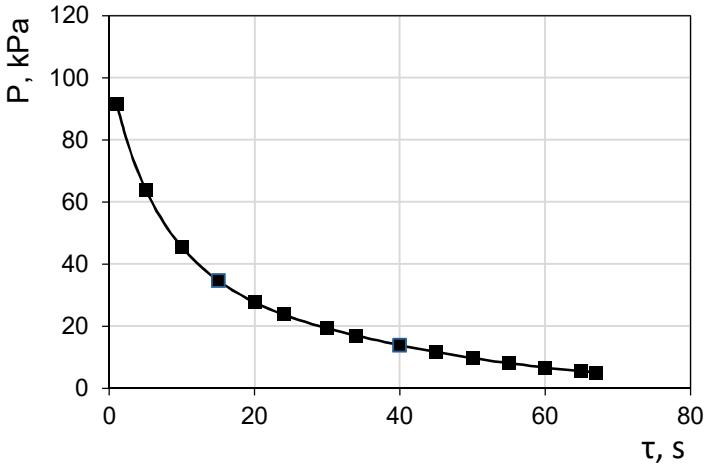

Figure 5. Calculated mode of vacuum creation in a vacuum chamber

As a result of calculations of the mathematical model of the process of vacuum cooling of a loaf of high-grade wheat flour weighing 0.5 kg, it is recommended to reduce the pressure of the vacuum chamber according to the dependence shown in Figure 5. Under these conditions, the cooling time is 68 seconds.

Summarizing and comparing the results

During the study of the operating parameters of vacuum cooling of the loaf, it was found that the crust formed during baking has a high resistance, which prevents the diffusion of water vapor from the middle of the loaf to the environment (Kozak et al., 2023). Therefore, the cooling rate is limited by the gas permeability of the crust and the structural and mechanical properties of the loaf crumb (Kozak et al., 2024).

If not properly adjusted, the pressure reduction in the vacuum chamber causes a pressure gradient between the vapor in the cooled product and the environment. This leads to cracking of the loaf crust (Figure 6) and detachment of the crumb from the bottom crust (Figure 7) (Kozak et al., 2023; 2024).

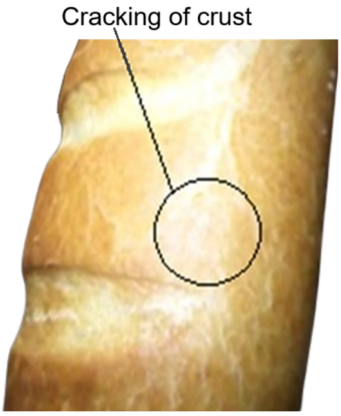

Figure 6. Loaf crust cracking as result of too much pressure reduction in vacuum chamber

In the experimental setup, we established the optimal mode of cooling the loaf to a temperature of 30 °C, which is shown in the graph in curve 1 (Figure 8). Curves 2 and 3 in Figure 8 correspond to samples 2 and 3 in Figure 7, and under such conditions, it was found that the crumb of the test sample was ruptured, which does not meet the established quality requirements (Kozak et al., 2023; 2024).

In the regime represented by curve 1 in Figure 3, the cooling time for a 0.5 kg loaf is 2 minutes, and the maximum rate of rarefaction does not exceed 4.5 kPa/s.

Figure 7. Destruction of loaf:
1 – specimen with a properly selected vacuum cooling mode;
2, 3 – samples with too intensive vacuum cooling mode

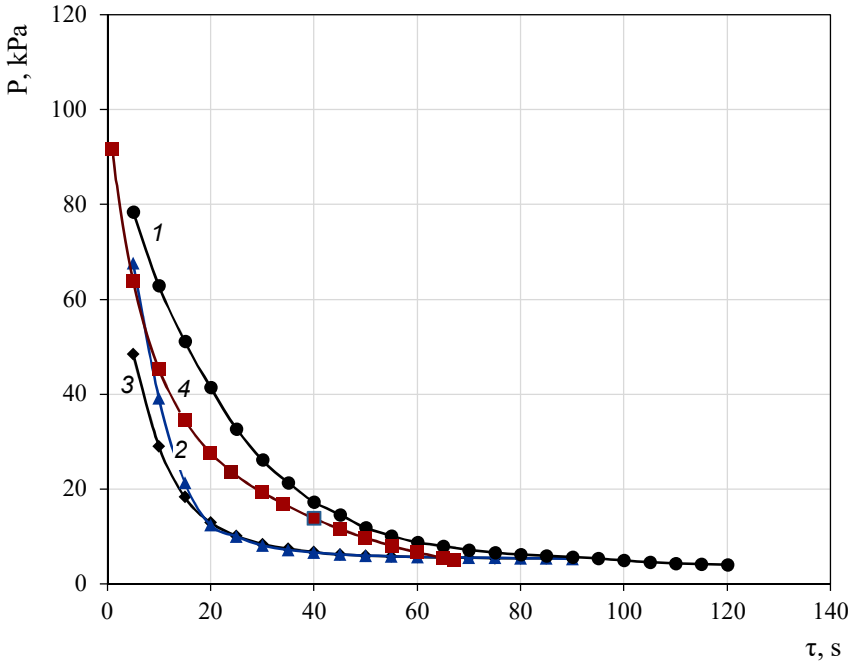

Figure 8. Curves of vacuum generation in vacuum chamber:
1 – experimentally found regime parameters of pressure change over time in a vacuum chamber at which no loaf destruction occurs;
2, 3 – experimentally found regime parameters of pressure change over time in a vacuum chamber at which the destruction of the loaf occurs;
4 – calculated mode of creating a vacuum in a vacuum chamber

Because of the studies, literature review, and mathematical model calculations, the regime parameters of pressure changes in the vacuum chamber were obtained, under which no loaf destruction occurs and the cooling time is 68 s.

Conclusions

1. The crust of the loaf formed during the baking process is characterized by low gas permeability (D = 0.32 $m^3/m^2 \cdot s$), which significantly hinders the escape of water vapor from the inner layers of the product.
2. The loaf crumb has high gas permeability, which contributes to the even evaporation of moisture throughout the product. Its structural and mechanical properties vary with temperature: at high temperatures, the crumb is less durable (1500 Pa at 100 °C, 3600 Pa at 30 °C) and more vulnerable to mechanical stress, which necessitates a controlled pressure drop.
3. In the process of vacuum cooling, phase transitions from liquid to vapor occur adiabatically, which ensures a rapid decrease in product temperature due to internal energy.
4. A mathematical model of the vacuum cooling process has been developed, which makes it possible to calculate the operating parameters under which crust cracking or detachment of the crumb from the lower crust does not occur. In particular, the model takes into account the structural and mechanical properties of the crumb, the gas permeability of the crust, heat and mass transfer processes during vacuum cooling.
5. According to the calculations of the mathematical model, a graph of pressure changes in the vacuum chamber as a function of time was constructed. According to the results of the calculations, the cooling time is 68 s instead of several hours when using traditional methods of cooling the loaf.

References

Ajani C.K., Zhu Z., Sun D.W. (2022), In situ investigation of cellular water transport and morphological changes during vacuum cooling of steamed breads, *Food Chemistry,* 381, 132211, https://doi.org/10.1016/j.foodchem.2022.132211

Ajani C.K., Zhu Z., Sun D.W. (2023), Shrinkage during vacuum cooling of porous foods: Conjugate mechanistic modelling and experimental validation, *Journal of Food Engineering*, 337, 111220, https://doi.org/10.1016/j.jfoodeng.2022.111220

Everington D. (2003), Vacuum technology for food processing, *Food Technology International Europe*, 5, pp. 71–74.

Gao J., Wang Y., Dong Z., Zhou, W. (2018), Structural and mechanical characteristics of bread and their impact on oral processing: A review, *International Journal of Food Science and Technology,* 53(4), pp. 858–872, https://doi.org/10.1111/ijfs.13671

Guo Z., Song X., Song Z., Liu B. (2018), An improved method of immersion vacuum cooling for small cooked pork: Bubbling vacuum cooling, *International Journal of Food Science and Technology*, 53(12), pp. 2748–2753, https://login.research4life.org/tacsgr1doi_org/10.1111/ijfs.13918

Ivanov V., Shevchenko O., Marynin A., Stabnikov V., Gubenia O., Stabnikova O., Shevchenko A., Gavva O., Saliuk A. (2021), Trends and expected benefits of the breaking edge food technologies in 2021–2030, *Ukrainian Food Journal,* 10(1), pp. 7-36, https://doi.org/10.24263/2304-974X-2021-10-1-3

Kinner M., Rüegg R., Weber C., Buchli J., Durrer L., Müller N. (2021), Impact of selected baking and vacuum cooling parameters on the quality of toast bread, *Journal of Food Science and Technology,* 58, pp. 4578–4586, https://doi.org/10.1007/s13197-020-04945-x

Kozak O.S., Telychkun V.I. (2023), Determination of the gas permeability of baton crush and crumb during vacuum cooling, *Food Industry*, pp. 33–34, pp. 62–70.

Kozak O.S., Telychkun Yu.S., Telychkun V.I. (2024), Determination of rheological characteristics of bread crumb for calculating the parameters of vacuum cooling process, *Scientific Works of NUFT,* 30(4), pp. 99–108, https://doi.org/10.24263/2225-2924-2024-30-4-9

McDonald K. (2001), The formation of pores and their effects in a cooked beef product on the efficiency of vacuum cooling, *Journal of Food Engineering*, 47(3), pp. 175–183, https://doi.org/10.1016/S0260-8774(00)00111-4

Primo-Martín C., Beukelaer H., Hamer R.J., Vliet T. (2008), Fracture behaviour of bread crust: Effect of bread cooling conditions, *Journal of Food Engineering*, 89(3), pp. 285–290, https://doi.org/10.1016/j.jfoodeng.2008.05.005

Peng Y., Cheng W. (2017), Experimental investigation on the effect of heat transfer enhancement of vacuum spray flash evaporation cooling using Al_2O_3–water nanofluid, *Energy Procedia*, 142, pp. 3766–3773, https://doi.org/10.1016/j.egypro.2017.12.274

Stefanov S., Gubenia O., Telychkun V. (2011), Regarding the bread, *ProPACK*, 2, pp. 8 – 15.

Wang N., Kan A., Huang Z., Lu J. (2020), CFD simulation of heat and mass transfer through cylindrical *Zizania latifolia* during vacuum cooling, *Heat Mass Transfer*, 56, pp. 627–637, https://doi.org/10.1007/s00231-019-02736-5

Zhu Z., Li Y., Sun D.W., Wang H.W. (2018), Developments of mathematical models for simulating vacuum cooling processes for food products – a review, *Critical Reviews in Food Science and Nutrition*, 59(5), pp. 715–727, https://doi.org/10.1080/10408398.2018.1490696

Zhang Z., Zhang Y., Su T., Zhang W., Zhao L., Li X. (2014), Heat and mass transfer of vacuum cooling for porous foods-parameter sensitivity analysis, *Mathematical Problems in Engineering*, 613028, https://doi.org/10.1155/2014/613028

Zhu Z., Li T., Sun D. W. (2020), Pressure-related cooling and freezing techniques for the food industry: fundamentals and applications, *Critical Reviews in Food Science and Nutrition*, 61(17), pp. 2793–2808, https://doi.org/10.1080/10408398.2020.1841729

Cite:

UFJ Style

Kozak O., Telychkun V. (2024), Mathematical model of vacuum cooling process for wheat bread, *Ukrainian Food Journal*, 13(4), pp. 780–793, https://doi.org/10.24263/2304-974X-2024-13-4-11

APA Style

Kozak, O., & Telychkun, V. (2024), Mathematical model of vacuum cooling process for wheat bread. *Ukrainian Food Journal*, *13*(4), 780–793. https://doi.org/10.24263/2304-974X-2024-13-4-11

Forecasting the financial performance of small and medium-sized enterprises: evidence from the Hungarian food retail sector

Dávid Sütő, Péter Bajnai, Veronika Fenyves

University of Debrecen, Debrecen, Hungary

Keywords:

SMEs
Food retail
Financial modelling
Forecast
Panel regression
Profit
Hungarian

Article history:

Received 12.02.2024
Received in revised form 29.08.2024
Accepted 30.12.2024

Corresponding author:

Péter Bajnai
E-mail: bajnai.peter@econ.unideb.hu

DOI:
10.24263/2304-974X-2024-13-4-12

Abstract

Introduction. This research aims to develop a financial model capable of performance measurement for food retail SMEs operating in a specific region of a typical Central and Eastern European emerging economy, Hungary, based on accounting statements and macroeconomic indicators, the utilisation of which enables managers to measure and improve financial performance.

Materials and methods. Multivariate stepwise linear regression was applied to select the indicators for the model, and multivariate linear panel regression was applied to develop the specific model. The database contained 972 company statements covering the period 2015-2019.

Results and discussion. Using panel data of financial indexes and macroeconomic indicators as independent variables, a multivariate linear regression function can be defined, allowing enterprises' operating profit to be estimated and predicted as a dependent variable with high accuracy and significance. The result of the modelling is a random-effects regression model that can predict 81.6% of the operating profit/loss of food retailers in Hungary's North Great Plain region. The practical results of the secondary research can be applied to the entire population of the study region based on statistical procedures. Among the financial ratios produced from the statements used in the course of the procedures, the application of ROA margin I, Net working capital, Net working capital ratio, Current assets ratio as key indicators, as well as Inventory turnover rate, Total assets turnover rate, Capital strength are suggested. Of the macroeconomic indicators, household income per capita and its change can provide guidance for planning, as food retail risk appears to be the most important macroeconomic indicator.

Conclusion. Businesses can use the model in their management accounting and control activities, either by substituting the relevant financial indicators into the final model to forecast the operating profit/loss or by making decisions with the support of the developed indicator system. Such scientifically established models can help improve SMEs' management accounting, thus maintaining or enhancing their decision-making processes and competitiveness.

Introduction

The role of small and medium-sized enterprises (SMEs) is fundamental in promoting economic growth in the national economies of the 21st century. The growth of economies heavily relies on the businesses within the SME sector, as emerging, renewed, and terminated companies keep the economy in constant motion. One of the most important areas of activity within the SME sector is trade. Regarding retail trade turnover, the largest proportion is represented by retail sales in non-specialised stores with food. The basis for the growth of iretail trade, including the growth of food retail, is the continuous increase in real wages, which is accompanied by an increase in consumer spending. There can be several ways of adaptation, including restructuring cost structures, cost reduction, diversification of activities, or shifting production costs onto consumers. Concerning the above cases, the development and preparation of decision alternatives play a crucial role, highlighting the importance of management control and performance measurement activities. There is a legitimate need for complex corporate financial performance evaluation and the development of management accounting and control methods that support corporate competitiveness within the context of businesses in the food retail sector.

Decision-makers measure the success of a business primarily through its financial performance, which is most easily captured by the information available from financial statements. In addition to being the basis for managerial decisions, financial statements can be used to analyse a company's performance and identify the reasons for deviations from previously projected values, and statistical organisations can use broader samples of financial statements to analyse and forecast the direction and level of economic development (Erdey, 2006; Osadchy et al., 2018).

Accounting information, completed with market data, is the basic input for financial analysis and planning, and the most important tools to use these inputs for decision-support planning and forecasting are various statistical methods, regression analysis, and operations research programming techniques. However, to extract useful inputs from financial statements, some form of measurement is required: most often, these are ratios, which put two pieces of data on an equivalent basis, thereby increasing their usefulness (Lee et al., 2023; Rákos et al., 2022). Financial ratio indicators are the oldest and simplest practical tools for evaluating and planning the performance of companies (Arkan, 2016). Financial ratio indicators play an important role in revealing the financial stability of an enterprise, preserving its competitive position, and eliminating potential financial risks (Belas et al., 2024; Kliestik et al., 2020; Tamimi and Orbán, 2022). Lukason and Camacho-Minano (2019) argue that financial ratio indicators measuring profitability, liquidity and leverage are the most relevant in bankruptcy forecasting.

The most commonly used statistical method for selecting the relevant financial indicators is a type of stepwise regression using the least squares method. The stepwise selection procedure helps in the selection of dependent variables (Voda et al., 2021). The most common area related to risks, based on financial indicators and using this method, is bankruptcy forecasting (Dankiewicz et al., 2022). There are numerous areas where a forecasting model based on financial indicators could be particularly useful (Földvári and Erdey, 2009) for the importance of exchange rate determination.

Taani (2011) investigated the impact of accounting information on earnings per share using five categories of financial ratios applying multiple regression methods and stepwise regression models. Asiri (2015) uses this method to investigate the correlation between the market capitalisation of 65 UK firms and their financial ratios – the aim is to examine the extent to which market value is determined by internal financial performance, such as

profitability, liquidity, or efficiency (Nugroho et al., 2024). Arkan (2016) examined the importance of financial ratios from financial statements in predicting stock prices in emerging markets. Using a stepwise multiple regression model, he tested the statistical power of 12 financial indicators in predicting the Kuwaiti financial market. Wang (2020) uses stepwise multiple regression to filter out the strong correlation factors as effective predictors among the many factors affecting the stock market return rate, examining the Chinese stock market. The South Asian case is investigated in detail by Gazi et al. (2024).

Of course, examples are not only available for modelling the market value of companies, stock market returns and risks. In many cases, the focus is on the operating profit of a company as the object of forecasting. Operating profit is the profit a company realises from its business before deducting taxes and interest, also known as earnings before interest and taxes (Nworie and Nwoye, 2023). According to the research of Owusu-Akomeah (2015), working capital management plays a very important role in achieving business success as it significantly impacts operating profit. Examining manufacturing firms listed on the Ghanaian stock exchange, they found that indicators such as inventory turnover, suppliers' and customers' turnover, and cash conversion cycle affect operating profit. Qianyu et al. (2021) used neural network models and financial statement information to forecast the profit of listed Chinese companies and compared it with the results predicted by analysts. The average accuracy of their model in profit forecasting is 88.6%, which is 13.52% higher than the average accuracy of analyst forecasts.

There are numerous examples of creating prediction models apart from bankruptcy prediction, and it is frequent to focus on profit, even operating profit. The above examples, however, mainly focus on larger firms – smaller companies need such models just as much as larger ones, if not more. The current research aims to build a model for small and medium-sized enterprises. According to the latest official European data from 2023, 99.8% of all enterprises are SMEs, comprising 51.8% of value-added and 64.4% of employment – they can be considered substantial contributors to employment and to the GDP growth in many countries (European Commission, 2023). In Hungary, the proportion of SMEs among registered businesses in 2013 was 99% in the corporate sector. SMEs accounted for 44.3% of gross value added and employed 68.4% of the workforce.

SMEs' role is essential in the economic development of many countries (Bilan et al., 2017; Straková et al., 2022; Woźniak et al., 2019). They form the most dynamic corporate sector of the world economy, which is the most productive one in terms of job creation, and they play a vital role in the development of human well-being (Naradda Gamage et al., 2020). The proper management of this sector is essential for the development of the business environment and transparent economic relations (Vasylieva et al., 2023). Still, it is also important to note that the weak capital base of these enterprises is associated with a high risk of financial loss and bankruptcy (Ślusarczyk and Grondys 2019). Start-ups often face funding gaps, as they are unable to obtain bank financing and at the same time venture capital and private equity is only available for companies with high growth potential (Fazekas and Becsky-Nagy, 2015; 2019; Nagy, 2004). As Bak et al. (2020) state, resilience is also a key factor for SMEs, although the related scholarly work is limited despite the sector's importance to the economy. SMEs are highly vulnerable due to such factors as the consumers' rapidly changing preferences, the SMEs' dependence on several actors or their lack of resources and credit (Bivona and Cruz 2021; Bucher et al., 2016; Roy and Shaw 2020).

Despite SMEs' importance and high vulnerability, they are often characterised by the lack of efficient management control or financial performance measurement tools and methods. Smaller companies use performance measurement tools less frequently and efficiently (Pešalj et al., 2018; Taylor and Taylor 2014). Garengo et al. (2005) studied the

constraints of using performance measurement systems in SMEs, which are the lack of financial and human resources, the short-term nature of planning, or the increased instability of the business environment. Cuzdriorean (2017) examined the use of management accounting and control practices in SMEs – performance measurement tools are among these practices –and found that the number of used practices is small compared to large companies. According to Lavia López and Hiebl (2015), SMEs use management control and performance measurement methods "not only to a lesser extent but also differently than large enterprises".

The aim of the present research is to develop a model suitable for performance measurement of businesses engaged in "non-specialised retail sale of food" activities operating in the Northern Great Plain region of Hungary, a European emerging market, based on accounting reports and macroeconomic indicators. The model should incorporate indicators that enable managers to measure and improve financial performance. The authors chose the timeframe of 2015-2019: in the years after 2020, a structural fracture happened in almost every economic sector due to the effects of the pandemic – our examined timeframe means an economically more stable, normal period to which companies can compare their present and future operations. Models formulated on historical data often provide great help even in the future.

The research hypothesis is that based on panel data and on the basis of financial indexes and macroeconomic indicators as independent variables calculated from the statements of the examined food retail enterprises, a multivariate linear regression function can be defined, which allows the operating profit or loss of the analysed enterprises to be estimated and predicted as a dependent variable with high accuracy and significance. An additional part of the hypothesis is that the random effects regression model is suitable for accurately and significantly predicting the operational profit/loss of food retail businesses, as opposed to the fixed effects regression model.

Materials and methods

Database of the study

The database for the secondary research was purchased from Opten Informatikai Ltd. The database contains the balance sheet and profit and loss account data of food retail enterprises in the sub-sector "Non-specialised retail sale of food", which are located in the Northern Great Plain region of Hungary, were established before 1 January 2015 and had at least one annual statement and a closed financial year in the period 2015-2019. A total of 972 statements were included in the survey over the indicated time period (2015 – 165, 2016 – 175, 2017 – 194, 2018 – 243, 2019 – 195). As it was articulated before, the reason behind the chosen timeframe of 2015-2019 is that in the years after 2020, a structural fracture happened in almost every economic sector due to the effects of the pandemic and, later, the Russo-Ukrainian war.

Limitation of data availability

A limitation of this study is the reliance on data collected between 2015 and 2019. While this dataset provides a robust foundation for analysis, it may not fully capture more recent trends in the field. Changes in technology or in the international economic and political situation since 2019 could influence the relevance of the findings to current contexts. However, as mentioned earlier, there are established and sound reasons behind the chosen

timeframe. Efforts were made to ensure the dataset's quality and relevance during the selected period; however, readers should exercise caution when generalizing the results to different timeframes. Future research could address this limitation by incorporating more recent data or extending the analysis to include longitudinal datasets covering a broader temporal range. This would enhance the study's robustness and applicability over time.

Applied methods

During the preparation and verification of the database and the calculation of the financial ratios, the following problems were encountered: in each year, there were enterprises that closed the current financial year without revenue, the balance sheet and profit and loss account data were not consistent, enterprises reported with the total cost method in one year and cost of sales method in another, and there were also outlier data. To solve the problems and thus to create a set of enterprises that could be included in the modelling, the following approach was adopted: enterprises with no revenue in the given financial year, enterprises with inconsistent data, enterprises with the cost of sales type profit and loss accounts, and enterprises with outliers and extreme outliers were filtered out and deleted.

To test the hypothesis, *multivariate linear panel regression* was performed on the database data. In a general sense, any database is a panel database in which observations can be distributed into a multidimensional structure. In the panel database, traditionally most commonly analysed, a given set of individuals is observed at fixed times over a given period. The observations thus consist of a certain set of properties of a given individual, the changes in these properties, and the time effect (Ahn et al., 2013; Freund et al., 2006).

In recent decades, panel econometrics has made steady progress, as has the analysis of panel data. Cross-sectional studies are usually carried out by analysing the data of the examined group(s) at a given point in time and looking for answers to the questions that arise at that point in time. Tarnóczi et al. (2015) argue that when analysing cross-sectional data over a longer period, it is difficult to detect individual and time effects, and therefore, panel analysis - a cross-sectional time series analysis - is a useful approach to address this problem. Depending on whether the elements of each panel are the same or different at the analysed time, a distinction is made between balanced and unbalanced panels. The panel database allows for a separate analysis of the time effect and the effects of each data group.

The analysis of panel data can also be understood as collecting several observations of cross-sectional data, which belong to different points in time. Panel regression is essentially a "cross-sectional time series analysis". Panel regression is not about increasing the size of the database to be analysed to obtain better statistical test results due to a higher degree of freedom. Panel data analysis allows the examination of economic questions that cannot be asked in cross-sectional or time-series analyses. Panel regression can also be interpreted as a multilevel model. Another advantage of panel data analysis is that models with more complex behaviour can be created and tested (Tarnóczi and Fenyves, 2017).

The mehod of panel regression analysis allows the examination of the regressive relationship between the data (panel matrix) of n variables with a time series of T periods. The basic equation of the model:

$$Yit = a + Xit\beta + Vi + \varepsilon it,\ i=1, ..., n \text{ and } t = 1, ..., T$$

where "a" stands for the constant term,

"β" are the coefficients of the model estimated by calculation,

"Vi + εit" represents the residual members (residues), i.e. "V" are the residues that refer to variables, which differ from unit to unit but are constant as variables (Madaras 2009).

Two main types of multivariate panel regression are distinguished by whether the error term (unobserved independent variable) "ε" is correlated with the independent variables in the model: fixed effects model and random effects model. In the fixed effects model, it is necessary to assume that the unobserved variable covering the variance of the error term is correlated with the explanatory variables in the model. In the random effects model, it is a condition that the so-called latent variable does not correlate with any of the independent variables in the model. The Hausman test is necessary to choose between fixed effects and random effects models. The null hypothesis of the Hausman test states that the random effects model provides consistent estimates. In this case, the random effects specification should be chosen over the fixed effects. Otherwise, the fixed effects model specification should be applied. Consistency should be examined based on the significance level, "p" value, associated with the Hausman test (Frondel and Vance 2010).

If the Hausman test indicates a $p>0.05$, the random effect panel regression model should be used; for a $p<0.05$, the fixed effect panel regression model should be used. If the assumption of the random effect estimation is true (i.e. there is no endogeneity in the model), the estimation is both consistent and efficient, i.e. it is more favourable than the fixed effect estimation (which is also consistent but not efficient). However, if the condition is not met, the random effect estimation is inconsistent (Berezvai 2015).

IBM SPSS Statistics version 26 and Stata version 13 were used for analysis and data management.

Results and discussion

Results of the multivariate stepwise linear regression

Before performing the multivariate linear panel regression, it was necessary to perform a multivariate stepwise linear regression for each analysed year to identify the financial indicators that most influence the profitability of the enterprises (Tömöri et al., 2022) in the database.

In the multivariate stepwise linear regression calculation, the dependent variable used is the "Operating profit/loss" of the examined companies. In the cross-sectional analysis, 21 financial indicators were selected as independent variables. The results of the regression show that, using the financial indicators calculated from the reports of the investigated food retail enterprises as independent variables for the given year, a multivariate linear regression function can be obtained using cross-sectional data for the time interval 2015-2019 as the independent variables, which allows the result of the operating profit/loss of the examined enterprises to be estimated as a dependent variable with high accuracy and significance.

Based on the cross-sectional modelling, the indicators used in the final models for the given years are ROA margin I, Net working capital, Net working capital ratio, Inventory turnover rate, Total assets turnover rate, Capital strength, Current assets ratio, PAT WC margin. Of these, the following financial ratios occurred as independent variables in each year in each model:

- ROA margin I. (Operating profit or loss / Total assets)
- Net working capital (Current assets - Current liabilities)
- Net working capital ratio (Net working capital / Total assets)

Based on the global interpretation of the t-tests, these three variables have the highest added value and impact in the models each year so that the above financial indicators can be defined as key indicators based on the analysis. It is expected that the above indicators will be included in the models following the panel regression procedure.

Multivariate linear panel regression

Because it is possible to handle both time and observed elements in panel databases based on grouping rules, the panel regression procedure also used macroeconomic data for modelling, either in balanced or unbalanced form, which are presented in Table 1.

Table 1

Applied macroeconomic variables

	EUR/HUF MNB annual average exchange rate in HUF (HUF)	5-year BIRS (average of the current year) (coefficient)	Annual net income per capita of households (thousand HUF)	Employment rate (current year) (coefficient)
2015	309.9	0.0215	1 150.303	0.57510343
2016	311.46	0.013	1 199.094	0.59702898
2017	309.21	0.0114	1 300.079	0.6096726
2018	318.87	0.0165	1 431.983	0.61978921
2019	325.35	0.0112	1 610.692	0.62603421

Source: own editing based on KSH (Central Statistical Office) data

SPSS and Stata statistical software were used for panel regression modelling. Based on the outputs of a backward regression procedure on panel data in SPSS, fixed effects and random effects panel regression models were constructed using Stata.

The "backward" procedure consists of including all independent variables in the model in the first round and excluding, in the course of iterations, those independent variables, the omission of which does not substantially reduce the amount of variance explained by the model (R^2). The aim of the "backward" regression on panel data is to find independent variables among financial and macroeconomic indicators that can be used in "fixed effects" and "random effects" regressions. Of the 21 financial indicators mentioned in subsection 4.1, those that were used in the final model for the year in question in the cross-sectional modelling were selected for backward regression: ROA margin I, Net working capital, Net working capital ratio, Inventory turnover rate, Total asset turnover rate, Capital strength, Current asset ratio, PAT WC margin.

Among the output data of the backward regression on the independent variables, the data in the "Coefficients" table are needed to make the decision. The "backward" procedure produced a satisfactory result after 9 iterations. After the 9^{th} iteration, the following variables were selected as independent input variables for the panel regressions based on the significance levels and multicollinearity measured by the VIF test.

The ROA margin I, Net working capital, and Net working capital ratio in Table 2 are included in the panel regression as independent variables using the backward procedure, which supports the result of the cross-sectional modelling that the financial ratios discussed can be defined as key indicators. The panel regression also includes the ratio of current assets to financial ratios as input explanatory variables. Among the macroeconomic indicators, the annual net income per capita of households is included in the panel models.

Table 2

Panel regression input independent variables

Coefficients							
Independent variable	Unstandardised coefficients		Standardised coefficients	t	Level of significance	Multicollinearity statistics	
	B	Standard error	Beta			Tolerance	VIF
Current assets ratio (Current assets / Total assets)	-588.099	97.424	-0.103	-6.036	0.000	0.656	1.526
Net working capital (Current assets - Current liabilities)	0.119	0.003	0.547	35.165	0.000	0.788	1.269
Net working capital ratio (Net working capital / Total assets)	-1313.946	87.341	-0.287	-15.044	0.000	0.524	1.907
ROA margin I. (Operating profit / Total assets)	10371.430	191.906	0.778	54.044	0.000	0.920	1.087
Annual net income per capita of households (thousand HUF)	0.297	0.117	0.036	2.550	0.011	0.932	1.073

Source: own editing

For the independent variables mentioned above, it can be stated that $p<0.05$, the VIF test values are between 1 and 2, i.e. they are significant, and there is no multicollinearity.

"Random effects - RE" panel regression results (STATA)

For both the random effects and fixed effects panel regressions, it is necessary to specify the time variables and the clustering variables, which in this case are the period 2015-2019 and the Opten ID of the companies.

The results of the RE panel regression are presented in Table 3. The Corrected R^2 is 0.8156, which means that the constructed random-effects regression model can predict the operating profit/loss of the enterprises in the North Great Plain region with 81.6% accuracy.

The STATA procedure uses the Wald Khi-square test for RE panel regression to determine whether the model applies only to the sample under consideration or to the entire population. The Wald test result is 4015.06, $p=0.00$, which leads to the conclusion that the model is applicable to the entire population. All variables in the model are significant.

The random effects model for food retailers in the North Great Plain can be written in the following form:

$$\text{Operating profit}_{Pred} = 210.5 + (-614.9 \times \text{Current Asset Ratio}) + (0.115 \times \text{Net Working Capital}) + (-1230.1 \times \text{Net Working Capital Ratio}) + (10306.3 \times \text{ROA Margin I}) + (0.315 \times \text{Annual Net Income per Capita Household})$$

Table 3

RE panel regression model summary

Name of the independent variable	Beta	Standard error	z test	Level of significance	Confidence interval (95%)	
Current assets ratio	-614.9	109.8	-5.60	0.000	-830.2	-399.6
Net working capital	0.115	0. 003	30.90	0.000	0.108	0.122
Net working capital ratio	-1230.1	96.4	-12.7	0.000	-1419.1	-1041.09
ROA margin I.	10306.3	191.1	53.9	0.000	9931.7	10680.9
Annual net income per capita of households (thousand HUF)	0.315	0.118	2.67	0.008	0.084	0.5469
Constant	210.5	168.3	1.25	0.021	-119.3	540.5
Corrected R^2	0.8156	**Wald Khi-square test result**	4015.06	**RE model significance level**	0.000	
Dependent variable: Operating profit/loss						

Source: own editing

"Fixed effects - FE" panel regression result (STATA)

The results of the FE panel regression are presented in Table 4. The corrected R^2 is 0.7874, which means that the constructed fixed effects regression model can predict the operating profit/loss of the companies in the North Great Plain region with an accuracy of 78.74%.

The STATA procedure applies an F test for the FE panel regression to determine whether the model applies only to the examined sample or to the entire population. The result of the F test is 291.62, p=0.00, which suggests that the model could be applied to the whole population. However, it is important to point out that the indicator for the proportion of current assets is not significant in the fixed effect model (p=0.789).

The random effects model for food retailer companies in the North Great Plain can be written in the following form:

$$\text{Operating profit/loss}_{Pred} = -427.57 + (-78.4 \times \text{Current asset ratio}) + (0.088 \times \text{Net working capital}) + (-884.2 \times \text{Net working capital ratio}) + (10492.6 \times \text{ROA margin I}) + (0.483 \times \text{Annual net income per capita households})$$

Table 4

Summary of FE panel regression model

Name of the independent variable	Beta	Standard error	t-test	Level of significance	Confidence interval (95%)	
Current assets ratio	-78.4	293.02	-0.27	0.789	-654.6	497.8
Net working capital	0.088	0.013	6.62	0.000	0.062	0.114
Net working capital ratio	-884.2	248.13	-3.56	0.000	-1372.2	-396.2
ROA margin I.	10492.6	290.08	36.17	0.000	9922.21	11063.1
Annual net income per capita of households (thousand HUF)	0.483	0.195	2.47	0.014	0.099	0.868
Constant	-427.57	331.54	-1.29	0.198	-1079.5	224.4
Corrected R^2	0.7874	**F test result**	291.62	**FE model significance level**	0.000	
Dependent variable: Operating profit/loss						

Source: own editing

Hausman test results

Based on primal logic, considering the determinative coefficient (FE (0.7874) < RE (0.8156)) and the explanatory power of the independent variables, as well as the significance level (in the case of the fixed effects model, the indicator of the current assets ratio is not significant, p=0.789), it is clear that the random effects model performs better.

The Hausman test was used to decide between random effects and fixed effects regression models. The significance level of the test is p=0.352, which means that the random effects model is practically applicable. The random effects model is consistent and effective for food retailers in the North Great Plain. The fixed effects model is effective but not consistent.

The results show that based on the panel data between 2015 and 2019, using the financial ratios of food retailers in the examined Hungarian region and macroeconomic indicators as independent variables, a multivariate linear regression function can be defined, which allows to estimate and predict the operational profit/loss of the examined companies as a dependent variable with high accuracy and significance. The random effects regression model can predict the operating profit/loss of the examined companies with high accuracy and significance; the fixed effects regression model cannot be used instead.

Conclusions

The primary objective of the research was to develop a decision-supporting performance measurement tool based on quantitative data. The research resulted in the development of a multivariate regression model and a financial indicator framework. The practical results of the secondary research can be applied to the entire population of the study region based on statistical procedures. The result of the modelling is a random-effects regression model that can predict 81.6% of the operating profit/loss of food retailers in Hungary's North Great Plain region.

Among the financial ratios produced from the statements used in the course of the procedures, the application of ROA margin I, Net working capital, Net working capital ratio, Current assets ratio as key indicators, as well as Inventory turnover rate, Total assets turnover rate, Capital strength are suggested. The indicators form a set of indexes that can contribute to the financial analysis, financial planning and decision-making of food retailers in the North Great Plain region. Of the macroeconomic indicators, household income per capita and its change can provide guidance for planning, as food retail risk appears to be the most important macroeconomic indicator.

It is concluded that, based on the panel data for the period 2015-2019, the financial ratios and macroeconomic indicators calculated based on the statements of the examined food retailing enterprises can be used as independent variables to define a multivariate linear regression function that can be used to estimate and predict the operating profit/loss of the examined companies under study as a dependent variable with high accuracy and significance – our hypothesis can be accepted. The main result of the research is that a performance evaluation panel regression model specific to food retailing enterprises in the North Great Plain region has been developed, which can be used to predict the outcome of the operating profit/loss of the studied companies. Based on the Hausman test, there is no endogeneity in the model, and the error terms do not correlate, which makes the application of the random effects model practical. The random effects model is consistent and effective for the sample, and the fixed effects model is effective but not consistent. The adjusted R^2 of the RE panel regression is 0.8156, which means that the constructed random effect regression model can predict the operating profit/loss of the North Great Plain companies with 81.6% accuracy. Based on the Wald Chi-squared test, the RE panel regression is applicable to the entire population.

It can be concluded that the analysis and interpretation of key indicators can help food retailers to produce higher operating profit. Based on the identified key indicators, the effectiveness of working capital management can be analysed at a high level of abstraction, which can be used as a basis for determining the appropriate action in operations to mitigate the problem. It can also be concluded that multiple indicators have been identified in the cross-sectional stepwise regression procedure, not all directly related to working capital management. However, their application can provide additional information for food retailers in the examined region. Although excluded from the panel model, the applicable indicators had explanatory power in the cross-sectional regressions: Inventory Turnover, Total Asset Turnover, and Capital Strength. It is also found that the variance explained by the dependent variables excluded from the panel model is partially equal to that explained by the remaining variables. In practical terms, this means that the two financial indicators provide partially or entirely the same information. From a professional point of view, the analyst should pay attention to the similarity of the information content when assessing performance.

The model resulting from the research can be used by food retailers in the examined region of Hungary in their financial analysis, management control and performance measurement activities. The companies have two options: they can either substitute the relevant financial indicators and the current level of the macroeconomic indicator into the final generic model to obtain a forecast of the operational profit/loss, or they can make decisions with the support of the developed indicator system. Of course, it is also possible to use both methods in combination, and it is recommended from a professional point of view. Following the steps of creating the present model, further financial performance measurement tools can be created for other samples of different sectors or geographical areas, which can help management and investors of SMEs to grasp the profitability of the companies better.

References

Ahn S. C., Lee Y. H., Schmidt P. (2013), Panel data models with multiple time-varying individual effects, *Journal of Econometrics*, 174, pp. 1-14, https://doi.org/10.1016/j.jeconom.2012.12.002

Arkan T. (2016), The importance of financial ratios in predicting stock price trends: A case study in emerging markets, *Finanse, Rynki Finansowe, Ubezpieczenia*, 79, pp. 13–26, https://doi.org/10.18276/frfu.2016.79-01

Asiri B. K. (2015), How investors perceive financial ratios at different growth opportunities and financial leverages, *Journal of Business Studies Quarterly*, 6(3), pp. 1-12.

Bak O., Shaw S., Colicchia C., Kumar V. (2020), A systematic literature review of supply chain resilience in small–medium enterprises (SMEs): A call for further research, *IEEE Transactions on Engineering Management*, 70(1), pp. 328–341, https://doi.org/10.1109/TEM.2020.3016988

Belas J., Kubalek J., Hlawiczka R., Bencsik A., Metzker Z. (2024), The impact of selected financial factors on business ethics in the SMEs segment in the V4 countries, *Economics and Sociology,* 17(2), 173-193, https://doi.org/10.14254/2071789X.2024/17-2/8

Berezvai Zs. (2015), A magyar malomipar piacszerkezetének modellezése, versenyintenzitással való összefüggéseinek bemutatása kvantitatív közgazdasági módszerekkel [Modeling the market structure of the Hungarian milling industry, presenting its correlation with competitive intensity using quantitative economic methods], *GVH országos tanulmányi verseny [*The national study competition of the Economic Competition Office], 16.

Bilan Y., Mishchuk H., Pylypchuk R. (2017), Towards sustainable economic development via social entrepreneurship, *Journal of Security & Sustainability Issues*, 6(4), 691-702, http://doi.org/10.9770/jssi.2017.6.4(13)

Bivona E., Cruz M. (2021), Can business model innovation help SMEs in the food and beverage industry to respond to crises? Findings from a Swiss brewery during COVID-19, *British Food Journal*, 123(11), pp. 3638–3660, https://doi.org/10.1108/BFJ-07-2020-0643

Bucher S., Urs P. J., Cardoza G. (2016), FUNDES: Becoming a strategically mindful non-profit, *Journal of Business Research*, 69(10), pp. 4489–4498, https://doi.org/10.1016/j.jbusres.2016.03.014

Cuzdriorean D. D. (2017), The use of management accounting practices by Romanian small and medium-sized enterprises: A field study, *Journal of Accounting and Management Information Systems*, 16(2), pp. 291–312, http://dx.doi.org/10.24818/jam is.2017.02004

Dankiewicz R., Balawejder B., Chudy-Laskowska K., Britchenko I. (2022), Impact factors and structural analysis of the state's financial security, *Journal of International Studies*, 15(4), pp. 80-92, doi:10.14254/2071-8330.2022/15-4/5

Erdey L. (2006), Adósságválságtól a NAFTA első évtizedéig - Mexikó gazdaságfejlődésének kérdőjelei [From debt crisis to the first decade of NAFTA – Questionmarks of Mexico's Economic Development], *Competitio,* 5(3), pp. 43-65, https://doi.org/10.21845/comp/2006/3/3

European Commission (2023), *Annual Report on European SMEs 2022/2023*, Available at: https://single-market-economy.ec.europa.eu/system/files/2023-08/Annual%20Report%20on%20European%20SMEs%202023_FINAL.pdf

Fazekas B., Becsky-Nagy P. (2015), The role of venture capital in the bridging of funding gaps – A real options reasoning, *Analele Universitatii Di N Oradea-Stiinte Economica / Annals of University of Oradea-Economic Science*, 24(1), pp. 825-830.

Fazekas B., Becsky-Nagy P. (2019), Mit jelez a tulajdonosi szerkezet? – A tulajdonosi szerkezet és a vállalkozások teljesítményének kapcsolata információs aszimmetriák mellett a magyarországi kockázatitőke-befektetések tükrében [What does the ownership structure indicate? - The relationship between ownership structure and firm performance in the presence of information asymmetries in venture capital investments in Hungary], *Vezetéstudomány*, 50(7-8), pp. 31-38, https://doi.org/10.14267/VEZTUD.2019.07.03

Földvári P., Erdey L. (2009), Do purchasing power and interest rate parities hold for the EUR/HUF exchange rate? A time-series analysis, *Acta Oeconomica*, 59(3), pp. 289-306, https://doi.org/10.1556/aoecon.59.2009.3.2

Freund R.J., Wilson W.J., Sa P. (2006), *Regression analysis*, Elsevier.

Frondel M., Vance C. (2010), Fixed, random, or something in between? A variant of Hausman's specification test for panel data estimators, *Economics Letters*, 107(3), pp. 327–329, https://doi.org/10.1016/j.econlet.2010.02.007

Garengo P., Biazzo S., Bititci U. S. (2005), Performance measurement systems in SMEs: A review for a research agenda, *International Journal of Management Reviews*, 7(1), pp. 25–47, https://doi.org/10.1111/j.1468-2370.2005.00105.x

Gazi M. A. I., Nahiduzzaman M., Sarker S. K., Amin M. B., Kabir M. A., Kouki F., Senathirajah A.R.S., Erdey, L. (2024), Should South Asian stock market investors think globally? Investigating safe haven properties and hedging effectiveness, *Economies*, 12(11), 309, https://doi.org/10.3390/economies12110309

Kliestik T., Valaskova K., Lazaroiu G., Kovacova M., Vrbka J. (2020), Remaining financially healthy and competitive: The role of financial predictors, *Journal of Competitiveness*, 12(1), pp. 74–92, https://doi.org/10.7441/joc.2020.01.05

Lavia López O., Hiebl M. R. (2015), Management accounting in small and medium-sized enterprises: current knowledge and avenues for further research, *Journal of Management Accounting Research*, 27(1), pp. 81-119, https://doi.org/10.2308/jmar-50915

Lee J., Chang J.R., Kao L.J., Lee C.F. (2023), Financial analysis, planning, and forecasting, In: *Essentials of Excel VBA, Python, and R*, Springer, Cham, https://doi.org/10.1007/978-3-031-14283-3_20

Lukason O., Camacho-Miñano M. (2019), Bankruptcy risk, its financial determinants and reporting delays: Do managers have anything to hide?, *Risks*, 7(3), 77, https://doi.org/10.3390/risks7030077

Madaras Sz. (2009), A munkanélküliség elemzése a Központi Régió megyéiben [Analysis of unemployment in the counties of the Central Region of Hungary], *Közgazdász Fórum*, 12, pp. 45–58.

Nagy P. (2004), A kockázati tőke szerepe a finanszírozási rések feloldásában, In: Mészáros T., Czakó E., Román Z., Perényi Á., Papanek G., Katona J., Kádár K., Barta Gy., Bagó E., Bélyácz I., (Eds.), Gazdasági szerkezet és versenyképesség az EU csatlakozás után: A VIII. Ipar- és Vállalatgazdasági Konferencia előadásai, Pécs, pp. 422-430.

Naradda Gamage S.K., Ekanayake E.M. ., Abeyrathne G.A.K.N.J., Prasanna R.P.I.R., Jayasundara J.M.S.B., Rajapakshe P.S.K. (2020), A review of global challenges and survival strategies of small and medium enterprises (SMEs), *Economies*, 8(4), pp. 79-103, https://doi.org/10.3390/economies8040079

Nugroho L., Orban I., Utami W., Hidayah N., Nugraha E. (2024), Liquidity surplus and profitability: How does liquidity affect profitability prior to and during COVID-19?, (Empirical Indonesian Banking Sector), *WSEAS Transactions on Business and Economics*, 21, pp. 59-70, https://doi.org/0.37394/23207.2024.21.6

Nworie G. O., Nwoye U. J. (2023), Drivers of Operating Profit: A focus on selected firms' costs, *CECCAR Business Review*, 4(2), pp. 62-72, https://doi.org/10.37945/cbr.2023.02.07

Osadchy E. A., Akhmetshin E. M., Amirova E. F., Bochkareva T. N., Gazizyanova Y., Yumashev A. V. (2018), Financial statements of a company as an information base for decision-making in a transforming economy, *European Research Studies Journal*, 21(2), pp. 339-350.

Owusu-Akomeah M. (2015), Working capital management and profitability of listed manufacturing companies in Ghana, *ADRRI Journal of Arts and Social Sciences*, 13(5), pp. 20-32, https://doi.org/10.55058/adrrijass.v13i5.190

Pešalj B., Pavlov A., Micheli P. (2018), The use of management control and performance measurement systems in SMEs: A levers of control perspective, *International Journal of Operations & Production Management*, 38(11), pp. 2169-2191, https://doi.org/10.1108/IJOPM-09-2016-0565

Qianyu Z., Dongping L., Xueying Z., Huaisen C., Xiaozhou Z. (2021), Enterprise profit forecast model based on long short-term memory neural network, *2021 International Conference on Big Data Analysis and Computer Science (BDACS)*, pp. 62–65, https://doi.org/10.1109/BDACS53596.2021.00021

Rákos M., Szenderák J., Erdey L., Kőmíves P. M., Fenyves, V. (2022), Analysis of the economic situation of energy companies in Central and Eastern Europe, *International Journal of Energy Economics and Policy*, 12(4), pp. 553-562, https://doi.org/10.32479/ijeep.12957

Roy P.K., Shaw K. (2023), A credit scoring model for SMEs using AHP and TOPSIS, *International Journal of Finance & Economics*, 28(1), pp. 372-391, https://doi.org/10.1002/ijfe.2425

Ślusarczyk B., Grondys K. (2019), Parametric conditions of high financial risk in the SME sector, *Risks*, 7(3), 84, https://doi.org/10.3390/risks7030084

Straková J., Talíř M., Váchal J. (2022), Opportunities and threats of digital transformation of business models in SMEs, *Economics and Sociology,* 15(3), 159171, https://doi.org/10.14254/2071-789X.2022/15-3/9

Taani K. (2011), The effect of financial ratios, firm size and cash flows from operating activities on earnings per share: an applied study on Jordanian industrial sector, *International Journal of Social Sciences and Humanity Studies,* 3(1), pp. 197-205.

Tamimi O., Orbán I. (2022), Financial engineering and its impact on audit efficiency in the opinion of experts, *Journal of International Studies*, 15(2), pp. 50-62.

Tarnóczi T., Fenyves V., Bács Z., Böcskei E. (2015), Versenyképesség és gazdasági etika. Vállalati teljesítmény elemzése panel regresszióval [Competitiveness and economic ethics. Analyzing company performance with panel regression], *Polgári Szemle*, 11, pp. 4-6.

Tarnóczi T., Fenyves V. (2017), Az Észak-Alföldi régió élelmiszer-kiskereskedelmi vállalatainak kockázatelemzése [Risk analysis of food retail companies in the North Great Plain region], *International Journal of Engineering and Management Sciences*, 2(4), pp. 539-540, https://doi.org/10.21791/IJEMS.2017.4.44.

Taylor A., Taylor M. (2014), Factors influencing effective implementation of performance measurement systems in small and medium-sized enterprises and large firms: a perspective from contingency theory, *International Journal of Production Research*, 52(3) pp. 847-866, https://doi.org/10.1080/00207543.2013.842023

Tömöri G., Bács Z., Felföldi J., Orbán I. (2022), Impact of pharmaceutical R&D activity on financial flexibility and bargaining power, *Economies*, 10(11), 277, https://doi.org/10.3390/economies10110277

Vasylieva T., Kasperowicz R., Tiutiunyk I., Lukács E. (2023),Transparency and trust in the public sector: Targets and benchmarks to ensure macroeconomic stability, *Journal of International Studies, 16*(4), 117-135, https://doi.org/10.14254/2071- 8330.2023/16-4/8

Voda A.D., Dobrotă G., Țîrcă D.M., Dumitrașcu D.D., Dobrotă D. (2021), Corporate bankruptcy and insolvency prediction model, *Technological and Economic Development of Economy*, 27(5), 1039-1056, https://doi.org/10.3846/tede.2021.15106

Wang S. (2020), Research on stock return prediction based on stepwise regression-incremental linear regression analysis, *International Core Journal of Engineering*, 6, pp. 211-217, https://doi.org/10.6919/ICJE.202004_6(4).0031

Woźniak M., Duda J., Gąsior A., Bernat T. (2019), Relations of GDP growth and development of SMEs in Poland, *Procedia Computer Science*, 159, pp. 2470-2480, https://doi.org/10.1016/j.procs.2019.09.422

Cite:

UFJ Style

Sütő D., Bajnai P., Fenyves V. (2024), Forecasting the financial performance of small and medium-sized enterprises: evidence from the Hungarian food retail sector, *Ukrainian Food Journal*, 13(4), pp. 794–808, https://doi.org/10.24263/2304-974X-2024-13-4-12

APA Style

Sütő, D., Bajnai, P., & Fenyves, V. (2024). Forecasting the financial performance of small and medium-sized enterprises: evidence from the Hungarian food retail sector. *Ukrainian Food Journal*, *13*(4), 794–808. https://doi.org/10.24263/2304-974X-2024-13-4-12

Evaluation of employer's brand of trade and food industry companies

Viktoriia Khmurova[1], Olena Dragan[2], Iryna Fedulova[3], Maryna Dzhulai[3], Alina Berher[2]

1 – Ben Gurion University of the Negev, Be'er Sheva, Israel;
2 – National University of Food Technologies, Kyiv, Ukraine;
3 – State University of Trade and Economics, Kyiv, Ukraine

Keywords:

EVP
Employer
Brand
Trade
Food
Industry

Article history:

Received 17.03.2024
Received in revised form 6.07.2024
Accepted 30.12.2024

Corresponding author:

Olena Dragan
E-mail: eidragan@ukr.net

DOI: 10.24263/2304-974X-2024-13-4-13

Abstract

Introduction. The purpose of the research is to identify the components of the employer's brand that contribute to its agreeability and effectiveness in attracting and retaining talented employees, as well as to provide a generalized assessment of the employer's brand, which involves identifying the strengths and weaknesses of its value proposition (EVP).

Materials and methods. Experts in employer's branding conducted an expert assessment development of the components' level of employer's brand value proposition. The assessment was based on the Likert scale, which includes 5 possible states from 1 is strongly agree with the best message about the EVP component to 0 is strongly disagree. The TOPSIS multicriteria assessment method to summarize and analyze the level of employer's brand development was used.

Results and discussion. The key components of the value proposition are revealed, such as salary level, additional benefits, career growth, company image and a comfortable workplace, which are the basis for forming an attractive employer brand.

The average expert assessment of EVP components of the employer's brand for all the surveyed companies showed that the advantages of the employer's brand of the surveyed companies are official employment (4.27); products and services (4.07); social projects (3.97) of the companies. The weaknesses of the employer's brand of the surveyed companies are the opportunity to gain international experience (1.42) and the possibility of moving to another city/country (1.55).

The generalized assessment of the employer's brand allowed us to rank the surveyed companies by the level of employer's brand development and to identify among them the leader (Auchan) and the outsider (Epicenter K).

The level of employer's brand development of value proposition components of the surveyed companies is the basis for the formation of the desired employer's brand. The assessments of each EVP component were categorized into 3 ranges: strength, average, and weakness. Based on the results of the categorization assessment, EVPs were identified for each company that are associated with the strengths or weaknesses of the employer brand. This made it possible to propose directions for the development of employer's brand for surveyed companies. In particular, improving weak EVP will reduce the negative brand perception among potential employees. Strengthening of a strong EVP will allow companies to stand out in the labor market. EVP components with the average value should be considered as the potential for possible improvement.

Conclusion. The proposed methodological approach allows the objective assessment of the state of an employer's brand development and identification of its strengths and weaknesses, which is an important step in formulating strategies for attracting and retaining the target audience.

Introduction

Creating an attractive employer image is the key task for any company. It helps to attract talented employees to the company, promotes staff retention, increases their motivation, level of engagement, marketing and sales effectiveness, facilitates attracting investments and partners to the company's activities, and creates a culture of risk and reputation management.

According to Tanwar and Prasad (2016), an employer's brand is the image and reputation of the company as an employer in the eyes of current and potential employees, as well as other stakeholders such as partners and customers. Tanwar and Prasad (2016) include in the employer's brand a set of perceptions, experiences and expectations that people associate with the company as the place where they want to work. In such circumstances, there is a need to determine the criteria for employer's brand formation, taking into account the requirements of the target audience.

Each company uses special attractive offers in the form of tangible and intangible benefits to define the desired image for potential candidates. Thus, the concept of employer's value proposition (EVP) arises (Barrow et al., 2005). According to the international audit and consulting company Deloitte, a high level of EVP is important for 80% of employers' top managers (HR Liga, 2019). According to Grc.ua (2024), for 84% of the surveyed job seekers, the company's reputation and active HR brand are important when choosing a future job. The economic impact for companies is reflected in a 10% reduction in labor costs, a 25% reduction in recruitment costs, and a 28% reduction in staff turnover (Grc.ua, 2024).

According to Liu (2020), Nagpal et al. (2019), Pawar and Charak (2015), the EVP is central to an employer's brand and is key to attracting and retaining talented employees. It defines the unique benefits and values that the company offers to its employees and helps to create an attractive employer image in the labor market. It is important that the value proposition is authentic, realistic, and reflects the actual experience of employees in the company (Staniec and Kalińska-Kula, 2021).

Jha Sr. and Jha Sh. (2015) conducted the research of employer's brand EVPs in six leading countries and determined that EVPs help to pay the attention of potential employees, especially those who has necessary skills and experience. EVP also helps employees to understand how their work contributes to the overall success of the company and how they can grow within the organization (Tanwar and Prasad, 2016). Unique EVP allocates a company apart from its competitors and makes it more attractive to potential employees. The most important attributes of EVP are stability and job security, followed by relationships in the company, high remuneration, and benefits (Palen-Tondel and Smolbik-Jeczmien, 2021). The value proposition is usually considered a set of associations and tangible and intangible offers that an employee receives from the company (Pawar and Charak, 2015).

Krummel et al. (2020) classified the needs of employees according to the factors of employer attractiveness using the ERG theory (existence, relatedness and growth) established by Alderfer (1969), which is a further development of Maslow's hierarchy of needs theory. According to this theory, a person has three basic needs that he or she seeks to satisfy, which include the needs for material existence, interpersonal relationships with other people, and the search for opportunities for personal development.

Valène (2024) considers EVP of employer's brand as an objectively defined set of values that the company offers its employees in the form of working and cultural environment, namely: the needs of material existence, consciousness-raising relationships with other people and society, opportunities for personal development, and work-life balance.

Nagpal A. and Nagpal G. (2019) showed that the EVP components directly affect employee's productivity, their loyalty to the employer, increase the value of fulfilling

promises to employees, and determine further communication in the company. It is undeniable that EVP employer's brand also focuses on its employees. Employees themselves have an impact on the formation of company values (Jha Sr. and Jha Sh., 2015). Satisfaction feedback is obtained through the following tools: anonymous audience surveys, interviews with dismissed employees, and analysis of labor market trends (Staniec and Kalińska-Kula, 2021). Quality interaction between the employer and the employee is the consistency between the desired and actual level of EVP.

The result of the research of HR consulting company "Sibson Consulting" there is the "Reward of Work" (ROW) model, which includes the winning elements and processes of creating an attractive workplace (Seemiler and Grace, 2017). This model is transformed into the employer's value proposition EVP.

Liu (2020) identified the following components of an EVP employer's brand as career development opportunities, personal value realization, corporate culture, financial remuneration, social responsibility, and workspace. First, the company's reputation determines the content of career pages and search sites pages, which in turn increases the EVP competitiveness (Liu et al., 2018).

Analysis of the literature has shown that most scientists consider that the main components of EVP are the level of salary, additional benefits (health insurance, bonuses), career development in the company, employee training and development system, the company's image as an employer, and comfortable workplace. Less important, but also influencing the choice of a future job, are the following factors: the company's business rating, the use of the latest technologies, company values, and the company's rating as an employer (Firsova et al., 2020; HR Liga, 2019; Liu, 2020; Nagpal A. and Nagpal G., 2019), 2019; Oberemchuk and Dehtiar, 2019; Palen-Tondel and Smolbik-Jeczmien, 2021; Pawar and Charak, 2015; Samoliuk et al., 2021; Seemiler and Grace, 2017; Shanmuga, 2021;Valène, 2024; Volobaeva et al., 2021; Zhovtyak, 2021). In the context of the digitalization of society, reviews about the company on various portals are also important (Gross et al., 2023; Liu et al., 2018; Mir and Salo, 2024; Seemiler and Grace, 2017). Liu (2020) note that in the current conditions, social projects, positive environmental impact, social responsibility, corporate culture, and favourable company atmosphere EVP components are also important. The value proposition of work-life balance refers to harmony in the level of satisfaction from work and life. It emphasizes the importance of work-life balance, as well as the overall well-being of employees. The ability to choose a schedule that fits individual needs can increase employee loyalty and company attractiveness (Pawar and Charak, 2015; Valène, 2024).

The diversity of employer's brand EVP components suggests that they contain a wide range of economic, emotional, and functional characteristics. There is still no established opinion on which EVP components best reflect the content of the employer's brand. The issues of systematizing the EVP components of the employer's brand remain unresolved, which could be used as a basis for assessing its state of development and attractiveness in the labor market.

The purpose of the research is to identify the components of the employer's brand and to evaluate the employer's brand of the companies, which serves as the basis for substantiating the ways of its development.

Materials and methods

Materials

The assessment of the employer's brand development was conducted based on the survey of leading experts of the surveyed enterprises in the retail and catering sector by EVP components.

To assess the state of the employer's brand, 6 companies were selected that are popular and well-known among consumers and job candidates. The companies were selected according to the following criteria: scale of operations, size of the coverage network (number of stores), number of officially hired employees (more than 5000), number of internship offers and vacancies on career sites, availability of the department or specialists engaged in employer's brand management, and previous employer's brand ratings. Six companies were selected for the servey: ATB, Auchan, McDonald's, Epicenter K, METRO, Fozzy Group. Half of the selected companies (Auchan, McDonald's, METRO) are international and operating in many global markets.

The survey was conducted in 2022. There were 7 HR and Employer's Branding specialists who understand the company's internal culture and external perception of it as an employer were involved in the survey. Google Forms was conducted for the survey.

The topic of employer's brand development is narrow-purpose; the goal was to obtain a qualitative assessment of the state of employer's brand development rather than a full quantitative analysis, so the sample of experts is sufficient to obtain objective results. The data was obtained directly from professionals who work in this area that ensures its significance.

Methods

For generalized brand assessment, it is proposed to use the TOPSIS (Technique for Order Preference by Similarity to Ideal Solution) method, one of the analytical methods for making multi-criteria decisions (Madanchian and Taherdoost, 2023). This method is used to compare alternatives by means of similarity to the ideal and anti-ideal solutions, taking into account the weighting of the criteria. It allows generalizing the employer's brand assessment by many criteria, which are used as value propositions. TOPSIS is a convenient, practical method that has a simple mathematical apparatus and can be used with Excel.

The algorithm for using the TOPSIS method to assess an employer brand can be described as follows:

1. Identification of criteria: determination of key value propositions that are important for employer's brand assessing.
2. Conducting an expert survey by Likert scale on the level of development of each component of the employer's brand value proposition.
3. Normalize the data to bring the values of each criterion to the same scale to ensure an adequate level of comparison.
4. Creating a decision matrix: rows – the studied employers, columns – normalized values of the employer's brand of value proposition indicators.
5. Identification of the ideal and anti-ideal employer for each value proposition in order to determine the best and the worst characteristics.
6. Setting the weight for each criterion according to their importance in the assessment.
7. Calculate the similarity to the ideal solution: use the Euclidean distance to determine the similarity of each employer to the ideal and anti-ideal solution.
8. Determination of the employer's brand ranks by the criterion of generalized evaluation.

The best message about the state of each EVP component was identified in the previous questionnaire for the expert. Below are the linguistic characteristics of the best message about each EVP component:

1. Dress code: the company provides restrained, modern, comfortable, easy-to-clean work wear that is not paid for by the employee at their own expense or does not impose special requirements for it.
2. Social projects of the company: the company has social projects to support the environment, low-income groups, and IDPs.
3. Possibility of moving to another city/country: the company helps with relocation to another place of work, provides financial support.
4. Business rating of the company: the company is high in the ranking of the largest taxpayers, has a large network of retailers, a high level of market recognition among consumers and positive feedback on the company's activities.
5. Creativity/design of the office, comfortable workplace: modern design, provision of computer equipment (if necessary), open space for work and communication with the team, a place to relax.
6. Reviews about the company on various portals: positive feedback about work, teamwork, salary and financial bonuses.
7. Rating of the company as an employer: high positions in the rating of the most attractive employers according to the results of a survey of candidates in the labor market, the company's nomination for the implementation of a successful HR project.
8. Location of the office: proximity to a transport interchange or residential area, the ability to get to the place of work by public transport or with the help of a company shuttle service.
9. Additional benefits (insurance, healthcare, transportation, etc.): availability of health insurance, reimbursement of transportation costs, and a system of bonuses with gifts from the company and bonus programs.
10. Official employment: compliance of the employment relationship with the employee with the labor legislation.
11. Products/services created by the company: certification of products/services according to international standards, high requirements for employee service, creation of a positive experience and customer impression.
12. Company's values: the company's internal and external communication of values when making business decisions or hiring new employees, and the actions taken to increase loyalty to the company.
13. The company's image as an employer: a clearly formed positive feedback on the interaction with recruiters during the selection stages of the vacancy, positive feedback on working in the company.
14. Opportunity to gain international experience: the company's provision of opportunities to work on projects with colleagues or contractors from other countries, the availability of a relocation program during work or career development.
15. Training and development system in the company: a formed and structured training system from the initial position to a high-level manager, which is available to every employee of the company, there is a career development system.
16. Work schedule: the ability to combine work and study as needed, a flexible approach to planning work shifts for the month, the ability to work remotely (if the position requires).
17. Salary level: compliance with the average level of pay in the labor market or even higher, timely payment of wages, 100% official payment to the employee's bank account.

The EVP was assessed by Likert scale from 1 to 5, where 1 is completely inappropriate and 5 is completely appropriate. The greatest advantages of this scale are its ease of use and relative reliability even with a small number of judgments.

The next step in the proposed employer's brand assessment methodology is to normalize the identified expert assessments. The normalization of the matrix of the determined ratings is carried out by the formula (Madanchian and Taherdoost, 2023):

$$t_{ij} = \frac{x_{ij}}{\sqrt{\sum_{i=1}^{n} x_{ij}^2}} \quad (1)$$

where x_{ij} – expert evaluation j-th component of the EVP for i-th enterprise; i – is the index of the analyzed enterprises; i=1…n n – is the number of enterprises under study; j – is the index of the EVP, $j=1...m$; m – is the number of EVP.

The next step in assessing the employer brand is to form a normalized dimensionless matrix, which is obtained because of the normalization behavior according to formula 1 and in which all values range from 0 to 1.

The weightiness of the criteria in the evaluation is determined by the formula (Madanchian and Taherdoost, 2023):

$$w_{ij} = \frac{M(x_{ij})}{\sum_{j}^{m} M(x_{ij})} \quad (2)$$

where $M(x_{ij})$ – expert evaluation of the weight j-th component of the EVP, $\sum_{j=1}^{m} W_{ij} = 1$.

The weight of EVPs in this study will be considered the same (0.059), since their number is large and it is impossible to identify the most significant ones.

The normalized scores are weighted according to the weighting of the EVP of the company. The normalized weighted scores are determined by the formula (Madanchian and Taherdoost, 2023):

$$T_{ij} = t_{ij} w_{ij} \quad (3)$$

where w_j– is the weight j-th component of the EVP, j=1, … , 17.

The next step is to calculate the squares of the distances of the expert assessment of the value proposition components. To do this, we calculate the squares of the distances from the ideal level – T_j^+ (the maximum value of T_{ij} to j) and the anti-ideal level – T_j^- (the minimum value of T_{ij} to j).

For each component of the value proposition, we calculate S_i+ та S_i- by formulas (Madanchian and Taherdoost, 2023):

$$S_i^+ = \sqrt{\sum_{j=1}^{n} (T_{ij} - T_j^+)^2} \quad (4)$$

$$S_i^- = \sqrt{\sum_{j=1}^{n} (T_{ij} - T_j^-)^2} \quad (5)$$

The generalized employer's brand score is determined by the formula (Madanchian and Taherdoost, 2023):

$$R_i = \frac{S_i^-}{S_i^- + S_i^+} \quad (6)$$

The proposed model will help to assess the state of development of the employer's brand.

In the process of using the TOPSIS methodology, the appraisal of the ideal (T_j^+) and anti-ideal (T_j^-) solutions are used as intermediate estimates. Such estimates can be used to justify the directions of forming the desired employer's brand in the context of individual components of its EVP.

T_j^+ reflects the key strengths of each company; T_j^- identifies the weaknesses that are least attractive to experts and need to be improved; average values demonstrate the company's balance according to the certain criteria.

This data can help each company to focus on improving its weaknesses and asign its strengths. For this purpose, we used equal division of the T_{ij} scores into 3 categories: strengths; average values; and weaknesses.

The interval for dividing the scores was determined by the formula:

$$(T_{ij\ max} - T_{ij\ min})/3 = I$$

The interval of EVP strengths was determined by the formula:

$$T_{ij\ max} \div T_{ij\ max} - I$$

The interval of average EVP values was determined by the formula:

$$T_{ij\ max} - I \div T_{ij\ max} - 2 * I$$

The interval of EVP weaknesses was determined by the formula:

$$T_{ij\ max} - 2 * I \div T_{ij\ max} - 3 * I$$

Hypothesis

The main hypothesis of the research is that in order to determine whether the current state of the employer's brand meets the desired views of the target audience, it is advisable to form the list of EVP brand, assess the level of their development, conduct a generalized assessment of the employer's brand in terms of all EVP components development and determine which EVP components are strong, medium or weak points of the employer's brand development.

Results and discussion

Assessing the components of the EVP employer's brand.

The purpose of the employer brand rating is to study the level of attractiveness of the EVP for candidates (Fedulova et al., 2024). Based on the results of the literature review and job search websites, main features and characteristics of companies that help them form the employer's brand and create its attractiveness in the labor market for job candidates the list of EVPs was formed, (Table 2).

The average expert assessment of EVPs of the surveyed companies is shown in Table 3.

Based on the data obtained on the average expert assessments of EVP employer's brand components for the surveyed companies, the following conclusions can be made. The main advantages of the employer's brand of the surveyed companies are official employment (4.27); products and services (4.07); and social projects (3.97) of the companies. Thus, the surveyed companies provide transparency and stability, are associated with quality products or services, which also increases their attractiveness as employers, and social responsibility is the important element for the employer's image.

The weaknesses of the employer's brand of the surveyed companies are the opportunity to gain international experience (1.42) and the possibility of relocation to another city/country (1.55). This indicates limited globalization or lack of international career opportunities in the companies, as well as the local orientation of the surveyed companies.

Table 3

Averaged expert assessment of EVP of employer brand of studied companies

Components of the EVP	ATB	Auchan	METRO	McDonald's	Epicenter K	Fozzy Group	Average value
Dress code	3.1	4.2	3.2	3.3	2.1	4.1	3.33
Social projects of company	4.1	5.0	4.1	3.3	3.1	4.2	3.97
The possibility of moving to another city/country	1.4	2.4	2.2	1.1	1.1	1.1	1.55
Business rating of company	4.1	4.3	3.1	4.1	3.2	4.1	3.82
Office creativity/design, comfortable workplace	3.3	4.4	3.2	2.1	3.1	4.1	3.37
Reviews about company on various portals	3.1	3.1	3.2	2.2	2.1	3.1	2.80
Rating of company as employer	3.4	3.2	3.2	2.3	2.1	3.1	2.88
Office location	4.1	4.1	2.1	2.3	3.1	4.2	3.32
Additional benefits (insurance, transportation, etc.)	3.3	4.1	4.1	3.1	3.1	4.2	3.65
Official employment	5.0	5.0	5.0	3.1	3.2	4.3	4.27
Products/services that the company creates	4.4	5.0	4.2	3.2	3.2	4.4	4.07
Company values	3.1	5.0	4.2	3.3	3.4	4.2	3.87
The image of company as employer	3.3	4.1	3.1	3.1	2.1	3.1	3.13
Opportunity to gain international experience	1.4	1.7	2.1	1.1	1.1	1.1	1.42
The system of training and development in company	3.3	5.0	3.1	3.2	2.4	3.1	3.35
Work schedule	3.3	5.0	3.1	3.2	3.3	3.1	3.50
Salary level	4.1	3.1	4.1	3.1	3.3	3.1	3.47

Source: Own study based on expert assessment

The company's rating as an employer (2.88) and reviews on portals (2.80) are relatively low, points out the defects in the perception of the company among employees and potential job seekers. This requires working on the corporate image. Fringe benefits (3.65) are relatively high, but there is still space for improvement in working conditions, which could increase the overall brand appeal.

Generalized employer's brand assessment.

The company's rating as an employer is an important indicator of attractiveness for candidates, as it is a generalized opinion of job seekers and employees about working for the

company. Thus, employer's brand assessment is the key element of human resource management strategy and corporate management in general (Tanwar and Prasad, 2016).

Table 4 shows the weighted normalized matrix of experts' ratings and the ideal T_j^+ and anti-ideal T_j^- appraisal.

Table 4

Normalized weighted matrix of expert opinions and T_j^+ , T_j^-

Components of the EVP	ATB	Auchan	METRO	McDonald's	Epicenter K	Fozzy Group	T_j^+	T_j^-
Dress code	0.022	0.030	0.023	0.023	0.015	0.029	0.030	0.015
Social projects of company	0.025	0.030	0.025	0.020	0.019	0.025	0.030	0.019
The possibility of moving to another city/country	0.020	0.035	0.032	0.016	0.016	0.016	0.035	0.016
Business rating of company	0.026	0.027	0.019	0.026	0.020	0.026	0.027	0.019
Office creativity/design, comfortable workplace	0.023	0.031	0.022	0.015	0.022	0.029	0.031	0.015
Reviews about company on various portals	0.026	0.026	0.027	0.019	0.018	0.026	0.027	0.018
Rating of company as employer	0.028	0.026	0.026	0.019	0.017	0.025	0.028	0.017
Office location	0.029	0.029	0.015	0.016	0.022	0.029	0.029	0.015
Additional benefits (insurance, transportation)	0.022	0.027	0.027	0.020	0.020	0.027	0.027	0.020
Official employment	0.028	0.028	0.028	0.017	0.018	0.024	0.028	0.017
Products/services that company creates	0.026	0.029	0.024	0.019	0.019	0.026	0.029	0.019
Company values	0.019	0.031	0.026	0.020	0.021	0.026	0.031	0.019
The image of company as employer	0.025	0.031	0.023	0.023	0.016	0.023	0.031	0.016
Opportunity to gain international experience	0.023	0.028	0.034	0.018	0.018	0.018	0.034	0.018
System of training and development in company	0.023	0.035	0.022	0.022	0.017	0.022	0.035	0.017
Work schedule	0.022	0.034	0.021	0.022	0.022	0.021	0.034	0.021
Salary level	0.028	0.021	0.028	0.021	0.023	0.021	0.028	0.021

Source: Own study based on expert assessment

Table 5 shows the results of the generalized employer's brand assessment using the formula (6).

Table 5

Generalized evaluation of the employer brand R_i

Indicators	ATB	Auchan	METRO	McDonald's	Epicenter K	Fozzy Group
S_i+	0.0314	0.0097	0.0296	0.0464	0.0494	0.0341
Si –	0.0308	0.0509	0.0348	0.0144	0.0103	0.0332
R_i	0.4954	0.8396	0.5405	0.2369	0.1720	0.4934
Ranking of employers by level of brand attractiveness	3	1	2	5	6	4

Source: Own study based on expert assessment

Auchan is the most attractive employer according to the results of the assessment (Ri = 0.8396). The employer's brand is formed among the target students during the educational process, i.e. the image of the company is formed before the job search. This is the most competitive approach compared to other selected companies. The second place is METRO (Ri = 0.5405), which attracts students with the opportunity to get managerial position and experience in international project after the internship. ATB (Ri = 0.4954) is the third most attractive employer, offering the highest salary among all other selected employers. This criterion is one of the most important when choosing your future job. Fozzy Group (Ri = 0.4934) ranks the 4th place in the ranking of employers surveyed. The company offers jobs not only in the retail chain but also in the office team. The competitive advantage of Fozzy Group is a quick opportunity to work and develop according to your future speciality, comparable to other selected employers. McDonald's (Ri = 0.2369) is losing its attractiveness for employment due to the intense workload. The least attractive employer is Epicenter K (Ri = 0.1720), as formed EVP are not aimed at fast and effective attraction of candidates.

Liu (2020) considered the model for assessing the level of competitiveness of employer's EVP, which is based on the Analytic Hierarchy Process (AHP) method. However, the author determined the EVP design and employer's attractiveness only from the perspective of online recruiting. Pawar (2016) proposed the employer's branding process, but this process did not take into account the characteristics and level of individual components development of EVP employer's brand. Shanmuga (2021) considered the comparison of work life balance, job security, leadership style, working environment and in which area employees get more attractive, but the issues of assessing the state development of these EVP components were reserved.

Most scientists in their researches of employer's brand limiting themselves by the taking into account EVP from the perspective of job seekers (Volobaieva et al., 2021) or existing staff (Staniec and Kalińska-Kula, 2021; Tanwar and Prasad, 2016). However, in our opinion, it would be advisable to propose the approach to assessing the employer's brand in terms of individual EVP components development from the point of view of leading experts in this field.

Table 6 shows the categories of employer's brand assessment components.

Table 6

Categories of strong, medium and weak values of employer brand EVP components

Components of the EVP	Strengths	Medium	Weaknesses
Dress code	$0.015<T_{ij}<0.020$	$0.021<T_{ij}<0.025$	$0.026<T_{ij}<0.03$
Social projects of company	$0.019<T_{ij}<0.022$	$0.023<T_{ij}<0.026$	$0.027<T_{ij}<0.03$
Possibility of moving to another city/country	$0.016<T_{ij}<0.022$	$0.023<T_{ij}<0.029$	$0.03<T_{ij}<0.035$
Business rating of company	$0.019<T_{ij}<0.022$	$0.023<T_{ij}<0.204$	$0.025<T_{ij}<0.027$
Office creativity/design, comfortable workplace	$0.015<T_{ij}<0.020$	$0.021<T_{ij}<0.025$	$0.026<T_{ij}<0.031$
Reviews about company on various portals	$0.018<T_{ij}<0.021$	$0.022<T_{ij}<0.024$	$0.025<T_{ij}<0.027$
Rating of the company as employer	$0.017<T_{ij}<0.021$	$0.022<T_{ij}<0.024$	$0.025<T_{ij}<0.028$
Office location	$0.015<T_{ij}<0.200$	$0.021<T_{ij}<0.025$	$0.026<T_{ij}<0.029$
Additional benefits (insurance, transportation, etc.)	$0.02<T_{ij}<0.203$	$0.024<T_{ij}<0.025$	$0.026<T_{ij}<0.027$
Official employment	$0.017<T_{ij}<0.021$	$0.022<T_{ij}<0.024$	$0.025<T_{ij}<0.028$
Products/services that company creates	$0.019<T_{ij}<0.022$	$0.023<T_{ij}<0.026$	$0.027<T_{ij}<0.029$
Company values	$0.019<T_{ij}<0.023$	$0.024<T_{ij}<0.027$	$0.028<T_{ij}<0.031$
The image of company as an employer	$0.016<T_{ij}<0.021$	$0.022<T_{ij}<0.026$	$0.027<T_{ij}<0.031$
Opportunity to gain international experience	$0.018<T_{ij}<0.023$	$0.024<T_{ij}<0.029$	$0.03<T_{ij}<0.034$
System of training and development in company	$0.017<T_{ij}<0.023$	$0.024<T_{ij}<0.029$	$0.03<T_{ij}<0.035$
Work schedule	$0.021<T_{ij}<0.025$	$0.026<T_{ij}<0.029$	$0.03<T_{ij}<0.034$
Salary level	$0.021<T_{ij}<0.024$	$0.025<T_{ij}<0.026$	$0.027<T_{ij}<0.028$

Source: Own study based on expert assessment

Table 7 shows, based on the assessment categories (Table 6), which components of the employer brand assessment are classified as strengths, weaknesses, or average values for each company.

Companies should pay attention to the components marked in dark grey as the most vulnerable aspects of the brand. Improving these aspects will help to reduce negative brand perceptions among potential employees.

Table 7

Heat matrix identifies strong, medium and weak values of employer brand EVP

Components of the EVP	ATB	Auchan	METRO	McDonald's	Epicenter K	Fozzy Group
Dress code	0.022	0.030	0.023	0.023	0.015	0.029
Social projects of company	0.025	0.030	0.025	0.020	0.019	0.025
The possibility of moving to another city/country	0.020	0.035	0.032	0.016	0.016	0.016
Business rating of company	0.026	0.027	0.019	0.026	0.020	0.026
Office creativity/design, comfortable workplace	0.023	0.031	0.022	0.015	0.022	0.029
Reviews about the company on various portals	0.026	0.026	0.027	0.019	0.018	0.026
Rating of the company as employer	0.028	0.026	0.026	0.019	0.017	0.025
Office location	0.029	0.029	0.015	0.016	0.022	0.029
Additional benefits (insurance, transportation, etc.)	0.022	0.027	0.027	0.020	0.020	0.027
Official employment	0.028	0.028	0.028	0.017	0.018	0.024
Products/services that company creates	0.026	0.029	0.024	0.019	0.019	0.026
Company values	0.019	0.031	0.026	0.020	0.021	0.026
The image of the company as employer	0.025	0.031	0.023	0.023	0.016	0.023
Opportunity to gain international experience	0.023	0.028	0.034	0.018	0.018	0.018
System of training and development in company	0.023	0.035	0.022	0.022	0.017	0.022
Work schedule	0.022	0.034	0.021	0.022	0.022	0.021
Salary level	0.028	0.021	0.028	0.021	0.023	0.021

Source: Own study based on expert assessment

Notes:

Strengths | Medium value | Weaknesses

For the components marked in white, it is worth maintaining the current level or investing in further development. Intensifying strengths will help the company to stand out in the labor market and increase its brand attractiveness.

Components with medium values (light grey) also deserve attention to improve competitiveness. In these cases, it is possible to focus on improving conditions that are already at a satisfactory level but still have potential for improvement.

For ATB, the strengths of the employer's brand are the company's business rating, reviews of the company on various portals; the company is rating as an employer, office

location, official employment, products/services created by the company, and salary levels. Weak messages of the employer's brand include the possibility of relocation to another place/country, company values, additional benefits (insurance, workplace, etc.), the opportunity to obtain international experience, training and development system, and work schedule.

The worst component of Auchan's EVP is the level of salary. Other components of the employer's brand are mostly well developed.

The best components of METRO's EVP are the opportunity to obtain international experience, the possibility of relocation to another city or country, official employment, salary level, additional benefits (insurance, etc.), reviews about the company on various portals, and the company's rating as an employer. The worst components of METRO's EVP are the company's business rating, office location, training and development system, and work schedule.

McDonald's has a high level of EVP in the business rating component. The dress code and the company's image as an employer have an average level. Other components have a low level of development in the labor market. Therefore, McDonald's needs to identify the reasons for this situation and improve the competitiveness of the employer's brand to better attract potential employees.

Epicenter K does not have a high-level of EVP. Epicenter K's mid-level employer's brand EVP includes office creativity/design, comfortable workplace, and office location. Other components need to be improved to increase the attractiveness of the employer's brand.

Fozzy Group's employer's brand strengths include dress code, company's business rating, office creativity/design, and comfortable workplace, reviews of the company on various portals, rating of the company as an employer, office location, and additional benefits. Weaknesses of the brand include the possibility of relocation to another city/country, the opportunity to obtain international experience, the training and development system, work schedule, and salary level.

Suggestions for the development of the employer's brand for each company should focus on maintaining strengths, improving medium strengths, and eliminating weaknesses. Such analysis helps to identify the primary problems faced by the companies, improve their image and create more attractive employer's brand.

Conclusions

It has been determined that in order to form an employer's brand, it is necessary to take into account and balance the qualities and characteristics that are important for potential job candidates. Based on the results of the analysis, the list of the main EVP employer's brands, which are important when choosing a job and internship, has been formed.

The research made it possible to use the employer's brand assessment methodology, which is based on the TOPSIS multi-criteria methodology, which includes the following steps:

- allocation of components of EVP employer's brand;
- selection of experts;
- experts assessment of the level of components of EVP employer's brand development on the Likert scale;
- normalization of the obtained estimates;

- construction of decision matrix, in which the rows show the components of the EVP employer's brand, and the columns show the surveyed enterprises;
- determination of the ideal and anti-ideal employer in terms of each component of EVP;
- calculation of the Euclidean distance to determine the degree of each employer compliance with the ideal and anti-ideal solution;
- calculation of generalized assessment of the employer's brand development level;
- establishing the employer's rank according to the generalized assessment of employer's brand;
- categorization of EVP components of the employer's brand into three levels: high, medium, and low;
- Identification of advantages and disadvantages in the employer's brand development according to the results of dividing the EVP components into strong, medium and weak points.

The main advantages of the proposed approach are the ability to calculate a generalized assessment of an employer's brand by the level of EVP components development and understanding the weaknesses and strengths for forming an effective and competitive employer's brand.

This approach can be used to substantiate the directions of employer's brand development that is important for potential job seekers.

The hypothesis has shown that assessing the level of employer's brand development at the surveyed enterprises allows substantiating the directions of its development and forming the desired level of employer's brand for the target audience.

References

Alderfer C. (1969), An empirical test of a new theory of human needs, *Organizational Behavior and Human Performance*, 4(2), pp. 142–175, https://doi.org/10.1016/0030-5073(69)90004-XGet rights and content

Barrow S., Mosley R. (2005), Bringing the best of brand management to people at work. NewYork: John Wiley & Sons Ltd.

Fedulova I., Dzhulai M., Dragan O., Zhukovska V., Mykolaichuk I., Bolotina I., Bezpalko O., Berher A. (2024), Formation of employer's image for representatives of Generation Z in the retail sector in conditions of instability, *Transformation of National Economies in Conditions of Instability* (in Press).

Firsova S., Kozhukhivska A. (2020), Strategic aspects of employer brand management, *Effective Economy*, 9, https://doi.org/10.32702/2307-2105-2020.9.51

Grc.ua: website. (2024), Step-by-step algorithm for building an employer's brand, https://grc.ua/article/24573

Gross J., Cui Z., Wangenheim V. (2023), How to make influencer advertising engaging on Instagram: Emotional storytelling in sponsored posts, *Journal of Interactive Advertising*, 23(4), pp. 388–408, https://doi.org/10.1080/15252019.2023.2211579

HR Liga: website. (2019), How to build a strong HR brand and what it will give you/ https://hrliga.com/index.php?module=news&op=view&id=19855

Jha Sr., Jha Sh. (2015), Leveraging employee value proposition for organizational effectiveness, Available at: http://dx.doi.org/10.2139/ssrn.2586380

Krummel D., Siegfried P., Michel A. (2020), Millenials' employer brand perception in a German retail context, *Journal of Human Resource and Sustainability Studies*, 8, pp. 396–418, https://doi.org/10.4236/jhrss.2020.84023

Liu F., Xiao D., Zhang J., Huang M. (2018), WeChat recruitment characteristics and employer attractiveness from the signal theory perspective–The moderating effect of corporate reputation, *Journal of Guangzhou University (Social Science Edition)*, 17(3), pp. 72–77, https://xb.gzhu.edu.cn/skb/EN/Y2018/V17/I3/72

Liu F. (2020), Analysis of employer value proposition competitiveness in online recruitment, *Industrial Engineering and Innovation Management*, Press Canada, 3, pp. 142–150, https://doi.org/10.23977/ieim.2020.030209

Madanchian M, Taherdoost H. (2023), A comprehensive guide to the TOPSIS method for multi-criteria decision making, *Sustainable Social Development,* 1(1), 2220, https://doi.org/10.54517/ssd.v1i1.2220

Mir I., Salo J. (2024), Analyzing the influence of social media influencer's attributes and content esthetics on endorsed brand attitude and brand-link click behavior: The mediating role of brand content engagement, *Journal of Promotion Management*, 30(1), pp. 1–28, https://doi.org/10.1080/10496491.2023.2251461

Nagpal A., Nagpal G. (2019), Influence of employee value proposition on employer brand. *International Journal of Innovative Technology and Exploring Engineering*, 8(12), pp. 673–676, https://doi.org/10.35940/ijitee.l1163.10812s19

Oberemchuk V., Dehtiar O. (2019), Employer brand and strategic guidelines for its development, *Bulletin of Kamenets-Podolsk National University named after Ivan Ohienko. Series: Economic Sciences*, 14, pp. 344–351, https://doi.org/10.32782/2524-0072/2024-59-28

Palen-Tondel P., Smolbik-Jeczmien A. (2021), Looking for a fulcrum- are preferred work values different for four generation cohorts co-existing in the labour market of Poland? *European Research Studies Journal*, 24(3), pp. 102-119, https://doi.org/10.35808/ersj/2343

Pandita D. (2022), Innovation in talent management practices: creating an innovative employer branding strategy to attract generation Z, *International Journal of Innovation Science*, 14(3/4), pp. 556–569, https://doi.org/10.1108/IJIS-10-2020-0217

Pawar A., Charak K. (2015), Employee value proposition leading to employer brand: The Indian organizations outlook, *International Journal of Management Research & Review*, 5, pp. 1195–1203.

Pawar A. (2016), Employee value proposition: A collaborative methodology for strengthening employer brand strategy, *Journal of Resources Development and Management*, 16, pp. 56–62,

Samoliuk N., Mishchuk H., Mishchuk V. (2021), Gender aspects of the employer value proposition formation on the labor market, *Bulletin of Khmelnitsky National University*, 4, pp. 147–155, https://www.doi.org/10.31891/2307-5740-2021-296-4-24

Seemiler C., Grace M. (2017), Generation Z: Educating and engaging the next generation of students, Wiley Online Library, 22(3), pp. 21–26, https://doi.org/10.1002/abc.2129

Shanmuga P. (2021), A study on strategy of employer branding and its impact on talent management in IT industries, *Elementary Education*, 20(5), pp. 3441–3451, https://doi.org/10.17051/ilkonline.2021.05.378

Staniec I., Kalińska-Kula M. (2021), Internal employer branding as a way to improve employee engagement, *Problems and Perspectives in Management*, 19(3), pp. 33–45, https://doi.org/10.21511/ppm.19(3).2021.04

Tanwar K., Prasad A. (2016), Exploring the relationship between employer branding and employee retention, *Global Business Review*, 17(3), pp. 186–206, https://doi.org/10.1177/0972150916631214

Valène J. (2024), Employee value proposition: The complete guide to building a great EVP, Available at: http://blog.haiilo.com/blog/6-steps-to-build-your-employees-value-proposition/

Volobaieva I., Kravchuk O., Varshava D. V. (2021), The value dimension of the employer brand: Influencing the staff engagement, *Business Inform,* 4, pp. 302–309, https://doi.org/10.32983/2222-4459-2021-4-302-309

Zhovtiak H. (2021), Building employer branding in the labor market, *Eastern Europe: Economy, Business and Management,* 30, pp. 74–78, https://doi.org/10.32782/easterneurope.30-12

Cite:

UFJ Style

Khmurova V., Dragan O., Fedulova I., Dzhulai M., Berher A. (2024), Evaluation of employer's brand of trade and food industry companies, *Ukrainian Food Journal*, 13(4), pp. 809–824, https://doi.org/10.24263/2304-974X-2024-13-4-13

APA Style

Khmurova, V., Dragan, O., Fedulova, I., Dzhulai, M., & Berher, A. (2024). Evaluation of employer's brand of trade and food industry companies. *Ukrainian Food Journal*, *13*(4), 809–824. https://doi.org/10.24263/2304-974X-2024-13-4-13

Characteristics and immunostimulating properties of chemical and microbial vaccine adjuvants

Tetiana Belemets, Viktoria Krasinko, Viktor Stabnikov

National University of Food Technologies, Kyiv, Ukraine

Keywords:

Chemical
Microbial
Vaccine
Adjuvant
β-glucan
Polysaccharides

Article history:

Received 01.02.2024
Received in revised form 12.10.2024
Accepted 30.12.2024

Corresponding author:

Tetiana Belemets
E-mail: Tatiana_Belemets@i.ua

DOI:
10.24263/2304-974X-2024-13-4-14

Abstract

Introduction. Currently, vaccination is the most cost-effective and efficient tool against infectious diseases helping reduce global morbidity and mortality. To increase the effectiveness of vaccines and ensure a stronger immune response in vaccinated people, various components – adjuvants - are added to them. This review focuses on the analysis of the immunological and characteristics of adjuvants of different nature.

Materials and methods. The modern scientific publications of leading periodicals on the topic of the use of adjuvants and their systems were studied: immunostimulating effect, efficiency, review of manufacturers, biotechnological production methods and the possibility of integration into the composition of tested vaccines.

Results and discussion. In contrast to the use of immunopotentiating agents of chemical origin, more and more scientific studies are appearing confirming the advisability of using adjuvants of microbial origin. These are vesicles of the outer membrane of bacteria *Escherichia coli*, *Streptococcus pneumoniae*, *Staphylococcus aureus*, *Bacillus anthracis*, *Enterococcus faecium*; the structural protein flagellin of the flagella of gram-negative bacteria; monophosphoryl lipid A (MPL-A R595), adjuvant systems based on a combination of liposomes from *Salmonella typhi* in the form of nanoparticles using the model antigen ovalbumin, as well as polysaccharides isolated from the fungi *Aspergillus oryzae*, yeast *Saccharomyces cerevisiae*, *Candida albicans*, bacteria *Xanthomonas campestris* and *Bacillus natto*. The polysaccharide β-glucan in the form β-1,3/1,6 is characterized by its appropriate immunogenicity because of its epigenetic properties due to the PAMP structure (β-linked chains), which is recognized by pattern recognition receptors. The most important sources of β-glucan are yeasts *Saccharomyces cerevisiae* and the mushroom *Grifola frondosa*.

Conclusions. Immunomodulation through targeting Toll-like receptors is fundamental in the creation of antigen-agnostic vaccines with epigenetic adjuvants of microbial origin. The polysaccharide β-glucan is a candidate for the status of a new type of immune adjuvant for new vaccines against a large number of diseases due to a wide range of immune responses regardless of the administration form. Such "universal vaccines" could have a significant impact during a pandemic when conventional vaccines that provide an antigen-specific immune response are not available.

Abreviations

APC – Antigen presenting cells
ASC – Apoptosis-associated speck-like protein containing a CARD
BVA – Bovine serum albumin
BMV – Bacterial membrane vesicle
CD – Cluster of differentiation
CpG – DNA section
DAMPs – Danger-associated molecular patterns
DC – Dendritic cells
Dectin – Natural killer (NK)-cell-receptor-like C-type lectin
EV – Extracellular vesicles
GSC – Glioma stem cells
HSPCs – Hematopoietic stem and progenitor cells
IFA – Indirect fluorescent antibody
IFN – Interferon
Ig – Immunoglobulins
IL – Interleukin
LPS – Bacterial lipopolysaccharides
MHC – Major histocompatibility complex
NF-κB – An ancient protein transcription factor
NK – Natural killer
OVA – Ovalbumin
OMV – Outer membrane vesicles
PAMP – Pathogen-associated molecular patterns
PRRs – Pattern recognition receptors
Th –T-helper
TNF – Tumor necrosis factor
TNF-α – Tumor necrosis factor alpha
TLR – Toll like receptors

Introduction

Despite rapid technological progress and global development of medicine, infectious diseases continue to occupy first place (after cardiovascular diseases) among the leading causes of death (Farina et al., 2023). With the beginning of the development and use of effective means of immunoprophylaxis in the world, there has been a significant reduction in mortality rates caused by the most common pathogens (whooping cough, polio, measles, tetanus, and diphtheria) (Karch et al., 2016). These cause-and-effect relationships are confirmed by the analysis of the course of the recent global pandemic of coronavirus infection caused by the zoonotic infectious agent SARS-CoV-2, which was largely overcome thanks to global immunization.

The World Health Organization recently released the first global priority list of endemic pathogens and noted the urgent need to develop vaccines for them. In particular, it includes HIV, tuberculosis and malaria, which annually claim 2.5 million lives worldwide, as well as those well known to mankind - streptococcal infection (the causative agent is group A streptococcus), hepatitis C (the causative agent is an RNA-containing virus belonging to the *Flaviviridae* family) and severe diseases caused by the causative agent *Klebsiella pneumoniae*. According to available statistics, over the past three years alone, the number of

confirmed cases of tuberculosis in Ukraine has increased from 75 to 112 (per 100,000 people) in 2020 and 2023, respectively (Statistics of the World Health Organization, 2024). Therefore, the development of new, scientifically based approaches to the creation of new vaccines and increasing the immunogenicity of existing drugs is a pressing task today.

In modern vaccinology, an adjuvant is an integral component of vaccines, the functionality of which is to stimulate the development of an immune response to an antigen, more intensive formulation of specific antibodies, and activation of the effector functions of T cells (Shah et al., 2017). In general, an ideal adjuvant should have no unacceptable side effects, should be proven safe and stable, should be easy to manufacture, cost-effective, and compatible with a wide range of vaccine components. Potential toxicity has generally remained a major constraint on the development of traditional adjuvants (Mohan et al., 2023).

The problem of adjuvant selecting is due to the widespread use of vaccines created based on inactivated pathogens, purified and recombinant antigens, which have insufficient immunogenicity and require the addition of adjuvants (Utama et al., 2022). However, currently only a small number of immunostimulants are allowed to be used in medical practice, and the approval of new types of adjuvants and their sources is associated with significant restrictions and is long-term, which hinders the implementation of innovations (Facciolà et al., 2022).

The issue of considering and selecting new adjuvants with high efficiency and safety for vaccine production is important and relevant for two main reasons: (a) absolutely all existing vaccination programs in the world require improvement of technologies and development of a new generation of vaccines; (b) there are still no clear generalized data on the mechanisms of action of adjuvants and their systems.

The aim of the present review is to systematize the data of scientific literature sources on the issues of analysis of the composition, structural features, immunological mechanisms of action and stimulating effects caused by the immunoadjuvant properties of immunopotentiating agents and their systems.

Immunological characteristics of chemical adjuvants

The correct selection of adjuvant is critical for immunopotentiating agent-mediated induction of the immune response of different types of vaccines. After all, the mechanism of activation of the immune response, its cellular and humoral links, is more moderate for vaccines without adjuvant. At the same time, vaccines with an adjuvant in their composition contribute to the maturation of a larger number of antigen-presenting cells, polarizing cytokines, multifunctional T-cells, and antibodies.

The scheme of manifestation of immunogenic properties of vaccines with and without adjuvants in their composition is shown in Figure 1.

Even if the antigen and adjuvant components are well matched individually, their mixture may be suboptimal or incompatible, which affects the safety and efficacy of the developed anti-infective agents (Harandi, 2018).

Currently, the following adjuvants are common in immunobiotechnological production: TLR9 agonist CpG1018, TLR4 agonist AS01b and AS04 5, 6, 7 or squalene-based adjuvants such as AS03 (containing α-tocopherol) and MF59 (oil-in-water nanoemulsion containing squalene). The list of adjuvants approved for use in licensed vaccines also includes Tween 80 and Span 85 (both are surface-active substances). In general, the most commonly used immunopotentiating agents are oil-in-water emulsion-based adjuvants (Chegrynets et al., 2021) and aluminum salts (Galson et al., 2016).

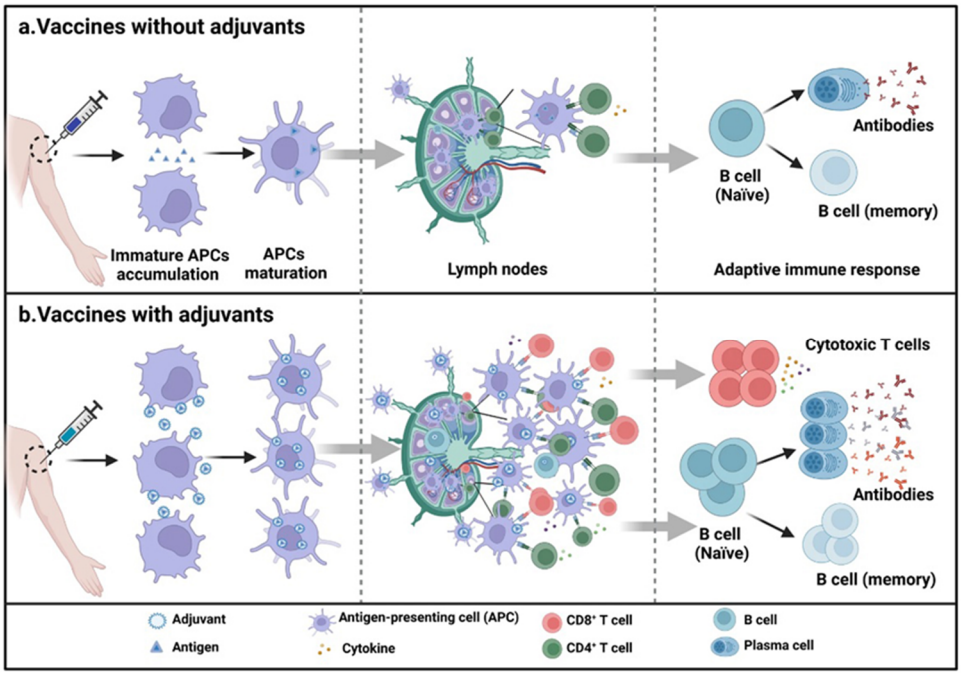

Figure 1. Generalized scheme of step-by-step manifestation of immunogenic properties of vaccines: a. vaccines without the use of adjuvants; b. vaccines with adjuvants in their composition (Adopted from Zhao et al., 2023)

Adjuvant based on an oil-water emulsion that has been widely used in animal experiments is Freund's adjuvant in two possible forms: incomplete (IFA) and complete (CFA). The latter also contains inactivated cells of *Mycobacterium tuberculosis* bacteria to enhance the immune effect by attracting macrophages and other immune cells to the injection site (usually used in primary immunization).

A typical CFA compositions comprises 1 mg *Mycobacterium tuberculosis*, heat killed and dried, with 0.85 ml paraffin and 0.15 ml Arlacel® 83 (a mixture of oleic, palmitic, stearic and linoleic acids from 2-(3,4-dihydroniglyceride)) (Malik et al., 2018). The active component derived from *Mycobacterium tuberculosis* is a dipeptide, N-acetylmuramyl-L-alanine-D-isoglutamine (MDP). MDP is a molecule that activates macrophages and dendritic cells via an oligomerization domain, which binds nucleotides containing 2 (NOD2) and skeletal elements of the bacterial cell wall. In addition to stimulating inflammation, this immunopotentiation agent causes aggregation and precipitation of soluble protein antigens to form particles that facilitate their efficient uptake by antigen-presenting cells (APCs). CFA also positively influences the Th1 cell subpopulation, the synthesis of IgG immunoglobulins (as opposed to the synthesis of IgM class), suppresses the induction of tolerance and promotes delayed hypersensitivity reactions. However, due to toxicity and adverse reactions, the use of this adjuvant is unacceptable for vaccines used for human immunization (unlike IFA, which exhibits less toxicity and is therefore suitable for clinical use) (Tadepalli et al., 2017).

Another squalene-based immunological adjuvant, MF59, has been associated with increased helper T-cell activity and higher immunoglobulin concentrations, particularly IgG1 and IgG2a isotypes. MF59 has also been reported to have the ability to induce a Th1 response in CD8+ T-cells in healthy people of different age groups (Yang et al., 2020).

In studies (Clark et al., 2009) it was shown that MF59 induces seroconversion (production of primary antibodies in the blood serum) and seroprotection (titer of protective antibodies) 21 days after the administration of the first vaccine against influenza A/H1N1. Moreover, the same vaccine produced higher rates of seroprotection and seroconversion after 21 and 42 days with adjuvant than without adjuvant. As for safety, mild to moderate reactions have been reported, including headache, muscle pain, and bruising at the injection site. However, none of these adverse reactions lasted more than 72 hours.

Among the existing invasive immunobiological products, squalene-based vaccines (AS03) are the leaders, with more than 20 million doses administered worldwide and biosafety results ranging from "acceptable" to "excellent" (Reed et al., 2009).

Several adjuvant formulas containing squalene and other compounds have already been tested: GLA-SE (an oil-in-water emulsion with squalene) and GLA (includes a glucopyranosyl lipid adjuvant) (Desbien et al., 2015). The GLA-SE formulation has been shown to induce strong signaling through the TLR-4, caspase, IL-18 and IFN-γ pathways, resulting in a Th1 response. It is currently used as an adjuvant in tuberculosis vaccines and is characterized by strong antibody responses with peak levels after the second immunization, and mild side effects including headaches and fatigue (Coler et al., 2018).

Studies in humans who received influenza vaccine with the squalene-based AS03 adjuvant showed long-lasting histone modifications and epigenetic changes in monocytes for up to 21 days after vaccine administration (Wimmers et al., 2021). It was found that epigenetically changed monocytes are more effective because they retain increased levels of chromatin of antiviral interferon regulatory factors (IRF) loci, including key antiviral immune regulators – RIG-1 (DDX58), IRF1, IRF8 and a number of genes stimulated by interferon of dengue fever and Zika virus. This is evidenced by a decrease in viral load after vaccination and a correlation of viral titers with the expression levels of interferon regulatory factors.

Now, given the lack of unanimous scientific thought, the first aluminum-based adjuvants available to mankind (aluminum hydroxide or aluminum alum) do not lose their popularity The three most commonly used and approved salts in 146 vaccines for preventive diseases are aluminum hydroxide, aluminum phosphate, and potassium aluminum sulfate (Kooijman et al., 2022). However, despite its widespread use to effectively potentiate the immune response, special care should be taken to ensure that the type of aluminum adjuvant does not affect the stability of the antigen composition (Agarwal et al., 2020).

The mechanisms of action of aluminum hydroxide and aluminum-based adjuvants in general include formation of aggregates (ensures continuous release of antigens), formation of partial structures (promotes phagocytosis of APCs) and induction of local inflammation (via the NLRP3 inflammasome), which causes the attraction and activation of macrophages, major histocompatibility complex (MHC II) molecules and antigen presentation. Inflammasome activation induces the secretion of mature IL-1 and IL-18 by dendritic cells, differentiation of Th2 cells, promoting B cell activation and subsequent antibody production (primarily IgG). However, studies have reported NLRP3-independent antibody production pathways and a non-phagocytic mode of action of aluminum hydroxide (Ho et al., 2018).

The effectiveness of aluminum salts is due to the creation of a "depot" of antigen in the place of administration, slowing down its release (it has the ability to be absorbed, which extends the time of contact of the vaccine with the immune system), a strong humoral response with weak induction of a cell-mediated immune response, and strengthening of phagocytosis. To prevent the development of an abscess (possible with subcutaneous injection), the introduction of vaccines with aluminum salts should be carried out exclusively intramuscularly. In general, this type of adjuvant allows the body to increase the titer of antibodies against pathologies of viral or bacterial origin (Powell et al., 2015).

However, it should also be noted that aluminum hydroxide is considered a genotoxic substance, which, when present in excess in the body, can lead to irreversible changes, impair memory, lead to mental disorders and Parkinson and Alzheimer's diseases. At the same time, there is a possibility of increased development of atherosclerosis and epilepsy (Pulendran et al., 2021).

Confirmation of possible negative consequences of using aluminum salts in vaccines was noted back in the early 2000s (Gherardi et al., 2001; Rivas et al., 2005). A number of studies have confirmed the formation of long-term deposits at the injection sites of vaccines containing aluminum salts, which can persist for decades after the vaccine, is administered (macrophagic myofasciitis). The depot effect was initially thought to be important for adjuvant activity, but this was later disproved by the demonstration of their adjuvant action even after depot withdrawal. At present, any harmful pathophysiological effect of long-term aluminum deposition in tissues and associated macrophage myofasciitis remain a matter of debate.

A new TLR7/8 agonist, a synthetic small molecule adjuvant 3M-052, has recently emerged, inducing potent antigen-specific immune responses by stimulating Th1 cells, antibodies and plasma cells (Arunachalam et al., 2020). Despite its effectiveness, the mechanism of the immunostimulating action of 3M-052 remains insufficiently studied. Current experimental data based on PLGA nanoparticle or gallium adjuvants primarily assess peripheral immune responses in the blood of non-human primates (NHPs), but have little coverage of responses occurring in the lymph nodes where immune responses are initiated. To date, there are no studies directly comparing the immune responses induced by 3M-052 vaccines with those elicited by live virus vaccines that provide long-lasting antibody production (Kasturi et al., 2020).

In support of the above, a molecular atlas of immunity to adjuvanted and live attenuated vaccines was studied in experimental mice using flow cytometry, single-stranded RNA (scRNA-seq) and single-cell sequencing ATAC (scATAC-seq) to create a comprehensive cellular, transcriptomic and epigenomic maps of the innate immune response in dLN at early and late stages after immunization with antigen with adjuvant YF-17D or 3M-052-Alum (Lee et al., 2020). Immunization with antigen plus 3M-052/Alum was found to induce activation and recruitment of myeloid cells into dLNs with a robust humoral response in mice at 14 and 28 days post-immunization, indicating high titers of IgG, IgG2c, and IgG. Immunization with 5 μg 3M-025-Alum significantly enhanced germinal center and T-follicular helper cell responses and increased antibody titers compared to alum alone as an adjuvant. Immunological response and possible effects of chemical adjuvants is given in Table 1.

Table 1

Immunological response and possible effects of chemically synthesized adjuvants

Immunological response	Possible effects	Reference
Chemically synthesized adjuvants		
Aluminum salts; Activation pathway: PRR		
Depot effect; increased presentation of antigen by antigen-presenting cells (APC) and production of IgG1, IgE; induction of danger-associated molecular patterns (DAMPs) production, activation of pattern-recognition receptors (PRRs) innate immune pathways, leading to production of IL-1β cytokines; activation of NLRP3 inflammasome, leading to production of IL-1, IL-18 with subsequent local inflammation and recruitment of APC.	Low protective efficacy; potential side effects; potential neurotoxicity; allergic reactions; may contribute to the development of ASIA (autoimmune/ inflammatory syndrome)	Moni et al., 2023
LNP (Lipid nanoparticles); Activation pathway: TLR 4		
Enhancement of humoral and cellular immunity to proteins and polysaccharide antigens; generation of Th 1, Th 2 or Th 1/Th 2 phenotypes, Th 1/Th 2 switch; modulation of generation of CD4+, CD8+ mediated immune responses is possible; transfer of PAMP-associated or specific immunomodulatory molecules, liposomes; can activate DU, macrophages and NK cells; greater influence of antigen on APC after vaccination; prolongation of the half-life of antigens in the blood.	Comprehensive immune protection; protection of antigen from degradation and increase of its stability in the body; potential side effects	Owen et al., 2021
Oil-in-water emulsion adjuvants		
MF59 (squalene-based oil-in-water emulsion); Activation pathway: MyD88, TLR 4,7,9		
Activation of myeloid cells (macrophages, DC), which respond by producing chemokines CC-chemokine ligand 2 (CCL2), CCL4, CCL5 and CXC-chemokine ligand 8 (CXCL8) also known as IL-8, which in turn recruit neutrophils, eosinophils, DC to the injection site; may work through NLRP3-independent activation pathways – ASC and TLR, MyD88; Th2-biased immune response and weak induction of Th1 response; induction of antibody response via MyD88-dependent mechanism; induction of transcriptional changes in muscle cells.	Dual function: antigen delivery and immune stimulation; side effects at the injection site; erythema and induration are possible	Zhao et al., 2023; Mancini et al., 2020

Immunological response	Possible effects	Reference
AS03 ("Adjuvant System 03" containing DL-α-tocopherol and squalene in an oil-in-water emulsion); Activation pathway: My-D88, TLR4,7,9		
Activation of NF-κB, inducing the secretion of cytokines and chemokines in muscles and lymph nodes, promoting the migration of innate immune cells; increased magnitude breadth of antibody and CD4+ T cell responses, resulting in increased protection through antibody production and higher levels of memory B cells; increased serum levels of IL-6, IP10 (CXCL10), transcriptional signatures of interferon signaling, antigen processing and presentation in DCs, monocytes and neutrophils.	Proven antioxidant and immunostimulating properties of α-tocopherol; strong immune response (after 6 months of vaccination); subjective intolerance	Facciolà et al., 2022; Mancini et al., 2020
CFA (Compete Freund's adjuvant with heat-killed cells of *Mycobacterium*); Activation pathway: TLR 2,4,9		
May lead to potentiation of IgG and IgA production; induction of predominantly Th2-biased response due to the "depot" at the injection site; stimulation of plasma cells producing antibodies; auxiliary activity of IFA is based on continuous release of antigen at the injection site; increase in antigen lifespan and strong local stimulation of innate immunity with phagocytosis, recruitment and infiltration of leukocytes; production of cytokines.	Long-term local inflammation; severe side effects; possible ulceration at the injection site; toxicity	Mohan et al., 2023

Thus, despite the fact that chemical adjuvants are now widely used in vaccine preparations, they have a number of significant drawbacks. In particular, aluminum salts are recognized as genotoxic substances with potential mutagenic and carcinogenic effects and the ability to provoke mental disorders, impair memory, cause Parkinson's and Alzheimer's diseases, and increase the likelihood of developing epilepsy and atherosclerosis. Finally, their weak induction of mucosal immunity also has a limiting effect on the development of vaccination efficacy (Eldred et al., 2006; Exley et al., 2014). CFA (Freund's adjuvant), despite the proven stimulation of a powerful immune response, is characterized by toxicity, leading to the formation of granulomas, inflammation at the injection site, due to the high content of waste oils that are not subject to biodegradation (Burny et al., 2017). Emulsion adjuvants are considered toxic for conventional human prophylactic vaccines and have an incomplete immune response after immunization. Injections of MF59-adjuvanted vaccine stimulate extracellular ATP release, the inhibition of which by local injections of apyrase may not enhance, but, on the contrary, weaken the immune response (Kim et al., 2020). Thus, the search for adjuvants of biological origin is a promising alternative direction for the selection of immunopotentiating agents.

Immunological characteristics of microbial adjuvants

Adjuvants of microbial origin are currently being proposed for use in vaccinology (Abbasi et al., 2022; Chang et al., 2021; Durães et al., 2021; Verma et al., 2023). For example, the adjuvant effect of spherical nanometric outer membrane vesicles (OMV) of Gram-negative bacteria *Escherichia coli* on antigen-specific priming of T cells was studied by Lee with co-authors (2021). Parmaksız et al. (2023) proposed an adjuvant system based on a combination of *Salmonella typhi* nanoparticles porins in the form of nanoparticles with liposomes (cationic and neutral) using the model antigen, ovalbumin. Taleghani and colleagues (2019) in one of the latest studies considered the possibility of using monophosphoryl lipid A (MPL-A), isolated mainly from the genetically engineered *Salmonella minnesota* strain R595, as the historically first TLR ligand approved for use as an adjuvant in the creation of human vaccines.

Flagellin, a structural protein of the flagella of gram-negative bacteria, is considered to be an efficient adjuvant. When entering the body, most bacterial flagellin molecules remain in the flagella, but some are released into the environment, allowing them to be recognized by the immune system through Toll-like receptors on the surface of immune cells (Hajam et al., 2017).

Confirmation of the presence of epigenetic characteristics of flagellin is given in the work (Murthy et al., 2014), according to the results of which, the hyperconserved N and C ends of flagellin can be recognized by molecules of the Toll-like receptor of immunocompetent cells, in particular TLR-5 (expressed on macrophages, lymphocytes, and dendritic cells). This recognition of TLR-5 by flagellin results in signaling through MyD88-dependent and MyD88-independent pathways, resulting in the induction of transcription factors AP-1, NF-κB, and IRF3, which induce the production of cytokines and chemokines. These proteins, in turn, recruit (direct) dendritic cells, as well as T and B-lymphocytes to the lymph nodes. In addition, flagellin can promote a strong antigen-specific CD4+ T cell response by interacting with TLR-5 on CD11c+ cells. The result of this interaction is a high titer of antibody formation, demonstrating the potential of flagellin as a protein adjuvant (Bates et al., 2019).

As an adjuvant, flagellin is used by co-administration with the main antigen and through fusion proteins obtained by adding epitopes associated with the flagellin molecule. It has been proven that physical binding of vaccine antigens to flagellin creates a significantly more powerful vaccine than simple mixing with the antigen. It has already been determined into which specific areas of the flagellin molecule epitopes should be inserted in order to maximize antibody titers, but conclusions are not yet available (Huleatt et al., 2018).

For example, optimal antibody titers were obtained by introducing a hemagglutinin (HA) epitope into the hypervariable region of flagellin (Song et al., 2009). To achieve the set goals, an approach was developed to bind agonists of the Toll-like receptor (TLR-5) flagellin to the self-sufficient protective subunit (globular head) of HA. The globular head domain includes most of the neutralizing epitopes of HA in the context of the flagellin fusion protein and stably refolds to precisely form these conformationally sensitive epitopes. It was found that the R3 vaccine (configuration – both ends of the globular head of HA are linked to flagellin) of several H5 subtype vaccines (based on the influenza virus A/Vietnam/1203/2004 (VN04)), in which the D3 domain of the flagellar is replaced by the HA head, is the most effective in eliciting protective HAI titers and protecting mice from disease and death.

However, in a study (Delaney et al., 2010), insertion of the L1R epitope into the hypervariable region not only does not cause the production of antibodies, but also, if used

specifically at the N-terminus of flagellin, can lead to the formation of antibodies capable of interacting with native L1R.

Lin et al. (2016) showed that insertion of epitopes into the C-terminus of flagellin can induce signaling through NLRC4 and NAIP5, leading to CD8+ T cell responses against tumor cells. The demonstrated diversity of immune system responses experimentally confirms the versatility of flagellin as an adjuvant with different target orientations depending on the area of antigen administration. However, further fundamental and applied scientific research is required to reveal the full potential of flagellin.

It should be noted that from a practical point of view, flagellin as an immunopotentiating agent has a number of safety advantages: only low doses are required to achieve effectiveness; no toxicity when administered intranasally in animal experiments. Thus, results have been obtained confirming the safety of using fused flagellin proteins as an adjuvant in vaccines against influenza A H1N1, since all existing systemic side effects in some research groups of people stabilize after 4 days of rest, and in others after taking non-steroidal anti-inflammatory drugs (Treanor et al., 2010).

Among the adjuvants of microbial origin, outer membrane vesicles (OMV) of gram-negative bacteria, in particular *E. coli*, stand out due to their powerful inflammatory potential and ability to stimulate the innate immune response. The immune response induced by spherical nanometric vesicles (proteoliposomes) is provided by lipopolysaccharides (LPS), peptide glycans, phospholipids, proteins, DNA, RNA, as well as virulence factors such as exotoxins.

The rationale for using bacterial membrane vesicles (BMVs) in vaccines is due to the presence of pathogen-associated molecular patterns (PAMPs) to induce strong immune responses, as well as the ability to present proteins of various sources ranging in size from 50 to 200 nm for efficient processing and delivery of antigens (they can be easily captured by immune cells). There are already a number of experimental BMV-based vaccines against a wide range of pathogens (Krishnan et al., 2022). Thus, BMVs can accumulate and transport nutrients, virulence factors and toxins, while neutralizing antibacterial molecules produced by the host organism. BMVs express bacterial surface antigens, which can be an important vaccine target (Mehanny et al., 2022).

Overall, bacterial vesicles have attracted increased attention as a powerful and versatile vaccine platform, as they are essentially immunostimulants capable of activating both innate and adaptive immune responses (CD4+ T-cell and B-cell responses) simultaneously. This mechanism is due to the recognition of LPS and other molecules on membranes by TLR molecules and the complement system, which leads to the recruitment of APC cells. Activated macrophages produce proinflammatory cytokines such as TNF-α and IL-6 and induce adaptive immune responses by enhancing the expression of the major histocompatibility complex class II (MHC-II) molecule HLADR, the costimulatory molecules CD80 and CD86, and intercellular adhesion molecules. Co-stimulation with molecules present in OMVs results in a more powerful response than that elicited by LPS alone. In this case, OMVs have the ability not only to induce the maturation of dendritic cells, which leads to enhanced capture of the antigen molecule and its presentation for the development of an adaptive immune response, but also to activate B cells to produce IgA, IgM, IgG and other antibodies (Zingl et al., 2020).

The studies (Buschmann et al., 2021; Elsharkasy et al., 2020; Vader et al., 2016) confirm the ability of BMV to induce long-term humoral and cellular immune responses when used in vaccines. These properties may be explained by the high density of pathogen-associated molecular patterns (PAMPs) on bacterial vesicles, which serve as potent immune stimulants.

Because BMVs carry a large number of antigens that can induce an immune response in vivo, a variety of BMVs including OMVs (outer membrane vesicles) and EVs (extracellular vesicles) are produced using wild-type or bioengineered bacteria (Treanor et al., 2010). Thus, a cloning system based on *Escherichia coli* and OMV derivatives fused with the outer membrane lipoprotein I (OprI) of *Pseudomonas aeruginosa* is currently in widespread use. This system has shown immunogenicity by stimulating dendritic cells/macrophages, demonstrating potential adjuvant properties.

Later, Gan with co-authors (2021) proposed the use of bacterial membrane vesicles OMV produced by gram-negative bacteria *Escherichia coli* and EV obtained from gram-positive bacteria (*Enterococcus faecium, Streptococcus pneumoniae, Staphylococcus aureus,* and *Bacillus anthracis*) as delivery systems for antigens in the fight against infections caused by bacterial pathogens. However, this use of OMVs and EVs as an adjuvant obtained using a bacterial producer also has its drawbacks. The problem is caused by the difficulty of maintaining the bacterial membrane due to the relative fragility of the structure, which can affect the uptake by antigen-presenting cells. Therefore, to solve this problem, it was proposed to coat MVs on nanoparticles to increase in vivo stability and circulation time (Gan et al., 2021).

In study of Afrough et al. (2020), the authors developed a vaccine candidate based on the fusion of PorA from serogroups A and B (*Neisseria meningitidis*) in combination with OMV, testing it in laboratory animals and comparing the efficacy of OMV with commonly used Freund's adjuvant. The elicited immune response in mice was assessed by enzyme-linked immunosorbent assay (ELISA) and serum bactericidal activity (SBA) assay. A significantly higher titer of bactericidal antibodies was observed in mice groups in response to injections with PorA+OMV compared to the groups receiving PorA+Freund's adjuvant. In this case, the recombinant PorA protein with OMV adjuvant additionally induces antibacterial antibody responses against capsular polysaccharides of serogroups A and B.

There is currently insufficient data on the specific effects of BMV and OMV adjuvants present in a number of vaccines against bacterial pathogens on the human immune system. The only licensed and widely used multicomponent meningococcal vaccine against *Neisseria meningitidis* is 4CMenB ("Bexsero") with OMV adjuvant in its composition (Masforrol et al., 2017).

Studies in recent years have shown the protective ability of the meningococcal vaccine containing OMVs against *Neisseria gonorrhoeae*, causative agent of gonorrhea, species close related to *Neisseria meningitidis*, a Gram-negative bacterium that can cause meningitis (Semchenko et al., 2019). Using enzyme immunoassay, it was shown that, as response to Bexsero (with OMV adjuvant) vaccination, human anti-gonococcal NHBA antibodies were generated providing additional cross-protection against gonorrhoea (Semchenko et al., 2019).

The potential impact of the outer membrane vesicle (OMV) meningococcal B vaccine, MeNZB, on specific immunogenicity and cross-protection against gonorrhoea were confirmed in study of Petousis-Harris et al. (2019).

Newly developed vaccines with OMV adjuvant in their composition have already begun to move to the clinical trial stage due to their preliminary demonstrated safety and efficacy. Thus, vaccines against allergens and shigellosis (the causative agent is *Shigella flexneri*) are in phase I clinical trials, and vaccines against influenza are in phase II. When administered intranasally, these immunobiological preparations induced the production of antibodies with very minor side effects, which emphasizes the potential of OMVs as immunopotentiating agents (Daleke-Schermerhorn et al., 2014; Martiñón et al., 2019).

However, the use of OMVs as adjuvants poses several additional challenges regarding their mass production, as OMV production is a complex procedure due to the need to control

the endotoxin content, which may be responsible for stimulating excessive inflammation. In particular, the lipopolysaccharide (LPS) dose needs to be carefully controlled, as OMVs with low LPS are less effective adjuvants, while excessive amounts of LPS may cause toxic effects (Martiñón et al., 2019).

Bacterial LPS and TLR4 ligands in vaccines are able to induce an immune response in the form of persistent epigenetic modification in bone marrow and myeloid progenitor cells with an increase in myeloid enhancers. This result is explained by the recognition of the TLR4 receptor by lipopolysaccharides and its transmission of immunological signals through the MyD88- and TRIF-dependent pathway (de Laval et al., 2020).

LPS-mediated resistance to infections is induced by increased leukocyte recruitment and attenuation of inflammatory processes. The manifestation of a stable immune response to bacterial antigens in the test mice after their vaccination using LPS is also shown (Rusek et al., 2018). It was found that transplanted hematopoietic stem and progenitor cells (HSPCs) from the bone marrow of LPS-exposed mice exhibit the ability to protect recipient mice from infectious diseases caused by *Pseudomonas aeruginosa*, demonstrating a reduced bacterial load in the spleen and liver (de Laval et al., 2020). However, despite existing studies on the immunostimulatory effects of LPS as an adjuvant, its use in clinical practice remains limited due to potential toxicity in humans (Hernandez et al., 2019).

Toll-like receptors as new generation adjuvants

According to previously established scientific ideas, immunological memory is a limited antigen-specific memory and is exclusively a privilege of the adaptive immune system, due to the work of lymphocytes. However, the description of specific memory in invertebrates, the system of acquired resistance in plants, antigen-specific memory in natural killer (NK) cells, as well as heterologous protection (provided by vaccines against smallpox, measles, and BCG) are evidence of the existence of an innate form of immune memory (Sánchez-Ramón et al., 2018).

Now, to reflect the possibility of the innate link of immunity to "remember"/adapter the first contact with a pathogen in order to create a robust immune response upon repeated exposure to a similar or dissimilar microbial stimulus, the term “trained immunity” has been proposed. It is noted that the molecular mechanisms that can form the basis of trained immunity include epigenetic, mechanical and functional reprogramming of progenitor cells of the myeloid line of hematopoiesis and the cell line of the innate link of immunity (Palgen et al., 2021).

According to evidence (Pulendran et al., 2021), the main functional task of adjuvants and their systems was previously attributed to enhancing the immunogenicity of vaccines by specifically targeting cells of the innate immune system. However, currently a number of other scientific works (Biering-Sørensen et al., 2017; Bruxvoort et al., 2022; Walk et al., 2019) show results indicating the actual possibility of pre-training the innate immune system, which can provide heterologous protection against secondary infection.

In addition, the ability of some immunopotentiating agents to induce persistent epigenetic reprogramming of the innate immune system in order to create improved resistance against pathogens is also emphasized. Such apotheosis testifies to the promising development of epigenetic adjuvants for the creation of new generation vaccine preparations.

Thus, it was confirmed the possibility of using transmembrane receptors of innate immunity (TLR) to provide longer-term protection against the next infectious agents due to the strengthening of innate immunity (Mifsud et al., 2014). At the same time, the FDA (Food and Drug Administration) in the USA has already approved several agonists of Toll-like

receptors for use as part of immunobiological drugs and recognized them as safe on a global scale.

Confirmation of heterologous protection (antigen-specific way) against a number of unrelated infectious agents is the results of epidemiological studies of immunization with measles vaccines (Aaby et al., 2010), BCG and OPG (Biering-Sørensen et al., 2017). The validity of these claims as a preventive measure against the disease of COVID-19 is described in the work (Bruxvoort et al., 2022), but is currently still at the stage of clinical trials.

Recent studies using Toll-like receptor (TLR) ligands have shown that antigens associated with their ligands can produce extremely high levels of antibodies and a rapid immune response. From the point of view of influencing the immune system cells, epigenetic adjuvants are able not only to stimulate persistent T- and B-cell responses, but also to provide additional protection against a wide range of pathogens by training innate immunity, which until recently was considered impossible. Therefore, when choosing an immunopotentiating agent for the creation of new vaccines, it is most appropriate to take into account its agonistic properties of Toll-like receptors and prospects for pharmaceutical use.

For example, it was proposed a description of the concept of "learned" (trained) immunity, in terms of which the probability of acquiring new properties by the cells of the innate immunity increases due to metabolism and epigenetic reprogramming (Wimmers et al., 2021). Evidence for this description is provided in the paper (Lee et al., 2022), which confirms the ability of selected vaccine adjuvants to induce epigenetic imprinting of innate immune cells and, as a result, to obtain a long-lasting state of antiviral protection of vaccinated individuals against a wide range of other pathogens. Currently, any precise parameters, basic mechanisms of the innate reprogramming process and its impact on protection against a wide range of pathogens remain poorly understood. In this regard, the issue of a more in-depth study of the influence of previous vaccination on the secondary immune response during revaccination in the context of adjuvants is relevant.

The publication (Ciarlo et al., 2020) reports on the analysis of the effect of trained immunity against a wide range of bacterial infections caused by *Listeria monocytogenes*, *Escherichia coli*, *Staphylococcus aureus*, *Citrobacter rodentium* and *Pseudomonas aeruginosa*. Trained immunity in laboratory mice was obtained by intraperitoneal injection of 1 mg of adjuvant - zymosan (a yeast cell wall preparation rich in β-glucans) 3 and 7 days before infection. The degree of activity of trained immunity was determined by the number of monocytes formed in the bone marrow, cytokine production (enzyme immunoassay), bactericidal blood analysis, and chromatin immunoprecipitation. Mice with pre-trained immunity showed an increase in the number of cytokines, leukocytes and phagocytes in blood samples, a decrease in the severity of diseases and better survival rates, combined with an overall decrease in bacterial load. A group of mice with "trained immunity" survived after infection with *Listeria monocytogenes*, the causative agent of listeriosis, while the entire control group died within 5 days after infection. The bacterial pathogen was not detected in the blood of "trained mice" on the 2nd and 3rd days after infection, while up to 10^5 colony-forming units (CFU)/ml was determined in the blood circulation of the control group. Immunological protection of mice with "trained immunity" is due to increased production of cytokines (IL-1β) in combination with stimulation of myelopoiesis in the bone marrow.

The possibility of inducing trained immunity due to the simultaneous use of bacterial LPS and fungal β-glucan was shown (Owen et al., 2021). This confirms the potential of epigenetic adjuvants to influence the innate immune system.

From a chemical point of view, β-glucans, as carbohydrate polymers, are characterized by various structural variations, conformations, and physicochemical parameters that directly affect their physiological functions. Variations in the structure of β-glucan directly depend

on the source of the polymer (fungi, yeast, bacteria, plant, and grain crops), as well as on the type of glycosidic bond, the degree of its branching and polymerization (Wang et al., 2017).

Carbohydrate polymers of the β-glucan type were studied as auxiliary substances in the composition of anti-infective vaccines and immunomodulators in anti-cancer therapy. First, this interest is due to the possibility of regulating the immune response due to the stimulation of the innate and adaptive links of immunity, as well as the possibility of increasing the immunogenicity of vaccines (Colaço et al., 2023).

The effectiveness of β-glucans as epigenetic adjuvants is due to the presence of a PAMP structure (β-linked pathways) that can be recognized by PRRs – Dectin-1 and CR3. The mechanism of immunostimulating effect of polysaccharide (β-1,3/1,6 glucan) can be explained by its pronounced selectivity in relation to specific receptors on the surface of macrophages (Dectin-1, Complement 3, Lactosylceramide, etc.), which can bind only to unbranched section of the β-glucan molecule. The activation of macrophages caused by this leads to the implementation of a number of processes of immune protection of the body - activation of the phagocytic functions of macrophages, increased induction and release of cytokines, epidermal cell growth factors, and angiogenesis (De Marco Castro et al., 2021).

β-glucan-activated macrophages and monocytes induce a metabolic shift via the Dectin-1 receptor toward aerobic glycolysis. Such changes in cellular metabolism from oxidative phosphorylation to aerobic glycolysis (the «Warburg effect») are crucial for the induction of β-glucan-induced trained immunity. β-glucan training of monocytes induces a resetting of cellular metabolism that modulates epigenetic programming of metabolic genes (Elder et al., 2017). According to (Dos Santos et al., 2019; Novakovic et al., 2016), the ability of β-glucan to affect "trained immunity" is associated with metabolic rearrangement, induction of transcription factors associated with aerobic glycolysis, and activation of the cholesterol synthesis pathway.

The adjuvant properties of β-1,3-D-glucans isolated from yeast and fungi in experiments on laboratory rats were demonstrated in (Han et al., 2020). It is noted that the polysaccharide from the walls of *Saccharomyces cerevisiae* increases the production of TNF-α in alveolar macrophages, increases the oxidative burst of leukocytes, and increases their antimicrobial activity.

Simultaneous application of a mixture of β-glucan and LPS activates the induction of myeloid reprogramming at the level of progenitor cells was shown (Mitroulis et al., 2018; Saeed et al., 2014). β-Glucan (as a component of the cell wall of fungi) binds Dectin-1 and the membrane protein CLEC7A with further modulation of this myelopoiesis in mouse bone marrow at the level of hematopoietic stem cells and progenitor cells, which persists up to 28 days after immunization.

Currently, the use of yeast β-glucan as a platform for antigen delivery targeting TLRs of antigen-presenting cells is promising. In the work (De Smet et al., 2014), such a platform is highly purified empty and porous shells of S. cerevisiae cell walls obtained by stepwise extraction with alkaline and acid solvents. It is characterized by β-1,3-linked glucopyranosyl residues, a smaller number of β-1,6-linked branches, which after alkaline and acid treatments consist mainly of β-1,3-glucan (> 85%), chitin/ chitosan (2%) and are free of proteins, lipids (1%) and mannans. If the antigen enters with a delivery platform made of β-glucan, the interaction of immune cell receptors with membrane receptors Dectin-1 and CR3 is noted. Binding of β-glucan to Dectin-1 on macrophages and dendritic cells induces their activation, maturation, and increases the production of proinflammatory cytokines such as TNF-α, IL-6, IL-2, IL-10, and IL-23. The delivery platform additionally stimulates dendritic cells to produce cytokines IFN-γ and IL-17 (observed when interacting with TLR receptors) (Mentrup et al., 2022).

Yeast β-glucan antigen delivery platforms have been used in (Huang et al., 2012; Hurtgen et al., 2012; Soto et al., 2012) for oral and parenteral targeted delivery (peptide/protein antigens, siRNA/DNA, and nanoparticles) in studies on laboratory animals. Positive results from the use of such yeast cell wall particles for the delivery of pathogenic DNA are described in the work (Mirza et al., 2017). The authors designed a delivery system using electrostatic interactions and presented an encapsulation strategy that provides high capacity and delivery of nucleic acids in combination with the oral bioavailability of β-glucan pures with their inherent ability to affect APC cells. The disadvantage of this technology is cytotoxicity caused by a high concentration of polymers.

The solution to the above-mentioned problem is described in the work (Hwang et al., 2018) and is carried out due to alternating stages of hydration and lyophilization in the process of loading antigenic material into the middle of β-glucan shells. Using this approach, the delivery technology platform has been extended to enable multi-complex co-delivery of TLR adjuvants and/or siRNA (in separate layers around the antigen core) to improve vaccine efficacy and safety (Soto et al., 2023).

The principles described by Soto were used in the study by De Smet et al. (2013) to produce β-glucan particles (GP) for oral immunization with GP-OVA to further evaluate the biocompatibility and efficacy of this model. Studies of the interaction between GP-OVA and intestinal epithelial cells were carried out "in vitro" and "in vivo". It was established that oral immunization with GP-OVA causes persistent humoral responses in the epithelial cells of the small intestine (mucosal IgA and serum IgG responses), as well as the release of cytokines and chemokines due to close contact with the mucosal surface.

The above-described immunostimulatory effects from oral immunization with antigens in combination with β-glucan particles (antigen delivery platform) to promote an enhanced adaptive immune response are reported in (Berner et al., 2018; De Smet et al., 2023). Proliferation, differentiation, and activation of APC cells Th1 and Th17 were noted after sensitization of mice for 3 days (De Smet et al., 2023). Sensitization was carried out with 100 μg/300 μg of OVA-containing compositions with stimulation on the 14th and 28th day. Such oral administration of GP-OVA in mice promoted the generation of cellular and humoral immune responses and additionally activated an increase in the amount of IgA and the secretory component in the intestine. The above research results are in good agreement with the work of Huang and colleagues (Huang et al., 2013), where invasive subcutaneous administration of the GP composition led to the stimulation of antigen-specific antibodies and T-lymphocytes as a response, as well as the production of cytokines - IFN-γ and IL17a by CD4+ Th1 and Th17 cells.

The use of β-glucans in the form of microparticles for stimulating the innate link of immunity remains a relevant issue for the world scientific community. For example, the work (Berner et al., 2005) describes in-depth "in vitro" studies of the natural immunostimulating activity of yeast β-glucans obtained from *S. cerevisiae* in soluble form and as microparticles. Laboratory mice were vaccinated with 1 mg/kg preparation of β-glucan microparticles. As a result, increased expression of costimulatory molecules B7.1 and B7.2 (required as a concomitant signal during T-cell activation and proliferation) and increased phagocytic activity of macrophages were observed in mice. In addition, a rapid phagocytic reaction of macrophages with subsequent induction of pro-inflammatory cytokines TNF-α, IL-6 and IL-1β was noted; this response was additionally enhanced because of IFN-γ priming.

According to research (Yu et al., 2015), yeast β-glucan can induce the recruitment of macrophages, effector T cells, and DCs to the liver with additional enhancement of the Th1 immune response, which promotes the removal of viral DNA from it.

In global practice, the potential of β-glucan is also used in anticancer therapy. Solid β-glucan particles have proven to be physiologically active molecules in the microenvironment of tumors due to the stimulation of immunosuppressive macrophages classically activated through Dectin-1 (Liu et al., 2015). The immunostimulating effect of β-glucan with potential anticancer activity in lung cancer (Peymaeei et al., 2020), cervix (Chaichian et al., 2020), and ovarian cancer (Sadoughi et al., 2022) is currently noted. According to the study of Sadoughi et al. (2022), the positive effect of the polysaccharide is due to its binding to the CR3 receptor and cytotoxic degranulation of tumor cells (coated with iC3b). Due to these properties, the use of β-glucans in anticancer therapy is a topical topic presented in a number of studies in recent years (Caseiro et al., 2022; Geller et al., 2019; Sadoughi et al., 2022).

Adjuvant properties of β-glucans: immunological features in the composition of vaccine preparations

Immunostimulating properties of β-glucan and its chains for the delivery of vaccine antigen in oral immunization were confirmed in (Berner et al., 2015; Cheng et al., 2014; De Smet et al., 2013; 2014). The main functional features of β-glucans discussed are pattern receptor (PRR) recognition by immunocompetent cells and moderate enhancement of immunostimulatory properties without causing their excessive activity, which may cause undesirable consequences in the form of autoimmune diseases (Miyamoto et al., 2018).

β-glucan-induced changes in cellular metabolism lead to the induction of "trained immunity" in monocytes with profound changes in their metabolic processes. The three metabolic pathways involved in trained immunity are glycolysis, glutaminolysis, and cholesterol synthesis, which are associated with β-glucan H3K4me3 enrichment (required for the formation of trained immunity). There is already evidence of the principle of metabolic-epigenomic circuits in innate immune memory, demonstrating the essential role of fumarate in modulating HIF1α degradation, histone methylation and acetylation; taking into account the work of metabolic-epigenomic chains is important if β-glucans are used in the composition of the latest vaccines (Cheng et al., 2014).

Confirmation of the above-mentioned potential of the polysaccharide is described and is explained by the binding and stimulating properties of receptors in relation to APC in the form of a receptor-targeted antigen delivery system (Baert et al., 2015). This delivery system may be promising in the development of the latest vaccines.

The immunostimulating effects of separately prepared β-glucan-CpG complexes with protein antigens was investigated (Kobiyama et al., 2016; Miyamoto et al., 2018; Mochizuki et al., 2015). It was found that the proposed complexes contribute to the release of cytokines and the induction of a powerful cytotoxic T-lymphocyte response, because of which the antigen is released. It is worth noting that the tested drug in these studies overcame unwanted aggregation and initiated stronger antigen-specific reactions with the participation of CD8+ T-cell responses.

The results presented above testify to the potential of β-glucan, both independently and in combination, to manifest adjuvant properties in the composition of immunobiological drugs. Adjuvant properties of β-glucan in DNA vaccines are described by Wang et al. (2020). Such vaccine preparations are able to induce a CD8+ T-cell-specific immune response. Synthetic β-1,6- and β-1,3-glucohexaose administered together with HBcAg DNA (pB144) promotes the recruitment and maturation of dendritic cells along with enhancement of virus-specific lymphocyte cytotoxicity and antibody response.

The results of using β-glucan particles (GP) from yeast *S. cerevisiae*, which are purified cell walls mainly with β1,3D-glucans for OVA encapsulation, are described in the work

(Huang et al., 2010). The developed platform is made using a series of alkaline and acid extraction steps, combining the function of antigen delivery and adjuvant action. Mice were immunized 3 times with an interval of 3 weeks using 100 µl of sterile PBS (control) and 50 µg of OVA complexed with 5 × 10 7 GPs (GP-OVA) by subcutaneous injection above the abdomen. It was noted that GP-loaded OVA is able to stimulate sustained humoral and T-cell responses, whereby the cellular response is driven by Th1 and Th17. In addition, strong antibody reactions were observed, with the titer of antibodies increasing with each subsequent stimulation.

In the formulations of many immunobiological drugs, polysaccharide β-glucan from various sources of origin has already demonstrated significant adjuvant activity in experimental studies on animal models (Table 2).

As can be seen from Table 2, the polysaccharide β-glucan is a candidate for the status of a new type of immune adjuvant for the latest vaccines against diseases caused by infectious agents of both bacterial and viral nature, due to a wide range of potentiation of immune responses regardless of the form of administration. One of the most recent successful integration of polysaccharides into vaccine preparations is the attempt to use their adjuvant properties in influenza (H5N1) vaccines with sulfated (degree of sulfation 0.16) yeast (*S. cerevisiae*) β-glucan (GSC in its composition) (Wang et al., 2016). It has been shown that GSCs are able to significantly promote lymphocyte proliferation independently or synergistically with Con A and LPS, increase the ratio of CD4 + /CD8 + due to an increase in the percentage of T cells, and also stimulate cells to secrete cytokines (INF-γ, IL-2). These results support the adjuvant effect of sulfated glucan as an effective immune adjuvant for inactivated influenza (H5N1) vaccines.

Successful attempts to use sulfated yeast β-glucans from *S. cerevisiae* (GSC) are presented in (Wang et al., 2024), where GSCs were used to enhance the immunogenicity of Newcastle disease vaccines. The aim of the work was to study the effect of GSC on the proliferation of chicken spleen lymphocytes "in vitro". During the study, 7, 14, 21, 28, 35, 42 days after the first vaccination of chickens, the titer of antibodies in the blood serum, the amount of produced interleukins (IL-2), interferons (IFN-γ), and the proliferation of lymphocytes were measured.

A significant increase in the immune efficiency of the vaccine due to GSC is noted because of the increase in the titer of antibodies in chickens, the proliferation of lymphocytes, as well as an increase in the amount of IL-2 and IFN-γ in blood serum.

The status of β-glucan, as a new type of immune adjuvant, is confirmed by Berner et al. (2015), who studied the use of an immunobiological preparation with microparticles of β-glucan (MG) conjugated with a vaccine antigen. In experiments, bone marrow dendritic cells (BMDC) were treated with OVA-conjugated MG. and then interacted with splenocytes from DO11.10 transgenic mice expressing the OVA peptide-specific T-cell receptor. BMDCs treated with MG:OVA were found to induce significantly more activated (CD25+ CD69+) OVA-specific CD4+ T cells than BMDCs treated with OVA alone. However, BMDC treated with MG: OVA increased the expression of CD86 and CD40. Such obtained "in vitro" results once again demonstrate the adjuvant capabilities of MG in matters of enhancing DC antigen presentation to naïve antigen-specific lymphocytes (CD4, CD8).

Table 2

Action of β-glucans when used as adjuvants vaccines

Object of study	β-glucan (source form of administration	Antigens	Effect	Reference
Mice	β-glucan (barley); subcutaneous	Meningococcal group Y, subcutaneous	Increase in specific CPS titer of IgG and IgG1	Qiao et al., 2015
Dogs	β-1,3/1,6-glucan (yeasts *S. cerevisiae*), oral	Bivalent vaccine containing inactivated cells *Bordetella bronchiseptica* and parainfluenza virus type 2, subcutaneous	Increased production of serum immunoglobulins IgA, IgM. IgG level remains unchanged	Stuyven et al., 2010
Mice	β-1,6-branched β-1,3-glucohexaose (synthetic), intraperitoneal	HBcAg DNA (pB144), intramuscular	Increase in the number of recruited and maturing dendritic cells, virus-specific CTL antibodies. Strengthening of the Th2 immune response.	Wang et al., 2020
Mice	β-1,6-branched β-1,3-glucohexaose (synthetic), intraabdominal	HBsAg, intraabdominal	Increase in the number of recruited and maturing macrophages, dendritic cells; production of specific antibodies. Strengthening of the Th2 immune response.	Dong et al., 2007
Mice	β-1,3-glucan hexasaccharide (synthetic), intraperitoneal	Inactivated (detoxified) diphtheria toxin, intradermal	Increase in the titer of antigen-specific antibodies	Donadei et al., 2017
Chickens	Sulphated β-1,3-glucan (*Lentinus edodes*), intraperitoneal	Newcastle disease vaccine, intramuscular	Higher antibody titer and lower mortality than non-sulfated and non-adjuvanted	Guo et al., 2009
Mice	β-glucan microparticles (*Saccharomyces cerevisiae*), oral	Bovine serum albumin, oral	Increased antibody response to vaccine antigens. Activation of antigen-presenting cells	Berner et al., 2018
Chickens	Sulphated β-1,3–1,6-glucan, intraperitoneal	Newcastle disease vaccine, intramuscular	Increased serum antibody titer. Serum IL-2 and IFN-γ concentration	Wang et al., 2014
Ducks and chickens	β-glucan (*Aureobasidium pullulans*), oral	H5N1 and H5N2 influenza vaccine, subcutaneous	Increase in the titer of antigen-specific antibodies	Le et al., 2021

The argument for the feasibility of using yeast β-glucans as a "pathogen-like" adjuvant for hepatitis B antigen is given in study (Soares et al., 2018). It was proposed the use of chitosan biopolymers in combination with β-glucan and additional surface localization of its particles to imitate the cell wall of some pathogens. This combination will stimulate immune cells expressing the Dectin-1 receptor. β-glucan particles (ChiGluPs) were obtained using the method of chitosan precipitation in an alkaline solution followed by genipin cross-linking. This optimized method made it possible to create particles with an average diameter of 837 nm for ChiP and 1274 nm for ChiGluP.

The obtained particles demonstrated sufficiently high efficiency of antigen loading in combination with low cytotoxicity. Blood analysis of pre-vaccinated mice confirms that ChiPs and ChiGluPs exert an adjuvant effect on hepatitis B surface antigen (HBsAg): ChiGluPs induces a 16-fold higher increase in serum anti-HBsAg class G immunoglobulins than ChIPs when 1.5 μg HBsAg is administered per dose. In addition, an increase for induction of IgG1 (by 5 times) and IgG3 (by 4 times) with the use of ChiGluP as opposed to the use of ChIP is noted.

The above results from the use of β-glucan (from *Pleurotus ostreatus*) in the composition of the latest vaccines rationalize the possibility of their recommendation for use as a prophylaxis for competitive infections. This is especially true in conditions of primary and secondary immunodeficiency of various etiologies, as well as allergic diseases such as allergic rhinitis, bronchial asthma, and atopic eczema (Urbancikova et al., 2020).

However, in contrast to a number of studies on the positive immunological effect of β-glucan, the mechanisms of its adjuvant properties require additional research. Although the adjuvantity of β-glucans is now generally accepted, there are studies reporting opposite results and conclusions (Pence et al., 2022). For example, the absence of an immunological stimulus was noted with oral administration of β-1,3/1,6 glucan in relation to an increase in the production of antigen-specific antibodies to fibroblast antigen F4 in experiments on pigs (Kobiyama et al., 2016).

An identical situation was reproduced in analyzes of a group of male volunteers under the condition of oral administration of β-glucan, which also did not lead to the induction of cytokines and microbial activity of leukocytes (Leentjens et al., 2014).

Taking into account the lack of unified data on the adjuvant properties of β-glucan, the questions of a more detailed examination of the immunostimulating effects of the polysaccharide and the mechanism of interaction with the receptors of immune cells (DC, macrophages and granulocytes) remain important.

β-glucan and biotechnological methods for its production

The production of β-glucan for further use as an immunostimulant in immunobiological preparations is the subject of modern research. β-glucan is a non-starch soluble polysaccharide presented in the cell walls of cereals, yeasts, bacteria, and algae. β-D glucose units in glucan are linked by glycosidic bonds at (1,3), (1,4) or (1,6) positions, and they can be linear or branched. The sources of β-glucan are represented by cereal (mainly oats and barley), and non-cereal (fungi, algae, and yeast) groups (Hu et al., 2020; Murphy et al., 2020). β-glucans from cereal or grains have β-(1,3) and β-(1,4) glycosidic linkages between glucose units, while β-(1,3) and (1,6) are characteristics of non-cereal β-glucans (Figure 2).

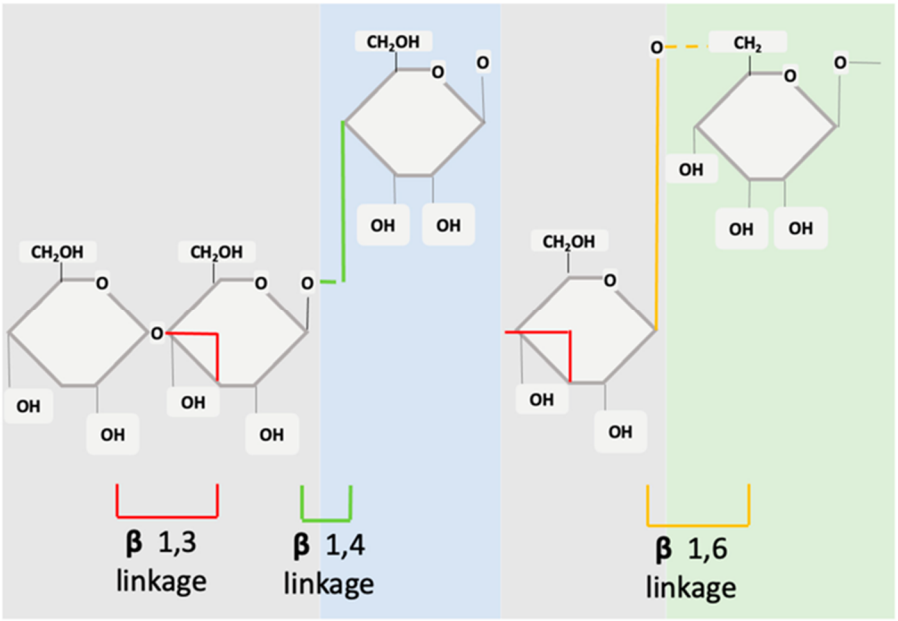

Figure 2. Structure of cereal β-glucans (1,3 1,4) and non-cereal β-glucans (1,3 1,6) (Adopted from Murphy et al., 2020)

β-glucan present in bacteria and algae is characterized by a linear structure, while β-glucan obtained from yeast, fungi, oats, and barley has a branched structure (Mudgil, 2017). The most biologically active form of β-glucans, known for their ability to optimise immune response, is β-1,3/1,6-glucan, having β(1-3) bonds between D-glucose units in the main chains and β(1-6) bonds in the side branches (De Marco Castro et al., 2021). Some prokaryotic (bacteria) and eukaryotic (yeasts, fungi, and algae) organisms proposed to be used for β-glucans production are shown in Table 3.

Table 3

Prokaryotic and eukaryotic organisms proposed to be used for β-glucans production

Glucan	Producer	Reference
β-1,3/1,6- glucan (branch-on-branch β-D-glucans structure)	Yeasts *Saccharomyces cerevisiae; Candida albicans*; *Candia utilis*	Philippini et al., 2012
β-1,3/1,6-glucan (highly branched) (extracellarly)	Yeast-like fungus *Aureobasidium pullulans*	Moriya et al., 2013
β-1,3/1,6-D-glucan (linear with 1,4-linked side branches)	*Pleurotus ostreatus* (white-rot fungus)	Dobsikova et al., 2012
β-1,3/1,6- glucan (linear with 1,6-linked β-glycoside side branches)	Algae *Laminaria* sp, *Eisenia bicyclis*; fungi *Schizophyllum commune*, *Aureobasidium pullulas, Grifola frondosa, Lentinula edodes*	Qu et al., 2021; Suzuki et al., 2021
β-1,3- glucan (linear and unbranched)	Bacteria *Alcaligenes faecalis;* algae *Euglena gracilis;* fungus *Poria cocos*	Suzuki et al., 2021

The attention is focused mostly on the following producers of β-1,3/1,6 glucans: yeasts *Saccharomyces cerevisiae* (Kim and Yun, 2006; Zhang et al., 2019), *Aureobasidium pullulans* (Chen et al., 2021; Moriya et al., 2013), actinomycetes *Streptomyces violaceus* and *S. lucensis* (Wu et al., 2018), microalgae (*Euglena gracilis*) (Qu et al., 2021), and Basidiomycetes fungi *Grifola frondosa* (hen-of-the-woods) and *Lentinula edodes* (shiitake) (Stabnikova et al., 2024).

One of the promising glucan producers is the mushroom *Grifola frondosa*, a Basidiomycete fungus, growing at the base of oaks or maples in Asia, Europe, and North America (Yang et al., 2023). This mushroom synthesizes a soluble homogeneous β-glucan with a β-D-(1-3)-linked glucan backbone with a single β-D-(1-6)-linked glucopyranosyl residue branched at C-6 on every third residue (Cui et al., 2020). The content of β-glucan in *G. frondosa* varied from 6.52% DM (Rodríguez-Seoane et al., 2018) to 25.99% DM (Sari et al., 2017).

Another suitable producer of β-glucan is the yeast *Saccharomyces cerevisiae*, which synthesizes linear β-1,3-glucan with a small amount of β-1,6-linked branches that accumulates in the cell walls (Kim and Yun, 2006). However, it should be noted that, according to the results of Boutros et al. (2022), the structure of glucan obtained from the yeast biomass of *S. cerevisiae* is influenced by both the yeast strain and the method used for its isolation and purification, so there may be slight chemical deviations in the structure of the final products. Cell wall accounts for up to 30% of the cell dry weight and is composed up to 55–65% β-glucan. The highest β-glucan content in cell wall among 10 *S. cerevisiae* strains cultuvated in a nutrient medium with glucose as a carbon source was 41.69% (Pengkumsri et al., 2022). 0.13 g of β-glucan per g of dried biomass was obtain during fed-batch cultivation of *S. cerevisiae* in medium with glucose as substrate for yeast growth (Kim and Yun, 2006).

The biological activity of β-glucan (immunostimulating, antitumor and antibacterial) is manifested only under the condition of increasing the degree of its solubility. At the same time, "soluble β-glucan" (molecular weight 130 kDa) refers to its water-soluble fragments (obtained by partial fragmentation of molecules) and various derivatives of the composition. In this regard, methods of obtaining polysaccharides with an increased degree of solubility using biotechnological modification are relevant (Kaur et al., 2019).

The influence of cultivation conditions and isolation methods on the yield of polysaccharides has been described in a number of studies, which demonstrate the possibility of significantly increasing the amount of β-glucan synthesized (Amer et al., 2021; Bzducha-Wróbel et al., 2020; Fu et al, 2022; Khadam et al., 2023; Utama et al., 2021; Zhang et al., 2019). During the cultivation of the yeast *S. cerevisiae*, it was found that the content of soluble polysaccharide and resistance to β-glucanase are higher in the early stationary phase of growth (Avramia et al., 2021). Under the condition of continuous cultivation, the content of soluble β-glucan and resistance to the action of the enzyme were higher.

To evaluate the immunomodulatory effect "in vivo" of β-glucan from yeast *S. cerevisiae*, laboratory mice were given 50, 100, 150 mg of dried β-glucan per kilogram of body weight (Pengkumsri et al., 2016). It was found that even a small dose of β-glucan induces the expression of selected pro-inflammatory (IL-17, IFN-γ) and significantly anti-inflammatory cytokines (IL-10); a relatively high dose is required to alter IL-6 and TGF-β expression. In general, the research data demonstrate that β-glucan extracted from *S. cerevisiae* HII31 cells can change the expression of pro-inflammatory and anti-inflammatory cytokines.

Taking into account all the above, the most important producers of β-glucan yeasts *Saccharomyces cerevisiae* and the mushroom *Grifola frondosa* can be considered.

Immunological response and possible effects of adjuvants of microbial origin is shown inTable 4.

Table 4

Immunological response and possible effects of microbial adjuvants

Immunological response	Possible effects	Reference
Adjuvants of microbial origin		
β-glucan; Activation pathway: Metabolic reprogramming and epigenetic modifications, Dectin-1, TLR 2,4,5		
Induces trimethylated histone H3 at Lys4 (H3K4me3) and H3 acetylated at Lys27 (H3K27ac) in monocytes and macrophages. Using the Dectin-1 receptor activates the PI3K (phosphoinositol-3-kinase)/AKT/ mTOR (mammalian target of rapamycin)/HIF-1α (hypoxia-inducible factor-1α) pathway and as a result of an activation, a metabolic shift towards aerobic glycolysis is induced enhancing glutaminolysis, which replenishes the tricarboxylic acid cycle, activates the cholesterol synthesis pathway and blocks the itaconate pathway. Formed and accumulated metabolites (fumarate, succinate, mevalonate) act as cofactors of epigenetic modifiers and enhancers of trained immunity. Induces the production of 1β [IL-1β], IL-32y, interleukin 6 [IL-6]); TNF; increases the total titer of serum immunoglobulins IgA, IgM, and IgG.	Epigenetic action and metabolic reprogramming of cells; no side effects	Kumar et al., 2019; Shah et al., 2009
OMV (Outer membrane vesicles); Activation pathway: TLR4		
Increases antigen absorption and induces the expression of cell surface molecules, receptors and costimulatory molecules, which leads to increased production of T cells; stimulates the production of T-helpers (Th1 and Th2), as well as cellular and humoral immunity. Activates embryonic kidney cells through the TLR-2/TLR-1 complex, increasing the titer of IgG.	Technological difficulty of obtaining; provocation of inflammatory processes; endotoxicity	Tan et al., 2018

In summary, the ideal adjuvant should be safe, stable and not cause unwanted side effects. Its production must be simple, cost-effective and compatible with all components of the vaccine. However, the toxicity of traditional adjuvants remains a key limiting factor for the development of new and improvement of existing immunobiological drugs. Thus, the long-term strategy for choosing of adjuvants is to select the optimal platform and identify key targets of innate immunity that ensure the generation of potent yet safe immune responses according to the nature of the pathogen targeted by the vaccine (Belemets et al., 2024).

According to the data given in Table 4, OMV adjuvants in combination with some TLR agonists can cause uncontrolled immune reactions in the type of excessive inflammation factor in addition to the possible provocation of inflammatory processes due to the presence of a significant amount of endotoxins in the composition of OMV. Accordingly, there is a need to rationalize their design to elicit an optimal immune response (Tan et al., 2018; Van Der Pol et al., 2015).

The disadvantages of using LPS as an immunopotentiating agent include toxicity, which makes it quite difficult to translate the use of LPS adjuvant into a clinical scenario. Moreover, problems with stability, production and quality assurance are the main factors in the absence of any registration of a liposome-based adjuvant for use as part of immunobiological drugs for humans (Facchini et al., 2021).

The use of polysaccharide β-glucan as an epigenetic adjuvant is appropriate due to its ability to influence the immune phenotype. This makes it possible to form the most effective immune response for each particular causative agent of the disease. Due to its epigenetic characteristics, β-glucan can be used for imprinting an enhanced antiviral state (resistance against a wide range of viruses in humans). This property may be particularly advantageous during a pandemic (the COVID-19 pandemic) to confer enhanced antiviral resistance for a limited period (approximately a few weeks) in a susceptible population (Arts et al., 2018).

Research results (Biering-Sørensen et al., 2017; Lee et al., 2022) demonstrate the induction of epigenetic imprinting of innate immune cells under the influence of epigenetic adjuvants, which leads to a long-lasting state of antiviral immunity and non-specific protection against re-infection. The promise of these adjuvants is enhanced by stimulation of robust T- and B-cell responses and protection against a wide range of pathogens through training of the innate immune system (Arts et al., 2016).

The epigenetic status of β-glucan has been repeatedly confirmed in a number of studies. It was noted that PAMPs induce trimethylated histone H3 at Lys4 (H3K4me3) and H3 acetylated at Lys27 (H3K27ac) in monocytes and macrophages. These changes persist for several weeks after elimination of stimuli, resulting in improved epigenetic status. However, what is important is the improvement of the epigenetic status, which induces increased expression of genes (related to metabolic, immune and host defense pathways), obtained during the secondary stimulus by the same or other PAMP. Thus, trained monocytes/macrophages produce increased levels of cytokines (tumor necrosis factor (TNF), interleukin 1β [IL-1β], and interleukin 6 (IL-6) when exposed to microbial compounds. This raises the attractive possibility of targeting small molecules to relevant cell types as immunological modulators to reprogram the epigenetic landscape of innate immune memory (Netea et al., 2017).

Vaccines using β-glucans as adjuvants of the new generation can be used both orally and parenterally, which makes them widely applicable in medical practice. Therefore, immunostimulating polysaccharides with inherent biocompatibility and biodegradability are considered a rational strategy for the development of new adjuvants that mimic the properties of pathogens ("pathogen-like") (Stothers et al., 2021).

Conclusions

Therefore, immunomodulation through targeting of TLRs opens up new perspectives in the development of new generation vaccines that use epigenetic adjuvants to persistently reprogram the innate immune system. This makes it possible to achieve long-term protection

against a wide range of pathogens, which is especially relevant in pandemic conditions, when traditional antigen-specific vaccines may not be available.

The selection of safe and effective adjuvants or their systems remains a key area of research. The development of new pharmacological drugs, molecules or a combination of excipients plays an important role in the progress of modern immunobiotechnology. In this context, the creation of innovative biotechnological approaches aimed at obtaining safe, stable and compatible adjuvants capable of ensuring the effectiveness of vaccination is of particular importance.

The widespread use of chemical adjuvants, such as aluminum salts or emulsion preparations, has significant limitations, including toxicity, potential mutagenic and carcinogenic effects, a number of side effects, and insufficient effectiveness in stimulating immunity. This creates a need to find alternative approaches, in particular adjuvants of microbial origin.

The β-glucan polysaccharide shows significant potential as an epigenetic adjuvant due to its ability to modulate the immune phenotype, enabling adaptive immune responses optimized for a specific pathogen. The biotechnological production of β-glucan is very simple, which contributes to its prospects in the development of new, safe and effective immunotherapeutic drugs.

References

Aaby P., Martins C.L., Garly M.L., Balé C., Andersen A., Rodrigues A., Ravn H., Lisse I.M., Benn C.S., Whittle H.C. (2010), Non-specific effects of standard measles vaccine at 4.5 and 9 months of age on childhood mortality: Randomised controlled trial, *BMJ*, 341, c6495, https://doi:10.1136/bmj.c6495

Abbasi A., Saadat T.R., Saadat Y.R. (2022), Microbial exopolysaccharides-β-glucans–as promising postbiotic candidates in vaccine adjuvants, *International Journal of Biological Macromolecules*, 223, pp. 346–361, https://doi.org/10.1016/j.ijbiomac.2022.11.003

Afrough P., Karam M.R.A., Vaziri F., Behrouzi A., Siadat S.D. (2020), Construction and assessment of the immunogenicity and bactericidal activity of fusion protein porin A from *Neisseria meningitidis* serogroups A and B admixed with OMV adjuvant as a novel vaccine candidate, *Iranian Journal of Basic Medical Sciences*, 23(6), pp. 737–743, https://doi.org/10.22038/ijbms.2020.40470.9

Agarwal S., Hickey J.M., McAdams D., White J.A., Sitrin R., Khandke L., Cryz S., Joshi S.B., Volkin D.B. (2020), Effect of aluminum adjuvant and preservatives on structural integrity and physicochemical stability profiles of three recombinant subunit rotavirus vaccine antigens, *Journal of Pharmaceutical Sciences*, 109(1), pp. 476–487, https://doi.org/10.1016/j.xphs.2019.10.004

Amer E.M., Saber S.H., Markeb A. A., Elkhawaga A.A., Mekhemer I.M.A., Zohri A.A., Abujamel T.S., Harakeh S., Abd-Allah E.A. (2021), Enhancement of β–glucan biological activity using a modified acid-base extraction method from *Saccharomyces cerevisiae*, *Molecules*, 26(8), 2113, https://doi.org/10.3390/molecules26082113

Arts R.J., Novakovic B., Ter Horst R., Carvalho A., Bekkering S., Lachmandas E., Rodrigues F., Silvestre R., Cheng S.C., Wang S.Y., Habibi E., Gonçalves L.G., Mesquita I., Cunha C., van Laarhoven A., van de Veerdonk F.L., Williams D.L., van der Meer J.W., Logie C., O'Neill L.A., Dinarello C.A., Riksen N.P., van Crevel R., Clish C., Notebaart R.A., Joosten L.A., Stunnenberg H.G., Xavier R.J., Netea M.G. (2016), Glutaminolysis and fumarate accumulation integrate immunometabolic and epigenetic programs in trained immunity. *Cell Metabolism*, 24(6), pp. 807–819, https://doi.org/10.1016/j.cmet.2016.10.008

Arts R.J.W., Moorlag S.J.C.F.M., Novakovic B., Li Y., Wang S.Y., Oosting M., Kumar V., Xavier R.J., Wijmenga C., Joosten L.A.B., Reusken C.B.E.M., Benn C.S., Aaby P., Koopmans M.P., Stunnenberg H.G., van Crevel R., Netea M.G. (2018), BCG vaccination protects against experimental viral infection in humans through the induction of cytokines associated with trained immunity, *Cell Host & Microbe*, 23(1), pp. 89–100, https://doi.org/10.1016/j.chom.2017.12.010

Arunachalam P.S., Charles T.P., Joag V., Bollimpelli V.S., Scott M.K.D., Wimmers F., Burton S.L., Labranche C.C., Petitdemange C., Gangadhara S., Styles T.M., Quarnstrom C.F., Walter K.A., Ketas T.J., Legere T., Jagadeesh Reddy P.B., Kasturi S.P., Tsai A., Yeung B.Z., Gupta S., Tomai M., Vasilakos J., Shaw G.M., Kang C.Y., Moore J.P., Subramaniam S., Khatri P., Montefiori D., Kozlowski P.A., Derdeyn C.A., Hunter E., Masopust D., Amara R.R., Pulendran B. (2020), T cell–inducing vaccine durably prevents mucosal SHIV infection even with lower neutralizing antibody titers, *Nature Medicine*, 26(6), pp. 932–940, https://doi.org/10.1038/s41591-020-0858-8

Avramia I., Amariei S. (2021), Spent brewer's yeast as a source of insoluble β–glucans, *International Journal of Molecular Sciences*, 22(2), pp. 825–851, https://doi.org/10.3390/ijms22020825

Baert K., de Geest B.G., de Rycke R., da Fonseca Antunes A.B., de Greve H., Cox E., Devriendt B. (2015), β–glucan microparticles targeted to epithelial APN as oral antigen delivery system, *Journal of Controlled Release,* 220*,* pp. 149–159, https://doi.org/10.1016/j.jconrel.2015.10.025

Bates J.T., Uematsu S., Akira S., Mizel S.B. (2019), Direct stimulation of tlr5+/+ CD11c+ cells is necessary for the adjuvant activity of flagellin, *The Journal of Immunology*, 182(12), pp. 7539–7547, https://doi.org/10.4049/jimmunol.0804225

Belemets T.O., Krasinko V.O., Udymovich V.M., Cheghrynets A.I. (2024), Potential adjuvants and theirs systems for creating the latest vaccines, *Scientific Works of NUFT*, 30(4), pp. 53-75, https://doi.org/10.24263/2225-2924- 2024-30-4-6

Berner M.D., Sura M.E., Alves B.N., Hunter K.W. (2005), IFN-γ primes macrophages for enhanced TNF–α expression in response to stimulatory and non–stimulatory amounts of microparticulate β–glucan, *Immunology Letters*, 98(1), pp. 115–122, https://doi.org/10.1016/j.imlet.2004.10.020

Berner V.K., Redelman D., Hunter K.W. (2015), Microparticulate β–glucan vaccine conjugates phagocytized by dendritic cells activate both naïve CD4 and CD8 T cells in vitro, *Cellular Immunology*, 298(1–2), pp. 104–114, https://doi.org/10.1016/j.cellimm.2015.10.007

Berner V.K., Sura M.E., Hunter K.W. (2018), Conjugation of protein antigen to microparticulate β–glucan from *Saccharomyces cerevisiae*: A new adjuvant for intradermal and oral immunizations, *Applied Microbiology and Biotechnology*, 80, pp. 1053–1061, https://doi.org/10.1007/s00253-008-1618-8

Biering–Sørensen S., Aaby P., Lund N., Monteiro I., Jensen K.J., Eriksen H.B., Schaltz–Buchholzer F., Jørgensen A.S.P., Rodrigues A., Fisker A.B., Benn C.S. (207), Early BCG–Denmark and neonatal mortality among infants weighing <2500 g: A randomized controlled trial, *Clinical Infectious Diseases*, 65(7), pp. 1183–1190. https://doi.org/10.1093/cid/cix525

Boutros J.A., Magee A.S., Cox D. (2022), Comparison of structural differences between yeast β–glucan sourced from different strains of *Saccharomyces cerevisiae* and processed using proprietary manufacturing processes, *Food Chemistry*, 367, 130708, https://doi.org/10.1016/j.foodchem.2021.130708

Bruxvoort K.J., Ackerson B., Sy L.S., Bhavsar A., Tseng H.F., Florea A., Luo Y., Tian Y., Solano Z., Widenmaier R., Shi M., Van Der Most R., Schmidt J.E., Danier J., Breuer T., Qian L. (2022), Recombinant adjuvanted zoster vaccine and reduced risk of coronavirus disease

2019 diagnosis and hospitalization in older adults, *The Journal of Infectious Diseases*, 225(11), pp. 1915–1922, https://doi.org/10.1093/infdis/jiab633

Burny W., Callegaro A., Bechtold V., Clement F., Delhaye S., Fissette L., Janssens M., Leroux-Roels G., Marchant A., van den Berg R.A., Garçon N., van der Most R., Didierlaurent A.M, ECR-002 Study Group. (2017), Different adjuvants induce common innate pathways that are associated with enhanced adaptive responses against a model antigen in humans, *Frontiers in Immunology*, 8, 943, https://doi.org/10.3389/fimmu.2017.00943

Buschmann D., Mussack V., Byrd J.B. (2021), Separation, characterization, and standardization of extracellular vesicles for drug delivery applications, *Advanced Drug Delivery Reviews*, 174, pp. 348–368, https://doi.org/10.1016/j.addr.2021.04.027

Bzducha-Wróbel A., Koczoń P., Błażejak S., Kozera J., Kieliszek M. (2020), Valorization of deproteinated potato juice water into β-glucan preparation of *C. utilis* origin: Comparative study of preparations obtained by two isolation methods, *Waste and Biomass Valorization*, 11, pp. 3257–3271, https://doi.org/10.1007/s12649-019-00641-w

Caseiro C., Dias J.N.R., de Andrade Fontes C.M.G., Bule P. (2022), From cancer therapy to winemaking: The molecular structure and applications of β-glucans and β-1, 3-glucanases, *International Journal of Molecular Sciences*, 23(6), pp. 3156–3191, https://doi.org/10.3390/ijms23063156

Chaichian S., Moazzami B., Sadoughi F., Haddad Kashani H., Asemi Z. (2020), Functional activities of beta-glucans in the prevention or treatment of cervical cancer, *Journal of Ovarian Research*, 13, pp. 1–12, https://doi.org/10.1186/s13048-020-00626-7

Chang M., Mahasenan K.V., Hermoso J.A., Mobashery S. (2021), Unconventional antibacterials and adjuvants, *Accounts of Chemical Research*, 54(4), pp. 917–929, https://doi.org/10.1021/acs.accounts.0c00776

Chegrynets A.I., Saliy O.O., Sobko I.A., Krasinko V.O. (2021), Immunological evaluation of inactivated Newcastle disease vaccine depending on adjuvant composition, *Regulatory Mechanisms in Biosystems*, 12(3), pp. 490–497, https://doi.org/10.15421/022167

Chen X., Wang Y., He C.Y., Wang G.L., Zhang G.C., Wang C.L., Wang D.H., Zou X., Wei G.Y. (2021), Improved production of β-glucan by a T-DNA–based mutant of *Aureobasidium pullulans*, *Applied Microbiology and Biotechnology*, 105(18), pp. 6887–6898, https://doi.org/10.1186/s13048-135-00223-9

Cheng S.C., Quintin J., Cramer R.A., Shepardson K.M., Saeed S., Kumar V., Giamarellos-Bourboulis E.J., Martens J.H., Rao N.A., Aghajanirefah A., Manjeri G.R., Li Y., Ifrim D.C., Arts R.J., van der Veer B.M., Deen P.M., Logie C., O'Neill L.A., Willems P., van de Veerdonk F.L., van der Meer J.W., Ng A., Joosten L.A., Wijmenga C., Stunnenberg H.G., Xavier R.J., Netea M.G. (2014), mTOR-and HIF-1α–mediated aerobic glycolysis as metabolic basis for trained immunity, *Science*, 345(6204), 1250684, https://doi.org/10.1126/science.1250684

Ciarlo E., Heinonen T., Théroude C., Asgari F., Le Roy D., Netea M.G., Roger T. (2020), Trained immunity confers broad-spectrum protection against bacterial infections, *The Journal of Infectious Diseases*, 222(11), pp. 1869–1881, https://doi.org/10.1093/infdis/jiz692

Clark T.W., Pareek M., Hoschler K., Dillon H., Nicholson K.G., Groth N., Stephenson I. (2009), Trial of 2009 influenza A (H1N1) monovalent MF59-adjuvanted vaccine, *New England Journal of Medicine*, 361(25), pp. 2424-2435, https://doi.org/10.1056/NEJMoa0907650

Colaço M., Roquito T., Costa J.P., Cruz M.T., Borges O. (2023), The effect of curcumin-loaded glucan nanoparticles on immune cells: Size as a critical quality attribute, *Pharmaceutics*, 15(2), pp. 623–638, https://doi.org/10.3390/pharmaceutics15020623

Coler R.N., Day T.A., Ellis R., Piazza F.M., Beckmann A.M., Vergara J., Rolf T., Lu L., Alter G., Hokey D., Jayashankar L., Walker R., Snowden M.A., Evans T., Ginsberg A., Reed S.G., TBVPX-113 Study Team, (2018), The TLR-4 agonist adjuvant, GLA-SE, improves

magnitude and quality of immune responses elicited by the ID93 tuberculosis vaccine: first-in-human trial, *NPJ Vaccines*, 3, 34, https://doi.org/10.1038/s41541-018-0057-5

Cui H., Zhu X., Huo Z., Liao B., Huang J., Wang Z., Song C., Hu X., Fang J. (2020), A β-glucan from *Grifola frondosa* effectively delivers therapeutic oligonucleotide into cells via dectin-1 receptor and attenuates TNFα gene expression, *International Journal of Biological Macromolecules*, 149, pp. 801–808, https://doi.org/10.1016/j.ijbiomac.2020.01.236

Daleke-Schermerhorn M.H., Felix T., Soprova Z., Ten Hagen-Jongman C.M., Vikström D., Majlessi L., Beskers J., Follmann F., de Punder K., van der Wel N.N., Baumgarten T., Pham T.V., Piersma S.R., Jiménez C.R., van Ulsen P., de Gier J.W., Leclerc C., Jong W.S., Luirink J. (2014), Decoration of outer membrane vesicles with multiple antigens by using an autotransporter approach, *Applied and Environmental Microbiology*, 80(18), pp. 5854–5865, https://doi.org/10.1128/AEM.01941-14

de Laval B., Maurizio J., Kandalla P.K., Brisou G., Simonnet L., Huber C., Gimenez G., Matcovitch-Natan O., Reinhardt S., David E., Mildner A., Leutz A., Nadel B., Bordi C., Amit I., Sarrazin S., Sieweke M.H. (2020), C/EBPβ-dependent epigenetic memory induces trained immunity in hematopoietic stem cells, *Cell Stem Cell*, 26(5), pp. 657–674, https://doi.org/10.1016/j.stem.2020.01.017

De Marco Castro E., Calder P.C., Roche H.M. (2021), β-1, 3/1, 6-glucans and immunity: State of the art and future directions, *Molecular Nutrition & Food Research*, 65(1), e1901071, https://doi.org/10.1002/mnfr.201901071

De Smet R., Allais L., Cuvelier C.A. (2014), Recent advances in oral vaccine development: Yeast-derived β-glucan particles, *Human Vaccines & Immunotherapeutics*, 10(5), pp. 1309–1318, https://doi.org/10.4161/hv.28166

De Smet R., Demoor T., Verschuere S., Dullaers M., Ostroff G.R., Leclercq G., Allais L., Pilette C., Dierendonck M., De Geest B.G., Cuvelier C.A. (2013), β-gucan microparticles are good candidates for mucosal antigen delivery in oral vaccination, *Journal of Controlled Release*, 172(3), pp. 671–678, https://doi.org/10.1016/j.jconrel.2013.09.007

Delaney K.N., Phipps J.P., Johnson J.B., Mizel S.B. (2010), A recombinant flagellin-poxvirus fusion protein vaccine elicits complement-dependent protection against respiratory challenge with vaccinia virus in mice, *Viral Immunology*, 23(2), pp. 201–210, https://doi.org/10.1089/vim.2009.0107

Desbien A.L., Reed S.J., Bailor H.R., Cauwelaert N.D., Laurance J.D., Orr M.T., Fox C.B., Carter D., Reed S.G., Duthie, M.S. (2015), Squalene emulsion potentiates the adjuvant activity of the TLR4 agonist, GLA, via inflammatory caspases, IL-18, and IFN-γ, *European Journal of Immunology*, 45(2), pp. 407–417, https://doi.org/10.1002/eji.201444543

Dobsikova R., Blahova J., Franc A., Jakubik J., Mikulikova I., Modra H., Novotna K., Svobodova Z. (2012), Effect of β-1.3/1.6-D-glucan derived from oyster mushroom *Pleurotus ostreatus* on biometrical, haematological, biochemical, and immunological indices in rainbow trout (*Oncorhynchus mykiss*), *Neuroendocrinology Letters*, 33(Suppl 3), pp. 96–106.

Donadei A., Balocchi C., Romano M.R., Panza L., Adamo R., Berti F., O'Hagan D.T., Gallorini S., Baudner B.C. (2017), Optimizing adjuvants for intradermal delivery of MenC glycoconjugate vaccine, *Vaccine*, *35*(32), pp. 3930–3937, https://doi.org/10.1016/j.vaccine.2017.06.018

Donadei A., Gallorini S., Berti F., O'Hagan D.T., Adamo R., Baudner B.C. (2015), Rational design of adjuvant for skin delivery: Conjugation of synthetic β-glucan dectin-1 agonist to protein antigen, *Molecular Pharmaceutics,* 12(5), pp. 1662–1672, https://doi.org/10.1021/acs.macromol.2c00854

Dong S.F., Chen J.M., Zhang W., Sun S.H., Wang J., Gu J.X., Boraschi D., Qu D. (2007), Specific immune response to HBsAg is enhanced by β-glucan oligosaccharide containing an α-(1→

3)-linked bond and biased towards M2/Th2, *International Immunopharmacology*, 7(6), pp. 725–733, https://doi.org/10.1016/j.intimp.2007.01.004

Dos Santos J.C., Barroso de Figueiredo A.M., Teodoro Silva M.V., Cirovic B., de Bree L.C.J., Damen M.S.M.A., Moorlag S.J.C.F.M., Gomes R.S., Helsen M.M., Oosting M., Keating S.T., Schlitzer A., Netea M.G., Ribeiro-Dias F., Joosten L.A.B. (2019), β-glucan-induced trained immunity protects against *Leishmania braziliensis* infection: A crucial role for IL-32, Cell Reports, 28(10), pp. 2659-2672, https://doi.org/10.1016/j.celrep.2019.08.004

Durães F., Szemerédi N., Kumla D., Pinto M., Kijjoa A., Spengler G., Sousa E. (2021), Metabolites from marine-derived fungi as potential antimicrobial adjuvants, *Marine Drugs*, 19(9), pp. 475–495, https://doi.org/10.3390/md19090475

Elder M.J., Webster S.J., Chee R., Williams D.L., Hill Gaston J.S., Goodall J.C. (2017), β-glucan size controls dectin-1-mediated immune responses in human dendritic cells by regulating IL-1β production, *Frontiers in Immunology*, 8, pp. 791–811, https://doi.org/10.3389/fimmu.2017.00791

Eldred B.E., Dean A.J., McGuire T.M., Nash A.L. (2006), Vaccine components and constituents: Responding to consumer concerns, *Medical Journal of Australia*, 184(4), pp. 170–175, https://doi.org/10.3440/md17560245

Elsharkasy O.M., Nordin J.Z., Hagey D.W., de Jong O.G., Schiffelers R.M., Andaloussi S.E., Vader P. (2020), Extracellular vesicles as drug delivery systems: Why and how?, *Advanced Drug Delivery Reviews*, 159, pp. 332–343, https://doi.org/10.1016/j.addr.2020.04.004

Exley C. (2014), Aluminium adjuvants and adverse events in sub-cutaneous allergy immunotherapy, *Allergy, Asthma & Clinical Immunology*, 10(1), pp. 1–5, http://www.aacijournal.com/content/10/1/4

Facchini F.A., Minotti A., Luraghi A., Romerio A., Gotri N., Matamoros-Recio A., Iannucci A., Palmer C., Wang G., Ingram R., Martin-Santamaria S., Pirianov G., De Andrea M., Valvano M.A., Peri F. (2021), Synthetic glycolipids as molecular vaccine adjuvants: Mechanism of action in human cells and in vivo activity, *Journal of Medicinal Chemistry*, 64(16), pp. 12261–12272, https://doi.org/10.1021/acs.jmedchem.1c00896

Facciolà A., Visalli G., Laganà A., Di Pietro A. (2022), An overview of vaccine adjuvants: Current evidence and future perspectives, *Vaccines*, 10(5), 819, https://doi.org/10.3390/vaccines10050819

Farina J.M., Liblik K., Iomini P., Miranda-Arboleda A.F., Saldarriaga C., Mendoza I., Zaidel E.J., Rubio-Campal J.M., Sosa-Liprandi A., Baranchuk A. (2023), Infections and cardiovascular disease: JACC focus seminar ¼, *Journal of the American College of Cardiology*, 81(1), pp. 71–80, https://doi.org/10.1016/j.jacc.2022.08.813

Fu W., Zhao G., Liu J. (2022), Effect of preparation methods on physiochemical and functional properties of yeast β-glucan, *LWT*, 160, pp. 113284–113290, https://doi.org/10.1016/j.lwt.2022.113284

Galson J.D., Trück J., Kelly D.F., van der Most R. (2016), Investigating the effect of AS03 adjuvant on the plasma cell repertoire following pH1N1 influenza vaccination, *Scientific Reports*, 6, pp. 37229–37345, https://doi.org/10.1038/srep37229

Gan Y., Li C., Peng X., Wu S., Li Y., Tan J.P.K., Yang Y.Y., Yuan P., Ding X. (2021), Fight bacteria with bacteria: Bacterial membrane vesicles as vaccines and delivery nanocarriers against bacterial infections, *Nanomedicine: Nanotechnology, Biology and Medicine*, 35, 102398, https://doi.org/10.1016/j.nano.2021.102398

Geller A., Shrestha R., Yan J. (2019), Yeast-derived β-glucan in cancer: novel uses of a traditional therapeutic, *International Journal of Molecular Sciences*, 20(15), pp. 3618–3734, https://doi.org/10.3390/ijms20153618

Gherardi R.K., Coquet M., Cherin P., Belec L., Moretto P., Dreyfus P.A., Pellissier J.F., Chariot P., Authier F.J. (2001), Macrophagic myofasciitis lesions assess long-term persistence of

vaccine-derived aluminium hydroxide in muscle, *Brain*, 124(Pt 9), pp. 1821–1831, https://doi.org/10.1093/brain/124.9.1821

Guo Z., Hu Y., Wang D., Ma X., Zhao X., Zhao B., Wang J., Liu P. (2009), Sulfated modification can enhance the adjuvanticity of lentinan and improve the immune effect of ND vaccine, *Vaccine*, 27(5), pp. 660–665, https://doi.org/10.1016/j.vaccine.2008.11.038

Gupta S., Pellett S. (2023), Recent developments in vaccine design: From live vaccines to recombinant toxin vaccines, *Toxins*, 15(9), 563, https://doi.org/10.3390/toxins15090563

Hajam I.A., Dar P.A., Shahnawaz I., Jaume J.C., Lee J.H. (2017), Bacterial flagellin — A potent immunomodulatory agent, *Experimental & Molecular Medicine*, 49(9), e373–e373, https://doi.org/10.1038/emm.2017.172

Han B., Baruah K., Cox E., Vanrompay D., Bossier P. (2020), Structure-functional activity relationship of β-glucans from the perspective of immunomodulation: A mini-review, *Frontiers in Immunology*, 11, 658, https://doi.org/10.3389/fimmu.2020.00658

Han X.Q., Yue G.L., Yue R.Q., Dong C.X., Chan C.L., Ko C.H., Cheung W.S., Luo K.W., Dai H., Wong C.K., Leung P.C., Han Q.B. (2014), Structure elucidation and immunomodulatory activity of a beta glucan from the fruiting bodies of *Ganoderma sinense*, *PLoS One*, *9*(7), e100380, https://doi.org/10.1371/journal.pone.0100380

Harandi A.M. (2018), Systems analysis of human vaccine adjuvants, In: T.H.M. Ottenhoff (Ed.), *Seminars in Immunology,* 39, pp. 30-34, Academic Press, https://doi.org/10.1016/j.smim.2018.08.001

Hernandez A., Patil N.K., Stothers C.L., Luan L., McBride M.A., Owen A.M., Burelbach K.R., Williams D.L., Sherwood E.R., Bohannon J.K. (2019), Immunobiology and application of toll-like receptor 4 agonists to augment host resistance to infection, *Pharmacological Research*, 150, 104502, https://doi.org/10.1016/j.phrs.2019.104502

Ho N.I., Huis In't Veld L.G.M, Raaijmakers T.K., Adema G.J. (2018), Adjuvants enhancing cross-presentation by dendritic cells: The key to more effective vaccines?, *Frontiers in Immunology*, 9, 2874, https://doi.org/10.3389/fimmu.2018.02874

Hu J., Wu Y., Xie H., Shi W., Chen Z., Jiang D., Hu H., Zheng X., Xu J., Yang Y., Liu Y. (2020), Purification, preliminary structural characterization, and in vitro inhibitory effect on digestive enzymes by β-glucan from *qingke* (Tibetan Hulless Barley), *Advances in Polymer Technology*, 2020, 2709536, https://doi.org/10.1155/2020/2709536

Huang H., Ostroff G.R., Lee C.K., Agarwal S., Ram S., Rice P.A., Specht C.A., Levitz S.M. (2012), Relative contributions of dectin-1 and complement to immune responses to particulate β-glucans, *The Journal of Immunology*, 189(1), pp. 312–317, https://doi.org/10.4049/jimmunol.1200603

Huang H., Ostroff G.R., Lee C.K., Specht C.A., Levitz S.M. (2013), Characterization and optimization of the glucan particle-based vaccine platform, *Clinical and Vaccine Immunology*, 20(10), pp. 1585–1591, https://doi.org/doi:10.1128/CVI.00463-13

Huleatt J.W., Nakaar V., Desai P., Huang Y., Hewitt D., Jacobs A., Tang J., McDonald W., Song L., Evans R.K., Umlauf S., Tussey L., Powell T.J. (2008), Potent immunogenicity and efficacy of a universal influenza vaccine candidate comprising a recombinant fusion protein linking influenza M2e to the TLR5 ligand flagellin, *Vaccine*, 26(2), pp. 201–214, https://doi.org/10.1016/j.vaccine.2007.10.062

Hurtgen B.J., Hung C.Y., Ostroff G.R., Levitz S.M., Cole G.T. (2012), Construction and evaluation of a novel recombinant T cell epitope-based vaccine against coccidioidomycosis, *Infection and Immunity*, 80(11), pp. 3960–3974, https://doi.org/10.1128/iai.00566-12

Hwang J., Lee K., Gilad A.A., Choi J. (2018), Synthesis of beta-glucan nanoparticles for the delivery of single strand DNA, *Biotechnology and Bioprocess Engineering*, 23, pp. 144–149, https://doi.org/10.1018/j.fsi.2018.08.019

Ji L., Sun G., Li J., Wang Y., Du Y., Liu X., Liu Y. (2017), Effect of dietary β-glucan on growth, survival and regulation of immune processes in rainbow trout (*Oncorhynchus mykiss*) infected by *Aeromonas salmonicida*. *Fish & Shellfish Immunology*, 64, pp. 56–67, https://doi.org/10.1016/j.fsi.2017.03.015

Karch C.P., Burkhard P. (2016), Vaccine technologies: From whole organisms to rationally designed protein assemblies, *Biochemical Pharmacology*, 120, pp. 1–14, https://doi.org/10.1016/j.bcp.2016.05.001

Kasturi S.P., Rasheed M.A.U., Havenar-Daughton C., Pham M., Legere T., Sher Z.J., Kovalenkov Y., Gumber S., Huang J.Y., Gottardo R., Fulp W., Sato A., Sawant S., Stanfield-Oakley S., Yates N., LaBranche C., Alam S.M., Tomaras G., Ferrari G., Montefiori D., Wrammert J., Villinger F., Tomai M., Vasilakos J., Fox C.B., Reed S.G., Haynes B.F., Crotty S., Ahmed R., Pulendran B. (2020), 3M-052, a synthetic TLR-7/8 agonist, induces durable HIV-1 envelope–specific plasma cells and humoral immunity in nonhuman primates, *Science Immunology*, 5(48), eabb1025, https://doi.org/10.1126/sciimmunol.abb1025

Kaur R., Sharma M., Ji D., Xu M., Agyei D. (2019), Structural features, modification, and functionalities of beta-glucan, *Fibers*, 8(1), 1, http://doi.org/10.3390/fib8010001

Khadam A.A., Salman J.A.S., Hijri M. (2023), Determination the optimum conditions for β-glucan production extracted from *Saccharomyces cerevisiae*, *Al-Mustansiriyah Journal of Science*, 34(2), pp. 32–43, http://doi.org/10.23851/mjs.v34i2.1298

Kim K.S., Yun H. S. (2006), Production of soluble β-glucan from the cell wall of *Saccharomyces cerevisiae*, *Enzyme and Microbial Technology*, 39(3), pp. 496–500, https://doi.org/10.1016/j.enzmictec.2005.12.020

Kim E.H., Woodruff M.C., Grigoryan L., Maier B., Lee S.H., Mandal P., Cortese M., Natrajan M.S., Ravindran R., Ma H., Merad M., Gitlin A.D., Mocarski E.S., Jacob J., Pulendran B. (2020), Squalene emulsion-based vaccine adjuvants stimulate CD8 T cell, but not antibody responses, through a RIPK3-dependent pathway, *eLife*, 9, e52687, https://doi.org/10.7554/eLife.52687

Kobiyama K., Temizoz B., Kanuma T., Ozasa K., Momota M., Yamamoto T., Aoshi T., Kuroda E., Ishii K.J. (2016), Species-dependent role of type I IFNs and IL-12 in the CTL response induced by humanized CpG complexed with β-glucan*, European Journal of Immunology,* 46(5), pp. 1142–1151, https://doi.org/10.1002/eji.201546059

Kooijman S., Vrieling H., Verhagen L., de Ridder J., de Haan A., van Riet E., Heck A.J.R., Kersten G.F.A., Pennings J.L.A., Metz B., Meiring H.D. (2022), Aluminum hydroxide and aluminum phosphate adjuvants elicit a different innate immune response, *Journal of Pharmaceutical Sciences*, 111(4), pp. 982–990, https://doi.org/10.1016/j.xphs.2022.01.014J

Krishnan N., Kubiatowicz L.J., Holay M., Zhou J., Fang R.H., Zhang L. (2022), Bacterial membrane vesicles for vaccine applications, *Advanced Drug Delivery Reviews*, 185, 114294, https://doi.org/10.1016/j.addr.2022.114294

Kumar S., Sunagar R., Gosselin E. (2019), Bacterial protein toll-like-receptor agonists: A novel perspective on vaccine adjuvants, *Frontiers in Immunology*, 10, pp. 1144–1166, https://doi.org/10.3389/fimmu.2019.01144

Le T., Le T., Doan T.H., Quyen D., Le K.X., Pham V., Nagataki M., Nomura H., Ikeue Y., Watanabe Y., Agatsuma T. (2021), The adjuvant effect of sophy β-glucan to the antibody response in poultry immunized by the avian influenza A H5N1 and H5N2 vaccines, *Journal of Microbiology and Biotechnology*, 21(4), pp. 405–411, https://doi.org/10.4014/jmb.1011.11024

Lee A., Scott M.K.D., Wimmers F., Arunachalam P.S., Luo W., Fox C.B., Tomai M., Khatri P., Pulendran B. (2022), A molecular atlas of innate immunity to adjuvanted and live attenuated vaccines in mice, *Nature Communications*, 13(1), 549, https://doi.org/10.1038/s41467-022-28197-9

Lee D.H., Kim S.H., Kang W., Choi Y.S., Lee S.H., Lee S.R., You S., Lee H.K., Chang K.T., Shin E.C. (2011), Adjuvant effect of bacterial outer membrane vesicles with penta-acylated lipopolysaccharide on antigen-specific T cell priming, *Vaccine*, 29(46), pp. 8293–8301, https://doi.org/10.1016/j.vaccine.2011.08.102

Leentjens J., Quintin J., Gerretsen J., Kox M., Pickkers P., Netea M.G. (2014), The effects of orally administered Beta-glucan on innate immune responses in humans, a randomized open-label intervention pilot-study, *PloS One*, 9(9), e108794, https://doi:10.1371/journal.pone.0108794

Lin K.H., Chang L.S., Tian C.Y., Yeh Y.C., Chen Y.J., Chuang T.H., Liu S.J., Leng C.H. (2016), Carboxyl-terminal fusion of E7 into Flagellin shifts TLR5 activation to NLRC4/NAIP5 activation and induces TLR5-independent anti-tumor immunity, *Scientific Reports*, 6(1), 24199, https://doi.org/10.1038/srep24199

Liu M., Luo F., Ding C., Albeituni S., Hu X., Ma Y., Cai Y., McNally L., Sanders M.A., Jain D., Kloecker G., Bousamra M. 2nd, Zhang H.G., Higashi R.M., Lane A.N., Fan T.W., Yan J. (2015), Dectin-1 activation by a natural product β-glucan converts immunosuppressive macrophages into an M1-like phenotype, *The Journal of Immunology*, 195(10), pp. 5055–5065, https://doi.org/10.4049/jimmunol.1501158

Malik A., Gupta M., Gupta V., Gogoi H., Bhatnagar R. (2018), Novel application of trimethyl chitosan as an adjuvant in vaccine delivery, *International Journal of Nanomedicine*, 2018(13), pp. 7959–7970, https://doi.org/10.2147/ijn.s165876

Mancini F., Rossi O., Necchi F., Micoli, F. (2020), OMV vaccines and the role of TLR agonists in immune response, *International Journal of Molecular Sciences*, 21(12), 4416, https://doi.org/10.3390/ijms21124416

Martiñón S., Cisneros A., Villicaña S., Hernández-Miramontes R., Mixcoha E., Calderón-Vargas P. (2019), Chemical and immunological characteristics of aluminum-based, oil-water emulsion, and bacterial-origin adjuvants, *Journal of Immunology Research*, 2019, 3974127, https://doi.org/10.1155/2019/3974127

Masforrol Y., Gil J., García D., Noda J., Ramos Y., Betancourt L., Guirola O., González S., Acevedo B., Besada V., Reyes O., González L.J. (2017), A deeper mining on the protein composition of VA-MENGOC-BC®: An OMV-based vaccine against *N. meningitidis serogroup* B and C, *Human Vaccines & Immunotherapeutics*, 13(11), pp. 2548–2560, https://doi.org/10.1080/21645515.2017.1356961

Mehanny M., Lehr C.M., Fuhrmann G. (2021), Extracellular vesicles as antigen carriers for novel vaccination avenues, *Advanced Drug Delivery Reviews*, 173, pp. 164–180, https://doi.org/10.1016/j.addr.2021.03.016

Mentrup T., Stumpff-Niggemann A.Y., Leinung N., Schlosser C., Schubert K., Wehner R., Tunger A., Schatz V., Neubert P., Gradtke A.C., Wolf J., Rose-John S., Saftig P., Dalpke A., Jantsch J., Schmitz M., Fluhrer R., Jacobsen I.D., Schröder B. (2022), Phagosomal signalling of the C-type lectin receptor Dectin-1 is terminated by intramembrane proteolysis, *Nature Communications*, 13(1), 1880, https://doi.org/10.1038/s41467-022-29474-3

Mirza Z., Soto E.R., Dikengil F., Levitz S.M., Ostroff G.R. (2017), Beta-glucan particles as vaccine adjuvant carriers, *Methods in Molecular Biology*, 1625, pp. 143–157, https://doi.org/10.2174/97816080521031110101

Mitroulis I., Ruppova K., Wang B., Chen L.S., Grzybek M., Grinenko T., Eugster A., Troullinaki M., Palladini A., Kourtzelis I., Chatzigeorgiou A., Schlitzer A., Beyer M., Joosten L.A.B., Isermann B., Lesche M., Petzold A., Simons K., Henry I., Dahl A., Schultze J.L., Wielockx B., Zamboni N., Mirtschink P., Coskun Ü., Hajishengallis G., Netea M.G., Chavakis T. (2018), Modulation of myelopoiesis progenitors is an integral component of trained immunity, *Cell*, 172(1), pp. 147–161, https://doi.org/10.1016/j.cell.2017.11.034

Miyamoto N., Mochizuki S., Sakurai K. (2018), Designing an immunocyte-targeting delivery system by use of beta-glucan, *Vaccine*, 36(1), pp. 186–189, https://doi.org/10.1016/j.vaccine.2017.11.053

Mochizuki S., Morishita H., Kobiyama K., Aoshi T., Ishii K.J., Sakurai K. (2015), Immunization with antigenic peptides complexed with β-glucan induces potent cytotoxic T-lymphocyte activity in combination with CpG-ODNs, *Journal of Controlled Release,* 220, pp. 495–502, https://doi.org/10.1016/j.jconrel.2015.11.008

Mohan T., Verma P., Rao D.N. (2023), Novel adjuvants & delivery vehicles for vaccines development: A road ahead, *The Indian Journal of Medical Research*, 138(5), 779–795.

Moni S.S., Abdelwahab S.I., Jabeen A., Elmobark M.E., Aqaili D., Ghoal G., Oraibi B., Farasani A.M., Jerah A.A., Alnajai M.M.A., Mohammad Alowayni A.M.H. (2023), Advancements in vaccine adjuvants: The journey from alum to nano formulations, *Vaccines*, 11(11), 1704, https://doi.org/10.3390/vaccines11111704

Moriya N., Moriya Y., Nomura H., Kusano K., Asada Y., Uchiyama H., Park E.Y., Okabe, M. (2013), Improved β-glucan yield using an *Aureobasidium pullulans* M-2 mutant strain in a 200-L pilot scale fermentor targeting industrial mass production, Biotechnology and Bioprocess Engineering, 18(6), pp. 1083–1089, https://doi.org/10.1007/s12257-013-0516-9

Mudgil D. (2017), The interaction between insoluble and soluble fiber, In: R.A. Samaan (Ed.), *Dietary Fiber for the Prevention of Cardiovascular Disease*, Academic Press, pp. 35–59, https://doi.org/10.1016/b978-0-12-805130-6.00003-3

Murphy E.J., Rezoagli E., Major I., Rowan N.J., Laffey J.G. (2020), β-glucan metabolic and immunomodulatory properties and potential for clinical application, *Journal of Fungi*, 6(4), 356, https://10.3390/jof6040356

Murthy K.G., Deb A., Goonesekera S., Szabó C., Salzman A.L. (2014), Identification of conserved domains in *Salmonella muenchen* flagellin that are essential for its ability to activate TLR5 and to induce an inflammatory response in vitro, *Journal of Biological Chemistry*, 279(7), pp. 5667–5675, https://doi.org/10.1074/jbc.M307759200

Netea M.G., van der Meer J.W. (2017), Trained immunity: an ancient way of remembering, *Cell Host & Microbe*, 21(3), pp. 297–300, http://dx.doi.org/10.1016/j.chom.2017.02.003

Novakovic B., Habibi E., Wang S.Y., Arts R.J.W., Davar R., Megchelenbrink W., Kim B., Kuznetsova T., Kox M., Zwaag J., Matarese F., van Heeringen S.J., Janssen-Megens E.M., Sharifi N., Wang C., Keramati F., Schoonenberg V., Flicek P., Clarke L., Pickkers P., Heath S., Gut I., Netea M.G., Martens J.H.A., Logie C., Stunnenberg H.G. (2016), β-Glucan reverses the epigenetic state of LPS-induced immunological tolerance, *Cell*, 167(5), pp. 1354-1368, http://dx.doi.org/10.1016/j.cell.2016.09.034

Owen A.M., Fults J.B., Patil N.K., Hernandez A., Bohannon J.K. (2021), TLR agonists as mediators of trained immunity: Mechanistic insight and immunotherapeutic potential to combat infection, *Frontiers in Immunology*, 11, 622614, https://doi.org/10.3389/fimmu.2020.622614

Palgen J.L., Feraoun Y., Dzangué-Tchoupou G., Joly C., Martinon F., Le Grand R., Beignon A.S. (2021), Optimize prime/boost vaccine strategies: Trained immunity as a new player in the game, *Frontiers in Immunology*, 12, 612747, https://doi.org/10.3389/fimmu.2021.612747

Parmaksız S., Pekcan M., Özkul A., Türkmen E., Rivero-Arredondo V., Ontiveros-Padilla L., Forbes N., Perrie Y., López-Macías C., Şenel S. (2023), In vivo evaluation of new adjuvant systems based on combination of *Salmonella typhi* porins with particulate systems: Liposomes versus polymeric particles, *International Journal of Pharmaceutics*, 648, 123568, https://doi.org/10.1016/j.ijpharm.2023.123568

Pence B.D., Hester S.N., Donovan S.M., Woods J.A. (2022), Dietary whole glucan particles do not affect antibody or cell-mediated immune responses to influenza virus vaccination in

mice, *Immunological Investigations*, 41(3), pp. 275–289, https://doi.org/10.3109/08820139.2011.628732

Pengkumsri N., Sivamaruthi B.S., Sirilun S., Peerajan S., Kesika P., Chaiyasut K., Chaiyasut C. (2016), Extraction of β-glucan from *Saccharomyces cerevisiae*: Comparison of different extraction methods and in vivo assessment of immunomodulatory effect in mice, *Food Science and Technology*, 37, pp. 124–130, https://doi.org/10.31557/APJCP.2020.21.3.837

Pengkumsri N., Sudiana A.D.G., Kuswendi H., Dewi V.Y.K., Balia R.L. (2022), The potential of ß-glucan from *Saccharomyces cerevisiae* cell wall as anti-cholesterol, *Journal of Animal Health and Production*, 9(1), pp. 72–77, http://dx.doi.org/10.17582/journal.jahp/2021/9.1.72.77

Petousis-Harris H., Radcliff F.J. (2019), Exploitation of *Neisseria meningitidis* group B OMV vaccines against *N. gonorrhoeae* to inform the development and deployment of effective gonorrhea vaccines, *Frontiers in Immunology*, 10, 683, https://doi.org/10.3389/fimmu.2019.00683

Peymaeei F., Sadeghi F., Safari E., Khorrami S., Falahati M., Roudbar Mohammadi S., Roudbary M. (2020), *Candida albicans* beta-glucan induce anti-cancer activity of mesenchymal stem cells against lung cancer cell line: An in-vitro experimental study, *Asian Pacific Journal of Cancer Prevention*, 21(3), 837, https://doi.org/10.31557/APJCP.2020.21.3.837

Philippini R.R., Martiniano S.E., dos Santos J.C., da Silva S.S., Chandel A.K. (2019), Fermentative production of beta-glucan: Properties and potential applications, In: G. Molina, V. Gupta, B. Singh, N. Gathergood (Eds.), *Bioprocessing for Biomolecules Production*, pp. 303–320, https://doi.org/10.1002/9781119434436.ch15

Powell B.S., Andrianov A.K., Fusco P.C. (2015), Polyionic vaccine adjuvants: another look at aluminum salts and polyelectrolytes, *Clinical and Experimental Vaccine Research*, 4(1), pp. 23–45, https://doi.org/10.7774/cevr.2015.4.1.23

Pulendran B.S., Arunachalam P., O'Hagan D.T. (2021), Emerging concepts in the science of vaccine adjuvants, *Nature Reviews Drug Discovery*, 20(6), pp. 454–475, https://doi.org/10.1038/ s41573-021-00163-y

Qiao W., Ji S., Zhao Y., Hu T. (2015), Conjugation of β-glucan markedly increase the immunogencity of meningococcal group Y polysaccharide conjugate vaccine, *Vaccine*, 33(17), pp. 2066–2072, https://doi.org/10.1016/j.vaccine.2015.02.045

Qu Y., Zhao X., Guo H., Meng Y., Wang Y., Zhou Y., Sun L. (2021), Structural analysis and macrophage activation of a novel β-glucan isolated from *Cantharellus cibarius*, *International Journal of Molecular Medicine*, 47(4), 50, https://doi.org/10.3892/ijmm.2021.4883

Reed S.G., Berthole, S, Coler R.N., Friede M. (2009), New horizons in adjuvants for vaccine development, *Trends in Immunology*, 30(1), pp. 23–32, https://doi.org/10.1016/j.it.2008.09.006

Rivas E., Gómez-Arnáiz M., Ricoy J.R., Mateos F., Simón R., García-Peñas J.J., Garcia-Silva M.T., Martín E., Vázquez M., Ferreiro A., Cabello A. (2005), Macrophagic myofasciitis in childhood: A controversial entity, *Pediatric Neurology*, 33(5), pp. 350–356, https://doi.org/10.1016/j.pediatrneurol.2005.05.024

Rodríguez-Seoane P., González-Muñoz M. J., Falqué E., Domínguez H. (2018), Pressurized hot water extraction of β-glucans from *Cantharellus tubaeformis*, *Electrophoresis*, 2018 doi: 10.1002/elps.201700399.

Rusek P., Wala M., Druszczyńska M., Fol M. (2018), Infectious agents as stimuli of trained innate immunity, *International Journal of Molecular Sciences*, 19(2), 456, https://doi.org/10.3390/ijms19020456

Sadoughi F., Asemi Z., Hallajzadeh J., Mansournia M.A., Yousefi B. (2022), Beta-glucans is a potential inhibitor of ovarian cancer: Based on molecular and biological aspects, *Current*

Pharmaceutical Biotechnology, 23(9), pp. 1142–1152, https://doi.org/10.2174/1389201022666210810090728

Saeed S., Quintin J., Kerstens H.H., Rao N.A., Aghajanirefah A., Matarese F., Cheng S.C., Ratter J., Berentsen K., van der Ent M.A., Sharifi N., Janssen-Megens E.M., Ter Huurne M., Mandoli A., van Schaik T., Ng A., Burden F., Downes K., Frontini M., Kumar V., Giamarellos-Bourboulis E.J., Ouwehand W.H., van der Meer J.W., Joosten L.A., Wijmenga C., Martens J.H., Xavier R.J., Logie C., Netea M.G., Stunnenberg H.G. (2014), Epigenetic programming of monocyte-to-macrophage differentiation and trained innate immunity, *Science*, 345(6204), 1251086, https://doi.org/10.1126/science.125108

Sánchez-Ramón S., Conejero L., Netea M.G., Sancho D., Palomares Ó., Subiza J.L. (2018), Trained immunity-based vaccines: a new paradigm for the development of broad-spectrum anti-infectious formulations, *Frontiers in Immunology*, 9, 2936, https://doi.org/10.3389/fimmu.2018.02936

Sari M., Prange A., Lelley J.I., Hambitzer R. (2017), Screening of beta-glucan contents in commercially cultivated and wild growing mushrooms, *Food Chemistry*, 216, pp. 45–51. doi: 10.1016/j.foodchem.2016.08.010.

Semchenko E.A., Tan A., Borrow R., Seib K.L. (2019), The serogroup B meningococcal vaccine Bexsero elicits antibodies to *Neisseria gonorrhoeae*, *Clinical Infectious Diseases*, 69(7), pp. 1101–1111, https://doi.org/10.1093/cid/ciy1061

Shah R.R., Hassett K.J., Brito L. A. (2017), Overview of vaccine adjuvants: Introduction, history, and current status, *Methods in Molecular Biology*, 1494, pp. 1–13, https://doi.org/10.1080/08998280.2005.11928028

Shah V.B., Williams D.L., Keshvara L. (2009), β-Glucan attenuates TLR2-and TLR4-mediated cytokine production by microglia, *Neuroscience Letters*, 458(3), pp. 111–115, https://doi.org/10.1016/j.neulet.2009.04.039

Soares E., Jesus S., Borges O. (2018), Chitosan: β-glucan particles as a new adjuvant for the hepatitis B antigen, *European Journal of Pharmaceutics and Biopharmaceutics*, 131, pp. 33–43, https://doi.org/10.1016/j.ejpb.2018.07.018

Song L., Zhang Y., Yun N.E., Poussard A.L., Smith J.N., Smith J.K., Borisevich V., Linde J.J., Zacks M.A., Li H., Kavita U., Reiserova L., Liu X., Dumuren K., Balasubramanian B., Weaver B., Parent J., Umlauf S., Liu G., Huleatt J., Tussey L., Paessler S. (2009), Superior efficacy of a recombinant flagellin: H5N1 HA globular head vaccine is determined by the placement of the globular head within flagellin, *Vaccine*, 27(42), pp. 5875–5884, https://doi.org/10.1016/j.vaccine.2009.07.060

Soto E.R., Caras A.C., Kut L.C., Castle M.K., Ostroff G.R. (2012), Glucan particles for macrophage targeted delivery of nanoparticles, *Journal of Drug Delivery*, 2012,143524, https://doi.org/10.1155/2012/143524

Soto E.R., Specht C.A., Rus F., Lee C.K., Abraham A., Levitz S.M., Ostroff G.R. (2023), An efficient (nano) silica-In glucan particles protein encapsulation approach for improved thermal stability, *Journal of Controlled Release*, 357, pp. 175–184, https://doi.org/10.1016/j.jconrel.2023.03.027

Stabnikova O., Stabnikov V., Paredes-López O. (2024), Wild and cultivated mushrooms as food, pharmaceutical and industrial products, *Ukrainian Food Journal*, 13(1), pp. 20–59, https://doi.org/10.24263/2304-974X-2024-13-1-4

Stothers C.L., Burelbach K.R., Owen A.M., Patil N.K., McBride M.A., Bohannon J.K., Luan L., Hernandez A., Patil T.K., Williams D.L., Sherwood E.R. (2021), β-glucan induces distinct and protective innate immune memory in differentiated macrophages, *The Journal of Immunology*, 207(11), pp. 2785–2798, https://doi.org/10.4049/jimmunol.2100107

Stuyven E., Verdonck F., Van Hoek I., Daminet S., Duchateau L., Remon J.P., Goddeeris B.M., Cox E. (2010), Oral administration of β-1, 3/1, 6-glucan to dogs temporally changes total

and antigen-specific IgA and IgM, *Clinical and Vaccine Immunology*, 17(2), pp. 281–285, https://doi.org/10.1128/CVI.00344-09

Suárez N., Ferrara F., Rial A., Dee V., Chabalgoity J.A. (2020), Bacterial lysates as immunotherapies for respiratory infections: Methods of preparation, *Frontiers in Bioengineering and Biotechnology*, 8(2), 545, https://doi.org/10.3389/fbioe.2020.00545

Suzuki T., Kusano K., Kondo N., Nishikawa K., Kuge T., Ohno N. (2021), Biological activity of high-purity β-1, 3-1, 6-glucan derived from the black yeast *Aureobasidium pullulans*: A literature review, *Nutrients*, 13(1), 242, https://doi.org/10.3390/nu13010242

Tadepalli G., Konduru B., Murali H.S., Batra H.V. (2017), Intraperitoneal administration of a novel chimeric immunogen (rOP) elicits IFN-γ and IL-12p70 protective immune response in BALB/c mice against virulent Brucella. *Immunology Letters,* 192, pp. 79–87, https://doi.org/10.1016/j.imlet.2017.10.013

Taleghani N., Bozorg A., Azimi A., Zamani H. (2019), Immunogenicity of HPV and HBV vaccines: Adjuvanticity of synthetic analogs of monophosphoryl lipid A combined with aluminum hydroxide, *APMIS*, 127(3), pp. 150–157, https://doi.org/10.1111/apm.12927

Tan K., Li R., Huang X., Liu Q. (2018), Outer membrane vesicles: current status and future direction of these novel vaccine adjuvants, *Frontiers in Microbiology*, 9, 783, https://doi.org/10.3389/fmicb.2018.00783

Tel-Çayan G., Çayan F., Deveci E., Duru M. E. (2021), Phenolic profile, antioxidant and cholinesterase inhibitory activities of four *Trametes* species: *T. bicolor*, *T. pubescens*, *T. suaveolens*, and *T. versicolor*, *Journal of Food Measurement and Characterization*, 15(5), pp. 4608–4616, https://doi.org/10.1007/s11694-021-01034-1

Toussaint B., Chauchet X., Wang Y., Polack B., Gouëllec A.L. (2023), Live-attenuated bacteria as a cancer vaccine vector, *Expert Review of Vaccines*, 12(10), pp. 1139-1154, https://doi.org/10.1586/14760584.2013.836914

Treanor J.J., Taylor D.N., Tussey L., Hay C., Nolan C., Fitzgerald T., Liu G., Kavita U., Song L., Dark I., Shaw, A. (2010), Safety and immunogenicity of a recombinant hemagglutinin influenza–flagellin fusion vaccine (VAX125) in healthy young adults, *Vaccine*, 28(52), pp. 8268–8274, https://doi.org/10.1016/j.vaccine.2010.10.009

Urbancikova I., Hudackova D., Majtan J., Rennerova Z., Banovcin P., Jesenak M. (2020), Efficacy of pleuran (β-glucan from *Pleurotus ostreatus*) in the management of herpes simplex virus type 1 infection, *Evidence-Based Complementary and Alternative Medicine*, 2020, 8562309. https://doi.org/10.1155/2020/8562309

Utama G.L., Dio C., Sulistiyo J., Chye F. Y., Lembong E., Cahyana Y., Verma D.K., Thakur M., Patel A.R., Singh S. (2021), Evaluating comparative β-glucan production aptitude of *Saccharomyces cerevisiae*, *Aspergillus oryzae*, *Xanthomonas campestris*, and *Bacillus natto*, *Saudi Journal of Biological Sciences*, 28(12), pp. 6765–6773, https://doi.org/10.1016/j.sjbs.2021.07.051

Utama G.L., Kurniawan M.O., Cahyana Y., Balia R.L. (2022), β-Glucan production through bioconversion of sugarcane bagasse by *Saccharomyces cerevisiae* and *Aspergillus niger*, In: H. Thatoi, S. Mohapatra, S.K. Das (Eds.), *Innovations in Fermentation and Phytopharmaceutical Technologies* (pp. 397–416). Elsevier, https://doi.org/10.1016/B978-0-12-821877-8.00009-9

Vader P., Mol E.A., Pasterkamp G., Schiffelers R.M. (2016), Extracellular vesicles for drug delivery, *Advanced Drug Delivery Reviews*, 106(Part A), pp. 148–156, https://doi.org/10.1016/j.addr.2016.02.006

Van Der Pol L., Stork M., van der Ley P. (2015), Outer membrane vesicles as platform vaccine technology. *Biotechnology Journal*, 10(11), pp. 1689–1706, https://doi.org/10.1002/biot.201400395

Verma S.K., Mahajan P., Singh N.K., Gupta A., Aggarwal R., Rappuoli R., Johri A.K. (2023), New-age vaccine adjuvants, their development, and future perspective, *Frontiers in Immunology*, 14, 1043109, https://doi.org/10.3389/fimmu.2023.1043109

Walk J., de Bree L.C.J., Graumans W., Stoter R., van Gemert G.J., van de Vegte-Bolmer M., Teelen K., Hermsen C.C., Arts R.J.W., Behet M.C., Keramati F., Moorlag S.J.C.F.M., Yang A.S.P., van Crevel R., Aaby P., de Mast Q., van der Ven A.J.A.M., Stabell Benn C., Netea M.G., Sauerwein R.W. (2019), Outcomes of controlled human malaria infection after BCG vaccination, *Nature Communications*, 10(1), 874, https://doi.org/10.1038/s41467-019-08659-3

Wang J., Dong S., Liu C., Wang W., Sun S., Gu J., Wang Y., Boraschi D., Qu D. (2020), β-Glucan oligosaccharide enhances T cells immune response induced by a DNA vaccine encoding hepatitis B virus core antigen, *BioMed Research International*, 2010, 645213, https://doi.org/10.1155/2010/645213

Wang M., Yang R., Zhang L., Meng X., Fei C., Zhang K., Wang X., Zheng W., Xiao S., Zhang S., Xue F., Hu Y. (2024), Sulfated glucan can improve the immune efficacy of Newcastle disease vaccine in chicken, *International Journal of Biological Macromolecules,* 70, pp. 193–198, https://doi.org/10.1016/j.ijbiomac.2014.05.048

Wang M., Zhang L., Yang R., Fei C., Wang X., Zhang K., Wang C., Zheng W., Xue F. (2016), Improvement of immune responses to influenza vaccine (H5N1) by sulfated yeast beta-glucan, *International Journal of Biological Macromolecules,* 93(Pt A), pp. 203–207, https://doi.org/10.1016/j.ijbiomac.2016.06.057

Wang Q., Sheng X., Shi A., Hu H., Yang Y., Liu L., Fei L., Liu H. (2017), β-Glucans: Relationships between modification, conformation and functional activities, *Molecules*, 22(2), 257, https://doi.org/10.3390/molecules22020257

Wimmers F., Donato M., Kuo A., Ashuach T., Gupta S., Li C., Dvorak M., Foecke M.H., Chang S.E., Hagan T., De Jong S.E., Maecker H.T., van der Most R., Cheung P., Cortese M., Bosinger S.E., Davis M., Rouphael N., Subramaniam S., Yosef N., Utz P.J., Khatri P., Pulendran B. (2021), The single-cell epigenomic and transcriptional landscape of immunity to influenza vaccination, *Cell*, 184(15), pp. 3915–3935, https://doi.org/10.1016/j.cell.2021.05.039

Yang J., Zhang J., Han T., Liu C., Li X., Yan L., Yang B., Yang X. (2020), Effectiveness, immunogenicity, and safety of influenza vaccines with MF59 adjuvant in healthy people of different age groups: A systematic review and meta-analysis, *Medicine (Baltimore)*, 99(7), e19095, https://doi.org/10.1097/MD.0000000000019095

Yang Y.M., Fu X., Cui F.J., Sun L., Zan X.Y., Sun W.J. (2023), Biochemical and structural characterization of a glucan synthase GFGLS2 from edible fungus *Grifola frondosa* to synthesize β-1, 3-glucan, *Biotechnology for Biofuels and Bioproducts*, 16(1), 163, https://doi.org/10.1186/s13068-023-02380-6

Yu X., Zhang D., Shi B., Ren G., Peng X., Fang Z., Kozlowski M., Zhou X., Zhang X., Wu M., Wang C., Yuan Z. (2015), Oral administered particulate yeast-derived glucan promotes hepatitis B virus clearance in a hydrodynamic injection mouse model, *PLoS One*, 10(4), e0123559, https://doi.org/10.1371/journal.pone.0123559

Yun C.H., Estrada A., Van Kessel A., Park B.C., Laarveld B. (2003), β-Glucan, extracted from oat, enhances disease resistance against bacterial and parasitic infections, *FEMS Immunology & Medical Microbiology*, 35(1), pp. 67–75, https://doi.org/10.1016/S0928-8244(02)00460-1

Zhang M., Jin X., Yang Y.F. (2019), β-Glucan from *Saccharomyces cerevisiae* induces SBD-1 production in ovine ruminal epithelial cells via the Dectin-1–Syk–NF-κB signaling pathway, *Cellular Signalling*, 53, pp. 304–315, https://doi.org/10.1016/j.cellsig.2018.10.018

Zhao T., Cai Y., Jiang Y., He X., Wei Y., Yu Y., Tian X. (2023), Vaccine adjuvants: Mechanisms and platforms, *Signal Transduction and Targeted Therapy*, 8(1), 283, https://doi.org/10.1038/s41392-023-01557-7

Zingl F.G., Leitner D.R., Schild S. (2020), Biogenesis of gram-negative OMVs, In: M. Kaparakis-Liaskos, T. Kufer (Eds.), *Bacterial Membrane Vesicles*, Springer, Cham, https://doi.org/10.1007/978-3-030-36331-4_2

Cite:

UFJ Style

Belemets T., Krasinko V., Stabnikov V. (2024), Characteristics and immunostimulating properties of chemical and microbial vaccine adjuvants, *Ukrainian Food Journal*, 13(4), pp. 825–861, https://doi.org/10.24263/2304-974X-2024-13-4-14

APA Style

Belemets, T., Krasinko, V., & Stabnikov, V. (2024). Characteristics and immunostimulating properties of chemical and microbial vaccine adjuvants. *Ukrainian Food Journal*, *13*(4), 825–861. https://doi.org/10.24263/2304-974X-2024-13-4-14

Instructions for authors

Dear colleagues!

The Editorial Board of scientific periodical
"**Ukrainian Food Journal**"
invites you for publication of your research results.

A manuscript should describe the research work that has not been published before and is not under consideration for publication anywhere else. Submission of the manuscript implies that its publication has been approved by all co-authors as well as by the responsible authorities at the institute where the work has been carried out.

It is mandatory to include a covering letter to the editor which includes short information about the subject of the research, its novelty and significance; state that all the authors agree to submit this paper to Ukrainian Food Journal; that it is the original work of the authors.

Manuscript requirements

Authors must prepare the manuscript according to the guide for authors. Editors reserve the right to adjust the style to certain standards of uniformity.

Language – English

Manuscripts should be submitted in Word.

Use 1.0 spacing and 2 cm margins.

Use a normal font 14-point Times New Roman for text, tables, and in the figure captions.

Present tables and figures in the text of manuscript.

Consult a recent issue of the journal for a style check.

Number all pages consecutively.

Abbreviations should be defined on first appearance in text and used consistently thereafter. No abbreviation should be used in title and section headings.

Please submit math equations as editable text and not as images (It is recommend software application MathType or Microsoft Equation Editor).

Minimal size of the article (without the Abstract and References) is 10 pages. For review article is 25 pages (without the Abstract and References).

Manuscript should include:

Title (should be concise and informative). Avoid abbreviations in it.

Authors' information: the name(s) of the author(s); the affiliation(s) of the author(s), city, country. One author has been designated as the corresponding author with e-mail address. If available, the 16-digit ORCID of the author(s) information on the title page .

Declaration of interest

Author Contribution Statement

Abstract. The **abstract** should contain the following mandatory parts:

Introduction provides a rationale for the study (2–3 lines).

Materials and methods briefly describe the materials and methods used in the study (3–5 lines).

Results and discussion describe the main findings (20–26 lines).

Conclusion provides the main conclusions (2–3 lines).

The abstract should not contain any undefined abbreviations or references to the articles.

Keywords. Immediately after the abstract provide 4 to 6 keywords.

Text of manuscript

References

Manuscripts should be divided into the following sections:

Introduction
Materials and methods
Results and discussion
Conclusions
References

Introduction. Provide a background avoiding a detailed review of literature and declare the aim of the present research. Identify unexplored questions, prove the relevance of the topic. This should be not more than 1.5 pages.

Materials and methods. Describe sufficient details to allow an independent researcher to repeat the work. Indicate the reference for methods that are already published and just summarize them. Only new techniques need be described. Give description to modifications of existing methods.

Results and discussion. Results should be presented clearly and concisely with tables and/or figures, and the significance of the findings should be discussed with comparison with existing in literature data.

Conclusions. The main conclusions should be drawn from results and be presented in a short Conclusion section.

Acknowledgments(if necessary)**.** Acknowledgments of people, grants, or funds should be placed in a separate section. List here those persons who provided help during the research. The names of funding organizations should be written in full.

Divide your article into sections and into subsections if necessary. Any subsection should have a brief heading.

References

Please, check references carefully.

The list of references should include works that are cited in the text and that have been published or accepted for publication.

All references mentioned in the reference list are cited in the text, and vice versa.

Cite references in the text by name and year in parentheses. Some examples:

(Drobot, 2008); (Qi and Zhou, 2012); (Bolarinwa et al., 2019; Rabie et al., 2020; Sengev et al., 2013).

Reference list should be alphabetized by the last name of the first author of each work.

If available, please always include DOIs links in the reference list.

Reference style

Journal article

Please follow this style and order: author's surname, initial(s), year of publication (in brackets), paper title, *Journal title (in Italic)*, volume number (issue), first and last page numbers. If available, please always include DOIs as full DOI links in your reference list (e.g. "https://doi.org/abc").

Popovici C., Gitin L., Alexe P. (2013), Characterization of walnut (*Juglans regia* L.) green husk extract obtained by supercritical carbon dioxide fluid extraction, *Journal of Food and Packaging Science*, *Technique and Technologies*, 2(2), pp. 104-108, https://doi.org/11.1016/22-33-85

Journal names should not be abbreviated.

Book

Deegan C. (2000), *Financial Accounting Theory*, McGraw-Hill Book Company, Sydney.

Book chapter in an edited book

Fordyce F.M. (2013), Selenium deficiency and toxicity in the environment. In: O. Selinus (Ed.), *Essentials of Medical Geology*, Springer, pp. 375–416, https://doi.org/10.14453/10.1007/978-94-007-4375-5_16

Kochubei-Lytvynenko O., Kuzmyk U., Yushchenko N. (2022), Spices for dairy products. In: O. Paredes-López, O. Shevchenko, V. Stabnikov, V. Ivanov (Eds.), *Bioenhancement and Fortification of Foods for a Healthy Diet*, CRC Press, Boca Raton, London, pp. 157-178, https://doi.org/10.1201/9781003225287-11

Online document

Mendeley J.A., Thomson, M., Coyne R.P. (2017), *How and When to Reference*, Available at: https://www.howandwhentoreference.com

Conference paper

Arych M. (2018), Insurance's impact on food safety and food security, *Resource and Energy Saving Technologies of Production and Packing of Food Products as the Main Fundamentals of Their Competitiveness: Proceedings of the 7th International Specialized Scientific and Practical Conference, September 13, 2018,* NUFT, Kyiv, pp. 52–57, https://doi.org/11.1016/22-33-85

Figures

All figures should be made in graphic editor using a font Arial.

The font size on the figures and the text of the article should be the same.

Black and white graphic with no shading should be used.

The figure elements (lines, grid, and text) should be presented in black (not gray) colour.

Figure parts should be denoted by lowercase letters (a, b, etc.).

All figures are to be numbered using Arabic numerals.

Figures should be cited in text in consecutive numerical order.

Place figure after its first mentioned in the text.

Figure captions begin with the term Figure in bold type, followed by the figure number, also in bold type.

Each figure should have a caption describing what the figure depicts in bold type.

Supply all figures and EXCEL format files with graphs additionally as separate files.

If you include figures that have already been published elsewhere, you must obtain permission from the copyright owner(s).

Tables

Number tables consecutively in accordance with their appearance in the text.

Place footnotes to tables below the table body and indicate them with superscript lowercase letters.

Place table after its first mentioned in the text.

Ensure that the data presented in tables do not duplicate results described elsewhere in the article.

Suggesting / excluding reviewers

Authors may suggest reviewers and/or request the exclusion of certain individuals when submitting their manuscripts.

When suggesting reviewers, authors should make sure they are totally independent and not connected to the work in any way. When suggesting reviewers, the Corresponding Author must provide an institutional email address for each suggested reviewer. Please note that the Journal may not use the suggestions, but suggestions are appreciated and may help facilitate the peer review process.

Submission

Email for all submissions and other inquiries:

ufj_nuft@meta.ua

Шановні колеги!

Редакційна колегія наукового періодичного видання «**Ukrainian Food Journal**» запрошує Вас до публікації результатів наукових досліджень.

Вимоги до оформлення статей

Мова статей – англійська.

Мінімальний обсяг статті – **10 сторінок** формату А4 (без врахування анотацій і списку літератури)**.**

Для всіх елементів статті шрифт – **Times New Roman**, кегль – **14**, інтервал – 1.

Всі поля сторінки – по 2 см.

Структура статті:

1. **Назва статті.**
2. Автори статті (ім'я та прізвище повністю, приклад: Денис Озерянко).
3. *Установа, в якій виконана робота.*
4. Анотація. **Обов'язкова** структура анотації:
   - Вступ (2–3 рядки).
   - Матеріали та методи (до 5 рядків)
   - Результати та обговорення (пів сторінки).
   - Висновки (2–3 рядки).
6. Ключові слова (3–5 слів, але не словосполучень).

Пункти 2–6 виконати англійською і українською мовами.

7. Основний текст статті. Має включати такі обов'язкові розділи:
   - Вступ
   - Матеріали та методи
   - Результати та обговорення
   - Висновки
   - Література.

За необхідності можна додавати інші розділи та розбивати їх на підрозділи.

8. Авторська довідка (Прізвище, ім'я та по батькові, вчений ступінь та звання, місце роботи, електронна адреса або телефон).
9. Контактні дані автора, до якого за необхідності буде звертатись редакція журналу.

Рисунки виконуються якісно. Скановані рисунки не приймаються. Розмір тексту на рисунках повинен бути **співрозмірним** (!) тексту статті. **Фотографії можна використовувати лише за їх значної наукової цінності.**

Фон графіків, діаграм – лише білий. Колір елементів рисунку (лінії, сітка, текст) – чорний (не сірий).

Рисунки та графіки EXCEL з графіками додатково подаються в окремих файлах.

Скорочені назви фізичних величин в тексті та на графіках позначаються латинськими літерами відповідно до системи СІ.

У списку літератури повинні переважати англомовні статті та монографії, які опубліковані після 2010 року.

Оформлення цитат у тексті статті:

Кількість авторів статті	Приклад цитування у тексті
1 автор	(Arych, 2019)
2 автора	(Kuievda and Bront, 2020)
3 і більше авторів	(Bazopol et al., 2022)

Приклад тексту із цитуванням: It is known (Arych, 2019; Bazopol et al., 2022), the product yield depends on temperature, but, there are some exceptions (Kuievda and Bront, 2020).

У цитуваннях необхідно вказувати джерело, звідки взято інформацію.

Список літератури сортується за алфавітом, літературні джерела не нумеруються.

Правила оформлення списку літератури

В Ukrainian Food Journal взято за основу загальноприйняте в світі спрощене оформлення списку літератури згідно стандарту Garvard. Всі елементи посилання розділяються **лише комами**.

1. Посилання на статтю:

Автори А.А. (рік видання), Назва статті, *Назва журналу (курсивом)*, Том (номер), сторінки, DOI.

Ініціали пишуться після прізвища.

Всі елементи посилання розділяються комами.

Приклад:

Popovici C., Gitin L., Alexe P. (2013), Characterization of walnut (*Juglans regia* L.) green husk extract obtained by supercritical carbon dioxide fluid extraction, *Journal of Food and Packaging Science, Technique and Technologies,* 2(2), pp. 104–108, https://doi.org/5533.935-3.

2. Посилання на книгу:

Автори (рік), *Назва книги (курсивом)*, Видавництво, Місто.

Ініціали пишуться після прізвища.

Всі елементи посилання розділяються комами.

Приклад:

Deegan C. (2000), *Financial Accounting Theory*, McGraw-Hill Book Company, Sydney.

3. Посилання на розділ у редагованій книзі:

Автори (рік), Назва глави, In: Редактори, *Назва книги (курсивом)*, Видавництво, Місто, сторінки.

Приклад:

Fordyce F.M. (2013), Selenium deficiency and toxicity in the environment. In: O. Selinus (Ed.), *Essentials of Medical Geology*, Springer, pp. 375–416, https://doi.org/10.14453/10.1007/978-94-007-4375-5_16

4. Тези доповідей конференції:

Arych M. (2018), Insurance's impact on food safety and food security, *Resource and Energy Saving Technologies of Production and Packing of Food Products as the Main Fundamentals of Their Competitiveness: Proceedings of the 7th International Specialized Scientific and Practical Conference, September 13, 2018,* NUFT, Kyiv, pp. 52–57, https://doi.org/5533.935-3.

5. Посилання на електронний ресурс:

Виконується аналогічно посиланню на книгу або статтю. Після оформлення даних про публікацію пишуться слова **Available at:** та вказується електронна адреса.

Приклад:

Cheung T. (2011), *World's 50 most delicious drinks*, Available at: http://travel.cnn.com/explorations/drink/worlds–50-most-delicious-drinks–883542

Список літератури оформлюється лише латиницею. Елементи списку українською та російською мовою потрібно транслітерувати. Для транслітерації з української мови використовується паспортний стандарт.

Зручний сайт для транслітерації з української мови: http://translit.kh.ua/#lat/passport

Стаття надсилається за електронною адресою:
ufj_nuft@meta.ua

УДК 663/664

Ukrainian Food Journal публікує оригінальні наукові статті, короткі повідомлення, оглядові статті, новини та огляди літератури.

Тематика публікацій в Ukrainian Food Journal:

Харчова інженерія	Процеси та обладнання
Харчова хімія	Нанотехнології
Мікробіологія	Економіка та управління
Фізичні властивості харчових продуктів	Автоматизація процесів
Якість та безпека харчових продуктів	Упаковка для харчових продуктів

Періодичність виходу журналу 4 номери на рік.

Результати досліджень, представлені в журналі, повинні бути новими, мати чіткий зв'язок з харчовою наукою і представляти інтерес для міжнародного наукового співтовариства.

Ukrainian Food Journal індексується наукометричними базами:

- Index Copernicus (2012)
- EBSCO (2013)
- Google Scholar (2013)
- UlrichsWeb (2013)
- CABI full text (2014)
- Online Library of University of Southern Denmark (2014)
- Directory of Open Access scholarly Resources (ROAD) (2014)
- European Reference Index for the Humanities and the Social Sciences (ERIH PLUS) (2014)
- Directory of Open Access Journals (DOAJ) (2015)
- InfoBase Index (2015)
- Chemical Abstracts Service Source Index (CASSI) (2016)
- FSTA (Food Science and Technology Abstracts) (2018)
- Web of Science (Emerging Sourses Citaton Index) (2018)
- Scopus (2022)

Рецензія рукопису статті. Матеріали, представлені для публікування в «Ukrainian Food Journal», проходять «Подвійне сліпе рецензування» двома вченими, призначеними редакційною колегією: один є членом редколегії і один незалежний науковець.

Детальна інформація про Журнал, інструкції авторам, приклади оформлення статті та анотацій розміщені на сайті:

http://ufj.nuft.edu.ua

Редакційна колегія

Наукове видання

Ukrainian Food Journal

Volume 13, Issue 4
2024

Том 13, № 4
2024

Підп. до друку 31.12.2024 р. Формат 70x100/16.
Обл.-вид. арк. 13.42. Ум. друк. арк. 13.54.
Гарнітура Times New Roman. Друк офсетний.
Наклад 100 прим. Вид. № 29н/24.

НУХТ. 01601 Київ–33, вул. Володимирська, 68

Свідоцтво про державну реєстрацію
друкованого засобу масової інформації
КВ 18964–7754Р
видане 26 березня 2012 року.